OPTICAL PROPERTIES OF THE DISSOLVED ORGANIC MATTER AS TRACERS OF MICROBIOLOGICAL AND GEOCHEMICAL PROCESSES IN MARINE ECOSYSTEMS

Cristina Romera Castillo

Optical properties of the dissolved organic matter as tracers of microbiological and geochemical processes in marine ecosystems

Cristina Romera Castillo

Directores: Dra. Cèlia Marrasé y Dr. Xosé Antón Álvarez Salgado

Universitat Politècnica de Catalunya

Programa de Doctorat en Ciències del Mar (MCD 2003-00141)
Departament d'Enginyeria Hidràulica, Marítima i Ambiental (EHMA)

Tesis presentada para obtener el título de Doctora por la Universitat Politècnica de Catalunya.

INDEX

Y después de este largo trayecto que parecía que se prolongaba exponencialmente ¡Por fin el momento de agradecer!

A mis directores de tesis, Celia y Pepe. Gracias por todo lo que me habéis enseñado, por vuestra paciencia infinita, por el tiempo dedicado a este trabajo y por los buenos momentos. Por vuestro valor científico y sobre todo, humano. Siempre dispuestos a "pringar" como cualquiera hasta horas infinitas analizando fluorescencias o lo que hiciera falta. Cèlia, por haberme dado la oportunidad de hacer este trabajo, por tu positividad y tus palabras de ánimo que siempre suben la moral. Tu buena predisposición y tu entusiasmo ante cualquier buena idea. Pepe, un gran honor que hayas sido director de mi tesis, gracias por todo lo que me has enseñado, tanto científicamente como de todo, un pozo de sabiduría! y siempre desafiante de la entropía de tu entorno. Por hacerme ver el sentido a las cosas en mis momentos de incredulidad. Por tantas historias y anécdotas contadas a la luz de la fluorescencia. Un enorme GRACIAS a los dos.

A Mar, componente importante de nuestro tele-grupo. Por tu ayuda siempre que la he necesitado. Por los buenos momentos en EEUU, Granada, Puerto Rico,.. y los que vengan! Al resto de co-autores de los capítulos de este trabajo, por su paciencia y sus rápidas correcciones, en la mayoría de los casos. Pep (visca la teva eficiència i les teves lliçons magistrals! han estat de gran ajuda), Hugo, Carmen, Xelu (por el trabajo que saldrá), Des Barton, Dan Repeta. A Mª Luisa, gran artista que ha sabido captar y plasmar la esencia de la materia coloreada en la portada. A Ernesto, por los retoques y opiniones de artista.

Al departament de biologia marina i ecologia de l'ICM en general. Déu n'hi do! Perquè tots heu contribuit en major o menor mesura a la realització d'aquesta tesi, encara que només hagi estat per generar bon ambient. Moltes gràcies!
Por las buenas amistades que he hecho aquí a lo largo de estos años. A Estela, por poner tanta "sal" a las comidas con historias y risas y por tu apoyo durante toda la tesis! A las que ya volaron pero fueron parte importante de este período, Lidia, Erika, Sofía, Bea Díez, Ceci.
A mis compañeros del "despacho molón", Mireia (por estar siempre a mi izquierda para comentar lo que fuera y animar), la ya Dra. Silvia (por más noches en la ópera!) y a los "chavalines", Claudio (el chileno más caluroso! harto de oirme decir "apaga el aire...") y Juancho (ánimo, a ver si le ganas a Mireia!). Por esas cervezas que quedan pendientes, no dejemos que caduquen esta vez!
A Irene, Vane y Clara, siempre prontas a solucionar cualquier problema. Evaristo, por tu ayuda y las conversaciones científicas. Berta, porque has sido de gran ayuda en nuestro mini-grupo desde que viniste. A Eva Flo, por tu amistad y tu alegría, y por ese viaje a morrocolandia que quedó pendiente por culpa de esta tesis… Isabel F., por tu buena predisposición y por los buenos momentos que ha habido y habrá!
A los que empezasteis a la vez que yo este "viaje" y con los que he pasado tan buenos momentos, Thomas (nous commençon et finisson ensemble! Por las risas que nos hemos echado juntos), Clara (mantén siempre esa alegría!), Arancha (la próxima eres tú!). Y a los demás que habéis compartido buenos momentos conmigo: Martí (hi ha alguna cosa que no sàpigues fer?), Rodrigo, Mariona, Ana

Gomes, Andrea, Elena, Pati, Itziar, Sara-Jeane, Xavi. A Bea F., Raquel, Montse, Ero (ya os queda poco a vosotras también!), Cristina (buena clase teórica de PCR y DGGE), Elisabet Sà y Elisabet Sañé, Miriam, Rachele…

A los "grandes jefes" que han aportado sabiduría a esta tesis, siempre dispuestos a resolver cualquier duda, Pep, Carles, Rafel, Cesc, Elisa, Miquel, Albert, Enric, Dolors, Carles Pelejero, Eva C., Montse, Ramón, Marta, Mikel Latasa... Porque todos y cada uno de vosotros, me habéis ayudado en algún que otro momento.
Al futuro inmediato de la oceanografía, los post-docs que cabalgan pacientes entre el "gran jefe" y la plebe de doctorandos, Silvia Acinas, Isabel, Hugo, Marta Sebastián.
A todos aquellos que pueblan los pasillos del instituto y saludan al pasar amenizando los largos trayectos hasta el baño o el laboratorio, Ana Mari, Fran, Pedro, Albert, Matina, Rodrigo(s), Roi, Guillem, Ramiro,…
A los que habéis ayudado en algún momento de este trabajo como parte de vuestras prácticas y que ha sido de gran ayuda! Fran, Encarna, Sandra, Adriá…

A los del departamento de física con quien tuve la suerte de compartir trabajo y campañas. Jose Luis Pelegrí, María Pastor, Maricel, Jaime, Paula, Mikhail,...

A aquellas personas que trabajan para la ciencia desde la administración y cuyo trabajo es imprescindible para que esto siga adelante, que en sus manos esta que la burocracia no acabe con nosotros y que esto marche. Por la eficiencia! Conchita, Genoveva, Nuria Angosto, Ramón, Jordi Estaña, Justo,...

A Gemma Vila, porque juntas hemos sabido sortear los inconvenientes externos a nosotras y ha sido una suerte que fueras tú mi homóloga de FDOM en Blanes! Mucho ánimo, que te queda muy poco y va a salir molt bé!

A todo el departamento de Oceanoloxía del IIM de Vigo. ¡Muchísimas gracias por la acogida! Porque me habéis hecho sentir como en casa desde el primer día, desde ayudándome con instalaciones informáticas varias (Fer y Antón), procesamiento de datos,…etc hasta ofreciéndome casa y dándome a conocer la vida (nocturna y diurna) de Vigo y su naturaleza. Merche, Diana, Miguel, Paola, Marquitos, Toni, Kiko, Thomas, Oscar, Bibiana. David, gracias por estar ahí y por las correcciones en gallego aguetense! A la alegría del departamento, que lo mismo te hacen un análisis de DOC que te bailan una conga, Rosa, Vane, Mónica y Antón (mi salvación en los últimos días de tesis en Vigo ayudándome a desconectar con divertidas historias de primos e informática), Fer (el único gallego capaz de pronunciar correctamente la "s" aspirada), Isabel (entaoooo!!! Gracias por tu apoyo y por lo bien que lo hemos pasado. Woooooo!!! Ahora síiii!!!). A Maria José, María "la rubia", Trini, Belén, que también habéis estado ahí siempre con una palabra amable en la boca. Y como no, este instituto también cuenta con "grandes jefes" que ayudan

cuando lo necesitas, Paco, Carmen, Des, Aida.

A los compañeros del laboratorio de Bremerhaven, por todo lo que me ayudasteis y lo bien que estuve allí aunque me tuviera que acostumbrar a comer en 15 min. Danke schön a Gerhard por su disponibilidad, a Boris y a Kai-Uwe, por enseñarme el análisis de amino ácidos. A Martin, Dittas, Oliver y Ruth, gracias por la acogida. Y a Luisa y Desi por aquellos días, hicisteis que esa estancia fuera genial. Vivan las cenas cubanas!

A Sofía y Joaquín, que me iniciaron en el maravilloso y precario mundo de la investigación científica, condimentado con laurel.

A mis compañeros (y ahora amigos) malaspineros, con los que he compartido una gran aventura y un viaje que no olvidaré. Nuestro equipo! Elena, Irene, Àngel, Victor, Paqui, Dani, Zuriñe (Su!), Ricardo, Rafel (no creo que encontremos nunca un mejor jefe de campaña ni compañero de aventuras selváticas, has deixat el llistó molt alt!). Por que nos encontremos todos otra vez, en la Antártida!

A mi Amiga Laura. Que aunque físicamente lejos estas siempre cerca. Mucha suerte en tu nueva etapa! A Majo, Irene y Lorena. A Jaime, "sin fallo" desde el principio (venga, que ya te queda poco a ti también!). A Max, incansable, siempre dispuesto a ayudar en lo que haga falta. A Roberto, presidente y fundador del Tupper-less, y a todos los tupperlesseros! A Francisco, Luca, Jacopo y Claudio. A mis flamenquitas! Catalanas salerosas!! Sandra y Montse (ea!), Irene y Olga. A los grandes navegantes, Ramón (eres un ejemplo de vitalidad admirable!) y Dani.

A la mia famiglia di Barcelona! Grazie mille! Perchè mi avete fatto sentire benissimo, per il vostro incoraggiamento, per il vostro affetto e amicizia, perchè non mi è mai mancato un posto a tavola! Ema, Ernesto, Lisilla, Ida, Silvio, Lorenzo, un enorme GRACIAS. Geo, por tu amistad y tu ayuda, próxima estación, Blanes.

A Lorenzo, pieza clave en estos años de tesis. Perque tutto quello che mi hai insegnato ha un valore incalcolabile. Per tuo amore e tuo affetto. Per essere el unico tera!

Y como no, un especial agradecimiento a mi familia. A mis padres y a mi hermana Marta, que siempre están dispuestos a escucharme y apoyarme. Que han vivido conmigo todas las aventuras de esta tesis. A mis tíos, Asún y Alfonso y a mis primos Paloma y David, que también están ahí siempre. Y a mis abuelos, grandes admiradores, siempre pendientes de cualquier barco que salga en la TV por si me ven dentro.

Espero no haber olvidado a nadie y si lo he hecho, le agradezco me disculpe.

A todos vosotros, Gracias, Merci, Graciñas, Grazie, Danke schön, Thanks!

Resumen

Los océanos albergan 685 Pg de carbono orgánico, de los que 662 Pg están en forma disuelta. La enorme diversidad de compuestos que constituyen la materia orgánica disuelta (DOM) y la baja concentración en que se encuentra cada uno de ellos, hace de la caracterización química y estructural de este material una ardua tarea. Es por eso que menos del 11% de la DOM está identificado en la actualidad. Una fracción variable de la DOM –entre el 20% en océano abierto y el 70% en zonas costeras– absorbe luz UV y visible, por lo que se conoce como DOM coloreada (CDOM). Parte de la CDOM, emite la radiación absorbida en forma de fluorescencia, si bien con un rendimiento cuántico bajo (en torno al 1%) y es conocida como DOM fluorescente (FDOM). El estudio simultaneo de la CDOM y FDOM combinando espectroscopia de absorción y fluorescencia permite –de forma relativamente simple, rápida y barata– ahondar en el conocimiento de (i) la estructura molecular de la DOM, en aspectos tales como su aromaticidad y peso molecular medio; y (ii) su reactividad biológica y fotoquímica, a través del estudio de la producción, consumo y/o alteración química de diferentes grupos cromóforos y fluoróforos en respuesta a la actividad de los microorganismos y la radiación solar en los océanos.

En esta Tesis se han realizado tanto experimentos de laboratorio como estudios de campo. En una serie de experimentos se ha profundizado en las fuentes microbiológicas de la CDOM y FDOM en condiciones controladas, demostrando que el fitoplancton marino produce un fluoróforo a Ex/Em = 320 nm/410 nm que es consumido por las bacterias marinas, que a su vez producen otro fluoróforo a Ex/Em = 340 nm/440 nm. Estos fluoróforos de naturaleza húmica, conocidos en la literatura especializada como "pico-M" y "pico-C", se consideraban característicos de ecosistemas marinos y continentales, respectivamente. Este trabajo sugiere que la diferenciación tiene más que ver con el tipo de células que las producen: eucariotas o procariotas.

Se ha caracterizado ópticamente DOM aislada por filtración tangencial (> 1 KDa) de diversas aguas naturales, observándose cambios significativos en la aromaticidad y peso molecular medio de las muestras en función de su origen continental o marino y de su exposición a la luz natural antes de ser colectadas. Igualmente, se realizaron experimentos controlados para estudiar la respuesta de estos materiales a la radiación natural, observándose degradación de los fluoróforos de naturaleza húmica "pico-M" y "pico-C" y generación de un fluoróforo de naturaleza protéica, conocido en la literatura como "pico-T".

Finalmente, se ha estudiado la importancia relativa de los procesos de mezcla de masas de agua de origen continental y marino, producción microbiana y degradación fotoquímica sobre la distribución de CDOM y FDOM en dos ecosistemas costeros con distintas condiciones: la Ría de Vigo y la Bahía de Blanes. La Ría de Vigo, sistema eutrófico enclavado en el afloramiento ibérico, se ve afectada periódicamente por episodios de afloramiento y hundimiento, resultando la producción microbiana el proceso dominante en condiciones de afloramiento y la descomposición fotoquímica en condiciones de hundimiento. Por otro lado, la Bahía de Blanes, en el oligotrófico Mediterráneo Nororiental, describe un marcado ciclo estacional dictado por la radiación natural incidente caracterizado por la acumulación estival de cromóforos y fluoróforos que absorben a <300 nm y la descomposición fotoquímica de los que lo hacen a > 300 nm.

Resum

Els oceans alberguen 685 Pg de carboni orgànic, dels quals 662 Pg estan en forma dissolta. L'enorme diversitat de compostos que constitueixen la matèria orgànica dissolta (DOM) i la baixa concentració en què es troba cadascun d'ells, fa de la caracterització química i estructural d'aquest material una àrdua tasca. És per això que menys del 11% de la DOM està identificat a dia d'avui. Una fracció variable de la DOM –entre el 20% a l'oceà obert i el 70% a zones costaneres– absorbeix llum UV i visible, per la qual cosa es coneix com DOM acolorida (CDOM). Part de la CDOM, emet la radiació absorbida en forma de fluorescència, si bé amb un rendiment quàntic baix (entorn del 1%) i és coneguda com DOM fluorescent (FDOM). L'estudi simultanei de la CDOM i la FDOM combinant espectroscòpia d'absorció i fluorescència permet –de forma relativament simple, ràpida i barata– aprofundir en el coneixement de (i) l'estructura molecular de la DOM, en aspectes tals com la seva aromaticitat i el pes molecular mitjà; i (ii) la seva reactivitat biològica i fotoquímica, a través de l'estudi de la producció, consum i/o alteració química de diferents grups cromòfors i fluoròfors en resposta a l'activitat dels microorganismes i la radiació solar en els oceans.

En aquesta Tesi s'han realitzat tant experiments de laboratori com estudis de camp. En una sèrie d'experiments s'ha aprofundit en les fonts microbiològiques de la CDOM i FDOM en condicions controlades, demostrant que el fitoplàncton marí produeix un fluoròfors a $Ex/Em = 320\ nm/410\ nm$ que és consumit pels bacteris marins, que al seu torn produeixen un altre fluoròfors a $Ex/Em = 340\ nm/440\ nm$. Aquests fluoròfors de naturalesa húmica, coneguts en la literatura especialitzada com "pic-M" i "pic-C", es consideraven característics d'ecosistemes marins i continentals, respectivament. Aquest treball suggereix que la diferenciació té més a veure amb el tipus de cèl·lules que les produeixen: eucariotes o procariotes.

S'ha caracteritzat òpticament DOM aïllada per filtració tangencial (> 1 KDa) de diverses aigües naturals, observant-se canvis significatius en la aromaticitat i pes molecular mitjà de les mostres en funció del seu origen continental o marí i de la seva exposició a la llum natural abans de ser mostrejades. Igualment, es van realitzar experiments controlats per estudiar la resposta d'aquests materials a la radiació natural, observant-se degradació dels fluoròfors de naturalesa húmica "pic-M" i "pic-C" i generació d'un fluoròfors de naturalesa protéica, conegut en la literatura com "pic-T".

Finalment, s'ha estudiat la importància relativa dels processos de barreja de masses d'aigua d'origen continental i marí, producció microbiana i degradació fotoquímica sobre la distribució de CDOM i FDOM en dos ecosistemes costaners diferents: la Ria de Vigo i la Badia de Blanes. La Ria de Vigo, sistema eutròfic enclavat en l'aflorament ibèric, es veu afectada periòdicament per episodis d'aflorament i enfonsament, resultant la producció microbiana el procés dominant en condicions d'aflorament i la descomposició fotoquímica en condicions d'enfonsament. D'altra banda, la Badia de Blanes, en el oligotròfic Mediterrani Nord-oriental, descriu un marcat cicle estacional dictat per la radiació natural incident caracteritzat per l'acumulació estival de cromòfors i fluoròfors que absorbeixen a <300 nm i la descomposició fotoquímica dels quals que ho fan a > 300 nm.

Resumo

Os océanos albergan 685 Pg de carbono orgánico, dos que 662 Pg están en forma disolta. A enorme diversidade de compostos que constitúe a materia orgánica disolta (DOM) e a baixa concentración na que se atopa cada un deles, fai da caracterización química e estrutural deste material unha árdua tarefa. É por iso que menos do 11% da DOM está identificada na actualidade. Unha fracción variable da DOM -entre o 20% no océano aberto e o 70% en zonas costeiras- absorbe luz UV e visible, polo que se coñece como DOM coloreada (CDOM). Parte da CDOM, emite a radiación absorbida en forma de fluorescencia, se ben cun rendemento cuántico baixo (en torno ó 1%) e é coñecida como DOM fluorescente (FDOM). O estudo simultáneo da CDOM e FDOM combinando espectroscopía de absorción e fluorescencia permite -de forma relativamente simple, rápida e barata- afondar no coñecemento de (i) a estrutura molecular da DOM, en aspectos tales como a súa aromaticidade e peso molecular medio; e (ii) a súa reactividade biolóxica e fotoquímica, a través do estudo da produción, consumo e/ou alteración química de diferentes grupos cromóforos e fluoróforos en resposta á actividade dos microorganismos e a radiación solar nos océanos.

Nesta Tese realizáronse tanto experimentos de laboratorio coma estudos de campo. Nunha serie de experimentos afondouse nas fontes microbiolóxicas da CDOM e FDOM en condicións controladas, demostrando que o fitoplancto mariño produce un fluoróforo a Ex/Em =320 nm/410 nm que é consumido polas bacterias mariñas, que á súa vez producen outro fluoróforo a Ex/Em =340 nm/440 nm. Estes fluoróforos de natureza húmica, coñecidos na literatura especializada como "pico-M" e "pico-C", considerábanse característicos de ecosistemas mariños e continentais, respectivamente. Este traballo suxire que a diferenciación ten máis que ver co tipo de células que as producen: eucarióticas ou procariotas.

Caracterizouse ópticamente DOM illada por filtración tanxencial (>1 KDa) de diversas augas naturais, observándose cambios significativos na aromaticidade e peso molecular medio das mostras en función da súa orixe continental ou mariña e da súa exposición á luz natural antes de ser colectadas. Igualmente, realizáronse experimentos controlados para estudar a resposta destes materiais á radiación natural, observándose degradación dos fluoróforos de natureza húmica "pico-M" e "pico-C" e xeración dun fluoróforo de natureza proteica, coñecido na literatura como "pico-T".

Finalmente, estudouse a importancia relativa dos procesos de mistura de masas de auga de orixe continental e mariña, produción microbiana e degradación fotoquímica sobre a distribución de CDOM e FDOM en dous ecosistemas costeiros con distintas condicións: a Ría de Vigo e a Baía de Blanes. A Ría de Vigo, sistema eutrófico encravado no afloramento ibérico, vese afectada periodicamente por episodios de afloramento e afundimento, resultando a produción microbiana o proceso dominante en condicións de afloramento e a descomposición fotoquímica en condicións de afundimento. Por outro lado, a Baía de Blanes, no oligotrófico Mediterráneo Nororiental, describe un marcado ciclo estacional ditado pola radiación natural incidente caracterizado pola acumulación estival de cromóforos e fluoróforos que absorben a <300 nm e a descomposición fotoquímica dos que o fan a >300 nm.

Abstract

Oceans store 685 Pg of organic carbon, 662 Pg of which are in the dissolved form. The diversity of compounds that comprise the dissolved organic matter (DOM) pool and the low concentration of each individual compound make the chemical characterization of this material a difficult task. For that reason, less than 11% of the oceanic DOM has been identified. A variable fraction of the DOM –between 20% in the open ocean and 70% in coastal areas– absorbs UV and visible radiation and it is known as coloured DOM (CDOM). A sub-fraction of CDOM emits the absorbed radiation as fluorescence with a low quantum yield (around 1%) and it is called fluorescent DOM (FDOM). The study of the CDOM and FDOM pools, combining absorption and fluorescence spectroscopy, allows to gain knowledge on (i) the molecular structure of DOM (e.g. aromaticity and average molecular weigh) and (ii) its biological and photochemical reactivity in a relatively simple, fast and economic mode. This can be done through the study of the production, utilization and/or chemical transformation of the different chromophores and fluorophores in response to the activity of microorganisms and solar radiation in the oceans.

The work presented in this thesis has involved both laboratory experiments and field studies. A series of experiments have been focused on the microbial sources of CDOM and FDOM. We have demonstrated that marine phytoplankton produces a fluorophore at Ex/Em 320/410 nm that is consumed by marine bacteria which, at the same, time produce another fluorophore at Ex/Em 340/440. These "humic-like" fluorophores, known in the literature as "peak-M" and "peak-C", are considered to be characteristic of marine and continental ecosystems, respectively. Our work suggests that they are more related to the type of cells that produce them: eukaryotic and prokaryotic cells.

DOM isolated by tangential ultrafiltration (> 1 KDa) from different aquatic environments has also been characterized optically. Significant changes were observed in the aromaticity and average molecular weigh of the samples depending on whether they were of continental or marine origin and also on the exposure to sunlight prior to collection. Moreover, controlled experiments were performed in order to study the response of these materials to the natural radiation. These experiments showed degradation of the humic-like fluorophores "peak-M" and "peak-C" and the formation of another protein-like fluorophore, known in literature as "peak-T".

Finally, we have also studied the relative importance of the processes of mixing between water masses of continental and marine origin, microbial production and photochemical degradation on the CDOM and FDOM distribution in two distinct coastal ecosystem: the "Ría de Vigo" and the Blanes Bay. The Ría de Vigo, an eutrophic coastal embayment in the Iberian upwelling system, is periodically affected by downwelling and upwelling events. Microbial production was the dominant process under upwelling conditions while photochemical decomposition prevailed under downwelling conditions. On the other hand, Blanes Bay, in the oligotrophic Northwest Mediterranean Sea, followed a marked seasonal cycle determined by natural radiation characterized by the summer accumulation of chromophores and fluorophores absorbing at < 300 nm and the photochemical decomposition of those absorbing at > 300 nm.

Glossary of relevant terms

$a_{CDOM}(\lambda)$	Absorption coefficient at wavelength λ (in nm)
$a*_{CDOM}(\lambda)$	Carbon specific CDOM absorption coefficient at λ nm
AOU	Apparent oxygen utilization
APER	Apparent percentage of net photosynthetic extracellular release
β	Universal constant for the calculation of the fluorescent quantum yield at 340 nm
BB	Bacterial biomass
CARD-FISH	Catalyzed reporter deposition Fluorescence In Situ Hybridization
CDOM	Coloured dissolved organic matter
DCAA	Dissolved combined amino acids
DOC	Dissolved organic carbon
DOM	Dissolved organic matter
EEM	Excitation Emission Matrix
ENACW	Eastern North Atlantic Central Water
FDOM	Fluorescent dissolved organic matter
$F(340/440)$	FDOM at Ex/Em 340 nm/440 nm or peak-C
$F(320/410)$	FDOM at Ex/Em 320 nm/410 nm or peak-M
$F(280/350)$	FDOM at Ex/Em 280 nm/350 nm or peak-T
$F(250/435)$	FDOM at Ex/Em 250 nm/435 nm or peak-A
HMW-DOM	High Molecular Weight Dissolved Organic Matter
LMW-DOM	Low Molecular Weight Dissolved Organic Matter
Peak-C	FDOM at Ex/Em 340 nm/440 nm
Peak-M	FDOM at Ex/Em 320 nm/410 nm
Peak-T	FDOM at Ex/Em 280 nm/350 nm
Peak-A	FDOM at Ex/Em 250 nm/435 nm
PER	Percentage of net photosynthetic extracellular release
POC	Particulate organic carbon
POM	Particulate organic matter
QSU	Quinine sulphate units
RDOM	Refractory Dissolved Organic Matter
S	Spectral slope
s	Salinity
SUVA(254)	Carbon specific absorption coefficient of CDOM at 254 nm
TDAA	Total dissolved amino acids
TIN	Total inorganic nitrogen
TOC	Total organic carbon
UDOM	Ultrafiltered Dissolved Organic Matter
UDOC	Ultrafiltered Dissolved Organic Carbon
UF	Ultrafiltration
$\Delta a*_{CDOM}(340)$	Residual of $a*_{CDOM}(340)$ with salinity
ΔAOU	Residual of AOU with salinity
$\Delta F*(340/440)$	Residual of C-specific fluorescence with salinity
$\Delta^2 F*(340/440)$	Residual of $\Delta F*(340/440)$ versus $\Delta a*_{CDOM}(340)$
$\Phi(340)$	Fluorescent quantum yield at 340 nm

Introduction
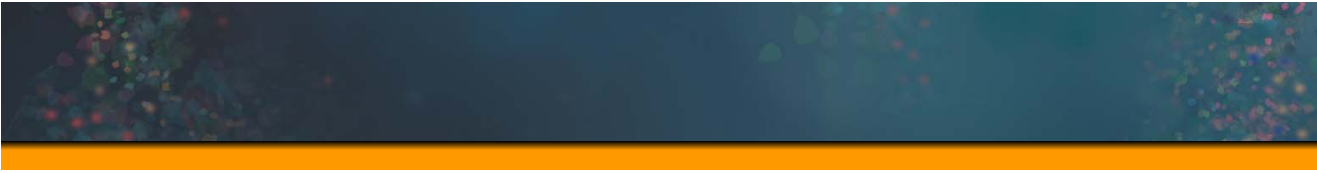
The role of DOC in the marine carbon cycle

The marine carbon cycle is driven by physical, chemical and biological processes which occur in the atmosphere, land and oceans (Sarmiento and Gruber, 2006). These processes determine the total carbon reservoir and also the relative weight of inorganic and organic marine carbon pools. The dynamics of this carbon compartment's net also regulates the capacity of the ocean to dissolve atmospheric CO_2 and consequently its study is crucial to understand the ocean's role in Earth's climate. However, and despite its interest, there is still a lack of knowledge about the chemical composition and transformations of the organic carbon compartments. The present study inquires into some key physical, chemical and biological factors governing the dynamics of the marine dissolved organic carbon (DOC) pool.

There are four major reservoirs of organic matter on the Earth's surface: organic matter in soils and in recently deposited marine sediments, dissolved organic matter (DOM) in seawater and plant biomass on land (Table 1, Hedges et al., 2000). Among them, oceanic dissolved organic matter (DOM) is the most important intermediate in the global carbon cycle (Hansell, 2002) and represents one of the largest and most dynamic reservoirs of reduced carbon on Earth (Hedges, 2002). The global DOC pool is estimated to be 662 Pg C (Hansell et al., 2009). This quantity is comparable to that of all living vegetation on the Earth's continents and the carbon stock of terrestrial biomass (600 Pg C) or the CO_2 accumulated in the atmosphere (720 Pg C, Hedges et al., 1992). Therefore, minor changes in the DOM pool could have a considerable impact on atmospheric CO_2 concentrations and the radiative balance on Earth (Hedges, 2002). Indeed, it has been speculated that a large-scale oxidation of DOM may have prevented a dramatic global glaciation ('snowball earth') in the Neoproterozoic period since DOM mineralization leads to an increase of atmospheric CO_2 enhancing greenhouse warming of the surface of the Earth (Peltier et al., 2007). Since the amounts of carbon in oceanic DOM and atmospheric CO_2 are similar, net oxidation of only 1% of the seawater DOM pool within 1 year would be sufficient to generate a CO_2 flux larger than that produced annually by fossil fuel combustion (Hedges, 2002).

Table 1. Main reservoirs of organic carbon in the Earth (from Hedges et al., 2000).
*Taken from Hansell et al. (2009).

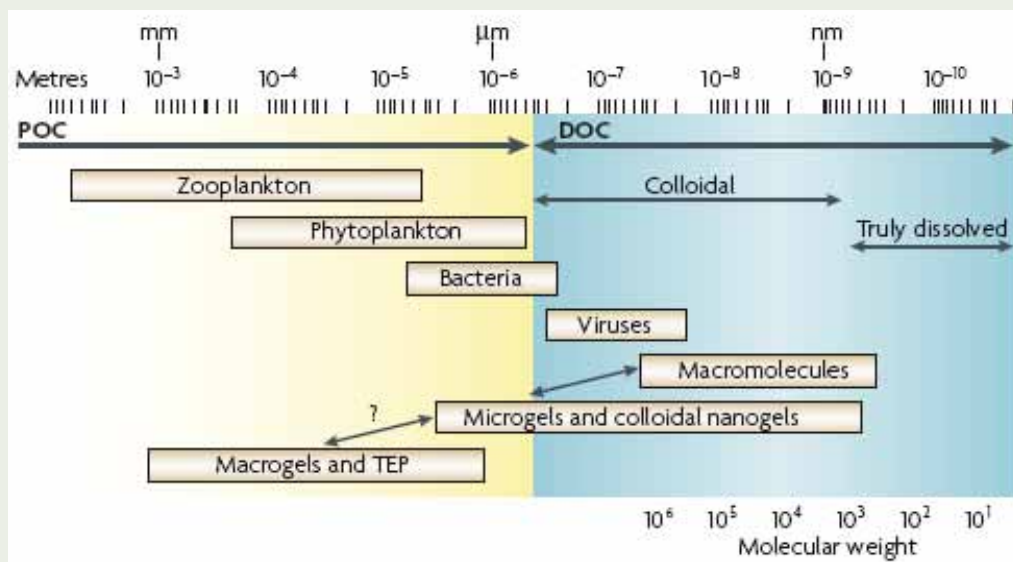| Reservoir	Carbon (Pg)
Soil humus	1600
Recent deposited marine sediments	1000
Dissolved in seawater	662*
Land plants	600
Marine organisms	3

Fig. 1. Size continuum of marine organic matter (from Azam and Malfatti, 2007).

Box 1. In the context of the carbon cycle, OM (organic matter) term refers, often, to its carbon content and, for this reason, the term OC (organic carbon) is, generally, used as synonym of OM (organic matter). Two pools of marine OM have been traditionally distinguished: Dissolved Organic Carbon (DOC), the fraction that passes through 0.2-1.0 µm filters, and Particulate Organic Carbon (POC), the fraction that is retained in these filters (Fig. 1). However, any division based on size is purely operational (Verdugo et al., 2004) since organic matter is formed by a continuum of discrete units ranging in size from small colloids to compounds of a few Da. Nevertheless, this distinction is useful since particles smaller than 1 µm are not prone to sinking (Hedges, 2002) and all living organisms other than viruses and small bacteria fall into the particulate fraction.

Oceans play a key role in controlling the World's climate and regulate atmospheric CO_2 levels through exchange across the air-sea interface. Net oceanic uptake of CO_2 is approximately 2 Pg C y^{-1} (Takahashi et al., 2009). This is feasible thanks to the carbon pump, the sequence of physical and biological processes by which atmospheric CO_2 is pumped to the deep ocean (Fig. 2). There are two main mechanisms that are responsible for this "pumping": the solubility pump and the biological pump, the later includes three types, the "organic carbon pump", the "carbonate pump" (Volk and Hoffert, 1985) and the "microbial carbon pump" (Jiao et al., 2010).

• The solubility pump is an essential process of atmospheric CO_2 sequestration by means of the dissolution of CO_2 at high ocean latitudes and subsequent subduction. This CO_2 is transported in the deep water masses until it reaches the lower latitudes where it warms up and upwells (Raven and Falkowsky, 1999).

• The biological pump:

• The organic carbon pump or soft-tissue pump, in which CO_2, together with inorganic nutrients and light, is used by phytoplankton to convert it to organic carbon, at a rate of about 50 Pg C y^{-1}, is the base of the marine food web (Chisholm, 2000). From this amount about 39 Pg C y^{-1} is respired in the upper layers of the ocean, converted to CO_2 and released back into
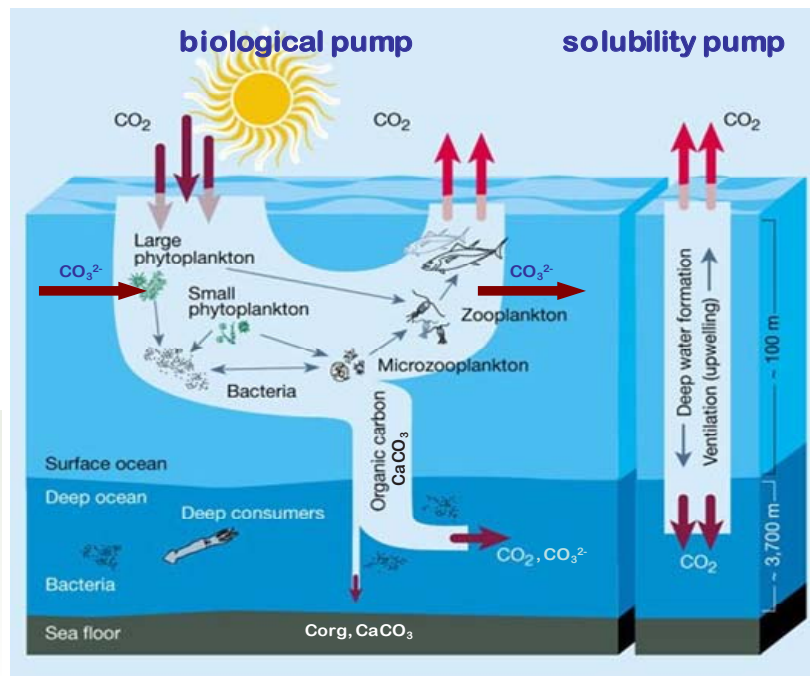

Fig. 2. Scheme of the solubility pump, organic carbon pump and carbonate pump (modified from Chisholm, 2000).

23

the atmosphere (Hansell et al., 2009). Only 11 Pg C y^{-1} reach the ocean interior, mainly in the form of sinking particles (Hansell et al., 2009) but also as dissolved organic matter (DOM) transported by vertical mixing or convection currents. The contribution of DOC to global export in the open ocean is in the range of $20 \pm 10\%$ (Hansell, 2002). Once in the ocean interior, the organic carbon is oxidized back to CO_2 by marine microheterotrophs and it accumulates, out of contact with the atmosphere, travelling with the water masses for decades to hundreds of years (Volk and Hoffert, 1985; Chisholm, 2000). The structure of the food web and the relative abundance of species influence how much CO_2 is pumped into the deep ocean. This structure is dictated largely by the availability of inorganic nutrients such as nitrogen, phosphorus, silicon and iron (Legendre and Le Fèvre, 1991).

• The carbonate pump is part of the biological pump and involves the production and dissolution of $CaCO_3$ by calcifying organisms (e.g. coccolithophores, foraminifers, and pteropods among others).This mechanism transports particulate inorganic carbon to the deep sea, which is formed in the surface ocean. However, whereas the soft-tissue is a CO_2 sink, the carbonate pump acts as a source at short time scales, reducing alkalinity and pH of seawater (Elderfield, 2002). When calcifying organisms die, their $CaCO_3$ structures are transported at depth through gravitational settling and active biotransport (Redfield et al., 1963; Elderfield, 2002). $CaCO_3$ dissolution occurs during this downward transport. Biologically mediated dissolution above the chemical lysocline in acid microenvironments such as zooplankton guts and the interior of flocculates and aggregates is still a matter of debate (e.g. Milliman et al., 1999; Feely et al., 2004; Friis et al., 2006). Dissolution in the CO_3^{2-} under-saturated conditions below the chemical lysocline is also favoured by the high pressures and low temperatures of the deep ocean.

• The microbial carbon pump, recently described by Jiao et al. (2010), includes the mechanisms related to the microbial production of refractory DOM (RDOM) by bacteria, Archaea and viruses and its storage, which occurs throughout the entire water column (Fig. 3). The results presented in chapter I of this thesis will complement the present view, suggesting that not only bacteria, Archaea and viruses but also phytoplankton could contribute to the microbial carbon pump.
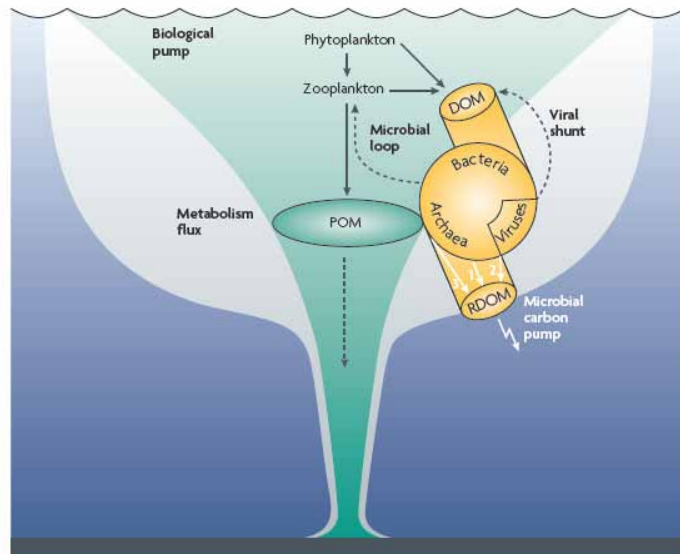
Fig. 3. Microbial Carbon Pump scheme (from Jiao et al., 2010).

DOC can be exported to the ocean interior mainly by means of two different processes:

1)   Convection currents: through this process the DOC accumulates in high concentrations in the mid-ocean gyres (Goldberg et al., 2009) and once there, it can be exported to depths of a few hundred meters by Ekman convergence of surface waters. Most of the DOC transported by this pathway is oxidized to CO_2 and returned for exchange with the atmosphere within months to years (Hansell et al., 2009).

2)   Thermohaline circulation: following this process the DOC can be transported from low to high latitudes and reach greater depth via meridional overturning circulation and ventilation of the ocean interior. In this case the DOC remains sequestered for decades to centuries (i.e., Hopkinson and Vallino, 2005).

Although the DOM export to deep waters is dictated by physical processes, the quantity and quality of DOM exported strongly depend on the biogeochemical transformations of carbon compounds in the photic zone. In this context, the study of these transformations is crucial to gain knowledge on the marine carbon cycle. The present work aims to be a contribution in such direction.

Ocean DOM. Composition and reactivity

The most abundant elements constituting the DOM pool are C, H, O, N and P. The stoichiometric relationship between them is C:N:P = 300:22:1 according to Benner (2002) or 374:27:1 according to (Hopkinson and Vallino, 2005) in surface waters, indicating that DOM is depleted in N and P relative to the average marine phytoplankton composition, C:N:P = 106:16:1 (Redfield et al., 1963). On the other hand, deep water DOM, is even more depleted in N and P than surface water DOM with C:N:P ratios ranging from 444:25:1 (Benner, 2002) to 3511:202:1 (Hopkinson and Vallino, 2005). The combination of these elements give rise to myriads of compounds of which only a small fraction (<11%) are known (Benner, 2002). This gap of knowledge is owing to the difficulty of isolating the variety of different compounds constituting the DOM pool and the low concentrations at which they are found. From the known fraction of DOM, neutral sugars, amino acids, amino sugars and lipids are the main constituents. In the surface ocean, 3.7-10.5% of DOC is constituted by carbohydrates (neutral and amino sugars, 2.4-6.6%), amino acids (1-3%) and lipids (0.2-0.9%). But this proportion reduces to 1.3-3.9% in the deep ocean. Concentrations of free sugars and amino acids are very low in these systems, so most of these biochemicals occur in combined form as oligomers and polymers (Benner, 2003).

Isolation of DOM is, nowadays, the best way to study the molecular composition of this pool. Different techniques are usually applied to separate DOM on basis of the polarity of their compounds (solid phase extraction Amberlite XAD resins and C18 phases) or their molecular size (tangential flow ultrafiltration) (e.g., Mopper et al., 2007). Other isolations methods recently used are osmosis linked to pulse electro-dialysis (Gurtler et al., 2008) or commercially pre-packed chemically modified hydrophilic styrene divinyl benzene polymers (Dittmar et al., 2008). However, among all these techniques, ultrafiltration has the advantage of does not modify the chemical structure of the DOM components. The most used pore size membranes range between 1-3 kDa (e.g. Benner et al., 1997; Rosenstock et al., 2005). Nevertheless, studies concerning the molecular weigh of DOM should to be interpreted carefully since the limits between the high and low molecular weight, depending on the pore size of the membrane used, are not fixed.

DOM is also classified attending to the turnover time of its components into: i) labile pool, with extremely rapid turnover times of a few hours to days; ii) semi-labile pool, with turnover times of month to years; iii) refractory pool, with turnover time of centuries to millennia (Nagata, 2008). Labile DOM in the surface ocean is estimated to be from a few to 10 μmol C kg^{-1} (Hansell, 2002). The occurrence of this labile fraction is supported by the measured uptake rate of bacteria (e.g., Amon and Benner, 1994) and the distribution of DOC within the ocean. The semilabile pool, of the order 10-30 μmol C kg^{-1} in surface waters (Hansell, 2002), is resistant to rapid microbial degradation and its consumption can occur at a location distant from where it was produced, therefore it is considered "exportable" (Nagata, 2008).

An estimation of a global export of DOC to the deep ocean of 1.8 Pg C y^{-1} was made by Hansell et al. (2009). The refractory pool in surface waters is of the order of 40 µmol C kg^{-1} (Hansell et al., 2009). This is the dominant pool in deep waters, with an average age of the order of 4000 years (Bauer, 2002). Its resistance to microbial degradation allows its storage in the ocean.

Distribution, sources and sinks of DOC

Despite its large global inventory, DOC in the open ocean is found at extremely low concentrations. Typical values of DOC are of about 80 µmol C kg^{-1} in the surface ocean dropping until approximately 40 µmol C kg^{-1} in the deep ocean (Fig. 4, Hansell et al., 2009). In the surface, DOC concentrations are higher in low than in high latitudes, although relatively low values are observed in the equatorial regions as compare with the surrounding subtropical gyres, because of the upwelling of DOC-poor subsurface waters. In deep waters the concentrations also change throughout the different oceans: deep waters from the North Atlantic present higher values (~48 µmol C kg^{-1}) than those from
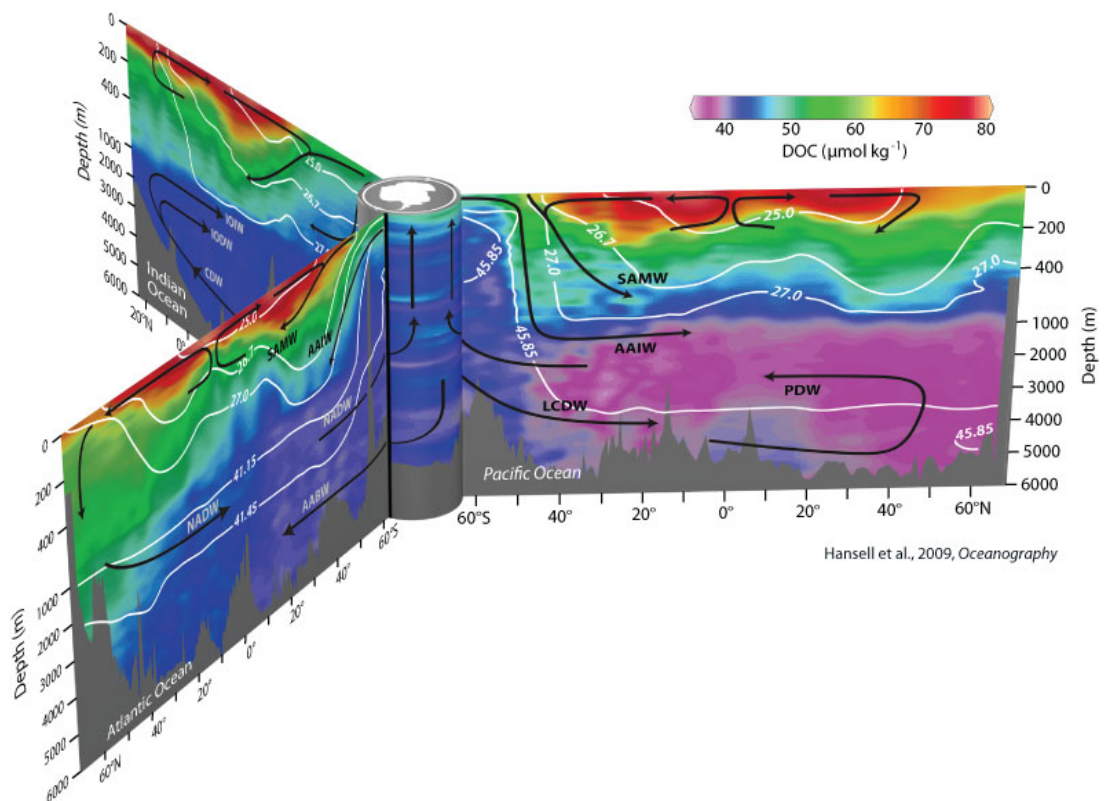

Fig. 4. Distribution of DOC (µmol C kg^{-1}) in the ocean (from Hansell et al., 2009).

the North Pacific (~34 µmol C kg^{-1}) because of the respiration of DOM along the deep ocean circulation pathway (Hansell et al., 2009). In coastal areas, the concentration of DOC is commonly higher than in the open ocean because of continental inputs and enhanced seasonal autochthonous production (Cauwet, 2002). However, DOC concentrations in coastal upwelling regions are comparatively lower because of the low DOC levels of the upwelled waters (Hansell and Carlson, 2001).

There are two main sources of dissolved organic matter in the ocean:

1) Inputs of terrestrial DOM which represents only 2–3% of the total oceanic DOM pool, although it may be a dominant source in the coastal ocean (Opsahl and Benner, 1997).

2) Autochthonous production accounts for more than 95% of total organic matter and is therefore the dominant source. This in situ production is mainly due to phytoplankton primary production (~50 Pg C y^{-1}), as a component of the biological pump. Through some biological processes (e.g. excretion, viral lysis, cell death, grazing, etc…) this DOM can be poured into the ocean where it constitutes the base of bacterioplankton growth and respiration (Azam and Cho, 1987). Bacteria can be grazed by flagellates and the trip of this carbon, through different trophic interactions, to higher trophic levels constitutes the so-called microbial loop (Fig. 5) (Azam et al., 1983). The recognition of the DOM as an important intermediate in the rapid cycling of bioactive elements within the ocean (Pomeroy, 1974; Azam and Hodson, 1977) has
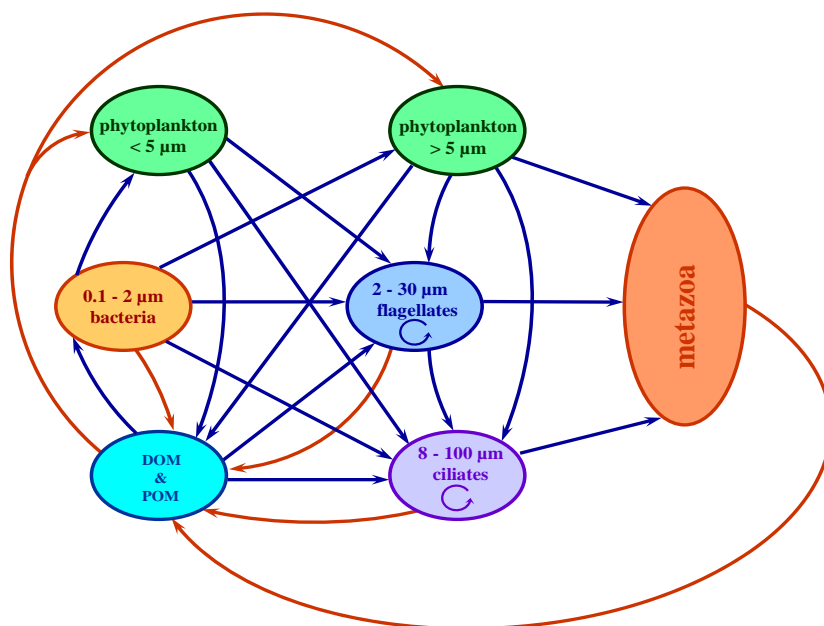

Fig. 5. Microbial loop scheme (from Sherr and Sherr, 1989).

also contributed to increase the awareness of the scientific community in relation to the DOM.

The fraction of organic carbon incorporated into the microbial biomass will be prone to pass to higher trophic levels. However, most of it will be oxidized by heterotrophs releasing CO_2, inorganic nutrients and recalcitrant forms of organic matter. The preservation of reduced carbon is the exception while the mineralization is the rule. The labile fraction only constitutes < 1% of the ocean DOC inventory owing to its very rapid turnover; the major part of DOC in the ocean (94%) is considered refractory DOM (RDOM, Hansell et al., 2009). Part of the RDOM pool is resistant to microbial degradation since its origin (e.g RDOM imported from land) while another portion of this pool is produced in situ as a by-product of different biological (bacterial respiration, viral lysis, grazing and egestion by protists etc.) or photochemical processes (Benner and Biddanda, 1998).

When the RDOM reaches the surface ocean, sunlight radiation, by means of photo-degradation processes, can transform the coloured fraction into labile DOM which becomes available for microbes (Benner and Biddanda, 1998; Obernosterer et al., 2001), re-starting the cycle. Not only labile DOM but also inorganic carbon (CO_2 and CO) and nitrogen are produced by photo-degradation of DOM. It has been estimated that between about 2 to 3% of the oceanic DOM pool is loss by photochemical degradation per year (Moran and Zepp, 1997).

Optical properties of DOM

A fraction of the DOM pool absorbs light at both ultraviolet (UV) and visible wavelengths and this is called coloured dissolved organic matter (CDOM; Coble, 2007) (Fig. 6). CDOM absorption is highest at UV wavelengths and decreases exponentially with increasing wavelength (Jerlov, 1976; Kirk, 1994). CDOM is one of the major absorption components of the ocean (Armstrong and Boalch, 1961). A sub-fraction of CDOM can emit blue fluorescence when irradiated with UV light and this is called fluorescent CDOM (FDOM; Coble 1996, 2007). FDOM can represent between 30% and 70% of the DOC depending on the aquatic system, being found the higher percentages in coastal areas (Chen and Bada, 1992; Chen, 2002; Kowalczuk et al., 2010).

The occurrence of coloured dissolved organic matter was reported for the first time by Kalle (1937) and called "gelbstoff", "gilvin" or "yellow substances". In 1966, the same author used DOM fluorescence to follow the entry of terrestrial organic matter via rivers into coastal waters (Kalle, 1966). Some years before, Weber (1961) devised a technique for elucidating the number of fluorescing compounds, i.e. fluorophores, in complex systems by variation of the excitation and emission wavelength and construction of a matrix of the resulting intensities. This technique allows obtaining the so-called fluorescence excitation-emission matrices (EEMs) and it was applied by Coble et al. (1990)

to characterize DOM. EEMs are obtained by combining the emission spectra collected at different excitation wavelengths into a three dimensional structure (Fig. 7). This technique has become common in aquatic studies from the mid-1990s since it provides a "map" of fluorophores.

Studies focused on CDOM and its characterisation have experienced a boost over the last two decades because of its interest for remote sensing. On the one side, ocean colour remote sensing stimulated the study of the use of CDOM absorption or fluorescence as a proxy for DOC concentration to capture synoptic DOC distributions in fine spatial and temporal resolution (e.g. Del Castillo and Miller, 2008; Kowalczuk et al., 2010). On the other side, CDOM absorption overlaps with that of chlorophyll in the blue region of the electromagnetic spectrum, and consequently corrections for this overlapping are necessary (e.g. Siegel et al., 2002; Coble, 2007).

Fluorescence techniques are frequently applied to distinguish between two main groups of fluorophores, depending of their excitation and emission (Ex/Em) wavelengths. One group, protein-like substances, fluoresces at wavelengths characteristic of the aromatic amino acids tryptophan (Ex/Em 280 nm/350 nm, peak-T) and tyrosine (Ex/Em 275 nm/305 nm, peak-B, Coble, 1996). However, fluorescence of peak-B is strongly affected by the Raman scattering band of water and it is not always observed. Moreover, its fluorescence can be quenched by that of tryptophan when they are being part of the same protein, reducing its intensity (Lakowicz, 2006). The other fluorescent amino acid, phenylalanine, is
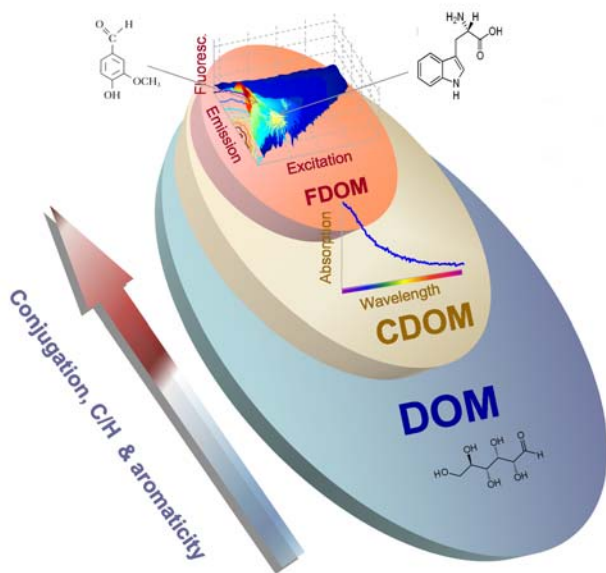
Fig. 6. Scheme of the colored and fluorescent DOM (CDOM and FDOM, respectively) fractions of the total DOM pool. The arrow indicates increasing aromaticity, conjugation, and carbon to hydrogen (C/H) ratio. Over the CDOM and FDOM fractions, examples of CDOM absorption spectra and excitation-emission matrices, respectively, are shown. Structure of tryptophan, a natural amino acid, and vanillin, a constituent of lignin, are shown as examples of fluorescent CDOM. The grey lines indicate the position of their respective fluorescence excitation-emission peaks (from Stedmon and Álvarez-Salgado, 2011).

30

generally present in much higher concentration than the other two (Yamashita and Tanoue, 2003) but its quantum yield in proteins is small (~0.03) and it can be quenched by tyrosine if it is bound in the same protein (Lakowicz, 2006). Phenylalanine has been identified by fluorescence only once in seawater (Jørgensen et al., 2011). The fluorescence of the protein-like group is thought to be due to amino acids being part of proteins as well as to free forms. The position of the amino acids in the proteins determines the intensity and Ex/Em wavelengths of the protein-like fluorescence peaks (Lakowicz, 2006). Protein-like fluorescence has also seen being part of microorganisms, as bacteria and phytoplankton (Determann et al., 1998). Some fractions of the protein-like compounds are taken more readily than others (Stedmon and Markager, 2005) suggesting different bioavailability. Another group fluoresces at pairs of wavelength characteristic of humic-like substances (Ex/Em 250/435 nm for peak-A, Ex/Em 320/410 nm for peak-M and Ex/Em 340/440 nm for peak-C, Fig. 7). Peak-C is called terrestrial humic-like peak because natural samples with a dominant terrestrial origin have been found to present a main peak at those wavelengths. On the other hand, peak-M, called marine humic-like peak, was found to be the main peak in natural marine samples (Coble et al., 1998). However, this view about the sources of the humic-like fluorophores should be revisited after the results of this thesis described in chapters I and II, where we analyse the production of FDOM by marine phytoplankton and bacteria. Some compounds likely to be responsible for the fluorescence of the humic-like substances are tannins, lignin, polyphenols and melanins (Coble, 2007). Moreover, quinone moieties have also been suggested to contribute to fluorescent humic-like substances (Cory and McKnight, 2005). Multivariate data analysis methods have been recently applied to analyse the large information contained in the EEMs. The most used are principal component analysis (PCA, Boehme et al., 2004) and parallel analysis factor (PARAFAC). The last one has been reported to be more adequate to be applied to the complex nature of the seawater EEMs than the former (Stedmon et al., 2003). PARAFAC can take overlapping
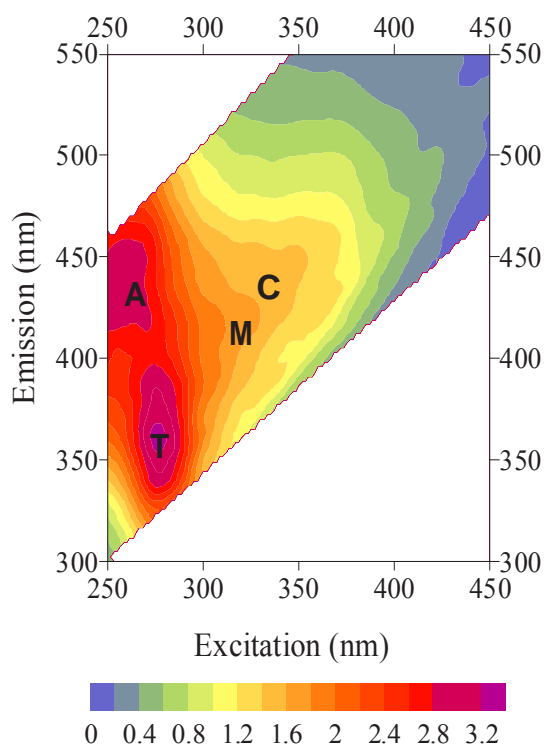

Fig. 7. Excitation-emission matrix of a surface seawater sample coming from Blanes Bay (NW Mediterranean Sea) expressed in quinine sulphate units (QSU). The position of peaks A, C, M and T is shown.

31

fluorescence spectra and decompose them into broadly defined fluorescence components. This has allowed going in depth in the study of the different fluorophores contributing to the FDOM.

Although it is not possible to generalize since there are few studies reporting the fluorescence of the different molecular fractions of DOM, it seems that protein-like substances are more abundant in the low molecular weight (LMW) fraction. This fraction corresponds to DOM with < 500 Da for Huguet et al. (2010) or < 5 kDa for Yamashita and Tanoue (2004). This agrees with the evidence that the highest concentrations of total hydrolysable amino acids (THAA) were found in the LMW fractions for fresh and seawater (Wu et al., 2003; Yamashita and Tanoue, 2004). However, the predominance of the fluorescent humic-like peaks is found in different fractions depending on the origin of the water sample. The highest fluorescence intensity of peak-M has been found in the LMW fraction, i.e. < 500 Da (Huguet et al., 2010) for estuarine samples and < 5 kDa for seawater samples (Yamashita and Tanoue, 2004). The fluorescence of peak-C was found to be predominant in the high molecular weight (HMW) fraction (> 1 kDa) in samples from freshwater (Belzile and Guo, 2006) but in the LMW fraction (< 5 kDa) for fresh and sea water samples (Wu et al., 2003; Yamashita and Tanoue, 2004), likely in the intermediate fraction between 500 Da and 1 kDa (Huguet et al., 2010). In this thesis, the optical properties and chemical characteristics of ultrafiltered DOM (> 1 kDa) from contrasting aquatic environment are examined to characterise the origin and biogeochemical transformations that they experienced in the environment before been collected (Chapter III).

Sources and sinks of CDOM

The main sources of CDOM in marine systems are: (i) continental runoff that transports DOM primarily formed and reworked from soils (Coble, 2007); (ii) abiotic condensation and transformation of biopolymers, e.g. photo-oxidized polyunsaturated lipids previously released into the water column by plankton (Kieber et al., 1997); and (iii) in situ biological production (Yentsch and Reichert, 1961; Kramer and Herndl, 2004). The in situ production of humic-like fluorescent CDOM in the ocean interior is 5-fold that of the terrestrial inputs (Yamashita and Tanoue, 2008). Even if in coastal areas, more affected by freshwater discharges, terrestrial inputs will gain importance, net fluorescent CDOM in situ production can exceed that of land runoff inputs. For example, in the eutrophic embayment of the Ria de Vigo (NW Spain) the in situ production of humic-like FDOM was 3-fold the continental input (Nieto-Cid et al., 2005). Within the autochthonous sources, CDOM can be produced as a by-product of microbial metabolism since bacterioplankton release CDOM during active growth (Kramer and Herndl, 2004). Furthermore, its production by copepods, krill, and other planktonic organisms has also been demonstrated in recent studies (Steinberg et al., 2004; Ortega-Retuerta et al., 2009). However, the production of CDOM by phytoplankton has been a controversial topic and for that reason it is one of the subjects that will be dealt with in chapter I of this thesis. Moreover, since bacteria and phytoplankton together represent a high percentage of marine plankton biomass (58-66%; Gasol et al., 1997), the study

of the quality and quantity of fluorescent DOM produced by each of them is crucial to better understand the dynamics of these coloured substances. This subject will be addressed in chapters I and II.

The main sink of CDOM is photodegradation, a key process to consider when examining the dynamics of DOM in aquatic systems (Moran et al., 2000). This process has been studied in chapter III of this thesis, where it is shown that changes of the optical properties of CDOM caused by sunlight depended on the origin of the organic matter.

Role of CDOM in the marine environment

CDOM can control both the intensity and spectral quality of light throughout the water column (Jerlov, 1976; Blough and Del Vecchio, 2002), either stimulating or hindering primary production and temperature stratification (e.g. Mopper and Kieber, 2002). A high concentration of CDOM can reduce photosynthetic available radiation reducing primary production in regions where light is limiting (Arrigo and Brown, 1996). On the other hand, it can also decrease harmful UV effects on phytoplankton cells as well as on bacterioplankton deoxyribonucleic acid (DNA) and physiology (Herndl et al., 1993). Another role of CDOM is the potential contribution of its refractory fraction to the sequestration of anthropogenic carbon by the already mentioned "microbial carbon pump" mechanism. Due to the bio-refractory character of this CDOM, its constituting carbon is thought to remain unavailable for hundreds to thousands of years when these substances are transported away from the sunlight. It should be mentioned that not all the refractory carbon is coloured. Another important role of CDOM is its capacity for metal scavenging by formation of complexes. Dissolved free and combined amino acids and humic substances are among the major biogenic CDOM compounds that act as metal ligands in seawater (Midorikawa and Tanoue, 1998; Lorenzo et al., 2007). This characteristic can be beneficial to the organisms when trace metals present in the medium reach toxic concentrations (Midorikawa and Tanoue, 1998). These metals can be later released into the marine environment during DOM mineralization. The rate of CDOM photodegradation is catalytically influenced by the presence of iron (Gao and Zepp, 1998). Furthermore, in rain-derived waters CDOM is likely to influence multiple atmospheric processes in addition to spectral attenuation of solar radiation such as the free radical and trace metal chemistry of the troposphere (Kieber et al., 2006).

CDOM distribution in marine systems

In general, coastal areas subject to important river inputs, exhibit high levels of CDOM. In absence of significant in situ sources and sinks or a complex mixing between water masses, CDOM absorption is inversely correlated with salinity presenting a conservative mixing behaviour. However, coastal margins not affected by river inputs generally show low values of $a_{CDOM}(355)$ (< 0.25 m^{-1}) and this is not or slightly correlated with salinity (Blough and Del Vecchio, 2002). General vertical

distribution of CDOM in the open ocean presents lower values at the surface than at the deep ocean due to photobleaching in the euphotic layer, and the highest values in the main thermocline (Nelson et al., 2010). In surface waters, high values have been registered in the subarctic zones ($a_{CDOM}(325) > 0.17$ m^{-1}), intermediate values in the Equatorial upwelling region and Southern Ocean ($a_{CDOM}(325) \sim 0.1$-0.15 m^{-1}) and low values in the sub-tropical gyres ($a_{CDOM}(325) < 0.05$ m^{-1}, Nelson et al., 2010). The combination of deep mixed layers and reduced light doses in the high latitudes compared to the tropics and subtropics is the reason behind the increasing concentrations of CDOM toward the poles (Nelson and Siegel, 2002). Vertical gradients of CDOM across the main thermocline are greater in the North Pacific and North Indian Oceans ($a_{CDOM}(325) \sim 0.22$ m^{-1}), than in the Atlantic basins (Nelson et al., 2010).

High values of CDOM in winter and low ones in summer owing to photo-degradation correspond to the typical seasonal distribution of CDOM in surface waters of temperate ecosystems (Nelson et al., 1998). In chapters IV and V of this thesis we looks at the seasonal and spatial distribution of CDOM in two temperate coastal systems with contrasting trophic status and different predominance of biogeochemical processes affecting its variability.

In the particular case of the fluorescent fraction of CDOM, protein-like compounds are present at high concentrations in the surface layer (0-200 m), decreasing in the mesopelagic layer (200-1000 m) and they are at lower concentrations in the bathypelagic layer (> 1000 m) (Mopper and Schultz, 1993; Yamashita and Tanoue, 2003). Humic-like substances are widely distributed throughout the ocean. They present low concentrations in the surface layer, increasing with depth (Chen and Bada, 1992; Yamashita et al., 2007). This profile is explained by the photosensitivity of these compounds to UV and visible radiation which bleach them in the surface layer (e.g. Chen and Bada, 1992). Peak-C and peak-M fluorescence are ubiquitous oceanic humic-like signal (Jørgensen et al., 2011). Their fluorescence intensities are relatively high in surface waters of the North Atlantic and in upwelling regions (Jørgensen et al., 2011).

Optical footprints as a tool to characterize DOM and to investigate sources and transformations of DOM

Biochemical characteristics of DOM can be linked to its optical properties (Stedmon et al., 2003; Hernes et al., 2009). Absorption coefficients and spectral slopes have proven to be good proxies to some characteristics of the molecular structure of CDOM. For example the absorption coefficient ratio at 254 nm/365 nm, $a_{CDOM}(254/365)$, has been used in freshwater research as an index of the average molecular weight of DOM (Dahlén et al., 1996; Engelhaupt et al., 2003) and the C-specific absorption coefficient at 254 nm, $a^*_{CDOM}(254)$, has worked as a reliable aromaticity index (Weishaar et al., 2003). Absorption spectral slopes, obtained by fitting the absorption spectra to an exponential equation, have been used as tracers for the chemical structure and origin of DOM in aquatic environments (Nelson

et al., 2004; Helms et al., 2008). They also allow distinguishing possible sources and sinks of CDOM at different depths (Bracchini et al., 2010) and they seem to be independent of CDOM concentration (Helms et al., 2008). The information of fluorescence excitation-emission matrices (EEMs) and single Ex/Em pair measurements have been used to identify terrestrial, marine and anthropogenic components of DOM in field studies (e.g. Coble, 1996; Cory and McKnight, 2005; Stedmon and Markager, 2005). Fluorescence also provides reliable information about the redox state, quality (humic- or protein-like materials) and biological and photochemical reactivity of DOM (Miller et al., 2006; Fellman et al., 2010). Fluorescence and absorbance measurements can also be combined through the fluorescence – absorption coefficient ratio, i.e. the fluorescence quantum yield, to gain knowledge on the chemical structure and the biogeochemical processes experienced by DOM (Birks, 1970; Turro, 1991; Green and Blough, 1994). Chapters IV and V of this thesis show how the optical properties of CDOM can help to quantify the relative importance of physical, photochemical and biological processes in coastal systems.

Aims of the thesis

The general aim or this thesis is to gain knowledge on the chemical composition, molecular structure and biogeochemical transformations experienced by natural DOM through its optical properties combining laboratory and field studies. The specific objectives are the following:

1) To characterize the DOM excreted by marine phytoplankton and bacterioplankton to test the hypotheses: a) Phytoplankton can produce FDOM and b) this FDOM is optically different from that produced by bacterioplankton (chapters I and II).

2) To analyse the optical properties of dissolved organic matter isolated from different geographical areas and its response to natural light exposure to check the following hypothesis: the provenance and transformation experienced by DOM are detectable observing the imprint left in the optical signals of DOM (chapter III).

3) To apply the knowledge gained in laboratory experiments to field studies of the optical properties of DOM. The hypothesis is that it is possible to discern, using DOM fluorescence and absorption characteristics, the relative importance of the physical and biogeochemical processes that modulate DOM dynamics in contrasting temperate coastal systems (chapters IV and V).

References

Amon, R.M.W., Benner, R., 1994. Rapid cycling of high-molecular-weight dissolved organic matter in the ocean. Nature 369, 549-552.

Armstrong, F.A.J., Boalch, G.T., 1961. The ultra-violet absorption of sea water. J. Mar. Biol. Ass. U. K. 41, 591-597.

Arrigo, K.R., Brown, C.W., 1996. Impact of chromophoric dissolved organic matter on UV inhibition of primary productivity in the sea. Mar. Ecol. Prog. Ser., 140, 207-216.

Azam, F., Hodson, R.E., 1977. Size distribution and activity of marine microheterotrophs. Limnol. Oceanogr. 22, 492-501.

Azam, F., Fenchel, T., Field, J. G., Gray, J.S., Meyer-Reil, L. A., Thingstad, F., 1983. The ecological role of water-column microbes in the sea. Mar.e Ecol. Prog. Ser., 10, 257-263.

Azam, F., Cho, B.C. 1987. Bacterial utilization of organic matter in the sea. In: Ecology of microbial communities. Fletcher, M., T.R.G. Gray, J.G. Jones (Eds). Cambridge University Press. Cambridge. 261-281.

Azam, F., Malfatti, F., 2007. Microbial structuring of marine ecosystems. Nat. Rev. Micro., 5, 782-791.

Bauer, J.E., 2002. Carbon isotopic composition of DOM. In: Hansell, D., Carlson, C. (Eds.), 2002. Biogeochemistry of marine dissolved organic matter. Academic Press, San Diego, pp. 405.

Belzile, C., Guo, L., 2006. Optical properties of low molecular weight and colloidal organic matter: Application of the ultrafiltration permeation model to DOM absorption and fluorescence. Mar. Chem. 98, 183-196.

Benner, R., Biddanda, B., Black, B., McCarthy, M., 1997. Abundance, size distribution, and stable carbon and nitrogen isotopic compositions of marine organic matter isolated by tangential-flow ultrafiltration. Mar. Chem. 57, 243-263.

Introduction

Benner, R., Biddanda, B., 1998. Photochemical transformations of surface and deep marine dissolved organic matter: effects on bacterial growth. Limnol. Oceanogr. 43, 1373-1378.

Benner, R., 2002. Chemical composition and reactivity. In: Hansell, D., Carlson, C. (Eds), Biogeochemistry of marine dissolved organic matter. Academic Press, San Diego, pp. 59-90.

Benner, R., 2003. Molecular indicators of the bioavailability of dissolved organic matter. In: S. Findlay and R. Sinsabaugh (Ed.), Aquatic ecosystems: Interactivity of dissolved organic matter. Academic Press, New York.

Birks, J.B., 1970. Photophysics of aromatic molecules. Willey-Interscience, London.

Blough, N.V., Del Vecchio, R., 2002. Chromophoric DOM in the coastal environment. In: Hansell, D., Carlson, C. (Eds.), Biogeochemistry of marine dissolved organic matter. Academic Press, New York, pp. 509–546.

Boehme, J., Coble, P., Conmy, R., Stovall-Leonard, A., 2004. Examining CDOM fluorescence variability using principal component analysis: seasonal and regional modeling of three-dimensional fluorescence in the Gulf of Mexico. Mar. Chem. 89, 3-14.

Bracchini, L., Tognazzi, A., Dattilo, A., Decembrini, F., Rossi, C., Loiselle, S., 2010. Sensitivity analysis of CDOM spectral slope in artificial and natural samples: an application in the central eastern Mediterranean Basin. Aquatic Sciences - Research Across Boundaries, 72, 485-498.

Cauwet, G., Déliat, G., Krastev, A., Shtereva, G., Becquevort, S., Lancelot, C., Momzikoff, A., Saliot, A., Cociasu, A., Popaet, L., 2002. Seasonal DOC accumulation in the Black Sea: a regional explanation for a general mechanism. Mar. Chem. 79, 193-205.

Coble, P.G., Green, S.A., Blough, N.V., Gagosian, R.B., 1990. Characterization of dissolved organic matter in the Black Sea by fluorescence spectroscopy. Nature, 348, 432-435.

Coble, P.G., 1996. Characterization of marine and terrestrial DOM in seawater using excitation-emission matrix spectroscopy. Mar. Chem. 51, 325-346.

Coble, P.G., Del Castillo, C.E., Avril, B., 1998. Distribution and optical properties of CDOM in the Arabian Sea during the 1995 Southwest Monsoon. Deep-Sea Res. II, 45, 2195-2223.

Coble, P.G., 2007. Marine optical biogeochemistry: the chemistry of ocean color. Chem. Rev. 107, 402-418.

Cory, R. M., D. M. McKnight. 2005. Fluorescence spectroscopy reveals ubiquitous presence of oxidized and reduced quinones in dissolved organic matter. Environ. Sci. Technol. 39:8142–49.

Chen, R.F., Bada, J.L., 1992. The fluorescence of dissolved organic matter in seawater. Mar. Chem. 37, 191-221.

Chen, R.F., Zhang, Y., Vlahos, P., Rudnick, S.M., 2002. The fluorescence of dissolved organic matter in the Mid-Atlantic Bight. Deep Sea Res. Part II 49, 4439-4459.

Chisholm, S.W., 2000. Oceanography: Stirring times in the Southern Ocean. Nature, 407, 685-687.

Dahlén, J., Bertilsson, S., Pettersson, C., 1996. Effects of UV-A irradiation on dissolved organic matter in humic surface waters. Environ. Int. 22, 501-506.

Del Castillo, C.E., Miller, R.L., 2008. On the use of ocean color remote sensing to measure the transport of dissolved organic carbon by the Mississippi River Plume. Remote Sensing of Environment, 112, 836-844.

Determann, S., Lobbes, J.M., Reuter, R., Rullkötter, J., 1998. Ultraviolet fluorescence excitation and emission spectroscopy of marine algae and bacteria. Mar. Chem. 62, 137-156.

Dittmar, T., Koch, B., Hertkorn, N., Kattner, G., 2008. A simple and efficient method for the solid-phase extraction of dissolved organic matter (SPE-DOM) from seawater. Limnol. Oceanogr.: Methods 6, 230-235.

Elderfield, H., 2002. Carbonate Mysteries. Science, 296, 1618-1621.

Engelhaupt, E., Bianchi, T.S., Wetzel, R.G., Tarr, M.A., 2003. Photochemical transformations and bacterial utilization of high-molecular-weight dissolved organic carbon in a southern Louisiana tidal stream (Bayou Trepagnier). Biogeochemistry 62, 39-58.

Feely, R.A., Sabine, C.L., Lee, K., Berelson, W., Kleypas, J., Fabry, V.J., Millero, F.J., Impact of anthropogenic CO_2 on the $CaCO_3$ system in the oceans, Science 305, 362–366, 2004.

Fellman, J.B., Hood, E., Spencer, R.G.M., 2010. Fluorescence spectroscopy opens new windows into dissolved organic matter dynamics in freshwater ecosystems: A review. Limnol. Oceanogr, 55, 2452-2462.

Introduction

Friis, K., Najjar, R.G., Follows, M.J., Dutkiewicz, S., 2006. Possible overestimation of shallow-depth calcium carbonate dissolution in the ocean. Global Biogeochemical Cycles, 20, GB4019, doi:10.1029/2006GB002727.

Gao, H., Zepp, R.G., 1998. Factors influencing photoreactions of dissolved organic matter in a coastal river of the Southeastern United States. Environmental Science & Technology, 32, 2940-2946.

Gasol, J. M., del Giorgio, P.A., Duarte, C.M., 1997. Biomass distribution in marine planktonic communities. Limnol. Oceanogr. 42, 1353-1363.

Goldberg, S.J., Carlson, C.A., Hansell, D.A., Nelson, N.B., Siegel, D.A., 2009. Temporal dynamics of dissolved combined neutral sugars and the quality of dissolved organic matter in the Northwestern Sargasso Sea. Deep Sea Res. Part I 56, 672-685.

Green, S.A., Blough, N.V., 1994. Optical absorption and fluorescence properties of chromophoric dissolved organic matter in natural waters. Limnol. Oceanogr, 39, 1903-1916.

Gurtler, B.K., Vetter, T.A., Perdue, E.M., Ingall, E., Koprivnjak, J.K., Pfromm, P.H., 2008. Combining reverse osmosis and pulsed electrical current electrodialysis for improved recovery of dissolved organic matter from seawater. J. Membr. Sci. 323, 328-336.

Hansell, D.A., 2002. DOC in the global ocean carbon cycle. In: Hansell, D., Carlson, C. (Eds.), 2002. Biogeochemistry of marine dissolved organic matter. Academic Press, San Diego, pp.685.

Hansell, D.A., Carlson, C.A., 2001. Marine dissolved organic matter and the carbon cycle. Oceanography, 14, 41-49.

Hansell, D.A., Carlson, C.A., Repeta, D.J., Reiner, S., 2009. Dissolved organic matter in the ocean. Oceanography, 22, 202-211.

Hedges, J.I., Hatcher, P.G., Ertel, J.R., Meyers-Schulte, K.J., 1992. A comparison of dissolved humic substances from seawater with Amazon River counterparts by 13C-NMR spectrometry. Geochim. Cosmochim.Ac. 56, 1753-1757.

Hedges, J.I., Eglinton, G., Hatcher, P.G., Kirchman, D.L., Arnosti, C., Derenne, S., Evershed, R.P., Kögel-Knabner, I., de Leeuw, J.W., Littke, R., Michaelis, W., Rullkötter, J., 2000. The molecularly-uncharacterized component of nonliving organic matter in natural environments. Org. Geochem. 31, 945-958.

Hedges, J.I., 2002. Why dissolved organic matter. In: Hansell, D., Carlson, C. (Eds.), 2002. Biogeochemistry of marine dissolved organic matter. Academic Press, San Diego, pp. 1-33.

Helms, J.R., Stubbins, A., Ritchie, J.D., Minor, E.C., Kieber, D.J., Mopper, K., 2008. Absorption spectral slopes and slope ratios as indicators of molecular weight, source, and photobleaching of chromophoric dissolved organic matter. Limnol. Oceanogr, 53, 955-969.

Herndl, G.J., Muller-Niklas, G., Frick, J., 1993. Major role of ultraviolet-B in controlling bacterioplankton growth in the surface layer of the ocean. Nature 361, 717-719.

Hernes, P.J., Bergamaschi, B.A., Eckard, R.S., Spencer, R.G.M., 2009. Fluorescence-based proxies for lignin in freshwater dissolved organic matter. J. Geophys. Res. 114, G00F03, doi:10.1029/2009JG000938.

Hopkinson, C.S., Vallino, J.J., 2005. Efficient export of carbon to the deep ocean through dissolved organic matter. Nature 433, 142-145.

Huguet, A., Vacher, L., Saubusse, S., Etcheber, H., Abril, G., Relexans, S., Ibalot, F., Parlanti, E., 2010. New insights into the size distribution of fluorescent dissolved organic matter in estuarine waters. Org. Geochem. 41, 595-610.

Jerlov, N.G., 1976. Marine optics. Elsevier, New York. 231.

Jiao, N., Herndl, G.J., Hansell, D.A., Benner, R., Kattner, G., Wilhelm, S.W., Kirchman, D.L., Weinbauer, M.G., Luo, T., Chen, F., Azam, F., 2010. Microbial production of recalcitrant dissolved organic matter: long-term carbon storage in the global ocean. Nat Rev Micro, 8, 593-599.

Jørgensen, L., Stedmon, C.A., Kragh, T., Markager, S., Middelboe, M., Søndergaard, M., 2011. Global trends in the fluorescence characteristics and distribution of marine dissolved organic matter. Mar. Chem. In Press, Corrected Proof.

Kalle, K., 1937. Nahrstoff Untersuchungen als Hydrographisehes Hilfsmittel zur Unterseheidung von Wasserkurpern. Ann. Hydrogr. Berlin 65, 276.

Kalle, K., 1966. The problem of the gelbstoff in the sea. Oceanogr. Mar. Biol. Ann. Rev. 4, 91-104.

Kieber, R.J., Hydro, L.H., Seaton, P.J., 1997. Photooxidation of triglycerides and fatty acids in seawater: implication toward the formation of marine humic substances. Limnol. Oceanogr. 42, 1454-1462.

Introduction

Kieber, R.J., Whitehead, R.F., Reid, S.N., Willey, J.D., Seaton, P.J., 2006. Chromophoric dissolved organic matter (CDOM) in rainwater, southeastern North Carolina, USA. J. Atmos. Chem. 54, 21-41.

Kirk, J.T.O., 1994. Light and photosynthesis in aquatic ecosystems, 2nd ed. Cambridge University Press, New York. 509.

Kowalczuk, P., Cooper, W.J., Durako, M.J., Kahn, A.E., Gonsior, M., Young, H., 2010. Characterization of dissolved organic matter fluorescence in the South Atlantic Bight with use of PARAFAC model: Relationships between fluorescence and its components, absorption coefficients and organic carbon concentrations. Mar. Chem. 118, 22-36.

Kramer, G.D., Herndl, G.J., 2004. Photo- and bioreactivity of chromophoric dissolved organic matter produced by marine bacterioplankton. Aquat. Microb. Ecol. 36, 239-246.

Lakowic, J.R., 2006. Principles of fluorescence spectroscopy. Springer.

Legendre, L., Le Fèvre, J., 1991. From individual plankton cells to pelagic marine ecosystems and to global biogeochemical cycles. In: Demmers, S. (Ed.), Particle analysis in oceanography. Springer, Heidelberg, Germany.

Lorenzo, J.I., Nieto-Cid, M., Álvarez-Salgado, X.A., Pérez, P., Beiras, R., 2007. Contrasting complexing capacity of dissolved organic matter produced during the onset, development and decay of a simulated bloom of the marine diatom Skeletonema costatum. Mar. Chem. 103, 61-75.

Midorikawa, T., Tanoue, E., 1998. Molecular masses and chromophoric properties of dissolved organic ligands for copper(II) in oceanic water. Mar.e Chemi. 62, 219-239.

Miller, M., McKnight, D., Cory, R., Williams, M., Runkel, R., 2006. Hyporheic exchange and fulvic acid redox reactions in an Alpine stream/wetland ecosystem, Colorado Front Range. Environmental science technology American Chem. Soc. 40, 5943-5949.

Milliman, J.D., Troy, P.J., Balch, W.M., Adams, A.K., Li, Y.H., Mackenzie, F.T., 1999. Biologically mediated dissolution of calcium carbonate above the chemical lysocline? Deep Sea Res. Part I: Oceanographic Research Papers, 46, 1653-1669.

Mopper, K., Schultz, C.A., 1993. Fluorescence as a possible tool for studying the nature and water column distribution of DOC components. Mar. Chem. 41, 229-238 229.

Mopper, K., Kieber, D.J., 2002. Photochemistry and the cycling of carbon, sulfur, nitrogen and phosphorus. In: Hansell, D.A., Carlson, C.A. (Eds.), Biogeochemistry of Marine Dissolved Organic Matter. Academic Press, New York, pp. 455–507.

Mopper, K., Stubbins, A., Ritchie, J.D., Bialk, H.M., Hatcher, P.G., 2007. Advanced instrumental approaches for characterization of marine dissolved organic matter: extraction techniques, mass spectrometry, and nuclear magnetic resonance spectroscopy. Chem. Rev. 107, 419-442.

Moran, M.A., Zepp, R.G., 1997. Role of photoreactions in the formation of biologically labile compounds from dissolved organic matter. Limnol. Oceanogr. 42, 1307-1316.

Moran, M.A., Sheldon, W.M., Zepp, R.G., 2000. Carbon loss and optical property changes during long-term photochemical and biological degradation of estuarine dissolved organic matter. Limnol. Oceanogr. 45, 1254-1264.

Nagata, T., 2008. Organic matter-bacteria interactions in seawater. In: Kirchman, D.L. (Ed.), Microbial ecology in the oceans. Wiley-Blackwell, Hoboken, pp. 207.

Nelson, N.B., Siegel, D.A., Michaels, A.F., 1998. Seasonal dynamics of colored dissolved material in the Sargasso Sea. Deep Sea Res. Part I: Oceanographic Research Papers 45, 931-957.

Nelson, N.B., Siegel, D.A., 2002. Chromophoric DOM in the open ocean. In: Hansell, D., Carlson, C. (Eds.), 2002. Biogeochemistry of marine dissolved organic matter. Academic Press, San Diego, pp. 547.

Nelson, N.B., Craig, A.C., Steinberg, D.K., 2004. Production of chromophoric dissolved organic matter by Sargasso Sea microbes. Mar. Chem., 89, 273- 287.

Nelson, N.B., Siegel, D.A., Carlson, C.A., Swan, C.M., 2010. Tracing global biogeochemical cycles and meridional overturning circulation using chromophoric dissolved organic matter. Geophys. Res. Let. 37, L03610.

Nieto-Cid, M., Álvarez-Salgado, X.A., Gago, J., Pérez, F.F., 2005. DOM fluorescence, a tracer for biogeochemical processes in a coastal upwelling system (NW Iberian Peninsula). Mar. Ecol. Prog. Ser. 297, 33-50.

Obernosterer, I., Sempéré, R., Herndl, G.J., 2001. Ultraviolet radiation induces reversal of the bioavailability of DOM to marine bacterioplankton Aquat. Microb. Ecol. 24, 61-68.

Introduction

Opsahl, S., Benner, R., 1997. Distribution and cycling of terrigenous dissolved organic matter in the ocean. Nature, 386, 480-482.

Ortega-Retuerta, E., Frazer, T.K., Duarte, C.M., Ruiz-Halpern, S., Tovar-Sánchez, A., Arrieta, J.M., Reche, I., 2009. Biogeneration of chromophoric dissolved organic matter by bacteria and krill in the Southern Ocean. Limnol. Oceanogr. 54, 1941–1950.

Peltier, W.R., Liu, Y., Crowley, J.W., 2007. Snowball Earth prevention by dissolved organic carbon remineralization. Nature 450, 813-819.

Pomeroy, L.R., 1974. The ocean's food web, A Changing Paradigm. Bioscience 24, 499-504.

Raven, J.A., Falkowski, P.G., 1999. Oceanic sinks for atmospheric CO_2. Plant Cell Environ. 22, 741-755.

Rosenstock, B., Zwisler, W., Simon, M., 2005. Bacterial consumption of humic and non-humic low and high molecular weight DOM and the effect of solar irradiation on the turnover of labile DOM in the Southern Ocean. Microb. Ecol. 50, 90-101.

Redfield, A.C., Ketchum, B.H., Richards, F.A., 1963. The influence of organisms on the composition of seawater. In: Hill, M.N. (Ed.), The sea. Vol. 2, Interscience, New York, pp. 26–77.

Sarmiento, J.L., Gruber, N., 2006. Ocean biogeochemical dynamics. Princeton university press, Princeton.

Sherr, E. and Sherr, B., 1988. Role of microbes in pelagic food webs: a revised concept. Limnol. Oceanogr. 33, 1225-1227.

Siegel, D.A., Maritorena, S. and Nelson, N.B., 2002. Global distribution and dynamics of colored dissolved and detrital organic materials. J. Geophys. Res. 107, 3228.

Stedmon, C.A., Markager, S., Bro, R., 2003. Tracing dissolved organic matter in aquatic environments using a new approach to fluorescence spectroscopy. Mar. Chem. 82, 239-254.

Stedmon, C.A.,Markager, S., 2005. Resolving the Variability in Dissolved Organic Matter Fluorescence in a Temperate Estuary and Its Catchment Using PARAFAC Analysis. Limnol. Oceanogr. 50, 686-697.

Stedmon, C.A., Álvarez-Salgado, X.A., 2011. Shedding light on a black box: UV-visible spectroscopic characterization of marine dissolved organic matter. In: Jiao, N., Azam, F., Sanders, S., (Eds.), Microbial carbon pump in the ocean. Science/AAAS Business Office. pp. 62.

Steinberg, D.K., Nelson, N.B., Carlson, C.A., Prusak, A.C., 2004. Production of chromophoric dissolved organic matter (CDOM) in the open ocean by zooplankton and the colonial cyanobacterium Trichodesmium spp. Mar. Ecol. Prog. Ser. 267, 45-56.

Takahashi, T. et al., 2009. Climatological mean and decadal change in surface ocean pCO2, and net sea-air CO2 flux over the global oceans. Deep Sea Rese. Part II 56(8-10), 554-577.

Turro, N.J., 1991. Modern molecular photochemistry. University Science Books.

Verdugo, P., Alldredge, A.L., Azam, F., Kirchman, D.L., Passow, U., Santschi, P.H., 2004. The oceanic gel phase: a bridge in the DOM-POM continuum. Mar. Chem. 92, 67-85.

Volk, T., Hoffert, M.l., 1985. Ocean carbon pumps: analysis of relative strengths and efficiencies in ocean-driven atmospheric CO_2 changes. In: Sunquist, E.T., Broeke, W.S. (Eds.), The carbon cycle and atmospheric CO2: natural variations archean to present. American Geophysical Union, Washington, D.C., pp. 99-110.

Weishaar, J.L., Aiken, G.R., Bergamaschi, B.A., Fram, M.S., Fujii, R., Mopper, K., 2003. Evaluation of specific ultraviolet absorbance as an indicator of the chemical composition and reactivity of dissolved organic carbon. Environ. Sci. Technol. 37, 4702-4708.

Weber, G., 1961.Enumeration of components in complex systems by fluorescence spectrophotometry. Nature 90, 27-29.

Wu, F.C., Tanoue, E., Liu, C.Q., 2003. Fluorescence and amino acid characteristics of molecular size fractions of DOM in the waters of Lake Biwa Biogeochemistry, 65, 245-257.

Yamashita, Y., Tanoue, E., 2003. Chemical characterization of protein-like fluorophores in DOM in relation to aromatic amino acids. Mar. Chem. 82, 255- 271.

Yamashita, Y., Tanoue, E., 2004. Chemical characteristics of amino acid-containing dissolved organic matter in seawater. Org. Geochem. 35, 679-692.

Introduction

Yamashita, Y., Tsukasaki, A., Nishida, T., Tanoue, E., 2007. Vertical and horizontal distribution of fluorescent dissolved organic matter in the Southern Ocean. Mar. Chem. 106, 498-509.

Yamashita, Y., Tanoue, E., 2008. Production of bio-refractory fluorescent dissolved organic matter in the ocean interior. Nat. Geosci. 1, 579-582.

Yentsch, C.S., Reichert, C.A., 1961. The interrelationship between water-soluble yellow substances and chloroplastic pigments in marine algae. Bot. Mar. 3, 65-74.

Chapter I

Production of chromophoric dissolved organic matter by marine phytoplankton

Chapter I

Co-authors:

H. Sarmento, X.A. Álvarez-Salgado, J.M. Gasol and C. Marrasé.

Abstract

Incubation experiments with axenic cultures of four common phytoplankton species of the genera *Chaetoceros*, *Skeletonema*, *Prorocentrum*, and *Micromonas* were performed to test for the production of fluorescent dissolved organic matter (FDOM) by marine phytoplankton. Our results prove that the four species exuded both fluorescent protein- and marine humic-like materials in variable amounts, with more production by the diatoms *Chaetoceros* sp. and *S. costatum* and less by *P. minimum*. Whereas the exudation of protein-like substances by healthy phytoplankton cells has been recognised, the in situ production of marine-humic like substances is still a matter of debate. Using axenic cultures, we demonstrate unequivocally that phytoplankton can directly contribute to the autochthonous production of coloured humic-like substances in the ocean. Extrapolation of these findings to the field suggests that about 20% of the marine humic-like substances produced in the highly productive coastal upwelling system of the Ría de Vigo could originate from growing phytoplankton. Therefore, the exudation of FDOM by marine phytoplankton should be considered in future studies of the dynamics of coloured DOM in marine systems.

Chapter I

Introduction

Marine dissolved organic matter (DOM) represents the largest pool of reduced carbon in the Earth. Phytoplankton is one of the major sources of DOM, which is released to the water column by exudation, excretion, and cell lysis due to viral attack, grazing, and sloppy feeding (Myklestad, 2000), and constitutes substrate that supports heterotrophic bacterial growth (Azam et al., 1983). The chemical composition, origin, and fate of the different components of the DOM pool in aquatic systems are still poorly known (Hansell, 2002).

Recent methodological advances have enabled identification of different fractions of DOM based on their optical properties in a way that is methodologically fast and simple, and that might provide indications about the origin and degradability of the DOM pool (Coble, 1996). A fraction of the DOM pool absorbs light at both ultraviolet (UV) and visible wavelengths and it is called coloured dissolved organic matter (CDOM; Coble, 2007). A sub-fraction of CDOM can emit blue fluorescence when it is irradiated with UV light and it is called fluorescent CDOM (FDOM; Coble, 1996, 2007). It is possible to distinguish between main groups of FDOM substances, depending on their excitation and emission (Ex/Em) wavelengths. One group fluoresces at wavelength pairs characteristic of the aromatic amino acids (Ex/Em 280 nm/350 nm) that corresponds to the peak-T reported by Coble (1996). This group, known as protein-like substances, has been considered as a proxy for labile DOM (Yamashita and Tanoue, 2003; Nieto-Cid et al., 2006). The other group, which emits radiation in the wavelength range of 380-420 nm when excited at 320 nm (peak-M as reported by Coble 1996), is called marine humic-like substances and it is considered to be photo-labile and bio-refractory (Chen and Bada, 1992; Nieto-Cid et al., 2006). Changes in FDOM are a good indication of biological (Chen and Bada, 1992; Nieto-Cid et al., 2006) and photochemical processes (Moran et al., 2000; Nieto-Cid et al., 2006) acting upon the bulk DOM pool.

The role of CDOM is key for ocean biogeochemical cycles since it can control light penetration in the water column. A high concentration of CDOM can reduce harmful UV effects on phytoplankton, acting as a photo-protector but it can also attenuate photosynthetic usable radiation, reducing primary production in regions where light is limiting (Arrigo and Brown, 1996). On the contrary, at low concentrations of CDOM, sunlight can damage not only phytoplankton cells but bacterioplankton physiology and deoxyribonucleic acid (DNA) as well (Herndl et al., 1993). Another important role of CDOM is the capacity for metal scavenging and the formation of complexes that can be beneficial to phytoplankton when metals present in the medium reach toxic concentrations (Midorikawa and Tanoue 1998).

Sources of CDOM include continental runoff that transports DOM primarily from soils (Coble, 2007); abiotic condensation and transformation of biopolymers, e.g., photo-oxidized polyunsaturated lipids released into the water column by plankton (Kieber et al., 1997); and in situ biological production (Yentsch and Reichert 1961; Kramer and Herndl 2004). Within these autochthonous sources, CDOM can be produced as a by-product of DOM metabolism, mainly by bacteria. But its production by copepods, krill, and other planktonic organisms has also been demonstrated in recent studies (Steinberg et al., 2004; Ortega-Retuerta et al., 2009).

The release of DOM by phytoplankton has been recognised as a major process in global biogeochemical cycles (Myklestad, 2000). The nature of the dissolved organic carbon (DOC) derived from phytoplankton is highly complex but major fractions include carbohydrates, followed by N-compounds namely protein, polypeptides, and amino acids (Goldman et al., 1992; Myklestad, 2000). However, the direct contribution of FDOM to the DOC released by phytoplankton is in controversy. On the one hand, a few field studies (Carder et al., 1989; Twardowski and Donaghay, 2001) and some culture experiments (Seritti et al., 1994) suggest that phytoplankton is a possible source of CDOM. But, other authors have reported the opposite, as they did not find a significant correlation between CDOM and phytoplankton biomass either in natural systems (Nelson et al., 1998) or in cultures (Rochelle-Newall and Fisher, 2002).

To better understand the sources and sinks of different types of organic matter in the ocean we must determine unequivocally whether phytoplankton produces CDOM. In this study, we have quantified the build-up of FDOM and DOC in axenic cultures of four common marine phytoplankton species (two diatoms, *Chaetoceros* sp. and *Skeletonema costatum*; a dinoflagelate, *Prorocentrum minimum*; and a prasinophyte, *Micromonas pusilla*) in order to determine whether phytoplankton is a direct source of CDOM, particularly of fluorescent humic-like substances.

Material and methods

Phytoplankton cultures

Four axenic species obtained from the Provasoli-Guillard National Center for Culture of Marine Phytoplankton (CCMP) (https://ccmp.bigelow.org/) were cultured in axenic conditions. The strains used were the diatoms *Chaetoceros* sp. (CCMP199) and *Skeletonema costatum* (CCMP2092) (Greville) Cleve, the dinoflagellate *Prorocentrum minimum* (CCMP1329) (Pavillard) J. Schiller, and the prasinophyte *Micromonas pusilla* (CCMP1545) (R.W. Butcher) I. Manton and M. Parke.

An inoculum of each species was added to 2 L of F/2 culture medium made with filtered and autoclaved coastal Mediterranean seawater. After gentle shaking, each mixture was distributed into three polystyrene bottles. Each bottle was filled with 600 mL and incubated at 20°C under artificial photosynthetic active radiation (PAR) radiation of 100 μmol photon m^{-2} s^{-1}, in a 16:8 hour light: dark cycle, until cell density increased about one order of magnitude.

Aliquots for phytoplankton counts, DOC concentration and DOM fluorescence were taken at the beginning and end of the incubation period: 3 days for all microalgae except for *P. minimum*, which was incubated for 7 days. Controls of the F/2 medium were also taken before adding the inoculum. Since the F/2 medium was the same for the four cultures, the differences between the initial values of the variables studied reflected the variable composition of the aliquots of the four cultures added to the F/2 medium.

Algal cultures were initially axenic, as guaranteed by the Provasoli-Guillard National Center for Culture of Marine Phytoplankton. To determine phytoplankton cell abundance and to check that the algal cultures were kept in axenic conditions, aliquots of 1 mL of each culture were fixed with 1% paraformaldehyde + 0.05% glutaraldehyde (final concentration), stained with DAPI (4,6 diamidino-2-phenylindole; 10 μg mL^{-1}, final concentration) and counted with an Olympus BX61 epifluorescence microscope under blue and UV wavelength excitation at the beginning and at the end of the experiment.

At the beginning and at the end of the incubation, DOC and FDOM samples were filtered onto 0.2 μm Sterivex filters. Milli-Q water was filtered through this filtration system and no significant changes were observed in DOC and FDOM analysis, proving that contamination did not occur during filtration. A control bottle containing only F/2 medium was incubated in the same conditions and no significant differences were observed at the end of the experiment (details not shown).

Phytoplankton biomass B, in pg C cell^{-1}, was estimated with the following conversion factors: B = 0.216·V $^{0.939}$ for *P.minimum* and *M. pusilla*, and B = 0.288·V $^{0.811}$ for diatoms (Menden-Deuer and Lessard 2000), where V is the cell volume in μm^3 and was calculated for the different species following the geometric models given by Sun and Liu (2003).

Determination of FDOM

To quantify the production of FDOM, samples were measured immediately after collection following Nieto-Cid et al. (2006). Single measurements and emission excitation matrices (EEMs) of the aliquots were performed with a LS 55 Perkin Elmer Luminescence spectrometer, equipped with a

xenon discharge lamp, equivalent to 20 kW for 8 μs duration. The detector was a red-sensitive R928 photomultiplier, and a photodiode worked as reference detector. Slit widths were 10.0 nm for the excitation and emission wavelengths; scan speed was 250 nm min^{-1}. Measurements were performed at a constant room temperature of 20°C in a 1 cm quartz fluorescence cell. The Ex/Em wavelengths used for single measurements were those established by Coble (1996): Ex/Em 280 nm/350 nm (peak T or $F(280/350)$) as indicator of protein-like substances and Ex/Em 320 nm/410 nm (peak M or $F(320/410)$) as indicator of marine humic-like substances. Following Coble (1996), fluorescence measurements were expressed in quinine sulphate units (QSU), i.e., in μg eq QS L^{-1}, by calibrating the LS 55 Perkin Elmer at Ex/Em 350 nm/450 nm against a quinine sulphate dihydrate (QS) standard made up in 0.05 mol L^{-1} sulphuric acid.

EEMs were performed to track possible changes in the position of the protein- and humic-like fluorescence peaks. These matrices were generated by combining 21 synchronous Ex/Em fluorescence spectra of the sample, obtained for excitation wavelengths from 250 to 400 nm and an offset between the excitation and emission wavelengths of 50 nm for the 1st scan and 250 nm for the 21st scan. Rayleigh scatter does not need to be corrected when the EEMs are generated from synchronous spectra and Raman scatter was corrected by subtracting the pure water (Milli-Q) EEM from the sample EEM.

Determination of dissolved organic carbon

Approximately 10 mL of water were collected in pre-combusted (450ºC, 12 h) glass ampoules for DOC analysis. H_3PO_4 was added to acidify the sample to pH < 2 and the ampoules were heat-sealed and stored in the dark at 4ºC until analysis. DOC was measured with a Shimadzu TOC-V organic carbon analyser. The system was standardized daily with a potassium hydrogen phthalate standard. Each ampoule was injected 3–5 times and the 3 replicates that yielded a standard deviation <1% were chosen to calculate the average DOC concentration of each sample. The performance of the analyser was tested with the DOM reference materials provided by Prof. D. Hansell (University of Miami). We obtained a concentration of 45.2 ± 0.3 μmol C L^{-1} for the deep ocean reference (Sargasso Sea deep water, 2600 m) minus blank reference materials, the day when the samples were analyzed. The nominal DOC value provided by the reference laboratory is 45 μmol C L^{-1}.

Phytoplankton cell densities, growth rates, and net percentage of extracellular release

Average of cell abundance ($\overline{C}$), biomass ($\overline{B}$), and growth rate (μ_C) for the four cultures were calculated considering that the species were in exponential growth. Since the cultures were kept in axenic conditions throughout the growing period, it can be assumed that organic carbon dynamics depended only on phytoplankton activity. A proxy for the percentage of net photosynthetic extracellular

release (PER) was calculated as APER = ΔDOC/(ΔDOC + ΔB) x 100, where APER is Apparent PER, and ΔDOC and ΔB are the net increase of DOC and phytoplankton biomass (both in µg C L^{-1}) through the incubation time, respectively.

Statistical tools

Paired Student-t-test was used to check for significant differences in the measured variables between the initial and final incubation times (Sokal and Rohlf, 1984). Regression model II was applied to calculate linear fitting parameters.

Results

Phytoplankton cell densities and growth rates

Average cell abundance in the different cultures varied between 12 x 10^3 cells mL^{-1} for *P. minimum* and 33 x 10^5 cells mL^{-1} for *M. pusilla* and biomass ranged from 990 µg C L^{-1} for *Chaetoceros* sp. to 2272 µg C L^{-1} for *S. costatum*. *Chaetoceros* sp. showed the highest exponential growth rates at 0.89 d^{-1} and *P. minimum* the lowest one at 0.45 d^{-1} (Table 1). These numbers are within the ranges reported in the literature (Rose and Caron, 2007).

Table 1. Average cell abundances ($\overline{C}$), biomass ($\overline{B}$), and growth rates (μ_C), calculated considering exponential algal growth. Apparent percentage of net photosynthetic extracellular release (APER) in each algal culture.

Algal culture	time (d)	$\overline{C}$ (cells mL^{-1})	$\overline{B}$ (µg C L^{-1})	μ_C (d^{-1})	APER (%)
Chaetoceros sp.	3	162 ± 5.2 x 10^3	990 ± 32	0.89 ± 0.02	11.7 ± 0.5
S. costatum	3	303 ± 21 x 10^3	2272 ± 158	0.87 ± 0.03	10 ± 2
P. minimum	7	12.0 ± 0.5 x 10^3	1254 ± 136	0.45 ± 0.02	18 ± 1
M. pusilla	3	3342 ± 29 x 10^3	1975 ± 13	0.59 ± 0.05	12.8 ± 0.8

Chapter I

Production of dissolved organic carbon

DOC increased significantly ($p < 0.01$) in all cultures. *P. minimum*, incubated for 7 days, showed the largest bulk DOC rise: 0.85 mg C L^{-1}. Total DOC production in the other three cultures, incubated for 3 days, varied from 0.35 to 0.64 mg C L^{-1} (Fig. 1a). Apparent PER (APER) values ranged between 10% and 18% (Table 1) and biomass-specific DOC production rates from 86 x 10^{-3} to 116 x 10^{-3} μg C μg C $^{-1}$ d^{-1} (Table 2). When we normalised to cell density instead of biomass, *P. minimum* presented the highest DOC production rates and *M. pusilla* the lowest. Both diatoms *Chaetoceros* sp. and *S. costatum* presented similar values of cell-specific DOC production rates (71.1 x 10^{-8} and 70.1 x 10^{-8} μg C $cell^{-1}$ d^{-1}, respectively), two orders of magnitude lower than *P. minimum* (10.2 x 10^{-6} μg C $cell^{-1}$ d^{-1}). Turnover rates of DOC, calculated assuming that they were proportional to cell growth rate and cells were in exponential growth, ranged from 0.04 to 0.07 d^{-1} (Table 3).

Production of FDOM

Fluorescence EEMs of the coloured dissolved organic matter (CDOM) produced by each culture during the incubation time are shown in Fig. 2. These EEMs were obtained by subtracting the fluorescence intensities at the beginning of the culture from the end values. In all cultures, EEMs presented marked fluorescence peaks in the protein- and humic-like areas. In the protein-like area, the most intense peak presented a maximum at Ex/Em 275 nm/358 nm for *Chaetoceros* sp., *P. minimum*, and *S. costatum* cultures, that was slightly displaced towards longer emission wavelengths compared to that established by Coble (1996) at Ex/Em 275 nm/340 nm (peak T). The *S. costatum* culture presented the highest fluorescence at peak T whereas *M. pusilla* showed the lowest value and it was centred at an emission wavelength of 345 nm. In the humic-like area all cultures showed a conspicuous peak within the range of the marine humic-like substances defined by Coble (1996) at Ex/Em 312 nm/380-420 nm (peak M).

Table 2. Net increase of the concentration of DOC and the fluorescence of peak-T and peak-M normalized to average biomass ($\overline{B}$) and incubation time (t).

Species	ΔDOC/ ($\overline{B} \cdot$ t) (μg C μg C^{-1} d^{-1})	Δpeak-T/ ($\overline{B} \cdot$ t) (μg eq QS μg C^{-1} d^{-1})	Δpeak-M/ ($\overline{B} \cdot$ t) (μg eq QS μg C^{-1} d^{-1})
Chaetoceros sp.	116 $\pm$ 11 x 10^{-3}	9.1 $\pm$ 0.8 x 10^{-4}	4.8 $\pm$ 0.1 x 10^{-4}
S. costatum	93 $\pm$ 13 x 10^{-3}	5.8 $\pm$ 0.1 x 10^{-4}	4.5 $\pm$ 0.1 x 10^{-4}
P. minimum	97 $\pm$ 9 x 10^{-3}	3.2 $\pm$ 0.2 x 10^{-4}	1.3 $\pm$ 0.03 x 10^{-4}
M. pusilla	86 $\pm$ 5 x 10^{-3}	2.6 $\pm$ 0.02 x 10^{-4}	3.0 $\pm$ 0.1 x 10^{-4}

The position of the fluorescence maxima in this area differed for each culture with excitation maxima slightly, but not significantly, displaced to shorter wavelength relative to peak M (Coble 1996). *Chaetoceros* sp. and *P. minimum* showed their maxima at Ex/Em 310 nm/399 nm and 316 nm/397 nm with an intensity of 1.36 QSU and 1.19 QSU, respectively. *S. costatum* and *M. pusilla* presented this maximum at Ex/Em 306 nm/396 nm and their fluorescence intensities were the most pronounced with 3.89 QSU and 2.03 QSU, respectively.

The EEM of *M. pusilla* also showed three peaks of lower fluorescence intensity at Ex/Em 348 nm/436 nm, 354 nm/447 nm, and 271 nm/432 nm. Finally, both diatoms showed a third peak that *M. pusilla* and *P. minimum* did not produce: *Chaetoceros* sp. at Ex/Em 280 nm/381 nm (1.56 QSU) and *S. costatum* at Ex/Em 289 nm/391 nm (3.73 QSU).

A significant ($p < 0.01$) net increase of FDOM (peak-M and peak-T) was observed in all cultures during the experiment (Fig. 1b, c). *S. costatum* exhibited the most pronounced increase: 3.05 ± 0.08 QSU for the humic-like substances. In the case of the protein-like substances, *S. costatum* also presented the highest increase (3.98 ± 0.06 QSU) whereas *M. pusilla* presented the lowest increase, 1.56 ± 0.01 QSU.

Fig. 1. Initial and final concentrations of: (a) DOC (mg C L^{-1}); (b) peak-M (F(320/410)) in QSU; (c) peak-T (F(280/350)) in QSU. Dark bars correspond to initial concentration (to) and grey bars to final concentration (tf).
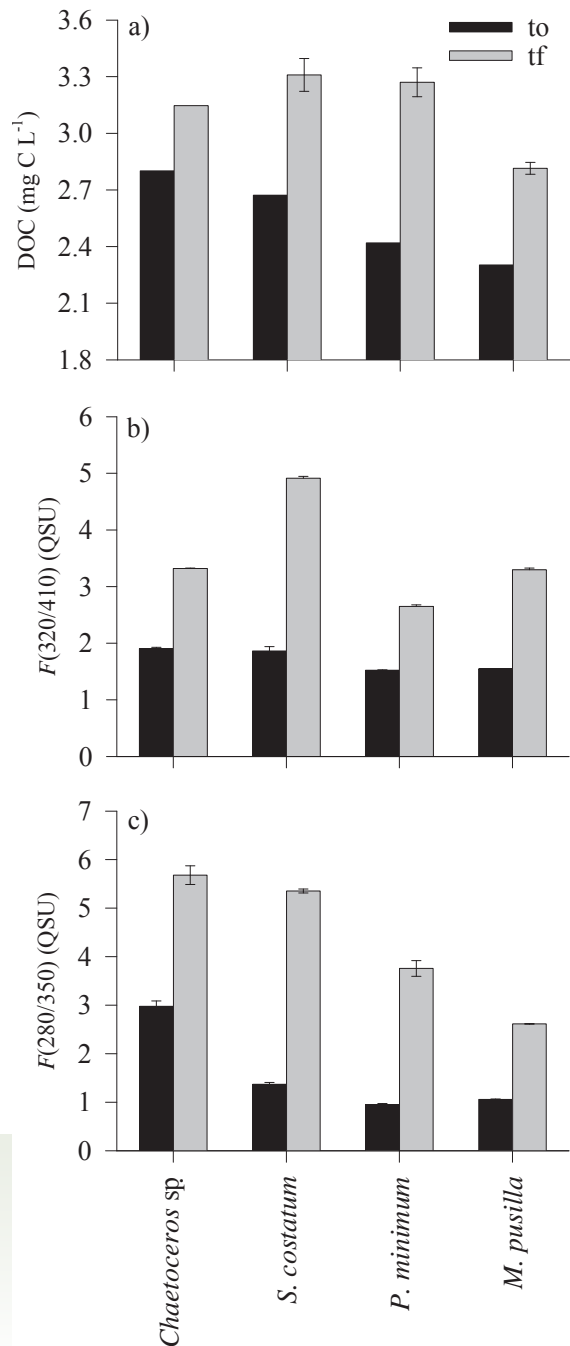
Table 3. Turnover rates of the concentration of DOC and the fluorescence of peak-T and peak-M for each culture calculated as $\mu_{DOC} = \ln[DOC(tf)/DOC(to)]/t$; $\mu_T = \ln[peak\text{-}T(tf)/peak\text{-}T(to)]/t$; and $\mu_M = \ln[peak\text{-}M(tf)/peak\text{-}M(to)]/t$.

Species	μ_{DOC} (d^{-1})	μ_T (d^{-1})	μ_M (d^{-1})
Chaetoceros sp.	$3.9 \pm 0.3 \times 10^{-2}$	$22 \pm 1 \times 10^{-2}$	$18.5 \pm 0.1 \times 10^{-2}$
S. costatum	$7.1 \pm 0.9 \times 10^{-2}$	$45.4 \pm 0.3 \times 10^{-2}$	$32.3 \pm 0.2 \times 10^{-2}$
P. minimum	$4.3 \pm 0.3 \times 10^{-2}$	$19.6 \pm 0.6 \times 10^{-2}$	$7.9 \pm 0.1 \times 10^{-2}$
M. pusilla	$6.7 \pm 0.4 \times 10^{-2}$	$30.16 \pm 0.06 \times 10^{-2}$	$25.2 \pm 0.3 \times 10^{-2}$

The biomass-specific FDOM production rates were the highest for *Chaetoceros* sp. (Table 2) in both protein- and humic-like peaks. *P. minimum* presented the lowest increase of humic-like substances, and *M. pusilla* the lowest rates of protein-like substances production. For the case of the cell-specific FDOM production rates (data not shown), *P. minimum* presented the highest and *M. pusilla* the lowest values in both fluorescent peaks. Diatoms showed similar cell-specific production rates of protein- and humic-like substances. The dimensionless Δpeak-T:Δpeak-M production ratio was calculated: it was maximum for *P. minimum* (2.49 ± 0.03) and minimum for *M. pusilla* (0.89 ± 0.03), whereas the diatoms presented intermediate values of 1.91 ± 0.05 for *Chaetoceros* sp. and 1.31 ± 0.03 for *S. costatum*.

Turnover rates of peak-T and peak-M were also calculated for all species (Table 3). *S. costatum* presented the highest values for both the protein- and humic-like fluorescence whereas *P. minimum* presented the lowest turnover rates.

Phytoplankton biomass was significantly correlated with the fluorescence of peak-M ($R^2 = 0.78$; $p < 0.0001$; Fig. 3a) when data for all species were included. Peak-T and DOC were significantly correlated with phytoplankton biomass (Fig. 3b, c), but with lower R^2 (0.36 and 0.44 for peak-T and DOC, respectively).

Discussion

Since all cultures were kept axenic during the course of the experiment, carbon dynamics were based exclusively on phytoplankton activity. We calculated a proxy to PER, apparent PER (APER), substituting ΔPOC (particulate organic carbon) by ΔBiomass, assuming that the production of transparent exopolymer particles (TEP) and DOC uptake did not occur during the course of the experiment. It is likely that these processes were negligible during the exponential phase of the cultures, but we have
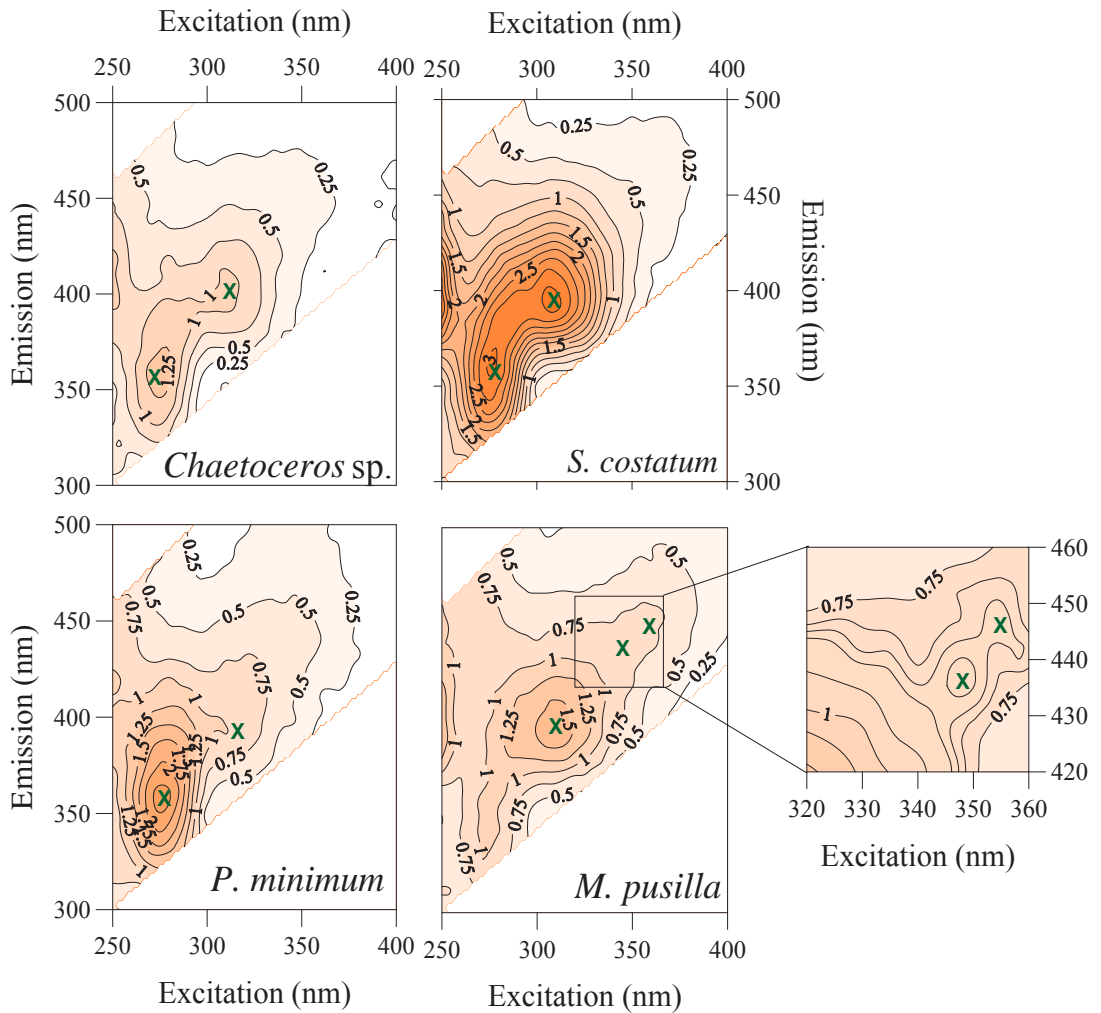
Fig. 2. Excitation-emission matrices (EEMs) of the FDOM produced in the cultures, in quinine sulphate units (QSU). Note that these values are neither normalized to incubation time nor to biomass. All the species were incubated for 3 days except *P. minimum* incubated for 7 days.

no direct evidence to prove it. The observed build-up of DOC concurs with many studies showing significant DOC excretion by phytoplankton (Bjørnsen, 1988). Net APER values obtained in this work were in the range of PER values found by other authors using the ^{14}C incorporation method. Mague et al. (1980) obtained a PER of 8% during the exponential growth phase of *S. costatum*, which is very close to the APER of 10% found in our study for the same species. According to Lancelot and Billen (1985), PER values are higher for microflagellates, with an inverse relationship to nutrient concentration. In our experiments, with excess nutrients, we obtained APER values of 13% for *Micromonas*, which is at the lower end of the PER range (10% to 60%) found by Lancelot and Billen (1985). Field-work carried out in the North Sea by Lancelot (1983) showed that, within the same range of inorganic nitrogen concentrations, flagellates presented higher PER values than diatoms. The same author obtained low PER values (<10%) when diatom species dominated the bloom, irrespective of nutrient conditions. We also found this trend in our experimental work: the cultures of *M. pusilla* and *P. minimum* presented higher APER values (13% and 18%, respectively) than the diatoms (< 12%).
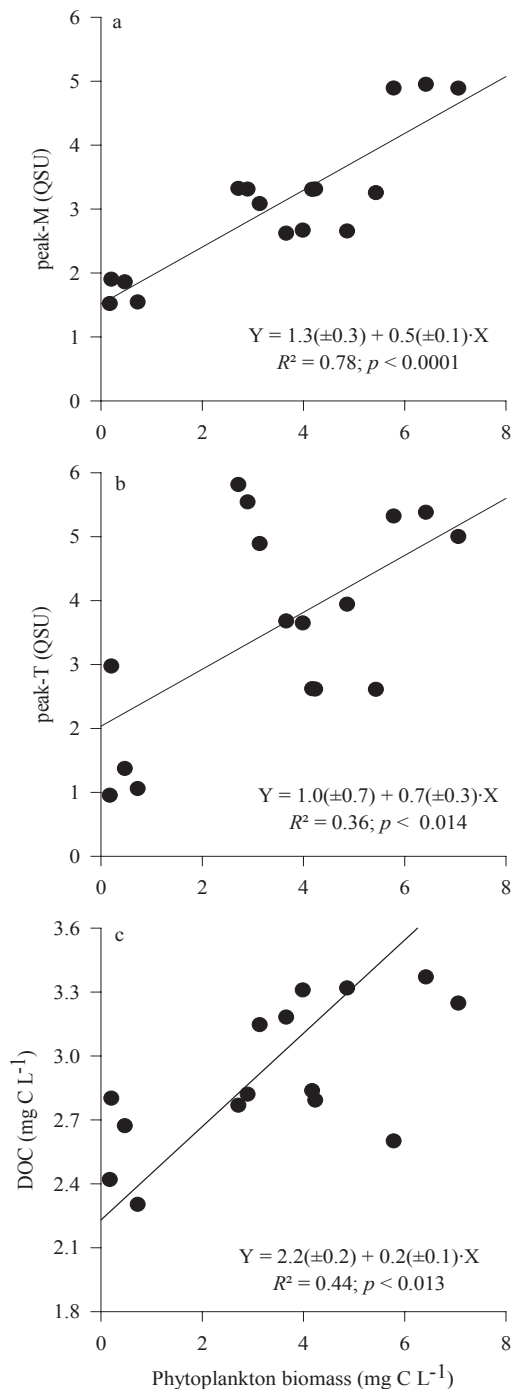
In all cultures, humic- and protein-like substances increased during the course of the incubations. Because bacteria were absent, it implies that the increases in DOC and FDOM were exclusively due to phytoplankton metabolism. The amount and quality of FDOM produced was different depending on the species. Factors such as nutrients, light and growth phase can affect PER (Obernosterer and Herndl, 1995); so, it is likely that FDOM, as a fraction of the released DOM, is affected by the same factors. Here, the four species were incubated under identical experimental conditions and, therefore, it can be assumed that the differences found on the excreted organic substances between cultures were attributable to specific differences in metabolic activity. The Δpeak-T:Δpeak-M ratio was significantly different among species, indicating that the selected dinoflagellates exuded relatively more protein-like than humic-like substances as compared with the diatoms, and the latter produced relatively more than the prasinophyte. A low value of this ratio would indicate a relative dominance of the exudation of the products of early degradation (respiration) over the synthesis products by healthy marine phytoplankton, since it has been reported that humic-like substances are a by-product of the microbial respiration (Nieto-Cid et al., 2006).

The variations in the position of the peak-T and peak-M fluorescence maxima in the EEMs indicate that different substances are being produced by each culture, i.e., that the quality of the organic matter produced by phytoplankton was different depending on the species. It is difficult to know the cause of those variations in the fluorescence maxima without concurrent molecular analysis. For example, tryptophan is highly sensitive to the polarity of its surrounding environment. Frequently, spectral shifts are observed as a result of binding ligands, protein-protein associations, and denaturation, among others (Lakowicz, 1983).

Both diatoms showed a peak at Ex/Em 280 nm/381 nm for *Chaetoceros* sp. and slightly displaced at longer wavelengths, 289 nm/391 nm, for *S. costatum*. A similar peak (Ex/Em 280 nm/370 nm) was found by Coble et al. (1998) in samples collected in the upper 100 m of a coastal upwelling system, where chlorophyll was high. That peak (called peak-N) had not been previously reported and the authors concluded that it could not be a humic-like peak but appeared to be associated with production of new CDOM in that marine environment. Our results support their conclusion as well as show that peak-N is produced by marine phytoplankton. The absence of this peak in the cultures of the other two species (*P. minimum and M. pusilla*), could indicate that the compounds associated to this peak are only produced by diatoms, or that the peak was masked by other fluorescence peaks in the other cultures. It would be worthwhile to explore in future experiments the possible specificity of FDOM compounds produced by different groups of phytoplankton.

The EEM of *M. pusilla* was compared with the EEM of a natural seawater sample, taken at the Blanes Bay Microbial Observatory (http://www.icm.csic.es/bio/projects/icmicrobis/bbmo/) in the NW Mediterranean Sea, during a *Micromonas* bloom (R. Massana personal communication), in February 2007 (details not shown). A peak at Ex/Em 283 nm/358 nm, which could correspond to the

Fig. 3. (a) Plot of peak-M fluorescence (F(320/410)) in QSU vs. phytoplankton biomass (mg C L^{-1}), (b) Plot of peak-T fluorescence (F(280/350)) in QSU vs. biomass (mg C L^{-1}), and (c) DOC (mg C L^{-1}) vs. biomass (mg C L^{-1}).

In panel (a): $Y = 1.3(\pm0.3) + 0.5(\pm0.1)\cdot X$; $R^2 = 0.78$; $p < 0.0001$

In panel (b): $Y = 1.0(\pm0.7) + 0.7(\pm0.3)\cdot X$; $R^2 = 0.36$; $p < 0.014$

In panel (c): $Y = 2.2(\pm0.2) + 0.2(\pm0.1)\cdot X$; $R^2 = 0.44$; $p < 0.013$

61

peak-T by Coble (1996), was found in the natural sample. This peak is slightly displaced to longer wavelengths than the peak T of the *M. pusilla* culture (Ex/Em 275 nm/345 nm). The EEM of the natural sample also showed a maximum at Ex/Em 348 nm/434 nm that coincided with the peak at Ex/Em 348 nm/436 nm detected in the axenic culture. These maxima coincide with the peak-C defined by Coble et al. (1998). Certainly, it should not be expected that the EEM of a natural sample, even if taken during an almost monospecific *Micromonas* bloom, would match completely the peaks found in a *Micromonas* axenic culture. The EEM of the *Micromonas* culture shown in Fig. 2 reflects the production of fluorescent materials only by this species. On the other hand, the fluorescence fingerprint of the natural sample results from the production and/or accumulation of FDOM due to the activity of plankton assemblages, the transformations by photo-chemical and biological reactions, and/or the inputs of terrestrial FDOM. With these considerations in mind, the correspondence between the EEM of a natural *Micromonas* bloom and that from a *Micromonas* axenic culture is indeed remarkable.

Several studies have confirmed that carbohydrates constitute the major fraction of compounds released by phytoplankton. The next largest fraction is composed of N-compounds with the most prominent members being amino acids, peptides, and proteins (Myklestad, 2000). Studies about dissolved free amino acids (DFAA) excreted by phytoplankton (Martin-Jézéquel et al., 1988) have found that the most prominent excreted free amino acids are Ser, Gly, Lys, Ala, Glu, Asp, Orn, and His (Myklestad, 2000). Yamashita and Tanoue (2003) observed a high correlation between protein-like fluorescence intensities and total amino acids in the ocean meaning that fluorescence intensities (i.e., peak-T) may be a useful indicator of the dynamics of dissolved amino acids. We found a significant increase of protein-like fluorescence per unit of biomass during the experiments for all the species examined suggesting that phytoplankton excretes fluorescent protein-like material during growth. Stedmon and Markager (2005) applied parallel factor analysis (PARAFAC) analysis to EEMs from a phytoplankton bloom sample and found two components in the protein-like region. One of them, with a maximum at Ex/Em 280 nm/338 nm was more susceptible to microbial degradation than the one that peaks at Ex/Em 275 nm/306 nm. Note that our peak-T is close to the former, more labile, component.

Microbial processes are an important source of humic-like compounds (Yentsch and Reichert, 1961). However, previous experimental and field studies have concluded that phytoplankton can not be a direct source of fluorescent humic-like substances, mainly because of a lack of correlation between phytoplankton biomass and CDOM (Nelson et al., 1998; Rochelle-Newall and Fisher, 2002). However, our study shows a clear increase of humic-like substances during the incubation of four different phytoplankton axenic cultures. This contrast may be attributable to a variety of causes. In field studies it is difficult to isolate the variables influencing CDOM dynamics and bacterial activity and UV radiation could mask the actual humic-like CDOM production role of phytoplankton as it has been shown that bacteria do produce such compounds (Tranvik, 1993; Nieto-Cid et al., 2006) and that natural UV radiation photodegrades them (Moran et al., 2000; Nieto-Cid et al., 2006). To our knowledge, ours

is the first study focusing on FDOM production, where phytoplankton cultures were maintained axenic until the end of the experiment. Therefore, the lack of a connection between humic-like CDOM and phytoplankton in previous experimental approaches could be caused by bacterial activity. Rochelle-Newall and Fisher (2002) analyzed fluorescence at longer wavelengths (Ex/Em 335 nm/450 nm) than those we used, in a region where we observed smaller increases in the intensity of fluorescence (data not shown). In our experiment, in absence of bacteria and UV radiation, the good correlation obtained between algal biomass and marine humic-like CDOM ($n = 16$, $R^2 = 0.78$, $p < 0.001$) indicates that phytoplankton is indeed a net source of humic-like CDOM.

Previous studies with natural samples had suggested that phytoplankton could release protein-like compounds, measured as peak-T (Nieto-Cid et al., 2006). The correlation between peak-T and biomass found here was also significant ($R^2 = 0.36$, $p < 0.01$) but lower than that between peak-M and biomass, suggesting that the dynamics of protein-like substances are species specific. Determann et al. (1998) observed the same pattern in non-axenic algae cultures that included cells and exudates. They found that fluorescence intensities (Ex/Em 230 nm/ 330 nm) normalized to phytoplankton cell numbers were a function of the species and also dependent on the physiological status. Moreover, it has been demonstrated that phytoplankton excretes amino acids but can take them up too (Paerl 1991). So, we cannot exclude the possibility of some uptake of protein-like substances by phytoplankton, and this could also contribute to a decrease in the correlation between peak-T and phytoplankton biomass.

How and why healthy phytoplankton cells release amino acids and humic substances to the medium is unclear. The DOC excretion by phytoplankton has been widely discussed. Bjornsen (1988) proposed passive diffusion as the most likely mechanism. It is known that phytoplankton exudes low molecular weight photosynthetic metabolites and by-products of the degradation of cellular polymeric material (Myklestad, 2000). In this sense, phytogenic marine humic substances can be considered a by-product of aerobic respiration.

To assess the relevance of our results in nature, we have roughly estimated the contribution of phytoplankton to the production of coloured humic-like substances in the highly productive coastal upwelling system of the Ría de Vigo (NW Iberian Peninsula). Seasonal cycles of peak-M (Nieto–Cid et al., 2006) and autotrophic carbon biomass (B) (Teixeira and Figueiras, 2009) were obtained in the surface layer of this ecosystem during year 2002. A significant positive linear relationship ($n = 8$, $R^2 = 0.78$, $p < 0.001$) was obtained between peak-M and biomass, with a slope of 2.9 ± 0.6 μg eq QS mg C^{-1}. Considering that the slope of the linear regression of the curve in Fig. 3a is 0.5 ± 0.1 μg eq QS mg C^{-1}, the contribution of phytoplankton to the build-up of peak-M in the surface layer of the coastal upwelling system of the Ría de Vigo should be $18 \pm 9\%$ if the relationships obtained in cultures were transferable to nature. Although this is certainly a rough estimation, it indicates that the contribution of phytoplankton to the production of coloured humic-like substances is potentially important, thus, further studies are necessary to assess the

contribution of phytoplankton to the autochthonous CDOM pool in the marine ecosystem.

The optical characterisation of exudates produced by axenic cultures of four common phytoplankton species showed that these organisms produced CDOM, detected by the build-up of fluorescent protein- and humic-like materials. Whereas the exudation of protein-like substances by healthy phytoplankton cells has been recognised as a common but intriguing process, the in situ production of marine-humic like substances has been traditionally associated with bacterial respiration. Although further studies are needed to examine the composition of the FDOM and its role in the physiology of phytoplankton, this work demonstrates unequivocally for the first time that phytoplankton cells in exponential growth also exude fluorescent humic-like substances and that the quality of this material is different for each species. As for the case of bacteria, it is hypothesised that the exudation of humic materials by phytoplankton could ultimately be derived from phytoplankton respiration. These results have clear implications for understanding the cycle of coloured DOM in the photic layer of coastal and open ocean waters by providing evidence for a previously unrecognized process contributing to the in situ production of CDOM.

Acknowledgements

References

Arrigo, K.R., Brown, C.W., 1996. Impact of chromophoric dissolved organic matter on UV inhibition of primary productivity in the sea. Mar. Ecol. Prog. Ser. 140, 207-216.

Azam, F., Fenchel, T., Field, J.G., Gray, J.S., Meyer-Reil, L.A., Thingstad, F., 1983. The ecological role of water-column microbes in the sea. Mar. Ecol. Prog. Ser. 10, 257-263.

Bjørnsen, P.K. 1988. Phytoplankton exudation of organic matter: Why do healthy cells do it? Limnol. Oceanogr. 33, 151-154.

Carder, K.L., Steward, R.G., Harvey, G.R., Ortner, P.B., 1989. Marine humic and fulvic acids: their effects on remote sensing of ocean chlorophyll. Limnol. Oceanogr. 34, 68-81.

Chen, R.F., Bada, J. L., 1992. The fluorescence of dissolved organic matter in seawater. Mar. Chem. 37, 191-221.

Coble, P.G., 1996. Characterization of marine and terrestrial DOM in seawater using excitation-emission matrix spectroscopy. Mar. Chem. 51, 325-346.

Coble, P.G., Del Castillo, C.E., Avril, B., 1998. Distribution and optical properties of CDOM in the Arabian Sea during the 1995 Southwest Monsoon. Deep-Sea Res II. 45, 2195-2223.

Coble, P.G., 2007. Marine optical biogeochemistry: the chemistry of ocean color. Chem. Rev. 107, 402-418.

Determann, S., Lobbes, J.M., Reuter, R., Rullköter, J., 1998. Ultraviolet fluorescence excitation and emission spectroscopy of marine algae and bacteria. Mar. Chem. 62, 137-156.

Goldman, J.C., Hansell, D.A., Dennett, M.R., 1992. Chemical characterization of three large oceanic diatoms: potential impact on water column chemistry. Mar. Ecol. Prog. Ser. 88, 257-270.

Hansell, D.A. 2002. DOC in the global ocean carbon cycle. In: Hansell, D.A. and Carlson, C.A. (Eds.), Biogeochemistry of marine dissolved organic matter. Academic Press, pp. 509-546.

Herndl, G.J., Müller-Niklas, G., Frick, J., 1993. Major role of ultraviolet-B in controlling bacterioplankton growth in the surface layer of the ocean. Nature 361, 717-719.

Kieber, R.J., Hydro, L.H., Seaton, P.J., 1997. Photooxidation of triglycerides and fatty acids in seawater: implication toward the formation of marine humic substances. Limnol. Oceanogr. 42, 1454-1462.

Kramer, G.D., Herndl, G.J., 2004. Photo- and bioreactivity of chromophoric dissolved organic matter produced by marine bacterioplankton. Aquat. Microb. Ecol. 36, 239-246.

Lakowicz, J.R., 1983. Principles of fluorescence spectroscopy. Plenum Press.

Lancelot, C., 1983. Factors affecting phytoplankton extracellular release in the Southern Bight of the North Sea. Mar. Ecol. Prog. Ser. 12, 115-121.

Lancelot, C., Billen, G., 1985. Carbon-nitrogen relationships in nutrient metabolism of coastal marine ecosystems. In: Jannasch, H.W., Williams, P.J.le B. (Eds.), Advances in aquatic microbiology, vol. 3. Academic Press, pp. 263-321.

Mague, T.H., Friberg, E., Hughes, D.J., Morris, I., 1980. Extracellular release of carbon by marine phytoplankton; a physiological approach. Limnol. Oceanogr. 25, 262-279.

Martin-Jézéquel, V., Poulet, S.A., Harris, R.P., Moal, J., Samain, J.F., 1988. Interspecific and intraspecific composition and variation of free amino acids in marine phytoplankton. Mar. Ecol. Prog. Ser. 44, 303-313.

Menden-Deuer, S., Lessard, E.J., 2000. Carbon to volume relationships for dinoflagellates, diatoms, and other protist plankton. Limnol. Oceanogr. 45, 569-579.

Midorikawa, T., Tanoue, E., 1998. Molecular masses and chromophoric properties of dissolved organic ligands for copper(II) in oceanic water. Mar. Chem. 62, 219-239.

Moran, M.A., Sheldon, W.M., Zepp, R.G., 2000. Carbon loss and optical property changes during long-term photochemical and biological degradation of estuarine dissolved organic matter. Limnol. Oceanogr. 45, 1254-1264.

Myklestad, S.M., 2000. Dissolved organic carbon from phytoplankton, In: Wangersky, P. (Ed.), The handbook of environmental chemistry. Marine chemistry, vol. 5D. Springer, pp. 111-148.

Nelson, N.B., Siegel, D.A., Michaels, A.F., 1998. Seasonal dynamics of coloured dissolved material in the Sargasso Sea. Deep-Sea Res I. 45, 931-957.

Nieto-Cid, M., Álvarez-Salgado, X.A., Pérez, F.F., 2006. Microbial and photochemical reactivity of fluorescent dissolved organic matter in a coastal upwelling system. Limnol. Oceanogr. 51, 1391-1400.

Obernosterer, I., Herndl, G.J., 1995. Phytoplankton extracellular release and bacterial growth: dependence on the inorganic N: P ratio. Mar. Ecol. Prog. Ser. 116, 247-257.

Ortega-Retuerta, E., Frazer, T.K., Duarte, C.M., Ruiz-Halpern, S., Tovar-Sánchez, A., Arrieta, J.M., Reche, I., 2009. Biogeneration of chromophoric dissolved organic matter by bacteria and krill in the Southern Ocean. Limnol. Oceanogr. 54, 1941–1950.

Paerl, H. W., 1991. Ecophysiological and trophic implications of light-stimulated amino acid utilization in marine picoplankton. Appl. Environ. Microbiol. 57, 473-479.

Rochelle-Newall, E.J., Fisher, T.R., 2002. Production of chromophoric dissolved organic matter fluorescence in marine and estuarine environments: an investigation into the role of phytoplankton. Mar. Chem. 77, 7 -21.

Rose, J.M., Caron, D.A., 2007. Does low temperature constrain the growth rates of heterotrophic protists? Evidence and implications for algal blooms in cold waters. Limnol. Oceanogr. 52, 886-895.

Seritti, A., Morelli, E., Nannicini, L., Del Vecchio, R., 1994. Production of hydrophobic fluorescent organic matter by the marine diatom Phaeodactylum tricornutum. Chemosphere 28, 117-129.

Sokal, F.F., Rohlf, F.J., 1984. Introduction to biostatistics. W.H. Freeman.

Stedmon, C.A., Markager, S., 2005. Tracing the production and degradation of autochthonous fractions of dissolved organic matter by fluorescence analysis. Limnol. Oceanogr. 50, 1415–1426.

Steinberg, D.K., Nelson, N.B., Carlson, C.A., Prusak, A.C., 2004. Production of chromophoric dissolved organic matter (CDOM) in the open ocean by zooplankton and the colonial cyanobacterium Trichodesmium spp. Mar. Ecol. Prog. Ser. 267, 45-56.

Sun, J., Liu D., 2003. Geometric models for calculating cell biovolume and surface area for phytoplankton. J. Plankton Res. 25,1331-1346.

Teixeira, I.G., Figueiras, F.G., 2009. Feeding behaviour and non-linear responses in dilution experiments in a coastal upwelling system. Aquat. Microb. Ecol. 55, 53-63.

Tranvik, L.J., 1993. Microbial transformation of labile dissolved organic matter into humic-like matter in seawater. FEMS Microb. Ecol. 12, 177-183.

Twardowski, M.S., Donaghay, P.L., 2001. Separating in situ and terrigenous sources of absorption by dissolved materials in coastal waters. J. Geophys. Res. 106, 2545-2560.

Yamashita, Y., Tanoue, E., 2003. Chemical characterization of protein-like fluorophores in DOM in relation to aromatic amino acids. Mar. Chem. 82, 255- 271.

Yentsch, C. S., Reichert, C.A., 1961. The interrelationship between water-soluble yellow substances and chloroplastic pigments in marine algae. Bot. Mar. 3, 65-74.

Chapter II

Net production/consumption of fluorescent coloured dissolved organic matter by natural bacterial assemblages growing on marine phytoplankton exudates

Chapter II

Co-authors:

H. Sarmento, X.A. Álvarez-Salgado, J.M. Gasol and C. Marrasé.

Abstract

The quantitative and qualitative analysis of the FDOM produced by phytoplankton and its comparison with that produced by bacteria is essential to better understand the distributions of CDOM in the oceans as well as the role of CDOM in the global carbon cycle. We examined the net uptake/release of coloured dissolved organic matter (CDOM) by a natural bacterial community growing on DOM exudates from four phytoplankton species cultured in axenic conditions. The species of phytoplankton DOM-producer did not influence the bacterial biomass yield. The phytoplankton exudates contained fluorescent humic- and protein-like substances. The humic-like substances excreted by phytoplankton (Ex/Em: 310 nm/392 nm; P. Coble's peak-M) were utilised by bacteria in different proportions depending on the phytoplankton species of origin; about 30% of the humic-like substances excreted by *S. costatum* were consumed while the percentages were reduced to 5% and 10% for *Chaetoceros* sp. and *M. pusilla*, respectively. Furthermore, bacteria produced humic-like substances that fluoresce at Ex/Em: 340 nm/440 nm (Coble's peak-C), i.e. more aromatic than those generated by phytoplankton. The induced fluorescent emission of the more aromatic CDOM produced by prokaryotes was significantly (p < 0.05) higher than that from the more aliphatic CDOM produced by eukaryotes. The final composition of the bacterial community growing on the exudates differed markedly depending on the phytoplankton species of origin. Among the bacterial group examined, *Alteromonas* and *Roseobacter* were the dominant bacterial groups during all the incubation on *Chaetoceros* spp. and *P. minimum* exudates, respectively. In *S. costatum* and *M. pusilla* exudates, the dominant bacterial group shifted during the course of the incubations. In the exponential growth phase, *Alteromonas* was the dominant group growing on *S. costatum* exudates, but it was replaced by *Roseobacter* afterwards. On *M. pusilla* exudates *Roseobacter* was replaced by *Bacteroidetes* after the exponential growth phase. The study of these fluorescence excitation-emission matrices in relation to different bacterial groups could be a step further in the characterization of DOM produced by bacteria and in the identification of the sources of DOM in the environment.

Chapter II

Introduction

Coloured dissolved organic matter (CDOM) is receiving increasing attention due to its important role in aquatic ecosystems. It regulates UV and visible light penetration in the water column thus influencing primary productivity (Arrigo and Brown, 1996) and preventing cellular DNA damage (Häder and Sinha, 2005; Herndl et al., 1993). CDOM can also form complexes with metals reducing the concentrations of free ions in seawater (Midorikawa and Tanoue, 1998). In addition, changes in the optical properties of CDOM are suitable to trace microbial and photochemical degradation processes (Nieto-Cid et al., 2006; Romera-Castillo et al., 2011, see Chapter IV) and, more specifically, the *in situ* formation of bio-refractory humic materials from bio-available DOM (Lønborg et al., 2010). Due to their optical properties, CDOM have also been the focus of remote sensing studies to map the global distribution and to correct the chlorophyll signal. The absorption spectrum of CDOM overlaps with that of chlorophyll *a*, affecting the satellite-derived estimates of phytoplankton biomass and activity in the oceans, especially in coastal areas (Siegel et al., 2002).

The fraction of CDOM that emits induced fluorescence light is called fluorescent dissolved organic matter (FDOM). Two main groups of fluorophores have been differentiated following Coble et al. (Coble et al., 1998): protein-like substances, which fluoresce around Ex/Em: 280 nm/350 nm (peak-T); and humic-like substances which fluoresce at two pairs of wavelengths, Ex/Em: 312 nm/380-420 nm of autochthonous (marine) origin (peak-M), and Ex/Em 340 nm/440 nm of allochthonous (terrestrial) origin (peak-C). Both peaks, -M and –C, have been found in samples from freshwater and seawater environments. However, a shift to longer wavelengths of the humic-like peaks in freshwater samples has been reported (Coble, 1996) because terrestrial humic substances are more aromatic than marine humic substances (Benner, 2003). Additionally, and independently of their origin, humic substances also fluoresce in the UV-C region of the spectrum, at Ex/Em: 250 nm/450 nm (Coble, 1996; Coble et al., 1998).

Humic materials have been traditionally considered photodegradable but resistant to bacterial degradation. In fact, when humic-like FDOM is not exposed to natural UV radiation levels, it can accumulate in the ocean at centennial to millennial time-scales within the global conveyor belt (Chen and Bada, 1992; Yamashita and Tanoue, 2008). Therefore, the formation of bio-resistant CDOM during the degradation of bio-available DOM would allow the sequestration of anthropogenic CO_2 in a dissolved organic form for hundreds to thousands of years, as part of the recently coined "microbial carbon pump" sequestration mechanism (Jiao et al., 2010).

Global carbon flux estimates require quantitative information about the degradation rates of biogenic organic matter. Although the bioavailability of phytoplankton exudates has been recurrently

studied (Obernosterer and Herndl, 1995; Sundh, 1992; Sundh and Bell, 1992), few works have dealt with the exudation of CDOM by phytoplankton (Romera-Castillo et al., 2010, see Chapter I). In fact, marine FDOM has been mainly considered a by-product of the bacterial metabolism (Chen and Bada, 1992; Nieto-Cid et al., 2006; Yamashita and Tanoue, 2008) until some recent studies have shown that it can be produced by zooplankton (Steinberg et al., 2004; Urban-Rich et al., 2006), krill (Ortega-Retuerta et al., 2009) and also by phytoplankton cells (Romera-Castillo et al., 2010, see Chapter I). Since phytoplankton is the most abundant organisms in terms of biomass among these FDOM producers. The analysis of the FDOM produced by phytoplankton and its comparison with that produced by bacteria is essential to better understand the role of CDOM in the global carbon cycle.

In addition, while bacterioplankton structure is modulated by the amount and quality of the available substrates (eg., (Pinhassi et al., 2004; Rooney-Varga et al., 2005), activity of different group of bacteria can shape organic matter composition. However, to the best of our knowledge, there is a lack of studies examining the changes in the fluorescence signal of the DOC and bacterial community composition in controlled conditions. Since fluorescence excitation-emission matrices are fingerprints of DOM structure, the study of these EEMs in relation to different bacterial groups could be a step further in the characterization of DOM produced by bacteria and in the identification of the sources of DOM in the environment.

The objective of the present work is to quantify the net production/consumption of CDOM by a natural bacterial community growing on exudates derived from four phytoplankton species (*Chaetoceros* sp., *Skeletonema costatum*, *Prorocentrum minimum* and *Micromonas pusilla*) cultured in axenic conditions. To this end, the time course of the induced fluorescent excitation-emission properties of CDOM was followed as well as its relationship with changes in the structure of the bacterial community. Moreover, we wanted to investigate whether the bacterial groups selected by the treatments can be associated to characteristic DOM fluorescent signals.

Material and methods

Phytoplankton cultures

Algal exudates were produced from axenic cultures of four phytoplankton species. The axenic species obtained from the Provasoli-Guillard National Center for Culture of Marine Phytoplankton (CCMP) (https://ccmp.bigelow.org/) were cultured in axenic conditions as described in Romera-Castillo et al. (2010, see Chapter I). The strains used were the diatoms *Chaetoceros* sp. (CCMP199) and *Skeletonema costatum* (CCMP2092) (Greville) Cleve, the dinoflagellate *Prorocentrum minimum*

(CCMP1329) (Pavillard) J. Schiller, and the prasinophyte *Micromonas pusilla* (R.W. Butcher) (CCMP1545) I. Manton and M. Parke. The four species produced significant amounts of FDOM (Romera-Castillo et al., 2010, see Chapter I).

The cultured volume (1.4 L) of each phytoplankton species was filtered through a 0.2 µm Sterivex cartridge and inoculated with 150 mL of natural seawater filtered twice through 0.6 µm polycarbonate filter to eliminate predators of bacteria, such as small flagellates. The inoculum was taken on 7 May 2008 from the Blanes Bay Microbial Observatory (http://www.icm.csic.es/bio/projects/icmicrobis/bbmo/). Then, each 1.55 L inoculated sample was distributed in 36 polycarbonate bottles of 60 mL filled with 40 mL of the inoculated exudates.

The bottles were incubated for 34 days and sampled at times 0 (T0), 4 (T4), 12 (T12), 21 (T21) and 34 days (T34). At each sampling time, 4 of the initial 36 bottles per treatment were sacrificed: three replicates were used for TOC, DOC and FDOM analysis and bacterial counts and one for Catalyzed reporter deposition Fluorescence In Situ Hybridization (CARD-FISH).

Bacterial community biomass and structure

Heterotrophic bacteria were counted in the four bottles with a FacsCalibur (Becton & Dickinson) flow cytometer equipped with a 15 mW Argon-ion laser (488 nm emission) as described in Gasol and del Giorgio (Gasol and Del Giorgio, 2000). For each sample, 4 mL of water were collected and fixed immediately with cold glutaraldehyde 10% (final concentration 1%), left in the dark for 10 min at room temperature and then stored at -80°C. Later, 400 µL of sample received a diluted SYTO-13 (Molecular Probes Inc., Eugene, OR, USA) stock (10:1) at 2.5 µmo L^{-1} final concentration, left for about 10 min in the dark to complete the staining and run in the flow cytometer. At least 30000 events were acquired for each subsample (usually 90000 events). Fluorescent beads (1 µm, Fluoresbrite carboxylate microspheres, Polysciences Inc., Warrington, PA) were added at a known density as internal standards. The bead standard concentration was determined by epifluorescence microscopy. Heterotrophic bacteria were detected by their signature in a plot of side scatter (SSC) vs. FL1 (green fluorescence). Data analysis was performed with the Paint-A-Gate software (Becton & Dickinson).

Bacterial cell size (V, in µm^3 cell^{-1}) was estimated using the relationship between the average bacterial size and the average fluorescence of the SYTO-13– stained sample relative to beads (FL1 bacteria/FL1 beads) reported by Gasol and del Giorgio (Gasol and Del Giorgio, 2000):

$$V = 0.0075 + 0.11 \cdot (FL1\ bacteria/FL1\ beads)$$

Bacterial biomass (BB, in Pg C cell^{-1}) was calculated by using the carbon-to-volume (V, in µm^3.cell^{-1})

relationship derived by Norland (Norland, 1993) from the data of Simon and Azam (Simon and Azam, 1989):

$$BB = 0.12 \cdot V^{0.7}$$

Bacterial community composition (BCC) was obtained by catalyzed reporter deposition fluorescent *in situ* hybridization (CARD-FISH). Three to five mL samples were fixed with paraformaldehyde (1% final concentration), and bacterial cells were collected onto 0.2 µm polycarbonate filters (Whatman) and kept at -80°C until hybridization. Four horseradish peroxidase probes were used, following the protocol of Pernthaler et al. (Pernthaler et al., 2004): ALT1413, CF319a, ROS537 and SAR11, targeting respectively the *Alteromonas*, the *Bacteroidetes*, the *Roseobacter* and SAR11 clades (further details in Sarmento & Gasol, submitted). The NON338 probe was used as a negative control. After permeabilization with lysozyme and achromopeptidase, several filter sections were cut and hybridized for 2h at 35°C (Pernthaler et al., 2004). Probe GAM42a was used with competitor oligonucleotides as described in (Manz et al., 1992). Filter portions were then counterstained with DAPI (1µg mL^{-1}) before enumeration with an epifluorescence microscope. A minimum of 10 fields per filter-portion were counted, and at least 400 cells per group were counted. The selected groups were expressed as a percentage relative to the total DAPI-stained bacterial cells.

Dissolved organic carbon (DOC) and fluorescent dissolved organic matter (FDOM)

Triplicate DOC and FDOM samples were filtered through GF/F filters with an acid-cleaned syringe. Milli-Q water was filtered through the filtration system and no significant enrichment was observed in DOC and FDOM concentrations, discarding contamination during filtration.

Approximately 10 mL of water were collected in pre-combusted (450ºC, 12 h) glass ampoules for DOC analysis. H_3PO_4 was added to acidify the sample to pH < 2 and the ampoules were heat-sealed and stored in the dark at 4ºC until analysis. DOC was measured with a Shimadzu TOC-V organic carbon analyser. The system was standardized daily with potassium hydrogen phthalate. Each ampoule was injected 3–5 times and the average area of the 3 replicates that yielded a standard deviation <1% were chosen to calculate the average DOC concentration of each sample after subtraction of the average area of the freshly-produced UV-irradiated milli-Q water used as a blank. The performance of the analyser was tested with the DOC reference materials provided by Prof. D. Hansell (University of Miami). We obtained a concentration of 45.2 ± 0.3 µmol C L^{-1} for the deep ocean reference (Sargasso Sea deep water, 2600 m) minus blank reference materials, the day when the samples were analyzed. The nominal DOC value provided by the reference laboratory (Certified Reference Materials for DOC analysis, Batch 04, 2004) is 45 µmol C L^{-1}.

Samples for FDOM analysis were measured immediately after collection. Single measurements at specific excitation-emission wavelengths as well as excitation-emission matrices (EEMs) of the aliquots were performed with a LS 55 Perkin Elmer Luminescence spectrometer, equipped with a xenon discharge lamp, equivalent to 20 kW for 8 μs duration. The detector was a red-sensitive R928 photomultiplier, and a photodiode worked as reference detector. Slit widths were 10.0 nm for the excitation and emission wavelengths and the scan speed was 250 nm min^{-1}. Measurements were performed at a constant room temperature of 20°C in a 1 cm quartz fluorescence cell. To compare with other works, the Ex/Em wavelengths used for single measurements were those established by Coble (Coble, 1996): Ex/Em: 280 nm/350 nm (peak T or $F(280/350)$) as indicator of protein-like substances and Ex/Em: 320 nm/410 nm (peak M or $F(320/410)$) and Ex/Em: 340 nm/440 nm (peak C or $F(340/440)$) as indicators of humic-like substances. Following Coble (Coble, 1996), fluorescence measurements were expressed in quinine sulphate units (QSU), i.e., in μg eq QS L^{-1}, by calibrating the LS 55 Perkin Elmer at Ex/Em: 350 nm/450 nm against a quinine sulphate dihydrate (QS) standard made up in 0.05 mol L^{-1} sulphuric acid.

EEMs were performed to track for possible changes in the position of the protein- and humic-like fluorescence peaks. These matrices were generated by combining 21 synchronous Ex/Em fluorescence spectra of the sample, obtained for excitation wavelengths from 250 to 400 nm and an offset between the excitation and emission wavelengths of 50 nm for the 1st scan and 250 nm for the 21st scan. Rayleigh scatter does not need to be corrected when the EEMs are generated from synchronous spectra and Raman scatter was corrected by subtracting the EEM of pure water (Milli-Q) from the EEM of the sample.

Paired Student-t-test was used to check for significant differences in the measured variables between, the initial, intermediate and final incubation times (Sokal and Rohlf, 1984).

Results

Time course of bacterial biomass

Bacterial biomass (BB) increased similarly in the four cultures throughout the initial 4 days of exponential growth (Fig. 1) reaching concentrations that ranged from 204 ± 17 to 244 ± 8 μg C L^{-1}. It kept increasing until day 12 only in the treatment
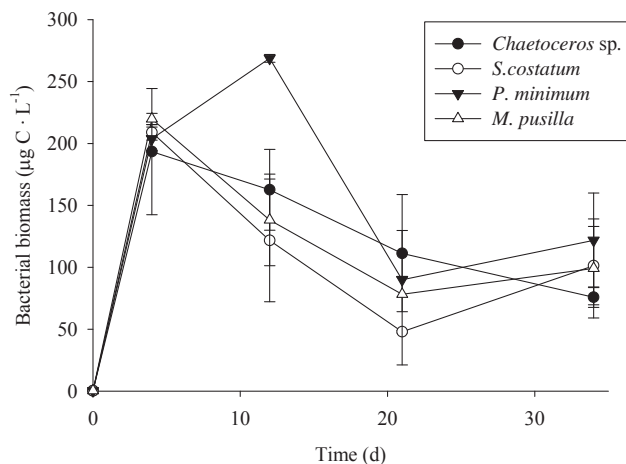

Fig. 1. Bacterial biomass (BB) during the incubation time.

with *P. minimum* exudates, reaching 269 ± 5 μg C L^{-1}. Bacterial biomass decreased significantly (p > 0.05) after day 4 except on P. minimum exudates, where it decreased after day 12. No significant changes were observed from day 12 until the end of the experiment in the rest of cultures.

Time course of dissolved organic carbon

Two phases can be distinguished in the time course of DOC concentrations (Fig. 2a). A sharp decrease of DOC occurred during the initial 4 days of bacteria exponential growth. The percentage of remained DOC regarding the initial concentration ranged from 47.1 ± 0.3 % to 59.5 ± 0.8 %. Diatom exudates presented the most abrupt DOC decrease and *P. minimum* exudates presented the smallest one. In the second phase, from day 4 to 34, DOC concentrations tended to increase significantly until final stagnation or small decrease.

Time course of fluorescent CDOM

To account for the net production/consumption of any CDOM fluorophore after 4 days of exponential growth, the fluorescence excitation-emission matrices (EEMs) at T0 were subtracted from the corresponding EMMs at T4 for each culture. At T4, all EEMs showed the production of a humic-like fluorophore that peaked around Ex/Em: 354 nm/424 nm (Figs. 3b, 4b, 5b and 6b); i.e. Coble's peak-C (Coble et al., 1998). After 34 days of incubation, peak-C was still present in the EEMs of all the cultures but its fluorescence intensity had increased (Figs. 3c, 4c, 5c and 6c). On the contrary, a second humic-like fluorophore that peaked around Ex/Em: 310 nm/392, Coble's peak-M (Coble et al., 1998), decreased after 4 days of exponential growth in 3 of the 4 cultures (Figs. 3b, 4b and 6b). In the *P. minimum* exudates peak-M took a bit longer to diminish (Figs. 5b and c).

Coble's UV protein-like peak-T (Coble et al., 1998), which peaks at around Ex/Em: 275 nm/ 361 nm, was also present in the exudates of the four phytoplankton species (Figs. 3a, 4a, 5a and 6a).

Table 1. Initial values of average bacterial biomass (BB), dissolved organic carbon (DOC), and fluorescence of CDOM at peak-M, peak-C and peak-T. Average ± SD values are reported.

Bacteria growth on exudates of	BB (μg C L^{-1})	DOC (μmol C L^{-1})	peak-M (QSU)	peak-C (QSU)	peak-T (QSU)
Chaetoceros sp.	0.41 ± 0.02	287.8 ± 2.2	3.12 ± 0.06	2.07 ± 0.01	4.32 ± 0.04
S. costatum	0.23 ± 0.03	304.5 ± 0.4	4.73 ± 0.01	2.22 ± 0.00	4.05 ± 0.02
P. minimum	0.31 ± 0.05	304.9 ± 1.0	2.96 ± 0.02	1.97 ± 0.03	3.77 ± 0.06
M. pusilla	0.35 ± 0.02	242.1 ± 0.6	3.00 ± 0.01	2.03 ± 0.02	2.91 ± 0.02

After 4 days of incubation, the intensity of peak-T increased in the cultures grown on *S. costatum*, *M. pusilla* and *P. minimum* exudates (Fig. 4b, 5b and 6b) but decreased slightly in the culture grown on *Chaetoceros* sp. exudates (Fig. 3b). In addition, all the EEMs showed the production of the Coble's UV humic-like peak-A (Coble et al., 1998) at around 261 nm/463 nm (Fig. 3b, 4b, 5b and 6b).

Changes in the intensity of peaks C, M and T, relative to values at T0, during the course of the incubations are presented in Fig. 2 for an easier comparison between the exudates of the different phytoplankton species. The initial values of these parameters are summarised in Table 1. Peak-C increased significantly (p < 0.001) until T21 in all cultures (Fig. 2b) with the highest variation during the first four days; the corresponding net production rates are summarised in Table 2. On the contrary, peak-M increased significantly ($p < 0.05$) only in the *P. minimum* exudates culture (Fig. 2c). For the other 3 species, a significant decrease ($p < 0.05$) occurred during the initial 4 days of incubation. The most pronounced decrease, by 30%, was observed in the culture grown on *S. costatum* exudates, prolonged until the end of the experiment. During the stationary phase, peak-M experienced a significant ($p < 0.05$) increase only from T12 to T21. Net bacterial production rates of peaks C and M per unit of carbon biomass and day were calculated for all treatments, during the exponential phase, to compare them with the net production rates of humic-like substances by marine phytoplankton during the exponential growth already obtained by Romera-Castillo et al. (2010, see Chapter I). We obtained net productions of peak-C between $15 \pm 2 \times 10^{-4}$ and $63 \pm 2 \times 10^{-4}$ QSU µg C^{-1} L d^{-1} and the highest net consumption of peak-M, $-117 \pm 4 \times 10^{-4}$ QSU µg C^{-1} L d^{-1}, corresponded to the bacteria grown on *S. costatum* exudates.
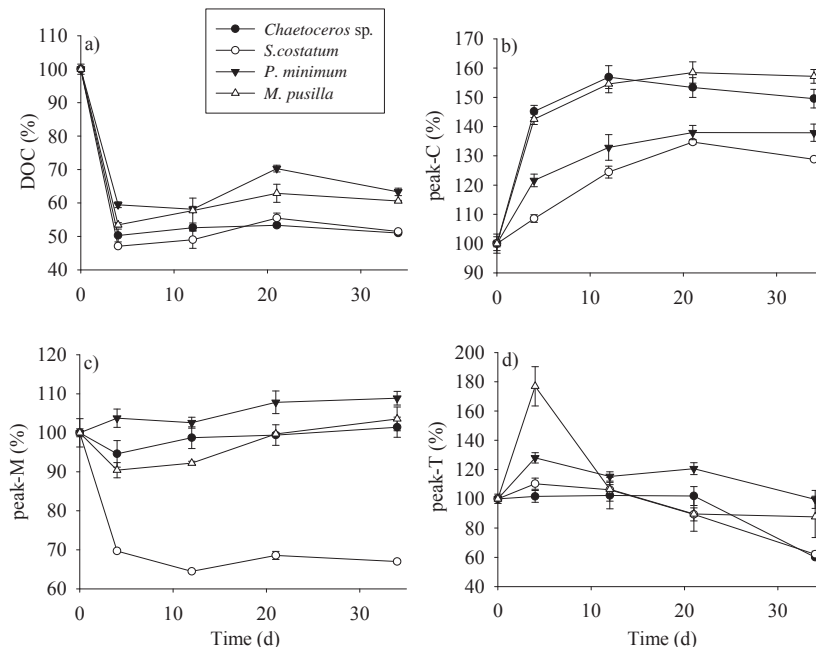

Fig.2. Percentages of a) DOC, b) peak-C ($F(340/440)$), c) peak-M ($F(320/410)$) and d) peak-T ($F(280/350)$) regarding to their initials values for all the incubations times.

In general, peak-T increased significantly in all cultures during the exponential growth phase (T4) and, then, decreased up to the end of the experiment (Fig. 2d). The bacterial culture on *M. pusilla* exudates underwent the largest increase (77%). However, *Chaetoceros* sp. did not show a significant variation of peak-T until the end of the incubation time (T34) when it sharply decreased by 41%. The net production of peak-T per carbon biomass and day ranged between 5 ± 5 x 10^{-4} and 164 ± 19 x 10^{-4} QSU µg C^{-1} L d^{-1}.

Time courses of bacterial community structure

The most abundant groups of bacteria were identified and counted by CARD-FISH to examine their response to the different substrates generated by the four phytoplankton species tested in this work (Fig. 7). Initial values of these bacterial groups were 2.49 x 10^4 cells mL^{-1}, 6.42 x 10^4 cells mL^{-1}, 1.21 x 10^6 cells mL^{-1} and 2.37 x 10^6 cells mL^{-1} for SAR11, *Alteromonas*, *Roseobacter* and *Bacteroidetes*, respectively. In *Chaetoceros* sp. exudates, *Alteromonas* was the dominant bacterial group during the course of the incubation. Among the studied groups on *S. costatum* exudates, *Alteromonas* was the dominant during the first 4 days, but it was replaced by *Roseobacter* thereafter. *Roseobacter* was also the dominant group in *P. minimum* exudates during all the incubation time. In *M. pusilla* exudates, *Roseobacter* was the most abundant group during the exponential phase but *Bacteroidetes* prevailed after T12. Subtracting the cell abundance of each group at T0 from T4, we observed that *Alteromonas* was the group that developed better on diatom exudates (1.1 x 10^6 cells mL^{-1} d^{-1} and 7.3 x 10^5 cells mL^{-1} d^{-1}, for *Chaetoceros* sp. and *S. Costatum*, respectively) while it was *Roseobacter* in the case of the *P. minimum* (9.1 x 10^5 cells mL^{-1} d^{-1}) and *M. pusilla* (3.4 x 10^5 cells mL^{-1} d^{-1}) exudates. SAR11, which was present at T0, decreased throughout the incubations in all exudates.

Table 2. Bacterial versus phytoplankton net production of dissolved organic carbon (DOC) and fluorescent CDOM in the four cultures during the exponential phase. B is average biomass of each kind of organism; t is time of incubation during the esponential phase.

	B from	ΔDOC/ (B·t)	Δpeak-T/ (B·t)	Δpeak-M/ (B·t)	Δpeak-C/ (B·t)
	Ti-T4	(µg C µg C^{-1} d^{-1})	(QSU µg C^{-1} L d^{-1})	(QSU µg C^{-1} L d^{-1})	(QSU µg C^{-1} L d^{-1})
Bacteria grown on					
Chaetoceros sp.	38.2 ± 0.8	-11.3 ± 0.4	5 ± 5 x 10^{-4}	-11 ± 3 x 10^{-4}	61 ± 2 x 10^{-4}
S. costatum	30.7 ± 1.0	-15.77 ± 0.08	34 ± 7 x 10^{-4}	-117 ± 4 x 10^{-4}	15 ± 2 x 10^{-4}
P. minimum	31.4 ± 1.6	-11.8 ± 0.2	84 ± 8 x 10^{-4}	9 ± 3 x 10^{-4}	34 ± 3 x 10^{-4}
M. pusilla	34.1 ± 0.8	-9.9 ± 0.1	164 ± 19 x 10^{-4}	-21 ± 3 x 10^{-4}	63 ± 2 x 10^{-4}
Production by					
Chaetoceros sp.		116 ± 11 x 10^{-3}	9.1 ± 0.8 x 10^{-4}	4.8 ± 0.1 x 10^{-4}	2.4 ± 0.05 x 10^{-4}
S. costatum		93 ± 13 x 10^{-3}	5.8 ± 0.1 x 10^{-4}	4.5 ± 0.1 x 10^{-4}	1.3 ± x 0.02 10^{-4}
P. minimum		97 ± 9 x 10^{-3}	3.2 ± 0.2 x 10^{-4}	1.3 ± 0.03 x 10^{-4}	0.8 ± 0.04 x 10^{-4}
M. pusilla		86 ± 5 x 10^{-3}	2.6 ± 0.02 x 10^{-4}	3.0 ± 0.1 x 10^{-4}	1.7 ± x 0.02 10^{-4}

Discussion

Net production/consumption of DOC and CDOM by marine bacteria

The growth of the natural bacterial community (ΔBB) was not significantly different ($p > 0.05$) among the four treatments amended with exudates of different phytoplankton species. Bacterial carbon consumption, during the exponential growth phase, was quite similar for the four phytoplankton exudates tested in this work; it ranged between $41 \pm 4\%$ and $53 \pm 2\%$ of the initial DOC. These proportions are similar to the 48% of labile DOM found by Puddu et al. (Puddu et al., 2003) in phytoplankton exudates obtained growing the diatom *Cylindrotheca closterium* in a nutrient balanced medium. On the contrary, the proportion of bioavailable FDOM excreted by phytoplankton was extremely different depending on the species: $30 \pm 0.3\%$ of the marine humic-like substances (peak-M) excreted by *S. costatum* were bioavailable while the proportion decreased to $5 \pm 2\%$ and $10 \pm 2\%$ in *Chaetoceros* sp. and *M. pusilla*, respectively. Since the incubations were performed in the dark, photo-bleaching of peak-M can be discarded. Previous works have demonstrated that bacteria can take up humic substances retained by XAD resins (Bussmann, 1999; Hunt et al., 2000). Indeed, during periods of low primary production bacteria seem to use humic substances as a substrate (Rosenstock et al., 2005; Sundh and Bell, 1992). Shimotori et al. (2009) also observed a decrease of the FDOM measured at Ex/Em 315 /410 nm (equivalent to peak-M) in their bacterial cultures, but only from incubation times of 20 to 30 days, when bacterial number started to decay. Their incubations consisted in artificial seawater amended with inorganic nutrients and glucose and inoculated with a natural bacterial community. They attributed the FDOM uptake by bacteria in the stationary phase to the depletion of the amended glucose, the only carbon source for bacterial growth in their cultures. In our experiment we used phytoplankton exudates that are known to be rich in carbohydrates (Myklestad, 2000) and the FDOM decrease that we observed occurred during the exponential growth phase of the experiments. Given the lability of the fresh materials exuded by phytoplankton, full consumption of the exuded carbohydrates and the subsequent utilisation of marine humic-like substances could have occurred in the short time elapsed between T0 and T4. It has been shown that humic substances retained by XAD resins can be adsorbed onto bacterial surfaces, although this adsorption is negligible at pH typical of marine waters for the number of bacteria that our incubation reached (Fein et al., 1999). The peak-M fluorophore consumed by bacteria in our experiment had been previously produced by phytoplankton (Romera-Castillo et al., 2010, see Chapter I). Therefore, phytoplankton cells exude fluorescence humic-like substances that are readily bioavailable to microbial degradation.

The different behaviour of peak-M and peak-C during the exponential phase of our incubations suggests a different origin and fate for both fluorophores. Peak-C was produced continuously in all cultures while peak-M was consumed during the exponential and produced during the senescence
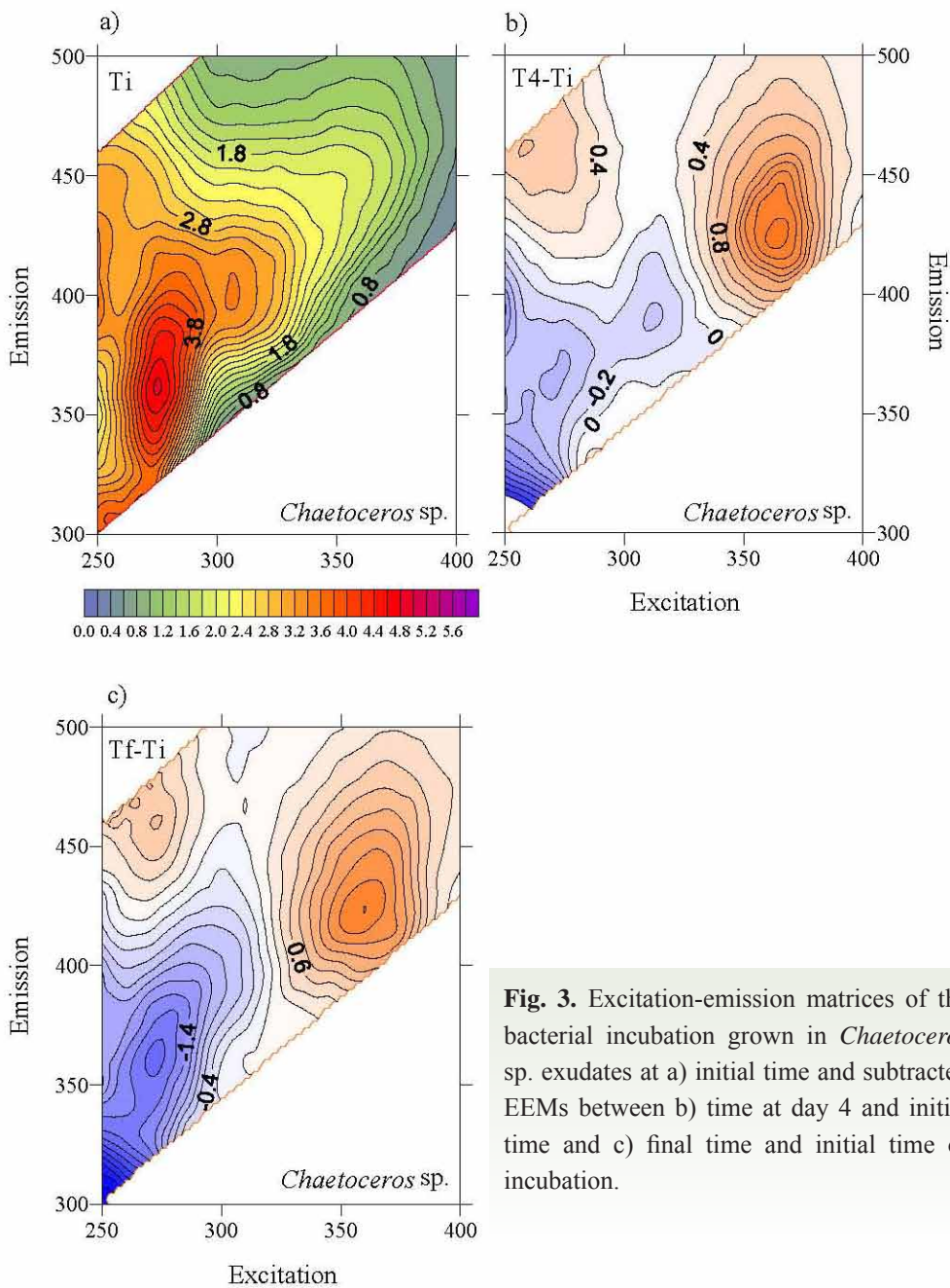
Fig. 3. Excitation-emission matrices of the bacterial incubation grown in *Chaetoceros* sp. exudates at a) initial time and subtracted EEMs between b) time at day 4 and initial time and c) final time and initial time of incubation.
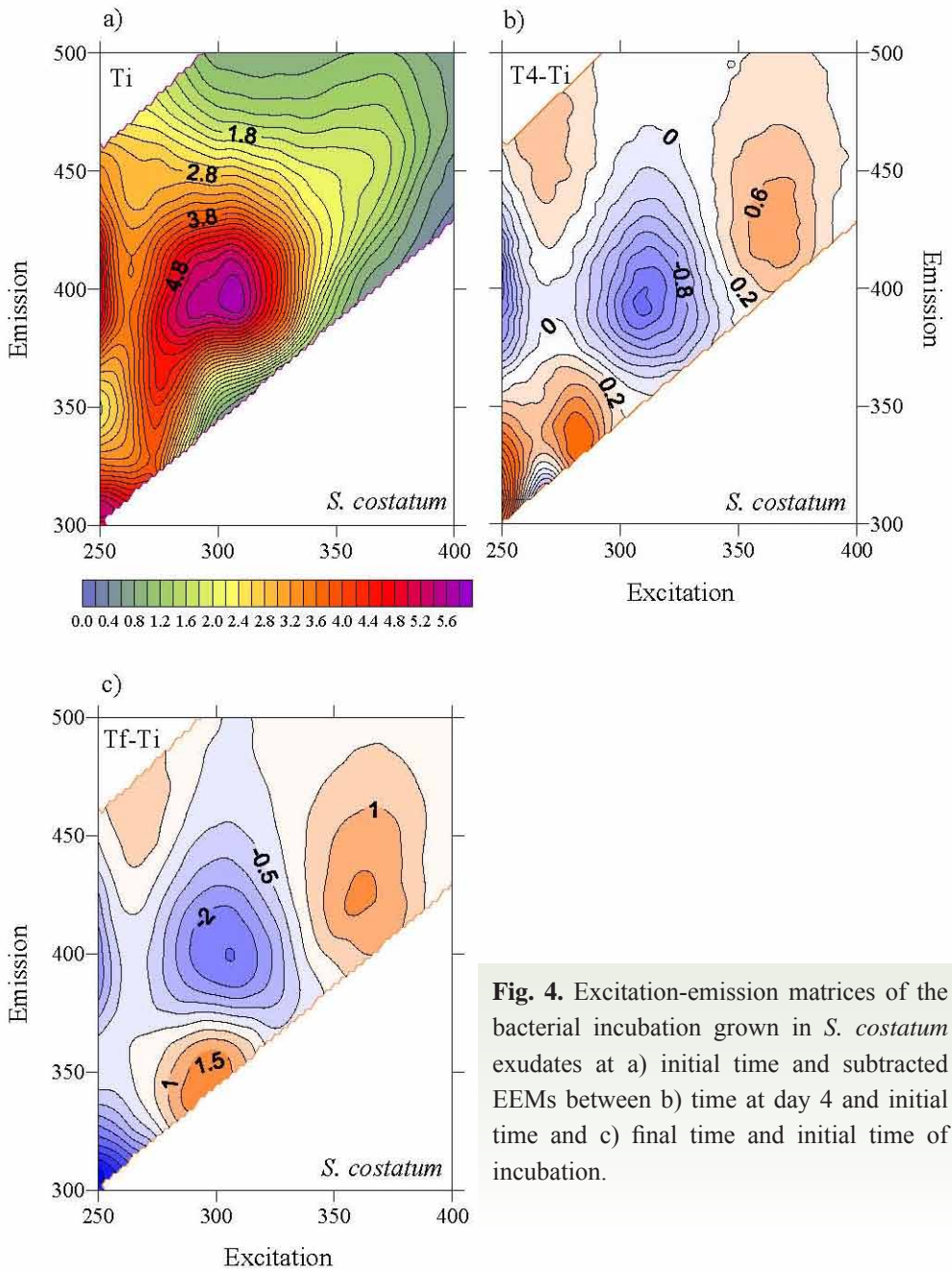
Fig. 4. Excitation-emission matrices of the bacterial incubation grown in *S. costatum* exudates at a) initial time and subtracted EEMs between b) time at day 4 and initial time and c) final time and initial time of incubation.

phase of the bacterial cultures. Since the ratio peak-M/peak-C did not change significantly from T12 onwards, it is likely that the fluorescence intensity observed at the Ex/Em wavelengths of peak-M during the senescence phase was mostly due to peak-C tailing.

Regarding peak-T, the release of this fluorophore by marine bacteria has been previously reported (Cammack et al., 2004). In our study, peak-T tended to increase during the exponential growth phase in almost all cultures and decreased after the bacterial populations reached the stationary growth phase. A similar pattern was observed by Cammack et al. (2004) in incubation experiments performed in lake waters of different trophic status. They suggested that peak-T reflects the balance between bacterial consumption and production of a small fraction of the DOM pool and that it could be a by-product of bacterial metabolism. The significant positive correlation that we found between peak-T and bacterial biomass ($R^2 = 0.40$; $p < 0.01$; $N = 16$) supports this statement. Kawasaki and Benner (Kawasaki and Benner, 2006) also found an increase of total dissolved amino acids (TDAA) matching a peak in bacterial biomass. This is consistent as well with our results since protein-like material increased, in general, during the bacterial exponential growth phase. However, since we have used GF/F filters that could have not retained 100% of the BB, a partial contribution of the aromatic amino acids contained in cells to the peak-T signal cannot be discarded.

Wavelength shifts in EEMs as indicators of changes in the chemical structure of CDOM

EEMs provide complementary information about the chemical structure, specially the aromaticity, of the FDOM produced or consumed by marine phytoplankton and bacteria. In all cultures except in that of *Chaetoceros* sp. bacteria produced protein-like substances and the peak-T shifted to slightly longer excitation and shorter emission wavelengths than the peak-T reported by Coble (Coble et al., 1998). Tryptophan is the most fluorescent of the three aromatic amino acids: tryptophan, tyrosine and phenylalanine (Lakowicz, 1983). Therefore, the fluorescence observed in the protein-like region should mainly due to the presence of this amino acid. The wavelength of the emitted light is a better indicator of the chemical environment of the fluorophore than the intensity. Tryptophan residues which are exposed to water have maximum fluorescence at emission wavelengths of about 340-350 nm, whereas totally buried residues (e.g., being part of peptides) fluoresce at about 330 nm (Lakowicz, 1983). The maximum intensities in the peak-T region found in our bacterial cultures, presented an Ex/Em maximum at 280 nm / 335 nm, which is an indication of the release of aromatic amino-acids by bacteria in a more buried combined form (e.g., bound to peptides) rather than in a free form. That maximum matches with the fluorescence maximum of the enzyme nuclease (Ex/Em 280 nm/334 nm, (Lakowicz, 1983). This exoenzyme could have been excreted by bacteria to hydrolyze DNA and consume their products (Paul et al., 1988). It differs from the protein-like substances excreted by phytoplankton since the maximum peak produced by three species of phytoplankton in that region was at Ex/Em 275 nm/358 nm (Romera-Castillo et al., 2010, see Chapter I).

At the same time of our incubations, a control test with Blanes Bay seawater filtered through 0.2 μm and inoculated with the same bacterial community than we used to inoculate the treatments was performed. In this control test, bacteria produced protein-like substances with a longer emission maximum wavelength (358 nm) than those grown on phytoplankton exudates. This could mean either that bacteria release different products depending on what they consumed as resource or that specific bacterial types, which release protein fluorescing at these wavelengths, have been selected in the control treatment, due to the substrate conditions. The later hypothesis is supported by the fact that CARD-FISH analyses showed differences in bacterial community composition depending on the phytoplankton species that produced the exudates. Indeed, the bacterial community selected in the control test was different from the one developing in the treatments with phytoplankton exudates (i.e. no *Bacteroidetes* appeared until T5, data not shown).

Polypeptides are part of the dissolved combined amino acids (DCAA) pool and some authors have reported that protein and DCAAs are relatively more important as bacterial substrates than DFAAs (Coffin, 1989; Keil and Kirchman, 1999; Kroer et al., 1994; Rosenstock and Simon, 1993), although others reported DFAA to be the preferred substrate by bacteria (Keil and Kirchman, 1993). Using radiolabelled proteins to examine the relative significance of protein versus DFAAs as bacterial substrates, Kiel and Kirchman (1993) found that bacteria preferred proteins in the oligotrophic Sargasso Sea (Keil and Kirchman, 1999), but DFAAs in the eutrophic Delaware Bay (Keil and Kirchman, 1993). Since our treatments with phytoplankton exudates were performed in nutrient-rich conditions, bacteria could have used DFAA and released peptides. Moreover, nutrients were in very low concentrations in the control treatment, where the released protein-like substances presented its emission maximum at 358 nm, which is characteristic of a free tryptophan residue.

Production of humic-like substances: marine phytoplankton *versus* marine bacteria

Peak-M has traditionally been associated to the humic materials produced in situ in marine ecosystems since the EEMs of natural seawater samples usually present a fluorescence maximum in that region. In contrast, the EEMs of natural samples with a predominant terrestrial origin present a fluorescence maximum at peak-C, shifted to significantly longer excitation and emission wavelengths than peak-M (Coble et al., 1998). Therefore, in our culture experiments with marine bacteria growing on marine phytoplankton exudates, production of peak-M fluorescence should be expected. However, our study demonstrates that the main humic-like fluorophore produced by marine bacteria grown on marine phytoplankton exudates was peak-C.
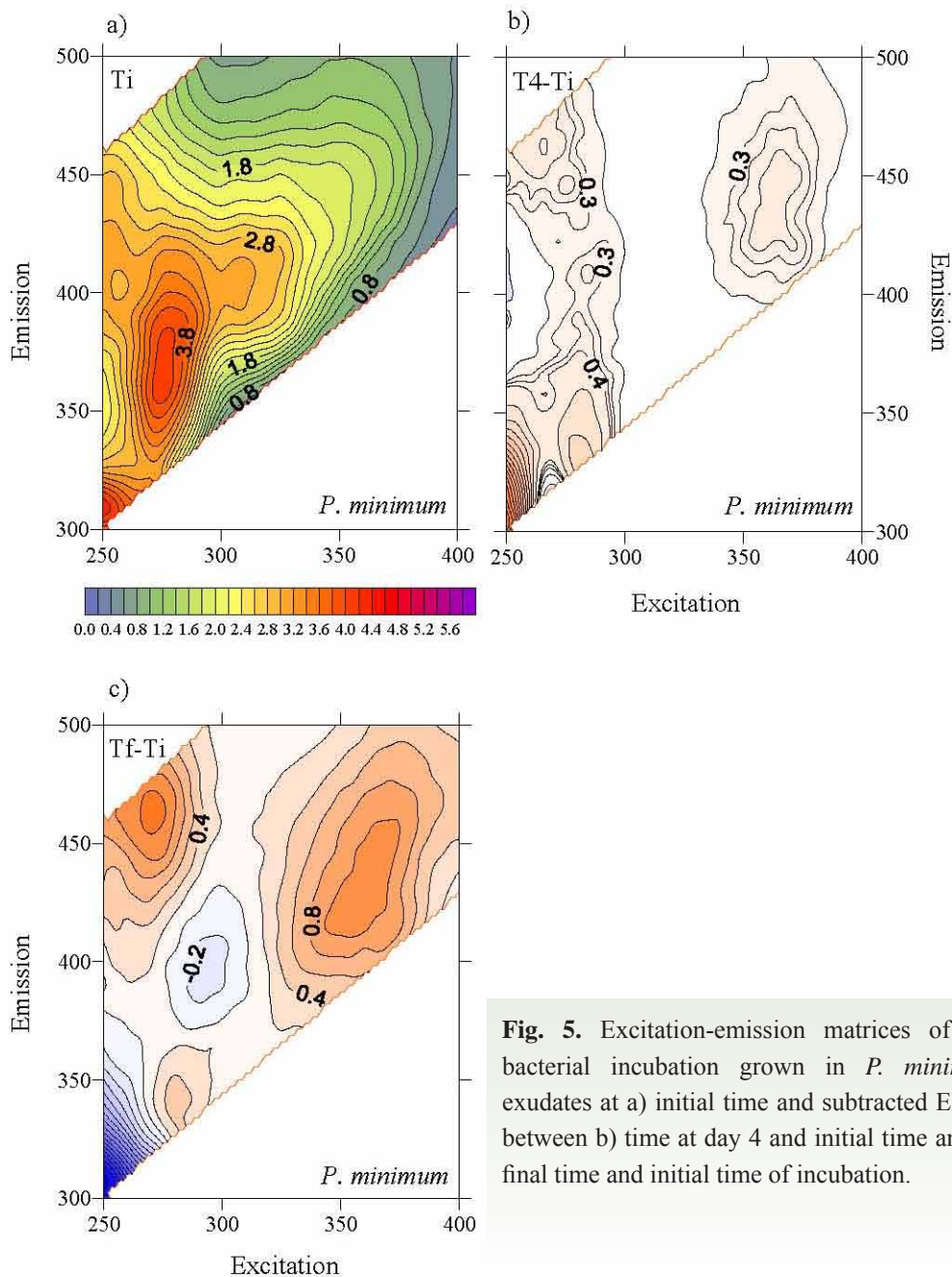
Fig. 5. Excitation-emission matrices of the bacterial incubation grown in *P. minimum* exudates at a) initial time and subtracted EEMs between b) time at day 4 and initial time and c) final time and initial time of incubation.
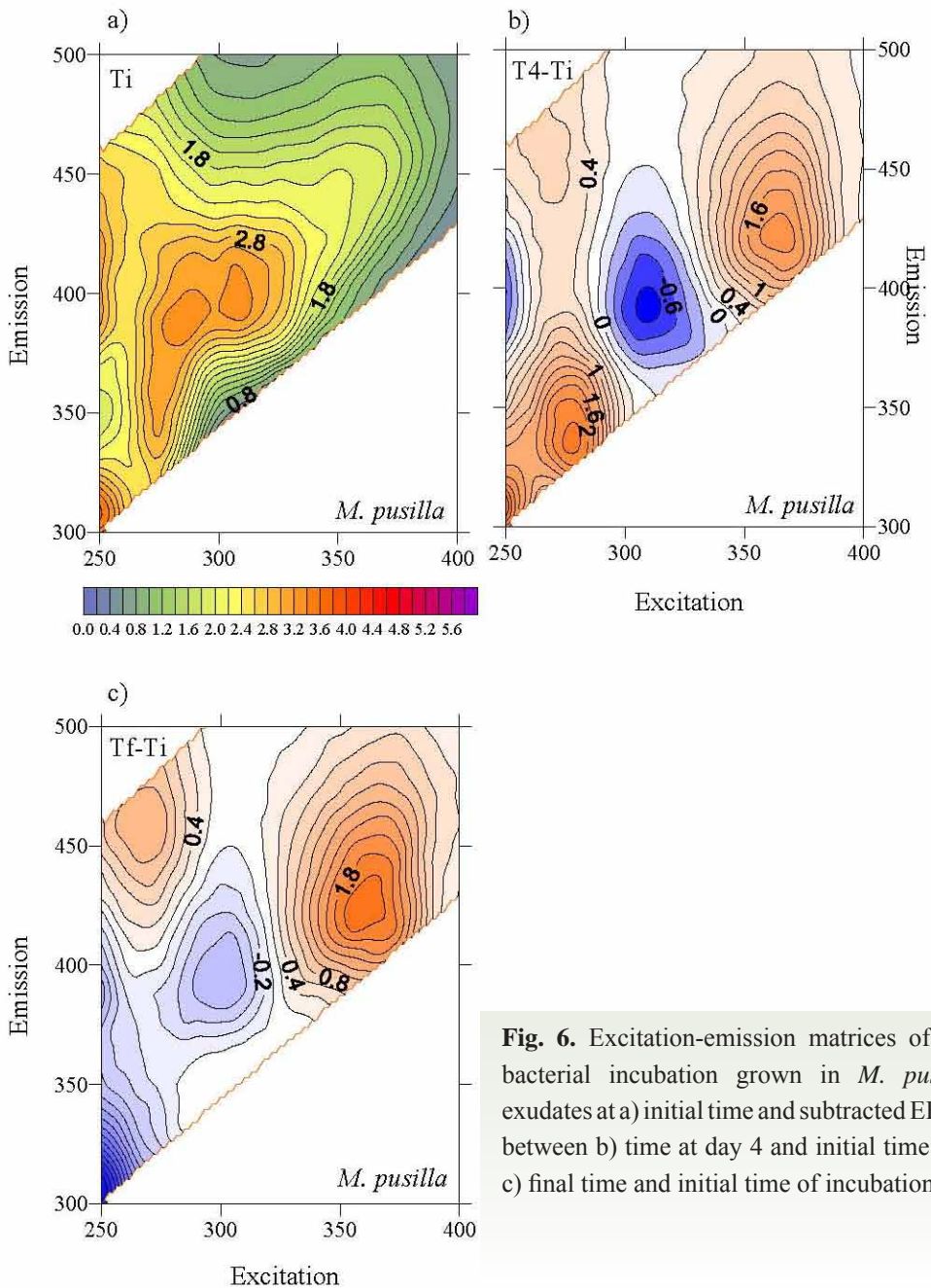
Fig. 6. Excitation-emission matrices of the bacterial incubation grown in *M. pusilla* exudates at a) initial time and subtracted EEMs between b) time at day 4 and initial time and c) final time and initial time of incubation.

Furthermore, our results show that marine phytoplankton is able to produce substances fluorescing at peak-M, which are consumed or transformed by marine bacteria that, in turn, produce other humic-like substances that fluoresce at peak-C, at significantly longer wavelengths. Any shift of a humic-like fluorescent emission maximum to longer wavelengths is an unequivocal indication of increased aromaticity and poly-condensation of humic materials (Chen et al., 2003). Therefore, attending to the position of both humic-like peak maxima, humic materials exuded by phytoplankton are more aliphatic (blue shifted) than the more aromatic humic materials produced by bacteria (red shifted). This does not necessarily mean that phytoplankton does not exude fluorescent substances in the Peak-C region; in fact, Romera-Castillo et al. (2010, see Chapter I) reported the production of this peak by *M. pusilla*, although maximum production was observed in the peak-M region. Preferential consumption of peak-M by marine bacteria concurs with other studies that reported a higher bioavailability with increasing aliphatic carbon moieties in a compound (Moran and Hodson, 1990; Sun et al., 1997).

Considering our results, we could hypothesise that the more aliphatic humic-like substances that fluoresce at peak-M are mostly produced as a by-product of the eukaryotes metabolism. Conversely, the more aromatic substances fluorescing at peak-C could be associated to prokaryotes by-products. This hypothesis is also supported by the evidence that copepods exude humic-like substances that fluoresce at peak-M (Urban-Rich et al., 2006) and that a strong signal in the peak-C region was found in cultures of *Synechoccocus* and *Procloroccocus* (data not shown). Furthermore, it has been reported that FDOM intensity at peak-M is higher in the euphotic zone (Coble, 1996), where phyto and microzooplankton are also abundant, and decreases with depth. However, the intensity of peak-C- increases with depth (Coble, 1996) and it is widely known that organic matter transformations in the twilight zone are dominated by bacterial activity which could generate higher fluorescence at this peak.

In general, the production of peaks T and C normalized to the bacterial biomass, during the exponential growth phase was about one order of magnitude higher for marine bacteria than for marine phytoplankton. This fact could explain the lack of correlation between chlorophyll and CDOM that some authors have reported (Nelson et al., 1998; Rochelle-Newall and Fisher, 2002), which they attributed to the in situ production of CDOM by bacteria concluding that phytoplankton was not a direct source of CDOM. Indeed, the consumption of the peak-M fluorophore by bacteria also contributes to reduce the expected correlation between phytoplankton biomass and CDOM.

Selection of bacterial groups growing on different phytoplankton exudates

Different bacterial groups were selected depending on the phytoplankton exudates on which they grew. This agrees with previous studies that concluded that bacterioplankton structure is determined by the amount and quality of the substrates available in the ecosystem (e.g., (Pinhassi et al., 2004; Rooney-Varga et al., 2005). It is well known that both SAR11 and *Roseobacter* are specialised in processing low

molecular weight organic substrates (Alonso and Pernthaler, 2006; Del Giorgio and Gasol, 2008; Moran et al., 2003), but the former prevail in oligotrophic and the latter in meso- and eutrophic environments (Fuhrman and Hagström, 2008). On the other hand, the group *Bacteriodetes* is specialised in processing high molecular weight organic substrates (Kirchman, 2004; Teira et al., 2008).

With these general considerations in mind, it can be straightforwardly explained why SAR11, which was present in the natural bacterial community of the (oligotrophic) Blanes Bay Observatory water that we used as inoculum, was not selected in any of our (eutrophic) cultures. The fact that after 4 days of incubation the highest cells numbers corresponded to the group *Alteromonas* grown on *Chaetoceros* sp. exudates could be the result of the production, by this diatom species, of a specific substrate, in which *Alteromonas* is specialised. Sarmento and Gasol (unpublished results), in short time (24h) incubations, have also found that the DOC from *Chaetoceros* sp. exudates was a highly
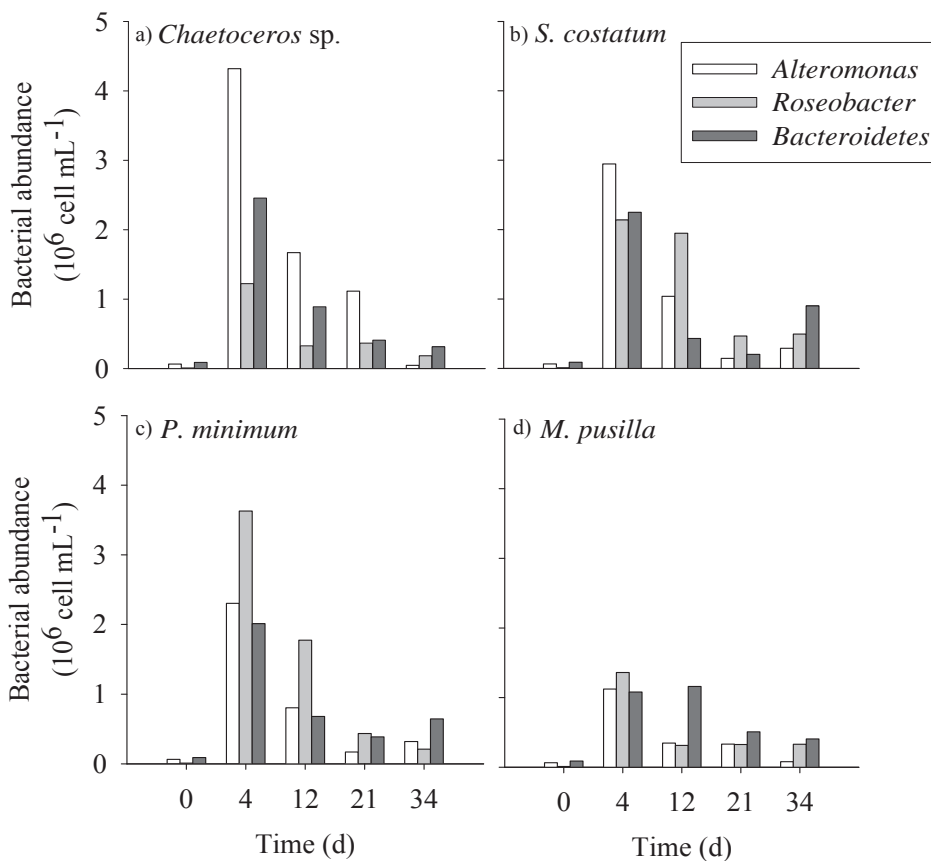

Fig. 7. Bacterial abundance of the main bacterial groups found in the exudates cultures of a) *Chaetoceros* sp., b) *S. costatum*, c) *P. minimum* and d) *M. pusilla*.

bioavailable substrate and that *Alteromonas* was again the bacterial group preferentially selected. Even if Schäfer et al. (2002) did not find *Gammaproteobacteria* in 6 mono-algal diatom non-axenic cultures, our work indicates that this class can also be associated with diatoms.

We did not observe significant correlations between humic-like peaks and bacterial numbers probably due to some factors: 1) humic-like peaks seem to present a different behaviour depending on the bacterial growth phase; 2) sometimes peak-M and peak-C tailings are overlapped to each others making the distinction between both peaks difficult. Therefore, if these correlations are hardly observed in lab experiments in a natural system these observations will be very difficult to see.

However, we observed a significant linear correlation between peak-T and bacterial biomass ($R^2 = 0.80$, $p < 0.001$, n = 20) when data from all times and all cultures are plotted together. Also the abundances of the bacterial groups *Roseobacter*, *Alteromonas* and *Bacteroidetes* cell numbers were significantly and positively correlated with the fluorescence intensity of peak-T: ($R^2 > 0.6$ $p < 0.01$, n = 20) although this correlation could be due to the good relationship between these bacterial groups and total bacterial biomass. This correlation had previously been observed in the Ría de Vigo (Teira et al., 2009) and could be indicative of the excretion of protein materials by bacteria.

Suzuki et al (2001) found that the growth of members of the *Flavobacteriaceae* (subgroup of *Bacteroidetes*) was not affected when inorganic nitrogen was excluded from the medium. These authors suggested this observation to indicate that these bacteria could utilize amino acids as sole nitrogen source. Others studies reported that this group of bacteria notably grow when abundant amounts of dissolved proteins are available (Cottrell and Kirchman, 2000; Pinhassi et al., 1999). In our experiment, the negative correlation found between the variation of peak-T (Δpeak-T) and the variation of *Bacteroidetes* (Δ*Bacteroidetes*) during the exponential phase supports this observation. Moreover, in the *M. pusilla* exudates, the largest amount of protein-like substances was produced during the exponential bacterial growth phase (Table 2, Fig. 2d). These protein-like substances were likely in the form of proteins rather than as free amino acids according to the shift of peak-T observed in the EEM (Fig. 5b). This could also explain the dominance of *Bacteroidetes* after T12 in the sample grown on *M. Pusilla* exudates.

Even if the fact that the phytoplankton exudates influence bacterial community composition in each treatment is observable from our results, the association of each bacterial group with a particular fluorescent humic-like peak is not clear. More studies are needed to asses it but from our results it could be suggested that the production of humic-like fluorescent material is a by-product of bacteria metabolism in general and not due to the activity of particular bacterial group(s).

Conclusions

Marine phytoplankton exudates contain fluorescent CDOM that is bioavailable to bacterial degradation. These exudates contain aliphatic blue-shifted fluorescent humic-like substances (P. Coble's peak-M) that are readily taken up by marine bacteria that, in turn, exude aromatic red-shifted humic-like substances (P. Coble's peak-C) during both the exponential and stationary growth phases. Based on this and previous results by other authors, we hypothesize that peak-M could be a by-product preferentially associated to catabolism of marine eukaryotic cells, whereas peak-C could be associated to catabolism of marine prokaryotes.

Marine bacteria produced humic- and protein-like substances an order of magnitude faster than phytoplankton when normalized to their respective biomasses. This fact, together with the photo degradability of aromatic compounds, is likely the reason behind the lack of correlation observed between phytoplankton biomass and CDOM in both, in situ measurements and satellite-derived estimates.

Although the type of algal species from which the exudates came from did not influence bacterial growth, the exudates influenced bacterial community structure by preferentially selecting bacterial groups with contrasting substrate preferences, such as *Altermonas*, *Roseobacter* or *Bacterioidetes*.

Acknowledgements

References

Alonso, C., Pernthaler, J., 2006. Roseobacter and SAR11 dominate microbial glucose uptake in coastal North Sea waters. Environ. Microbiol. 8, 2022-2030.

Arrigo, K.R., Brown, C.W., 1996. Impact of chromophoric dissolved organic matter on UV inhibition of primary productivity in the sea. Mar. Ecol. Prog. Ser. 140, 207-216.

Benner, R. 2003. Molecular indicators of the bioavailability of dissolved organic matter. In: Findlay, S., Sinsabaugh, R. (Eds.), Aquatic ecosystems: interactivity of dissolved organic matter. Academic Press, New York, p.121-137.

Bussmann, I., 1999. Bacterial utilization of humic substances from the Arctic Ocean. Aquat. Microb. Ecol. 19, 37-45.

Cammack, W.K.L., Kalff, J., Prairie, Y.T., Smith, E.M., 2004. Fluorescent dissolved organic matter in lakes: relationships with heterotrophic metabolism. Limnol. Oceanogr. 49, 2034-2045.

Coble, P.G. 1996. Characterization of marine and terrestrial DOM in seawater using excitation-emission matrix spectroscopy. Mar. Chem. 51, 325-346.

Coble, P.G., Del Castillo, C.E., Avril, B., 1998. Distribution and optical properties of CDOM in the Arabian Sea during the 1995 Southwest Monsoon. Deep-Sea Res. II 45, 2195-2223.

Coffin, R.B., 1989. Bacterial uptake of dissolved free and combined amino acids in estuarine waters. Limnol. and Oceanogr. 34, 531-542.

Cottrell, M.T., Kirchman, D.L., 2000. Natural assemblages of marine proteobacteria and members of the Cytophaga-Flavobacter cluster consuming low- and high-molecular-weight dissolved organic matter. Appl. Environ. Microbiol. 66, 1692-1697.

Chen, J., LeBoeuf, E.J., Dai, S., Gu, B., 2003. Fluorescence spectroscopic studies of natural organic matter fractions. Chemosphere 50, 639-647.

Chen, R.F., Bada, J.L., 1992. The fluorescence of dissolved organic matter in seawater. Mar Chem 37, 191-221.

Del Giorgio, P.A., Gasol, J.M., 2008. Physiological structure and single-cell activity in marine bacterioplankton. In: Kirchman, D.L. (Ed.), Microbial ecology of the oceans, 2nd ed. Wiley-Blackwell, p. 243–285.

Fein, J.B., Boily, J.-F., Güçlü, K., Kaulbach, E., 1999. Experimental study of humic acid adsorption onto bacteria and Al-oxide mineral surfaces. Chem. Geol. 162, 33-45.

Fuhrman, J.A., Hagström, Å., 2008. Bacterial and archaeal community structure and its patterns. In: Kirchman, D.L. (Ed.), Microbial Ecology of the Oceans. Wiley, p. 45-90.

Gasol, J.M., Del Giorgio, P.A., 2000. Using flow cytometry for counting natural planktonic bacteria and understanding the structure of planktonic bacterial communities. Scientia Marina 64, 197.

Häder, D.-P., Sinha, R.P., 2005. Solar ultraviolet radiation-induced DNA damage in aquatic organisms: Potential environmental impact. Mutation Research 571, 221–233.

Herndl, G.J., Muller-Niklas, G., Frick, J., 1993. Major role of ultraviolet-B in controlling bacterioplankton growth in the surface layer of the ocean. Nature 361, 717-719.

Hunt, A.P., Parry, J.D., Hamilton-Taylor, J., 2000. Further evidence of elemental composition as an indicator of the bioavailability of humic substances to bacteria. Limnol. Oceanogr. 45, 237-241.

Jiao, N., Herndl, G.J., Hansell, D.A., Benner, R., Kattner, G., Wilhelm, S.W., Kirchman, D.L., Weinbauer, M.G., Luo, T., Chen, F., Azam, F., 2010. Microbial production of recalcitrant dissolved organic matter: long-term carbon storage in the global ocean. Nat. Rev. Micro. 8, 593-599.

Kawasaki, N., Benner, R., 2006. Bacterial release of dissolved organic matter during cell growth and decline: Molecular origin and composition. Limnol. Oceanogr 51, 2170-2180.

Keil, R.G., Kirchman, D.L., 1993. Dissolved combined amino acids: chemical form and utilization by marine bacteria. Limnol. Oceanogr. 38, 1256-1270.

Keil, R.G., Kirchman, D.L., 1999. Utilization of dissolved protein and amino acids in the northern Sargasso Sea. Aquat. Microb. Ecol. 18, 293-300.

Kirchman, D.L., 2004. A primer on dissolved organic material and heterotrophic prokaryotes in the oceans. In: Follows, M., Oguz, T. (Ed.), The ocean carbon cycle and climate, NATO Science Series. Academic Publishers, Dordrecht, the Netherlands: Kluwer, p. 31-66.

Kroer, N.S., Jorgensen, N.O.G., Coffin, R.B., 1994. Utilization of dissolved nitrogen by heterotrophic bacterioplankton: a comparison of three ecosystems. Appl. Environ. Microbiol. 60, 4116-4123.

Lakowicz, J.R., 1983. Principles of fluorescence spectroscopy. Plenum Press.

Lønborg, C., Alvarez-Salgado, X.A., Martinez-Garcia, S., Miller, A.E.J., Teira, E., 2010. Stoichiometry of dissolved organic matter and the kinetics of its microbial degradation in a coastal upwelling system. Aquat. Microb. Ecol. 58,117-126.

Manz, W., Amann, R., Ludwig, W., Wagner, M., Schleifer, K.H., 1992. Phylogenetic oligodeoxynucleotide probes for the major subclasses of Proteobacteria—problems and solutions. Syst. Appl. Microbiol. 15, 593–600.

Midorikawa, T., Tanoue, E., 1998. Molecular masses and chromophoric properties of dissolved organic ligands for copper(II) in oceanic water. Mar. Chem. 62, 219-239.

Moran, M.A., Hodson, R.E., 1990. Bacterial production on humic and nonhumic components of dissolved organic carbon. Limnol. Oceanogr. 35, 1744-1756.

Moran, M.A., Sheldon, W.M., Zepp, R.G., 2000. Carbon loss and optical property changes during long-term photochemical and biological degradation of estuarine dissolved organic matter. Limnol. Oceanogr. 45, 1254-1264.

Moran, M.A., González, J.M., Kiene, R.P. 2003. Linking a bacterial taxon to sulfur cycling in the sea: studies of the marine *Roseobacter* group. Geomicrob. J. 20, 375 – 388.

Myklestad, S.M., 2000. Dissolved organic carbon from phytoplankton. In: Wangersky, P. (Ed.), The handbook of environmental chemistry, vol. 5. Part D. Marine chemistry. Springer-Verlag, Berlin Heidelberg, p.111-148.

Nelson, N.B., Siegel, D.A., Michaels, A.F., 1998. Seasonal dynamics of colored dissolved material in the Sargasso Sea. Deep Sea Res. I 45, 931-957.

Nieto-Cid, M., Álvarez-Salgado, X.A., Pérez, F.F., 2006. Microbial and photochemical reactivity of fluorescent dissolved organic matter in a coastal upwelling system. Limnol. Oceanogr. 51, 1391-1400.

Norland, S., 1993. The relationship between biomass and volume of bacteria. In: Kemp, P., Sherr, B.F., Sherr, E.B., Cole, J.J. (Ed.), Handbook of methods in aquatic microbial ecology. Lewis Publishing, p. 303–307.

Obernosterer, I., Herndl, G.J., 1995. Phytoplankton extracellular release and bacterial growth: dependence on the inorganic N: P ratio. Mar. Ecol. Progr. Ser. 116, 247-257.

Ortega-Retuerta, E., Frazer, T.K., Duarte, C.M., Ruiz-Halpern, S., Tovar-Sánchez, A., Arrieta, J.M., Reche, I., 2009. Biogeneration of chromophoric dissolved organic matter by bacteria and krill in the Southern Ocean. Limnol. Oceanogr. 54, 1941–1950.

Paul, J.H., DeFlaun, M.F., Jeffrey, W.H., 1988. Mechanisms of DNA utilization by estuarine microbial populations. Appl. Environ. Microbiol. 54, 1682-1688.

Pernthaler, A., Pernthaler, J., Amann, R., 2004. Sensitive multi-color fluorescence in situ hybridization for the identification of environmental microorganisms. In: Kowalchuk, G.A., Bruijn, F.J.d., Head, I.M., Akkermans, A.D., van Elsas, J.D. (Ed.), Molecular microbial ecology manual, second ed, vol. 3.11. Springer, p. 711-726.

Pinhassi, J., Azam, F., Hemphälä, J., Long, R.A., Martinez, J., Zweifel, U.L., Ake, H., 1999. Coupling between bacterioplankton species composition, population dynamics, and organic matter degradation. Aquat. Microb. Ecol. 17, 13-26.

Pinhassi, J., Sala, M.M., Havskum, H., Peters, F., Guadayol, O., Malits, A., Marrase C., 2004. Changes in bacterioplankton composition under different phytoplankton regimens. Appl. Environ. Microbiol. 70, 6753-6766.

Puddu, A., Zoppini, A., Fazi, S., Rosati, M., Amalfitano, S., Magaletti, E., 2003. Bacterial uptake of DOM released from P-limited phytoplankton. FEMS Microbiol. Ecol. 46, 257-268.

Rochelle-Newall, E.J., Fisher, T.R., 2002. Production of chromophoric dissolved organic matter fluorescence in marine and estuarine environments: an investigation into the role of phytoplankton. Mar. Chem. 77, 7 -21.

Romera-Castillo, C., Sarmento, H., Álvarez-Salgado, A.X., Gasol, J.M., Marrasé, C., 2010. Production of chromophoric dissolved organic matter by marine phytoplankton. Limnol. Oceanogr. 55, 446–454.

Romera-Castillo, C., Nieto-Cid, M., Castro, C.G., Marrasé, C., Largier, J., Barton, E.D., Álvarez-Salgado, A.X., 2011. Fluorescence: absorption coefficient ratio - tracing photochemical and microbial degradation processes affecting coloured dissolved organic matter in a coastal system. Mar. Chem. 125, 26-38.

Rooney-Varga, J.N., Giewat, M.W., Savin, M.C., Sood, S., LeGresley, M., Martin, J. L., 2005. Links between phytoplankton and bacterial community dynamics in a coastal marine environment. Microb. Ecol. 49 49, 163-175.

Rosenstock, B., Simon, M., 1993. Use of dissolved combined and free amino acids by planktonic bacteria in lake constance. Limnol. Oceanogr. 38, 1521-1531.

Rosenstock, B., Zwisler, W., Simon, M., 2005. Bacterial consumption of humic and non-humic low and high molecular weight DOM and the effect of solar irradiation on the turnover of labile DOM in the Southern Ocean. Microb. Ecol. 50, 90-101.

Schäfer, H., Abbas, B., Witte, H., Muyzer, G., 2002. Genetic diversity of 'satellite' bacteria present in cultures of marine diatoms. FEMS Microbiol. Ecol. 42, 25-35.

Shimotori, K., Omori, Y., Hama, T., 2009. Bacterial production of marine humic-like fluorescent dissolved organic matter and its biogeochemical importance. Aquat. Microb. Ecol. 58, 55-66.

Siegel, D.A., Maritorena, S., Nelson, N.B., 2002. Global distribution and dynamics of colored dissolved and detrital organic materials. J. Geophys. Res. 107, 3228.

Simon, M., Azam, F., 1989. Protein content and protein sintesis rates of planktonic marine bacteria. Mar. Ecol. Prog. Ser. 51, 201–213.

Sokal, F.F., Rohlf, F. J., 1984. Introduction to biostatistics. W. H. Freeman.

Sun, L., Perdue, E.M., Meyer, J.L., Weis, J., 1997. Use of elemental composition to predict bioavailability of dissolved organic matter in a Georgia River. Limnol. Oceanogr. 42, 714-721.

Sundh, I., 1992. Biochemical composition of dissolved organic carbon derived from phytoplankton and used by heterotrophic bacteria. Appl. Environ. Microbiol. 58, 2938-2947.

Sundh, I., Bell, R.T., 1992. Extracellular dissolved organic carbon released from phytoplankton as a source of carbon for heterotrophic bacteria in lakes of different humic content. Hydrobiologia 229, 93-106.

Suzuki, M.T., Preston, C.M., Chavez, F.P., DeLong, E.F., 2001. Quantitative mapping of bacterioplankton populations in seawater: field tests across an upwelling plume in Monterey Bay. Aquat. Microb. Ecol. 24,117-127.

Teira, E., Gasol, J.M., Aranguren-Gassis, M., Fernández, A., González, J., Lekunberri, I., Álvarez-Salgado, X.A., 2008. Linkages between bacterioplankton community composition, heterotrophic carbon cycling and environmental conditions in a highly dynamic coastal ecosystem. Environ. Microbiol. 10, 906-917.

Teira, E., Nieto-Cid, M., Álvarez-Salgado, X.A., 2009. Bacterial community composition and colored dissolved organic matter in a coastal upwelling ecosystem. Aquat. Microb. Ecol. 55, 131-142.

Urban-Rich, J., McCarty, J.T., Fernández, D., Acuña, J.L., 2006. Larvaceans and copepods excrete fluorescent dissolved organic matter (FDOM). J. Exp. Mar. Biol. Ecol. 332, 96- 105.

Yamashita, Y., Tanoue, E., 2008. Production of bio-refractory fluorescent dissolved organic matter in the ocean interior. Nature Geosci. 1, 579-582.

Chapter III

Optical properties of ultrafiltered dissolved organic matter (UDOM) from contrasting aquatic environments and their alteration by sunlight

Chapter III

Co-authors:

M. Nieto-Cid, C. Marrasé, D.J. Repeta, X.A. Álvarez-Salgado.

Abstract

We have determined the absorption and induced fluorescence spectra of natural dissolved organic matter isolated by tangential flow filtration (1 kDa cut off) from estuarine, interstitial, coastal, enclosed sea and open ocean waters. Absorption coefficients at fixed wavelengths, absorption spectral slopes over different wavelength ranges, fluorescence intensities at the Ex/Em wavelengths of protein- and humic-like fluorophores, and the fluorescence quantum yield at 340 nm have been used as simple, fast and inexpensive proxies for the chemical charcteristics of the isolated materials. By this approach the average molecular weight and aromaticity of the ultrafiltered dissolved organic matter decreased significantly from estuarine > coastal > enclosed sea > open ocean waters and increased significantly with depth; a pattern that can be explained on basis of the continental or marine origin of the samples and their exposure to natural radiation. Exposure of the isolates to sunlight revealed that the absorption and fluorescence emission intensities decreased at wavelengths > 300 nm due to the photobleaching of the humic-like fluorophores. Exposure to sunlight increased absorption at wavelengths < 300 nm, in open ocean samples, perhaps due to conformational changes in the humic substances containing bound proteins, which give rise to change in the resonance energy transfer among amino acids residues, or to the cleavage of amino acids or protein moieties bound to humic substances by natural radiation.

Chapter III

Introduction

Oceanic dissolved organic matter (DOM) is one of the largest and most dynamic reservoirs of reduced carbon on Earth; the global dissolved organic carbon pool is estimated to be 662 Pg C (Hansell et al., 2009), comparable to the carbon stock of terrestrial biomass, 600 Pg C, or the CO_2 accumulated in the atmosphere, 720 Pg C (Hedges et al., 1992). Therefore, minor changes in the DOM pool could considerably impact atmospheric CO_2 concentrations and the radiation balance on Earth (Hedges et al., 2002; Peltier et al., 2007). Despite its importance in global change and ocean biogeochemical cycles, the chemical composition and structure of only about 10% of the constituents of the DOM pool are currently known (Benner, 2002).

Molecular and structural characterisation of marine DOM requires isolation of the material from seawater and enrichment to higher concentrations. The heterogeneity of the DOM pool, which covers a broad range of chemical affinities and molecular weights, makes difficult a quantitative and representative extraction with the conventional methods of solid phase extraction (SPE) and ultrafiltration (UF). On the one hand, SPE Amberlite XAD resins and C18 phases separate on basis of the polarity of the substances, retaining the more hydrophobic components that hardly represent more than 1/3 of the bulk DOM (Mopper et al., 2007; Guo and Sun, 2009; Perdue and Benner, 2009). Other sorbents recently used in SPE methods are the commercially pre-packed chemically modified hydrophilic styrene divinyl benzene polymers, particularly PPL, which are able to recover up to about 2/3 of the DOM pool (Dittmar et al., 2008). However SPE methods require low pH and/or the elution with organic solvents, which could alter the structure and composition of the isolated material, specifically resulting in significantly altered optical properties (Green and Blough, 1994). On the other hand, UF techniques separate the DOM components based upon size, even though the material (hydrophilic or hydrophobic) of the membrane, the operation conditions (filtration pressure, concentration factor) and the matrix effects (e. g., ionic strength and pH) influences the efficiency of the method (Benner, 2002; Perdue and Benner, 2009). UF has the additional advantages of processing large volumes of seawater allowing the isolation of hundreds of milligrams of material and it is thought to yield DOM extracts that are more representative of the original material (Mopper et al., 1996). Molecular weight cut-off ranges for UF membranes used to isolate DOM are typically 1 to 3 kDa (Benner et al., 1997; Rosenstock et al., 2005). From 10 to 40% of the DOC in seawater can be isolated and concentrated with these membranes (Benner et al., 1997; Mopper et al., 2007). Finally, more recently, reverse osmosis linked to pulse electro-dialysis (RO/ED) has successfully isolated >60% of water and salt-free unbiased marine DOM (Gurtler et al., 2008).

The high molecular weight fraction of DOM (HMW-DOM) includes materials that are able to absorb the UV and visible radiation and to re-emit it as fluorescent light (Wheeler, 1976; Thurman, 1985; Mopper et al., 1996; Engelhaupt et al., 2003). Optical characterisation of the coloured (CDOM) and

induced fluorescent (FDOM) fractions of ultrafiltered DOM (UDOM) by absorption and fluorescence spectroscopy do not provide specific information about the molecular components of DOM as the state-of-the-art high resolution molecular magnetic resonance or mass spectroscopy techniques (Mopper et al., 2007). However, they are reliable probes for the changes in average molecular weight and aromaticity experienced by the DOM pool as a consequence of photochemical and biological processes (Coble, 1996; 2007; Moran et al., 2000; Stedmon and Markager, 2005; Nieto-Cid et al., 2006). Absorption coefficients at particular wavelengths, absorption coefficient ratios and spectral slopes have been used as indicators for the molecular size and the conjugation of UDOM (Carder et al., 1989; Dahlén et al., 1996; Weishaar et al., 2003). Fluorescence excitation-emission matrices allow distinguishing between fluorophores characteristic of protein- and humic-like substances (Coble, 1996; 2007; Stedmon and Markager, 2005). Moreover, indices combining the absorption and fluorescence properties of DOM, such as the fluorescence quantum yield, also provide relevant information on the chemical structure of these materials (Green and Blough, 1994; Romera-Castillo et al., 2011a, see Chapter IV).

CDOM and FDOM produced from the decomposition of nonliving terrestrial plant material is introduced in the oceans by rivers and streams (Sulzberger and Durisch-Kaiser, 2009) and, to a lesser extend, by rain water (Kieber et al., 2006). This terrestrial CDOM is relevant only in coastal areas affected by strong continental runoff. However, most of the CDOM in the oceans is produced in situ, mainly in the form of humic substances generated as a by-product of bacterial degradation processes (Chen and Bada, 1992; Stedmon and Markager, 2005; Nieto-Cid et al., 2006; Yamashita and Tanoue, 2008; Romera-Castillo et al., 2011b, see Chapter II). Production of CDOM by phytoplankton, zooplankton and krill has also been reported in some recent studies (Steinberg et al., 2004; Ortega-Retuerta et al., 2009; Romera-Castillo et al., 2010, see Chapter I). Humic substances can also be produced in the surface ocean through complex photochemical reactions of photo-humification (Kieber et al., 1997). Conversely, photo-degradation by natural sunlight is able to break down CDOM into colourless organic substances, CO and CO_2 (Moran and Zepp, 1997), producing dramatic losses of absorption and induced fluorescence (Skoog et al., 1996; Del Castillo et al., 1999; Moran et al., 2000; Nieto-Cid et al., 2006).

Absorption and fluorescence spectra of DOM isolated by cross–flow ultrafiltration from contrasting riverine, interstitial sediments, estuarine, coastal, enclosed and open ocean natural water samples will be examined in this study. An assortment of indices will be produced — including bulk and specific absorption and induced fluorescence coefficients and ratios at relevant wavelengths, spectral slopes and fluorescence quantum yields — to characterise the isolated materials and learn about their origin and the biogeochemical transformations that they experienced in the environment before been collected. In addition, the alteration produced by the natural sunlight on the optical properties of these materials will also be reported and discussed.

Materials and Methods

Ultrafiltered dissolved organic matter (UDOM) samples

DOM was concentrated from natural waters collected in contrasting aquatic environments: riverine, estuarine, coastal, enclosed and open ocean sites. The riverine sample was taken in the Delaware River; estuarine samples were collected in Chesapeake Bay and West Neck Bay (Long Island, NY), being the latter from surface interstitial sediment waters; the coastal sample was from Woods Hole; and ocean samples from the enclosed Black Sea and the open Subtropical North Pacific at Hawaii. Black sea and Hawaii samples were collected at three and two depths, respectively (Table 1).

A large amount of water (> 300 L) was concentrated through a flow–cross ultra–filtration system, following the methodology described by Repeta et al. (2002). Briefly, samples were filtered through a Whatman GF/F and/or 0.2 µm polycarbonate capsule filter to remove particulate matter and the high molecular weight fraction concentrated (10-100 x) using a 1 kDa spiral-wound filter (Amicon, Separation Engineering). UDOM concentrates were rendered largely salt-free by repeated dilution/ concentration with ultrapure Milli-Q water. The remaining water was removed by lyophilization to yield a final product that was 15-38% carbon by weight (Table 1).

Approximately 0.6 mg of the dried concentrate was diluted in 0.2 µm filtered aged surface Sargasso Sea water (150 mL). Aliquots were taken for the analysis of the concentration of DOC, and the absorption and fluorescence excitation-emission spectra of DOM. The carbon content and optical properties of the aged Sargasso Sea water (control) were also determined.

DOC concentration of UDOM dissolved in aged Sargasso Sea water

Approximately 10 mL of water were collected in pre-combusted (450ºC, 12 h) glass ampoules for DOC analysis. H_3PO_4 was added to acidify the sample at pH < 2 and the ampoules were heat-sealed and stored at 4ºC. DOC was measured with a Shimadzu TOC-CVS organic carbon analyser. The system was standardised daily with potassium hydrogen phthalate. The precision of the DOC measurements was ±0.01 mg L^{-1} of C. DOM reference materials provided by Prof. D. Hansell (Miami University) were analysed daily in order to test the performance of the analyser. We obtained average concentrations of 0.55 ± 0.02 mg L^{-1} of C for the deep ocean reference (Sargasso Sea deep water, 2600 m) minus blank reference materials. The nominal DOC value provided by the reference laboratory is 0.53 ± 0.02 mg L^{-1} of C.

The concentrations of DOC (UDOC, in mg L^{-1} of C) and DOM (UDOM, in mg L^{-1}) added to the aged surface Sargasso Sea water were calculated as:

$$UDOC = DOC - DOC_{SSW} \qquad (1)$$

$$UDOM = \frac{UDOC}{\% C} \qquad (2)$$

where DOC and DOC$_{SSW}$ are the concentrations of DOC in the solution and in the aged surface Sargasso Sea water, respectively; and %C is the percentage of carbon in the dried UDOM as determined with a Perkin Elmer 2400 CHN analyser (Table 1). %C increases from 14.7% for the Delaware River to 37.8% for Chesapeake Bay. %N, also provided in Table 1, varied from 0.83% for the Delaware River to 2.7% for the Hawaii surface sample. The C/N ratio (w/w) of the dried UDOM samples ranged from 12 for Chesapeake Bay to 21 for the Black Sea surface sample and it was as low as 10 for West Neck Bay surface sediments. Initial DOC and salinity values of the ultrafiltered seawater samples are also reported in Table 1.

Optical properties of UDOM dissolved in aged Sargasso Sea water

Absorption spectra from 250 to 700 nm were recorded in a Varian Cary 50 Bio Spectrophotometer. Measurements were performed at constant room temperature (20ºC) in a 10cm quartz cell. MQ water was used as blank. The absorption coefficient at each wavelength, $a_{CDOM}(\lambda)$ (in m^{-1}), was calculated as 23.03·Abs(λ), where Abs(λ) is the absorbance at wavelength λ. After the subtraction of the aged Sargasso Sea $a_{CDOM}(\lambda)$, the $a_{CDOM}(\lambda)$ spectra divided by the concentration of UDOC, i.e. the C-specific absorption coefficient spectra, $a^*_{CDOM}(\lambda)$, were fitted to the equation:

$$a^*_{CDOM}(\lambda) = a^*_{CDOM}(254) \cdot \exp\left[S \cdot (\lambda - 254)\right] + K \qquad (3)$$

where $a^*_{CDOM}(254)$ is the C-specific absorption coefficient at the reference wavelength of 254 nm (in m^2 g^{-1} of C), also named as SUVA(254) in the literature (Weishaar et al., 2003); S is the spectral slope over the range 250–500 nm (in nm^{-1}); and K is a background constant caused by fine size particles, micro air bubbles or colloidal material present in the sample, refractive index differences between the sample and the reference, or attenuation not due to organic matter (in m^2 g^{-1} of C). From $a^*_{CDOM}(254)$ and S we also obtain (1) the absorption coefficient ratio at 254 nm and 365 nm, $a_{CDOM}(254/365)$; and (2) the C-specific absorption coefficient at 340 nm, $a^*_{CDOM}(340)$. Apart from the spectral slope over the range 250-500 nm, slopes over two narrower wavelength ranges, $S(275-295)$ and $S(350-400)$ were also calculated using linear regressions of the log-transformed C-specific absorption spectra following Helms et al., (2008).

Table 1. Geographic origin (depth, position), salinity and dissolved organic carbon (DOC) concentration of the original samples and elemental carbon (%C) and nitrogen (%N) proportions of the corresponding ultrafiltered materials.

Sample	Depth (m)	Latitude (degree)	Longitude (degree)	Salinity	DOC (mg C · L^{-1})	%C	%N
Black Sea	Surface	41° 18.25'–42° 31.00' N	29° 05.66'–30° 30.00' E	18.1	-	34.93	1.66
Black Sea	90m	42° 31.00' N	30° 43.53' E	20.4	-	30.57	2.34
Black Sea	750	41° 24.99' N	29° 05.66' E	22.2	-	35.79	2.26
Hawaii	Surface	19° 43' 38.48" N	156° 03' 32.57" W	35.7	0.84	35.43	2.79
Hawaii	600	19° 43' 38.48" N	156° 03' 32.57" W	35.4	0.43	32.21	2.53
Woods Hole	Surface	41° 31' 50.83" N	70° 38' 43.34" W	30.7	1.22	32.40	2.48
Chesapeake Bay	Surface	36°47' N	75°51' W	35.3	1.07	37.81	3.23
Delaware River	Surface	39° 37' N	75° 33' W	1.5	2.26	14.73	0.83
West Neck Bay(NY)	Sediments	41° 04' N	72° 21' W	ND	26.4	22.15	2.14

Chapter III

Single excitation-emission (Ex/Em) fluorescence measurements were performed with a Photon Technology International (PTI) Model A1010 spectrofluorometer equipped with a double excitation monochromator, a single emission monochromator, and a cooled photomultiplier assembly. The slit widths were set to 4 nm. The specific Ex/Em wavelengths pairs were those established by Coble (1996): peak T or $F(280/350)$, at Ex/Em 280/350, an indicator of protein-like substances; peak M or $F(320/410)$, at Ex/Em 320/410, an indicator of marine humic-like substances; and peak C or $F(340/440)$, at 340/440 nm, an indicator of terrestrial humic-like substances. Although recently, it has been reported that compounds fluorescing at peak-C are produced by bacteria and those fluorescing at peak-M are produced by phytoplankton (Romera-Castillo, et al., 2010, 2011b, see Chapter I and II, respectively). Fluorescence measurements were expressed in quinine sulphate units (QSU) by calibrating the spectrofluorometer at Ex/Em 350 nm/450 nm against a quinine sulphate dihydrate (QS) standard in 0.1N sulphuric acid. A solution of sulphuric acid 0.1 N in Milli-Q water was used as a blank. The equivalent concentration of each peak was determined by subtracting the blank height from the average peak height, and dividing by the slope of the standard curve. Again, the fluorescence of the aged surface Sargasso Sea water was subtracted from the samples and the resulting values were divided by the concentration of UDOC, to obtain the corresponding C-specific induced fluorescence intensities.

Fluorescence excitation-emission matrices of the UDOM dissolved in aged surface Sargasso Sea water were performed with a Hitachi F-4500 Fluorescence Spectrophotometer equipped with a xenon discharge lamp. Slit widths were 5 nm for the excitation and emission wavelengths and scan speed 2400 nm/min. Measurements were performed at a constant room temperature of 20°C in a 1cm quartz fluorescence cell. Emission scans were recorded between 300 nm and 550 nm at 2 nm intervals for excitation wavelengths between 250 nm and 450 nm at 5 nm intervals. Factory-set excitation and emission corrections of the instruments were used. Rayleigh scatter was corrected by setting to zero any fluorescence value recorded at λem ≤ λex + 20 nm. Second order Rayleigh scattering peaks at twice the wavelength of the exciting light were also corrected. Raman scatter was corrected by subtracting the EEM of the aged surface Sargasso Sea water that was used as a blank. Since the absorption coefficients of all samples at any wavelength were < 10 m^{-1}, it was not necessary to correct for inner filters effects (Stedmon and Bro, 2008). Fluorescence units were converted into QSU and, then, divided by the concentration of UDOC to be expressed in C-specific fluorescence units, QSU mg C^{-1} L.

Finally, the quantum yield of fluorescence at excitation 340 nm, $\Phi(340)$, is the portion of the light absorbed by the UDOM solutions at 340 nm that is re-emitted as fluorescent light. $\Phi(340)$ of the samples was calculated by comparison to the fluorescence emission between 400 and 600 nm from the quinine sulphate standard in 0.1 N H$_2$SO$_4$ using the equation:

$$\Phi(340) = \frac{F(400-600)}{a_{\text{CDOM}}(340)} \cdot \frac{a_{\text{CDOM}}(340)_{\text{QS}}}{F(400-600)_{\text{QS}}} \cdot \Phi(340)_{\text{QS}} \tag{4}$$

Where $a_{CDOM}(340)_{QS}$ is the absorption coefficients of the QS standard at 340 nm (in m^{-1}); $F(400-600)$ and $F(400-600)_{QS}$ are the average integrated fluorescence spectra between 400 and 600 nm at a fixed excitation wavelength of 340 nm (in QSU) of the sample and the QS standard, respectively; and $\Phi(340)_{QS}$ is the dimensionless fluorescence quantum yield of the QS standard, 0.54 according to Melhuish (1961).

Fig. 1a shows the relationship between $F(400–600)_{QS}$ and $F(340/440)_{QS}$ for the quinine sulphate standards and Fig. 1b the same relationship for the UDOM samples. Given that $F(400–600)_{QS}$ and $F(400–600)$ can be estimated from $F(340/440)_{QS}$ and $F(340/440)$ using the dimensionless conversion factors obtained from the regressions showed in Fig. 1 (0.71 ± 0.01 for QS and 0.94 ± 0.03 for the UDOM samples), the ratios $F(400–600)_{QS}/a_{CDOM}(340)_{QS}$ and $F(400–600)/a_{CDOM}(340)$ of eq. (4) can be obtained from the ratios $F(340/440)_{QS}/a_{CDOM}(340)_{QS}$ and $F(340/440)/a_{CDOM}(340)$ respectively. Therefore, eq. 4 can be rewritten as:

Fig. 1. Linear correlation of a) average integrated fluorescence emission between 400 and 600 nm, F(400-600), versus the fluorescence emission at 440 nm, F(340/440), when excited at 340 nm for quinine sulphate; b) F(400-600) versus F(340/440) for the UDOM samples; c) F(340/440) versus absorption coefficient at 340 nm, aCDOM(340), for quinine sulphate.
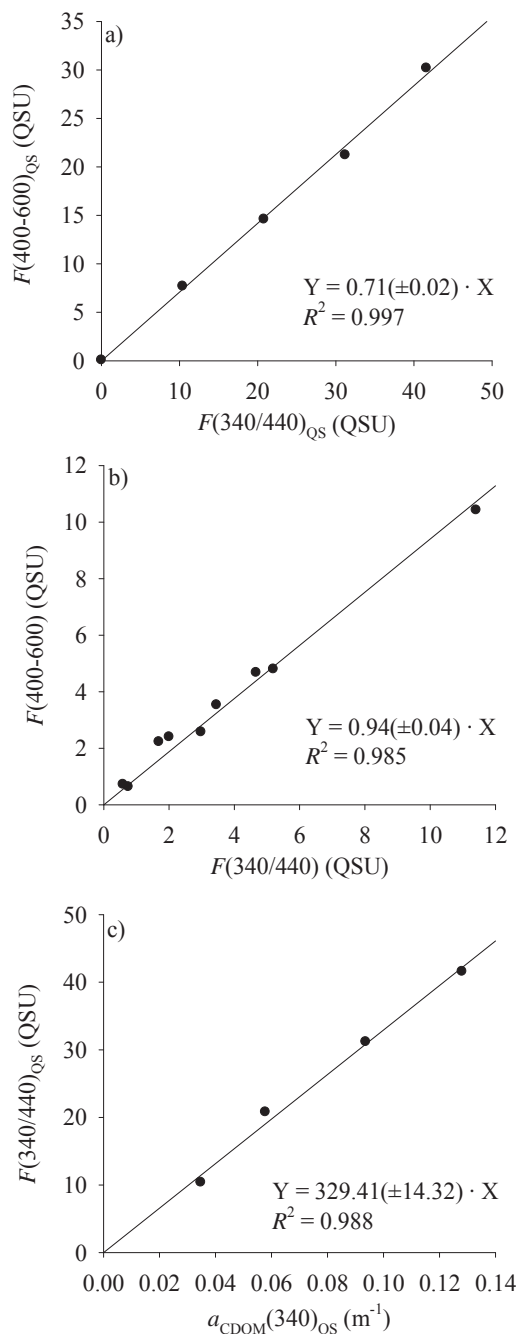
$$\Phi(340) = \beta \cdot \Phi(340)_{QS} \cdot \frac{F(340/440)}{a_{CDOM}(340)} = 2.2(\pm 0.1) \cdot 10^{-3} \cdot \frac{F(340/440)}{a_{CDOM}(340)} \qquad (5)$$

Where $\beta = 4 \cdot 10^{-3}$ is a dimensionless factor that accounts for the conversion of punctual into integrated fluorescence of the QS standards and the samples (Figs. 1a and b) and for the $F(340/440)_{QS}/a_{CDOM}(340)_{QS}$ factor of 329 ± 14 QSU m obtained from the regression in Fig. 1c.

Photo-reactivity experiments

Four of the UDOM samples (Delaware River (DwR), Woods Hole (WHC) and Hawaii at surface and 600m (Hi0 and Hi600, respectively) were chosen to study their response to the exposure to natural sunlight attending to their contrasting origins (riverine, coastal, and surface and deep open ocean samples) and optical properties.

Approximately 16 mg of the dried concentrates were dissolved in 0.2 μm filtered aged surface Sargasso Sea water (4 L), to reach a UDOC concentration ranging between 0.45 and 1.28 mg L^{-1} of C. The resulting solutions were filtered again through a 0.2 μm membrane Millipore filter (GTTP). The 0.2 μm filtered aged surface Sargasso Sea water was used as a control.

Acid cleaned and combusted quartz flasks (500 mL) were filled in triplicate with each solution. The samples were exposed to natural sunlight in a water bath on the roof of a building of the Woods Hole Oceanographic Institution, MA, during 57 hours. Dark controls were placed in triplicate in wrapped quartz flask in the same bath. The average irradiation over the incubation period was 272 W m^{-2} (ranging from 0 to 900 W m^{-2}) in the Martha's Vineyard Coastal Observatory. Solar radiation is measured at the top of the meteorological mast at the shore laboratory using an Eppley Model PSP (Precision Spectral Pyranometer). The PSP uses a glass dome that uniformly transits radiation between 0.285 and 2.8 μm. A calibration factor is applied to provide the total solar irradiance in watts per square meter (http://mvcodata.whoi.edu/cgi–bin/mvco/mvco.cgi). Since the experiments were performed in April, there was not water recirculation or refrigeration in the bath. Ambient temperature ranged from 3.0 to 13.5ºC with a mean value of 7.8ºC. DOM absorbance and fluorescence and DOC concentrations were measured in the light and dark samples at the beginning (0 h) and end (57 h) of the incubation period.

Results and Discussion

Optical characterisation of UDOM

Significant differences ($p < 0.001$) were observed in the C-specific absorption spectra of the materials characterised in this work (Fig. 2). $a^*_{CDOM}(254)$ decreased ocean-wards: river UDOM absorbs more short UV radiation than estuarine and coastal UDOM, and the latter more than UDOM from the surface ocean (Table 2). This 20-fold increase of $a^*_{CDOM}(254)$ in Delaware river compared to the surface water off Hawaii is consistent with the high concentrations of CDOM transported by rivers, which originates from the decomposition of nonliving plant material and are introduced into aquatic systems via leaching and runoff (Sulzberger and Durisch-Kaiser, 2009). These are progressively diluted in estuarine, coastal and open ocean waters (Vodacek and Blough, 1997; Coble, 2007). Apart from the relevance of leaching for the colour of continental waters, the Delaware River sample was collected at the turbidity maximum zone (TMZ) of Delaware Bay that results from a combination of flocculation induced by gravitational circulation and tidal resuspension of bottom sediments (Biggs et al., 1983).
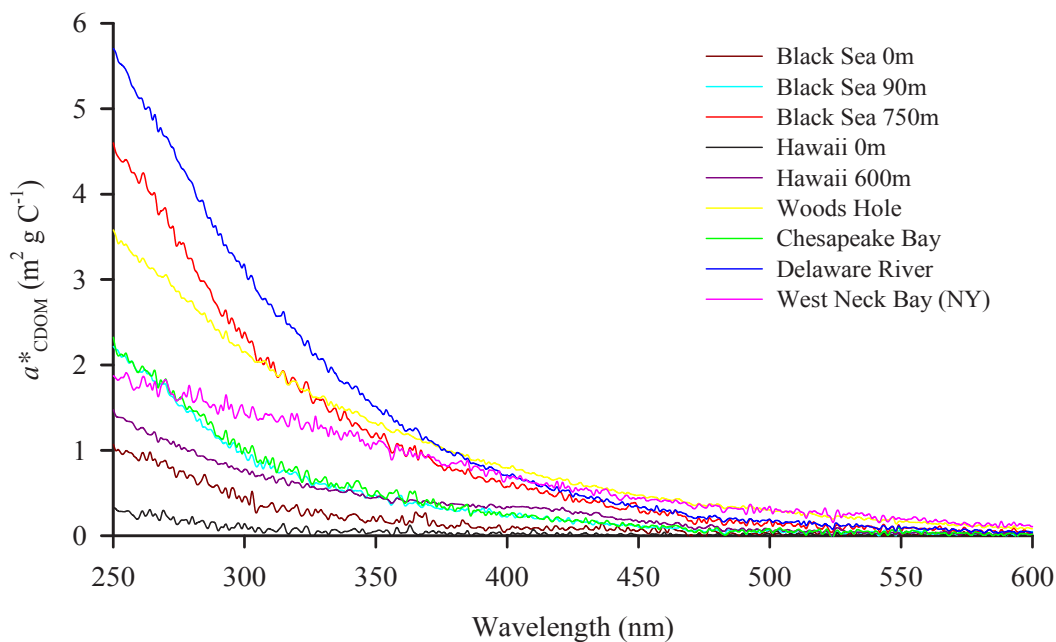

Fig. 2. C-specific absorption spectra of the UDOM samples.

Chapter III

Annual mean of salinity at the TMZ is about 5 pss throughout the year (Mannino and Harvey, 2004) and, in addition, the sampling site is immediately downstream of Philadelphia, which is an area of substantial shipping, industrial, and urban activity (Albert, 1988). Regarding the estuarine and coastal samples, whereas the West Neck Bay (NY) collection site receives copious anthropogenic inputs, the Woods Hole and Chesapeake Bay sites can be considered pristine. $a*_{CDOM}(254)$ of the surface UDOM of the enclosed Black Sea was 4-fold than in the surface open Subtropical North Pacific at Hawaii. This is again owing to the surface Black sea receives important inputs of CDOM–rich continental waters from the surrounding lands and, conversely, the surface layer of the subtropical gyre of the North Pacific is an open ocean area not affected by continental waters. Exposure to the natural UV radiation prior to collection should have a minor effect on the $a*_{CDOM}(254)$ of the UDOM samples since the higher loss of absorption occur at irradiation wavelengths (Del Vecchio and Blough, 2002) and only a few photons of $\lambda < 295$ nm reach the Earth surface.

By contrast, coefficient $a*_{CDOM}(340)$ was sensitive to the natural UV-A radiation (320-400 nm) on the Earth surface; it has been reported that UV-A radiation is more important for the photolysis of DOM molecules >1 kDa than UV-B radiation (Engelhaupt et al., 2003). For this reason, both the high levels of CDOM transported by rivers and its exposure to natural UV-A during mixing in estuaries, coasts, enclosed seas and open oceans, have to be claimed to explain the variability of $a*_{CDOM}(340)$ observed in Table 2 (Sulzberger and Durisch-Kaiser, 2009; Vodacek and Blough, 1997). Whereas $a*_{CDOM}(340)$ was about 40% of $a*_{CDOM}(254)$ in river, estuarine and coastal UDOM samples, it reduced to 20% of $a*_{CDOM}(254)$ in the permanently exposed to the natural UV-A surface waters of the Black Sea and the Subtropical North Pacific at Hawaii. The annual mean shortwave radiation in the western cyclonic gyre of the Black Sea is 148 Wm^{-2} (Schrum et al., 2001) whereas in Hawaii it is 230 W m^{-2} (Letelier et al., 2008). This, and the fact that Hawaii surface waters receive lower terrestrial inputs, could be the reasons why this UDOM sample presented the lowest $a*_{CDOM}(340)$ value.

$a*_{CDOM}(254)$ and $a*_{CDOM}(340)$ of UDOM in the ocean increased significantly with depth, both in the Black Sea and the Hawaii samples (Table 2), as a consequence of the production and accumulation of CDOM during bacterial degradation processes (Nelson et al., 2002; Yamashita and Tanoue, 2008; Swan et al., 2009). The Black Sea is a unique environment almost completely isolated from the World Ocean (Özsoy and Ünlüata, 1997). The three samples from this enclosed sea were from the western cyclonic gyre at depths characterised by contrasting optical and chemical conditions: (1) the surface layer sample is affected by natural UV radiation and it is well oxygenized; (2) the 90 m sample is residually affected by the UV radiation and it is within the sub–oxic layer, where oxygen concentration is low and nitrate is the primary electron acceptor; and (3) the 750 m sample was collected from the anoxic Black Sea, characterized by a complete lack of oxygen and a high concentration of hydrogen sulphide (Yakushev et al., 2005). Oxygen depletion in the suboxic and anoxic layers of the Black Sea as a result of the respiration of sinking organic matter during decades to centuries (Hay et al., 1990;

Table 2. C-specific absorption coefficients at 254 nm, $a^*_{CDOM}(254)$, and 340 nm, $a^*_{CDOM}(340)$, ratio of $a_{CDOM}(254/365)$ and absorption spectral slopes in the 250-500 nm, $S(250-500)$, 275-295 nm, $S(275-295)$, and 350-400nm, $S(350-400)$, wavelength ranges for all the UDOM materials dissolved in aged Sargasso Sea water. R is the correlation coefficient of the fitting of $a^*_{CDOM}(\lambda)$ to eq. (3).

Sample	$a^*_{CDOM}(254)$ (m² g C⁻¹)	$S(250-500)$ (10⁻³ nm⁻¹)	R	$a^*_{CDOM}(340)$ (m² g C⁻¹)	$a_{CDOM}(254/365)$ (dimensionless)	$S(275-295)$ (10⁻³ nm⁻¹)	$S(350-400)$ (10⁻³ nm⁻¹)
Black Sea 0m	1.01 ± 0.01	17.0 ± 0.2	0.989	0.24 ± 0.01	7.2 ± 0.2	20.9 ± 2.0	20.0 ± 2.0
Black Sea 90m	2.11 ± 0.01	15.92 ± 0.08	0.998	0.54 ± 0.01	6.11± 0.08	20.7 ± 1.0	12.2 ± 1.0
Black Sea 750m	4.50 ± 0.03	13.97 ± 0.05	0.999	1.35 ± 0.03	4.71 ± 0.04	16.8 ± 1.0	13.8 ± 0.4
Hawaii 0m	0.28 ± 0.00	20.8 ± 0.6	0.951	0.05 ± 0.01	12 ± 1	39.0 ± 9.0	20.1 ± 5.0
Hawaii 600m	1.32 ± 0.01	10.75 ± 0.08	0.995	0.52 ± 0.01	3.16 ± 0.06	13.3 ± 1.0	5.8 ± 0.3
Woods Hole	3.48 ± 0.03	10.14 ± 0.02	0.999	1.45 ± 0.02	2.96 ± 0.01	11.45 ± 0.40	10.2 ± 0.1
Chesapeake Bay	2.14 ± 0.01	15.24 ± 0.08	0.998	0.58 ± 0.01	5.58 ± 0.08	20.0 ± 1.0	15.7 ± 1.0
Delaware River	5.70 ± 0.04	13.75 ± 0.04	0.999	1.74 ± 0.03	4.45 ± 0.03	14.4 ± 0.2	15.2 ± 0.2
West Neck Bay (NY)	2.11 ± 0.02	7.41 ± 0.06	0.992	1.06 ± 0.04	1.90 ± 0.03	5.3 ± 2.0	8.5 ± 0.4

Yakushev et al., 2005) is the reason behind the high $a^*_{CDOM}(254)$ and $a^*_{CDOM}(340)$ values in the dark layers of the Black Sea. By contrast, comparatively lower $a^*_{CDOM}(254)$ and $a^*_{CDOM}(340)$ values were recorded in the more ventilated North Pacific Intermediate Water that was collected off Hawaii at 600 m depth, where dissolved oxygen levels are above 50 µmol kg⁻¹ (http://hahana.soest.hawaii.edu/hot/hot_jgofs.html).

Spectral slopes, S, ranged from 7.4 and 20.8 10⁻³ nm⁻¹, and vary inversely to $a^*_{CDOM}(254)$ or $a^*_{CDOM}(340)$, i.e. they were higher in open ocean (Hawaii) than in enclosed seas (Black Sea), coastal, estuarine or river samples. This agrees with other studies: spectral slopes for UDOM >1 kDa calculated by Engelhaupt et al. (2003) between 300 and 450 nm were also higher for open ocean samples than for the coastal ones. This is the expected pattern found in natural samples from estuarine, coastal and oceanic waters, and it is mainly due to the photochemical transformation of terrestrial CDOM in surface waters of the shelf and slope and its replacement by CDOM generated in situ mostly by microbial respiration (Coble, 2007).

Significant differences ($p < 0.001$) were also observed in the C-specific fluorescence EEMs of the UDOM characterised in this work (Fig. 3). As for the case of the C-specific absorption spectra, the
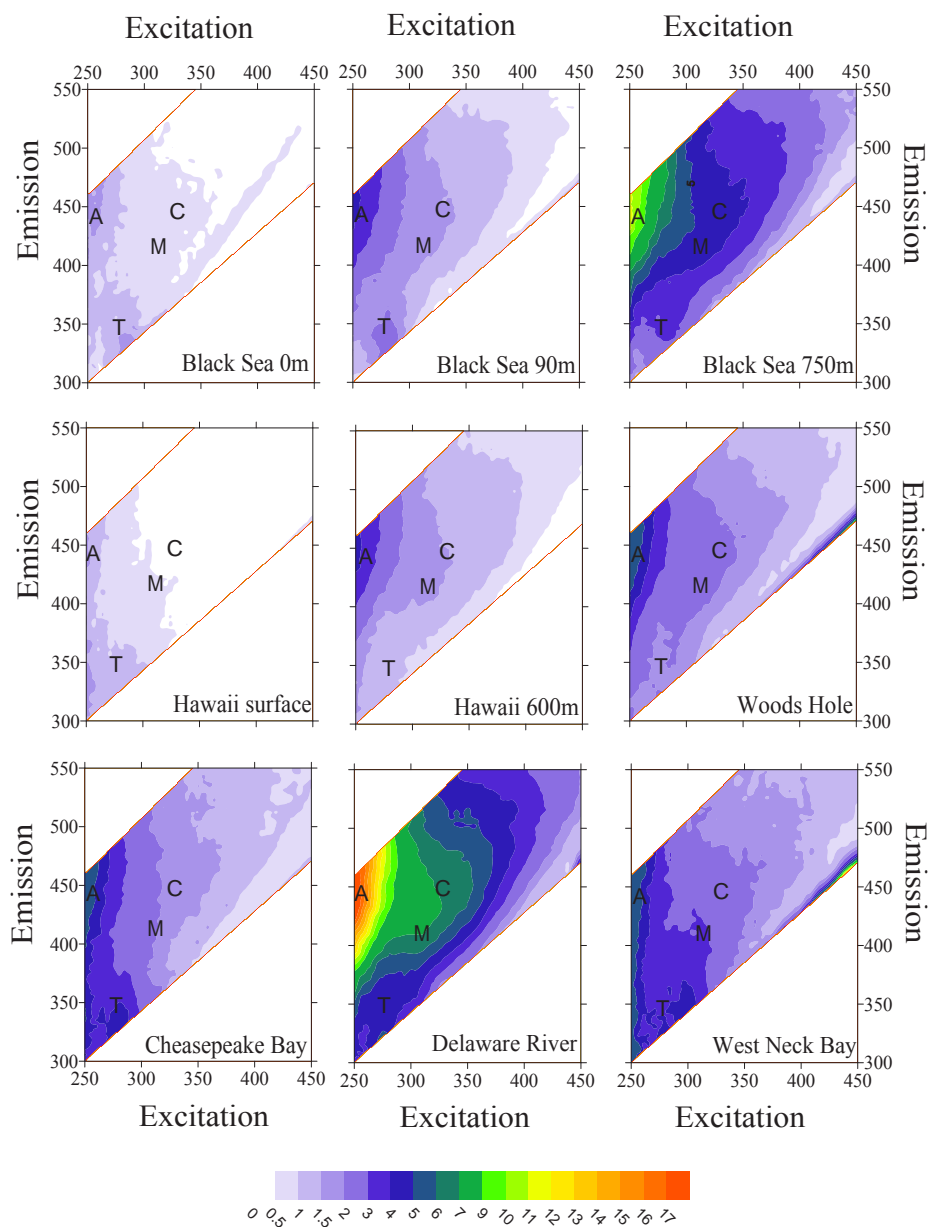
Fig. 3. Excitation-emission matrices of the UDOM samples normalized to DOC (in QSU mg C^{-1} L).

highest fluorescence intensity was recorded in the Delaware River sample and decreased ocean-wards. In the ocean, fluorescence increased with depth in the Hawaii and Black Sea samples. The most intense emission signal in the EEMs of all UDOM samples was observed from 425 to 460 nm when excited at 250 nm. It corresponds to the peak-A defined by Coble (1996), which is characteristic of humic substances, either terrestrial or marine. As for the case of $a^*_{CDOM}(254)$, the intensity of peak-A decreased in the order river > coastal > estuarine > surface ocean samples. The remarkable intensity of peak-A in the anoxic waters of the Black Sea at 750 m may results from the accumulation of humic material produced by bacterial respiration (Nieto-Cid et al., 2006; Yamashita and Tanoue, 2008).

The terrestrial and marine humic-like peaks C and M, were also detectable in all EEMs except in the surface ocean waters from Hawaii and the Black Sea, i.e. the samples that experienced a longer exposure time to the natural radiation. The protein-like peak-T is also present in almost all the UDOM samples. It was not significant in the Hawaii samples and it was very low in the Woods Hole one. In the Black Sea, the intensity of peak-T increased with depth. Table 3 summarized the C-specific fluorescence of peaks C and M and T (in QSU mg C^{-1} L). The humic-like fluorophores followed the same pattern than $a^*_{CDOM}(340)$, i.e. they increased shore- and downwards. C-specific peak-T fluorescence in the Black Sea was twice at 750 m than at the surface layer and the lowest values, < 0.20 QSU mg C^{-1} L, were recorded in Hawaii. The largest C-specific peak-T values, > 0.95 QSU mg C^{-1} L, were recorded in the coastal and riverine samples.

The proportion of organic nitrogen in the dried materials (%N; Table 1) correlated positive and significantly ($p < 0.05$) with the salinity of the water samples from which they were isolated (Fig. 4a). This agrees with the observations made by other authors who found evidences of a higher proportion of proteins in marine than in terrestrial UDOM samples (Repeta et al., 2002; Benner, 2003). Higher proportions of protein-like peak-T fluorescence in the dried materials would be expected in samples with higher %N. However, the plot of these two variables shows three groups of samples (Fig. 4b). The black dots shows the group formed by the West Neck Bay, the Chesapeake Bay and the three samples from the Black Sea, which follow the expected positive and significant ($R^2 = 0.91$, $p < 0.001$) linear correlation between %N and peak-T. The Delaware River samples (grey dot) is characterised by higher than expected peak-T fluorescence. It could be explained by the presence of hydrocarbons derived from substantial shipping, industrial, and urban activities in the sample collection area, which also fluoresce in the peak-T region of the spectrum. Finally, the white dots show a group formed by the Woods Hole and Hawaii samples, which are characterised by lower peak-T fluorescence than expected. This behaviour could be due to a lower proportion of fluorescent aromatic amino acids in the isolated protein material from these samples and/or the relative position of the fluorescent residues in the protein and the presence of other moieties. The latter affects the resonance energy transfer among tryptophan residues (Lakowicz, 2006) that could lead to relatively low peak-T fluorescence for a given proportion of proteins.
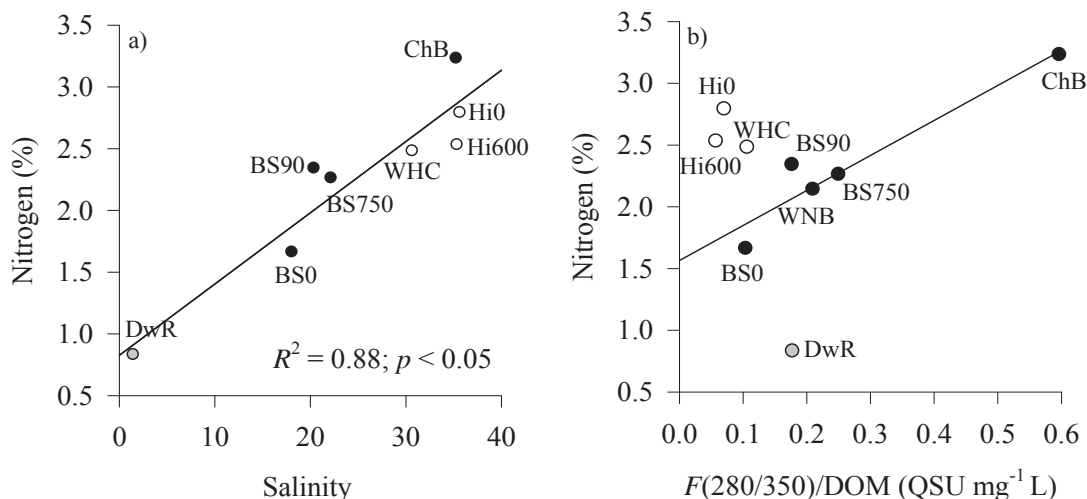
Fig. 4. Relationships between the nitrogen proportion in the UDOM isolates (%N) and a) the salinity of the samples and b) the protein-like fluorescence, $F(280/350)$/DOM, of UDOM dissolved in aged Sargasso sea water. BS0, Black Sea surface; BS90, Black Sea 90 m; BS750, Black Sea 750 m; ChB, Chesapeake Bay; DwR, Delaware River; Hi0, Hawaii surface; Hi600, Hawaii 600 m; WHC, Woods Hole Coastal; WNB, West Neck Bay. Note that the x-axis in plot b) the protein-like is referred to mg L^{-1} of ultrafiltered material calculated as peak-T/DOC • %C in the sample.

Average molecular weight and aromaticity of the UDOM

The optical properties of UDOM provide useful information about some molecular characteristics of the samples such as the average molecular weight or the degree of aromaticity. $a^*_{CDOM}(254)$ is commonly used to determine the relative abundance of aromatic C=C bonds in substituted benzenes or polyphenols and has been suggested as an index of the average number of rings and their condensation degree in natural DOM samples by Weishaar et al. (2003). These authors found a good correlation between $a^*_{CDOM}(254)$ and the percentage of aromaticity determined by ^{13}C–NMR spectroscopy. In our study, $a^*_{CDOM}(254)$ indicated that aromaticity increased with depth and from open ocean to river samples (Table 2).

The absorption coefficient ratio $a_{CDOM}(254/365)$, commonly used in freshwater research as an optical index of the average molecular weight of DOM (Dahlén et al. 1996; Engelhaupt et al. 2003), decreased downwards both in the Black Sea and the Hawaii samples and was higher in the oceanic

than in near shore and river samples (Table 2). Since the higher the a_{CDOM}(254/365) ratio the lower the average molecular weight of DOM (Dahlén et al., 1996; Engelhaupt et al., 2003; Dalzell et al., 2009), our results support that humification processes either in continental drainage basins, estuaries, coasts, or ocean waters produce HMW-DOM. On the other hand, the increasing value of this ratio ocean-ward and upward suggests that low molecular weight DOM (LMW-DOM) compounds are more abundant in the surface and in the open ocean. This is likely due to the photo-degradation processes which break down HMW-DOM into LWM-DOM in surface waters.

More recently, Helms et al. (2008) have suggested the use of the short UV wave range spectral slope S(275–295) and the long UV wave range spectral slope S(350–400) as a proxy to the average molecular weight of DOM and its alteration by dark aerobic microbial processes and exposure to UV light. These authors reported that the ratio S(275–295)/S(350–400) is >1 for marine samples and the opposite trend holds for highly coloured, terrestrially dominated samples. The values of S(275–295) and S(350–400) for our UDOM samples showed this pattern (Table 2): S(275–295) is lower than S(350–400) only for the Delaware River and the pore water West Neck Bay samples, i.e. those containing elevated proportions of terrestrially derived highly aromatic DOM, either natural or anthropogenic.

To estimate the fluorescent quantum yield, Φ(340), the dimensionless factor β (= 4($\pm$0.1)$\cdot10^{-3}$) was calculated from all the UDOM samples. This conversion factor was not significantly different from that obtained with natural samples of the Ría de Vigo (Romera-Castillo et al., 2011a, see Chapter IV). It suggests that the value of β is universal and can be used to obtain the fluorescent quantum yield in any aquatic ecosystem independently of the instrument used.

Table 3. C-specific fluorescence intensities at peaks C (F(340/440)), M (F(320/410)) and T (F(280/350)), and fluorescence quantum yield at 340 nm, Φ(340), for all the UDOM materials dissolved in aged Sargasso Sea water.

Sample	F(340/440)/DOC (QSU mg C^{-1} L)	F(320/410)/DOC (QSU mg C^{-1} L)	F(280/350)/DOC (QSU mg C^{-1} L)	Φ(340) (%)
Black Sea 0m	0.26 ± 0.01	0.48 ± 0.02	0.30 ± 0.02	0.24 ± 0.01
Black Sea 90m	1.29 ± 0.03	1.37 ± 0.04	0.58 ± 0.02	0.52 ± 0.01
Black Sea 750m	3.73 ± 0.08	3.8 ± 0.1	0.70 ± 0.10	0.59 ± 0.01
Hawaii 0m	0.10 ± 0.01	0.28 ± 0.01	0.20 ± 0.01	0.5 ± 0.1
Hawaii 600m	1.12 ± 0.03	1.14 ± 0.02	0.18 ± 0.02	0.46 ± 0.01
Woods Hole	1.61 ± 0.05	1.62 ± 0.04	0.33 ± 0.01	0.24 ± 0.01
Chesapeake bay	0.93 ± 0.03	1.13 ± 0.03	1.58 ± 0.04	0.35 ± 0.01
Delaware River	5.9 ± 0.2	5.5 ± 0.1	1.21 ± 0.08	0.73 ± 0.02
West Neck Bay (NY)	1.37 ± 0.07	1.88 ± 0.09	0.95 ± 0.04	0.28 ± 0.01

The quantum yields of the samples studied here ranged between 0.24 and 0.73%, somewhat lower than the mean value of 1% obtained in natural non concentrated samples (Green and Blough, 1994; Vodacek et al., 1995; Ferrari et al., 1996; Vodacek and Blough, 1997; Ferrari, 2000; Zepp et al., 2004; Romera-Castillo et al., 2011a, see Chapter IV). The Black Sea surface sample showed the lowest $\Phi(340)$, which increased sharply below the photic layer (Table 3). Since the higher $\Phi(340)$ the higher the aromaticity of DOM (Birks, 1970; Turro, 1991), the increase of $\Phi(340)$ with depth in the Black Sea is consistent with the change observed in $a^*_{CDOM}(254)$. Mopper et al. (1996) also found higher fluorescence to absorption ratios in deep relative to surface marine waters. Consistently, Benner (1992) reported that UDOM (> 1 kDa) from surface waters had a lower relative abundance of aromatic or olefinic carbons than UDOM from deep waters. However, for the case of the Hawaii samples we obtained a constant with depth values of $\Phi(340)$ instead of the increase observed in $a^*_{CDOM}(254)$.

UDOM isolated from the Delaware River presented the highest $\Phi(340)$, which decreased in estuarine and, even more, in coastal samples. A higher percentage of aromatic carbons for riverine samples have also been reported in comparison with marine samples (Coble, 1996). This observation is also valid for the UDOM fraction > 1 kDa, since the ^{13}C–NMR analysis of HMW-DOM from river and ocean samples showed that terrestrial humic substances are more aromatic and isotopically depleted in ^{13}C relative to marine organic matter (Repeta et al., 2002; Benner, 2003). Consistently, the terrestrial material was predominant in the site where the Delaware River sample was collected (Mannino and Harvey, 1999). The lower $\Phi(340)$ of estuarine and coastal samples can be explained by a lower contribution of aromatic terrestrial humic substances. In addition, the possible reduction of $\Phi(340)$ by photodegradation increases with the exposure time of the samples to the natural UV radiation. In this sense, river samples have a lower residence time than estuarine samples and the later lower than coastal samples.

Photo-reactivity of UDOM

Subtraction of the irradiated from the dark absorption spectra of each sample indicated that maximum colour loss occurred between 300 and 350 nm (data not shown), i.e. not only in the UV-B range but also in almost all the UV-A range of the spectrum, as observed by Vähätalo et al. (2000). It has been shown that the highest loss of absorption and fluorescence occurs at the irradiation wavelengths with smaller secondary (indirect) losses occurring outside the irradiation wavelengths (Del Vecchio and Blough, 2002). Since very few photons of λ < 295 nm reach the Earth surface, a limited loss of CDOM absorption should be expected for wavelengths in the UV-C range of the spectrum. Accordingly, non significant differences in $a^*_{CDOM}(254)$ between the irradiated samples and their respective dark controls were observed in the control aged Sargasso Sea Water and the UDOM of the Delaware River and the coast of Woods Hole (Fig. 5a). However, the irradiated UDOM samples from Hawaii showed a significant increase of $a^*_{CDOM}(254)$ compared with its dark control (p < 0.01 for the surface sample and

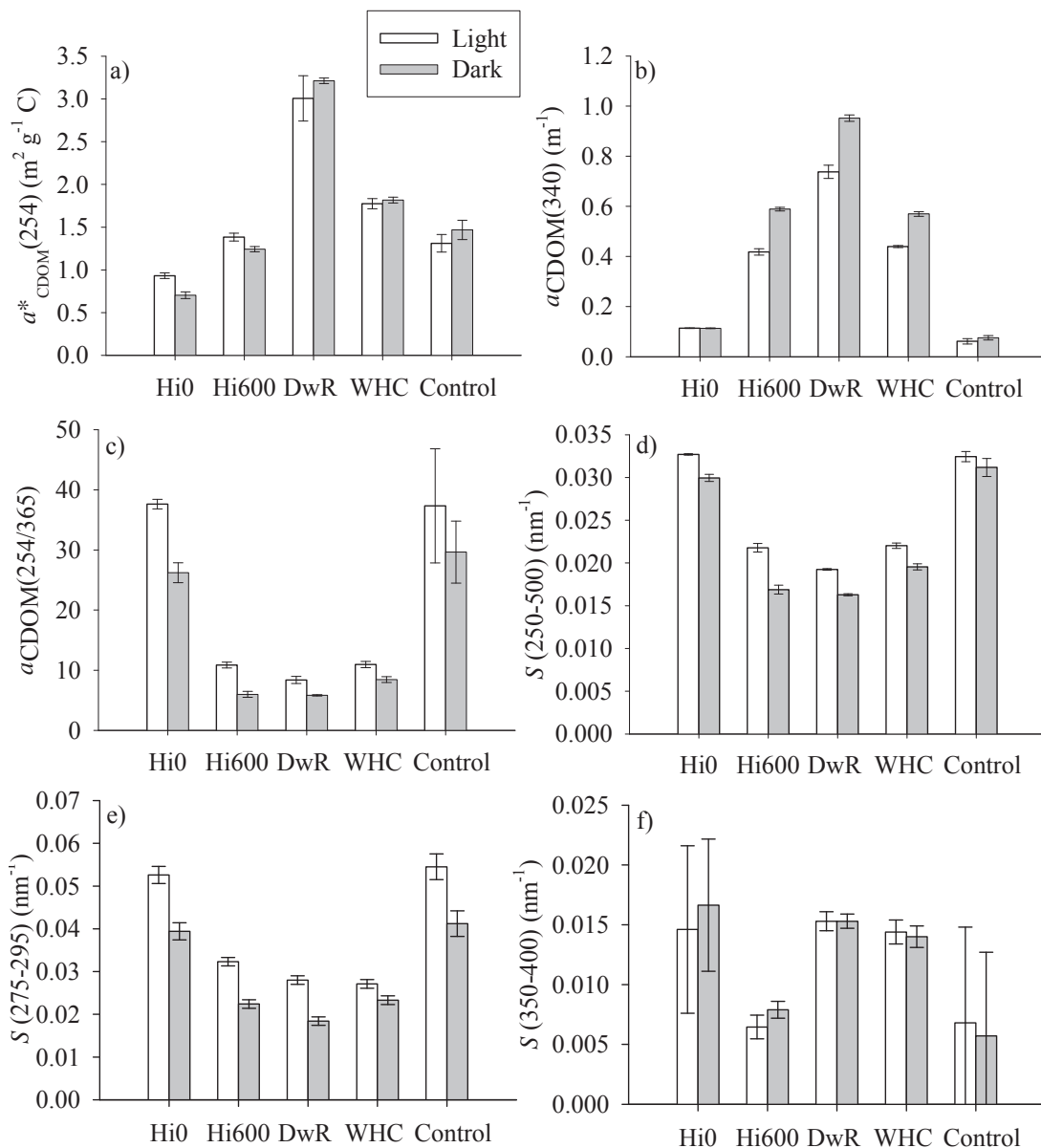**Fig. 5.** a) C-specific absorption coefficient at 254 nm, $a*_{CDOM}(254)$; b) absorption coefficient at 340 nm, $a_{CDOM}(340)$; c) 254 nm to 365 nm absorption coefficient ratio, $a_{CDOM}(254/365)$; spectral slopes at d) 250–500 nm e) 275–295 nm and f) 350–400 nm at the end of the incubation time. White bars: irradiated samples; Black bars: dark controls. DwR, Delaware River; Hi0, Hawaii surface; Hi600, Hawaii 600 m; WHC, Woods Hole Coastal and Control (aged Sargasso Seawater).

$p < 0.05$ for the 600 m sample). Colour loss at wavelengths < 295 nm after irradiation has been widely reported in the literature (e.g. Moran et al., 2000; Spencer et al., 2009; Ortega-Retuerta et al., 2010), but colour increase has also been observed (Kieber et al., 1997; Ortega-Retuerta et al., 2010). The production of new compounds absorbing at wavelengths < 295 nm could be occurring in our Hawaii samples as a consequence of photo-humification by means of condensation processes (Kieber et al., 1997) or by conformational changes in the irradiated molecules.

All the naturally irradiated UDOM samples but Hawaii surface presented a significant decrease of $a_{CDOM}(340)$ compared with the corresponding dark controls (Fig. 5b). It should be noted that the aged surface Sargasso Sea water used to dissolve the UDOM does not respond significantly to UV irradiation. The Hawaii 600 m sample showed the highest percentual decrease, about 30%, followed by the Delaware River and Woods Hole UDOM samples that showed a similar colour loss of about 23%.

The $a_{CDOM}(254/365)$ ratio increased in all UDOM irradiated samples compared with the corresponding dark controls (Fig. 5c), suggesting a decrease of the average molecular weigh of the coloured substances degraded to colourless compounds by natural radiation. This concurs with other studies that analysed the production of LMW-DOM from HMW-DOM mediated by photochemical reactions (Allard et al., 1994; Moran and Zepp, 1997). The increase of the $a_{CDOM}(254/365)$ ratio in the irradiated samples regarding the dark controls was larger in the Hawaii surface ocean UDOM sample (11 ± 2) followed by the Hawaii sample at 600 m (4.9 ± 0.7). River and coastal samples presented lower values of 2.6 ± 0.6 and 2.5 ± 0.7, respectively.

The spectral slope $S(250\text{-}500)$ increased significantly with the natural irradiation (Fig. 5d) due to the relatively faster photo bleaching in the UV-A range of the spectrum (e.g. Kowalczuk et al., 2003). At the end of the incubation time, $S(275\text{-}295)$ was significantly ($p < 0.05$) higher for all irradiated UDOM samples than for the corresponding dark controls whereas $S(350\text{–}400)$ remained invariable (Figs. 5e-f). Therefore, $S(275\text{–}295)$ is more sensitive to radiation than $S(350\text{–}400)$, resulting more useful to trace photochemical processes in seawater. As noted by Fichot and Benner (2011), any natural photon absorbed would produce a larger change of the absorption at 295 nm than at 275, increasing the $S(275\text{–}295)$. On the contrary, the decrease of absorption in the 350-400 nm range is more similar at all wavelengths because it overlaps with the photochemically active part of the natural solar spectrum leading to a minor change in the $S(350\text{-}400)$.

All irradiated UDOM samples showed a significant decrease of the fluorescence at peak-C compared with the corresponding dark controls (Fig. 6a). Fluorescence photobleaching was larger in the Delaware River sample (about 60%), it decreased in coastal UDOM samples and was minimum in open ocean samples suggesting a higher photo-reactivity of samples with a higher content of terrestrial DOM. In Hawaii, the sample from 600 m underwent a decrease of fluorescence higher than the one collected

at the surface. These results concur with those obtained by other authors who found that deep-water DOM is more photo-reactive than DOM from surface waters (Mopper et al., 1991; Obernosterer et al., 2001; Nieto-Cid et al., 2006).

Fluorescence intensity at peak-T tended to increased in all the irradiated samples (Fig. 6b), especially in Hawaii surface and deep ones. Note that the Hawaii samples exhibited a lower than expected peak-T fluorescence for the %N that they contain (Fig. 4b), which has been related to the position of the tryptophan residues and the presence of other moieties that can affect the fluorescence intensity of proteins (Lackowik, 2006). Given that most of the nitrogen in humic substances is in the form of amino acids (Schnitzer, 1985; Rosenstock et al., 2005), we hypothesised that the observed increments of the fluorescence intensity at peak-T after irradiation could occur through the cleavage of amino acids or protein moieties bound to humic substances by natural radiation. The concentration of humic-bound dissolved amino acids constitutes from 34% to 64% of the total dissolved amino acids (Rosenstock et al., 2005). The irradiation could break such combined molecules and release protein material which would have lower molecular weight and higher induced fluorescence at peak-T than when it was bounded. In support of this hypothesis, it has been shown that the fluorescence efficiency of tryptophan bound to phytoplankton
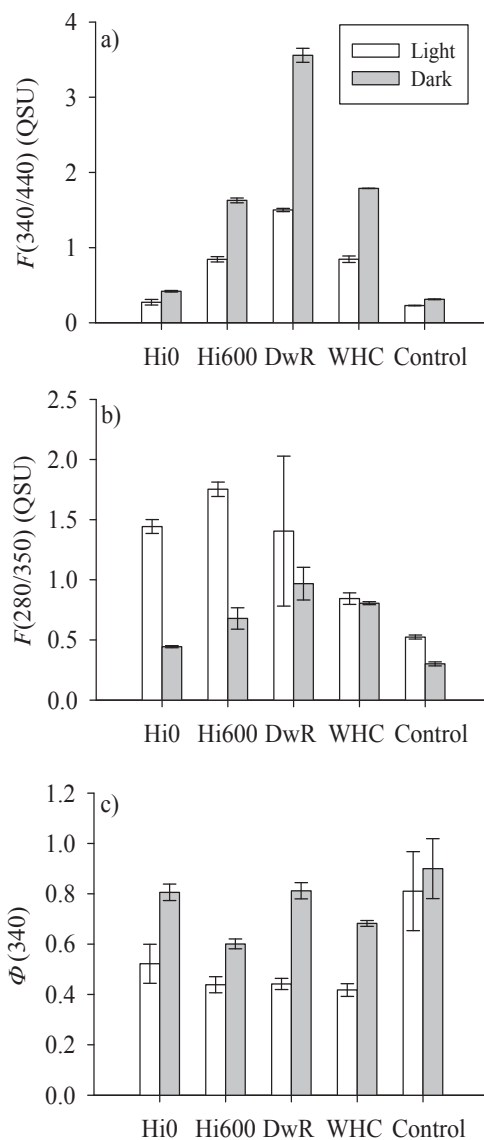

Fig. 6. Fluorescence intensity at a) peak-C, $F(340/440)$, and b) peak-T, $F(280/350)$ and c) fluorescence quantum yield at 340 nm at the end of the incubation time. White bars: irradiated samples; Black bars: dark controls. DwR, Delaware River; Hi0, Hawaii surface; Hi600, Hawaii 600 m; WHC, Woods Hole Coastal and Control (aged Sargasso Seawater).

proteins is about two orders of magnitude lower than the fluorescence efficiency of the dissolved free amino acid (Determann et al., 1998). The increase in $a^*_{CDOM}(254)$ of Hawaii samples could be as well due to this fact.

Finally, a significant decrease of the quantum yield (at 340) was observed in all the irradiated UDOM samples compared with the corresponding dark controls (Fig. 6c), i.e. the decrease of fluorescence is larger than the decrease of absorption when the UDOM is irradiated with natural sunlight. The Delaware River UDOM sample presented the largest percentual loss of quantum yield (46%) and the Hawaii samples the lowest. This contrast with the results found by Vodacek and Blough (1997), who reported no change in quantum yield with photo-degradation, but concurs with results by De Haan (1993), who observed a quicker decrease of fluorescence than absorption with radiation.

Acknowledgements

References

Albert, R.C., 1988. The historical context of water quality management for the Delaware Estuary. Estuaries, 11, 99-107.

Allard, B., Borén, H., Petterson, C., Zhang, G., 1994. Degradation of humic substances by UV-irradiation. Environ. Int. 20, 97–101.

Benner, R., Pakulski, J.D., McCarthy, M., Hedges, J.l., Hatcher, P.G., 1992. BuIk Chemical Characteristics of Dissolved Organic Matter in the Ocean. Science, 255, 1561-1564.

Benner, R., Biddanda, B., Black, B., McCarthy, M., 1997. Abundance, size distribution, and stable carbon and nitrogen isotopic compositions of marine organic matter isolated by tangential-flow ultrafiltration. Mar. Chem. 57, 243-263.

Benner, R., 2002. Chemical composition and reactivity. In: Hansell, D., Carlson, C. (Eds.), 2002. Biogeochemistry of marine dissolved organic matter. Academic Press, San Diego, pp. 59-90.

Benner, R., 2003. Molecular indicators of the bioavailability of dissolved organic matter. In: Findlay, S. and Sinsabaugh, R. (Eds.), Aquatic ecosystems: interactivity of dissolved organic matter. Academic Press, New York, pp. 121-137.

Biggs, R.B., Sharp, J. H., Church, T.M., Tramontano J.M., 1983. Optical properties, suspended sediments, and chemistry associated with the turbidity maxima of the Delaware Estuary. Can. J. Fish. Aquat. Sci. 40, s172–s179.

Birks, J.B., 1970. Photophysics of aromatic molecules. Willey-Interscience, London.

Carder, K.L., Steward, R.G., Harvey, G.R., Ortner, P.B., 1989. Marine humic and fulvic acids: their effects on remote sensing of ocean chlorophyll. Limnol. Oceanogr. 34, 68-81.

Chen, R.F., Bada, J.L., 1992. The fluorescence of dissolved organic matter in seawater. Mar. Chem. 37, 191-221.

Coble, P.G., 1996. Characterization of marine and terrestrial DOM in seawater using excitation-emission matrix spectroscopy. Mar. Chem. 51, 325-346.

Coble, P.G., 2007. Marine optical biogeochemistry: the chemistry of ocean color. Chem. Rev. 107, 402-418.

Dahlén, J., Bertilsson, S., Pettersson, C., 1996. Effects of UV-A irradiation on dissolved organic matter in humic surface waters. Environ. Int. 22, 501-506.

Dalzell, B.J., Minor, E.C., Mopper, K.M., 2009. Photodegradation of estuarine dissolved organic matter: a multi-method assessment of DOM transformation. Org. Geochem. 40, 243-257.

De Haan, H., 1993. Solar UV-Light Penetration and photodegradation of humic substances in Peaty Lake water. Limnol. Oceanogr. 38, 1072-1076.

Del Castillo, C.E., Coble, P.G., Morell, J.M., López, M.J., Corredor, J.E., 1999. Analysis of the optical properties of the Orinoco River plume by absorption and fluorescence spectroscopy. Mar. Chem. 66, 35-51.

Del Vecchio, R., Blough, N.V., 2002. Photobleaching of chromophoric dissolved organic matter in natural waters: kinetics and modeling. Mar. Chem. 78, 231-253.

Determann, S., Lobbes, J.M., Reuter, R., Rullkötter, J., 1998. Ultraviolet fluorescence excitation and emission spectroscopy of marine algae and bacteria. Mar. Chem. 62, 137-156.

Dittmar, T., Koch, B., Hertkorn, N., Kattner, G., 2008. A simple and efficient method for the solid-phase extraction of dissolved organic matter (SPE-DOM) from seawater. Limnol. Oceanogr.: Methods 6, 230-235.

Engelhaupt, E., Bianchi, T.S., Wetzel, R.G., Tarr, M.A., 2003. Photochemical transformations and bacterial utilization of high-molecular-weight dissolved organic carbon in a southern Louisiana tidal stream (Bayou Trepagnier). Biogeochemistry, 62, 39-58.

Ferrari, G.M., Dowell, M.D., Grossi, S., Targa, C., 1996. Relationship between the optical properties of chromophoric dissolved organic matter and total concentration of dissolved organic carbon in the southern Baltic Sea region. Mar. Chem. 55, 299-316.

Ferrari, G.M., 2000. The relationship between chromophoric dissolved organic matter and dissolved organic carbon in the European Atlantic coastal area and in the West Mediterranean Sea (Gulf of Lions). Mar. Chem. 70, 339-357.

Fichot, C.G., Benner, R., 2011. A novel method to estimate DOC concentrations from CDOM absorption coefficients in coastal waters. Geophys. Res. Lett., 38, L03610.

Green, S.A., Blough, N.V., 1994. Optical Absorption and Fluorescence Properties of chromophoric dissolved organic matter in natural waters. Limnol. Oceanogr, 39, 1903-1916.

Guo, L., Sun, M.-Y., 2009. Isotope composition of organic matter in seawater. In: Wurl, O. (Ed.), Practical Guidelines for the Analysis of Seawater. Taylor and Francis Group, LLC, pp. 97-123.

Gurtler, B.K., Vetter, T.A., Perdue, E.M., Ingall, E., Koprivnjak, J.K., Pfromm, P.H., 2008. Combining reverse osmosis and pulsed electrical current electrodialysis for improved recovery of dissolved organic matter from seawater. J. Membr. Sci. 323, 328-336.

Hansell, D.A., Carlson, C.A., Repeta, D.J., Reiner, S., 2009. Dissolved organic matter in the ocean. Oceanography, 22, 202-211.

Hay, B.J., Honjo, S., Kempe, S., Ittekkot, V.A., Degens, E.T., Konuk, T., Izdar, E., 1990. Interannual variability in particle flux in the southwestern Black Sea. Deep sea Res. 37, 911-928.

Hedges, J.I., Hatcher, P.G., Ertel, J.R., Meyers-Schulte, K.J., 1992. A comparison of dissolved humic substances from seawater with Amazon River counterparts by 13C-NMR spectrometry. Geochim. Cosmochim. Ac. 56, 1753-1757.

Hedges, J.I., Baldock, J.A., Gélinas, Y., Lee, C., Peterson, M.L., Wakeham, S.G., 2002. The biochemical and elemental compositions of marine plankton: A NMR perspective. Mar. Chem. 78, 47-63.

Helms, J.R., Stubbins, A., Ritchie, J.D., Minor, E.C., Kieber, D.J., Mopper, K., 2008. Absorption spectral slopes and slope ratios as indicators of molecular weight, source, and photobleaching of chromophoric dissolved organic matter. Limnol. Oceanogr. 53, 955-969.

Kieber, R.J., Hydro, L.H., Seaton, P.J., 1997. Photooxidation of triglycerides and fatty acids in seawater: implication toward the formation of marine humic substances. Limnol. Oceanogr. 42, 1454-1462.

Kieber, R.J., Whitehead, R.F., Reid, S.N., Willey, J.D., Seaton, P.J., 2006. Chromophoric dissolved organic matter (CDOM) in rainwater, southeastern North Carolina, USA. J. Atmos. Chem. 54, 21-41.

Kowalczuk, P., Cooper, W.J., Whitehead, R.F., Durakao, R.J., M., Sheldon, W., 2003. Characterization of CDOM in an organic rich river and surrounding coastal ocean in the South Atlantic Bight. Aquat. Sci., 65, 381–398.

Lakowicz, J.R., 2006. Principles of Fluorescence Spectroscopy. Springer.

Letelier, R.M., Strutton, P.G., Karl, D.M., 2008. Physical and ecological uncertainties in the widespread implementation of controlled upwelling in the North Pacific Subtropical Gyre. Mar. Ecol. Prog. Ser. 371, 305–308.

Mannino, A., Harvey, H.R., 1999. Lipid composition in particulate and dissolved organic matter in the Delaware Estuary: sources and diagenetic patterns. Geochim. Cosmochim. Ac. 63, 2219-2235.

Mannino, A., Harvey, H.R., 2004. Black carbon in estuarine and coastal ocean dissolved organic matter. Limnol. Oceanogr. 49, 735-740.

Melhuish, W.H., 1961. Quantum efficiencies of fluorescence of organic substances: effect of solvent and concentration of the fluorescent solute J. Phys. Chem., 65, 229-235.

Mopper, K., Zhou, X., Kieber, R.J., Kieber, D. J., Sikorski, R.J., Jones, R.D., 1991. Photochemical degradation of dissolved organic carbon and its impact on the oceanic carbon cycle. Nature 353, 60-62.

Mopper, K., Feng, Z., Bentjen, S.B., Chen, R.F., 1996. Effects of cross-flow filtration on the absorption and fluorescence properties of seawater. Mar. Chem. 55, 53-74.

Mopper, K., Stubbins, A., Ritchie, J.D., Bialk, H.M., Hatcher, P.G., 2007. Advanced instrumental approaches for characterization of marine dissolved organic matter: extraction techniques, mass spectrometry, and nuclear magnetic resonance spectroscopy. Chem. Rev. 107, 419-442.

Moran, M.A., Zepp, R.G., 1997. Role of photoreactions in the formation of biologically labile compounds from dissolved organic matter. Limnol. Oceanogr. 42, 1307-1316.

Moran, M.A., Sheldon, W.M., Zepp, R.G., 2000. Carbon loss and optical property changes during long-term photochemical and biological degradation of estuarine dissolved organic matter. Limnol. Oceanogr. 45, 1254-1264.

Nelson, N.B., Siegel, D.A., 2002. Chromophoric DOM in the open ocean. In: Hansell, D.A. and Carlson C.A. (eds), Biogeochemistry of marine dissolved organic matter. Academic Press, San Diego, CA. pp. 547-578.

Nieto-Cid, M., Álvarez-Salgado, X.A., Pérez, F.F., 2006. Microbial and photochemical reactivity of fluorescent dissolved organic matter in a coastal upwelling system. Limnol. Oceanogr. 51, 1391-1400.

Obernosterer, I., Sempéré, R., Herndl, G.J., 2001. Ultraviolet radiation induces reversal of the bioavailability of DOM to marine bacterioplankton. Aquat. Microb. Ecol. 24, 61-68.

Ortega-Retuerta, E., Frazer, T.K., Duarte, C.M., Ruiz-Halpern, S., Tovar-Sánchez, A., Arrieta, J.M., Reche, I., 2009. Biogeneration of chromophoric dissolved organic matter by bacteria and krill in the Southern Ocean. Limnol. Oceanogr. 54, 1941–1950.

Ortega-Retuerta, E., Reche, I., Pulido-Villena, E., Agustí, S. and Duarte, C.M., 2010. Distribution and photoreactivity of chromophoric dissolved organic matter in the Antarctic Peninsula (Southern Ocean). Mar. Chem. 118, 129-139.

Özsoy, E., Ünlüata, Ü., 1997. Oceanography of the Black Sea: A review of some recent results. Earth-Sci. Rev. 42, 231-272.

Peltier, W.R., Liu, Y., Crowley, J.W., 2007. Snowball Earth prevention by dissolved organic carbon remineralization. Nature 450, 813-819.

Perdue, E.M., Benner, R., 2009. Marine organic matter. In: Biophysico-chemical processes involving natural nonliving organic matter in environmental systems, N. Senesi, B. Xing, and P. M. Huang (eds), IUPAC Book Series, Wiley, NJ, pp. 407-449.

Repeta, D.J., Quan, T.M., Aluwihare, L.I., Accardi, A., 2002. Chemical characterization of high molecular weight dissolved organic matter in fresh and marine waters. Geochim. Cosmochim. Ac. 66, 955–962.

Romera-Castillo, C., Sarmento, H., Álvarez-Salgado, A.X., Gasol, J.M., Marrasé, C., 2010. Production of chromophoric dissolved organic matter by marine phytoplankton. Limnol. Oceanogr., 55, 446–454.

Romera-Castillo, C., Nieto-Cid, M., Castro, C.G., Marrasé, C., Largier, J., Barton, E.D., Álvarez-Salgado, X.A., 2011a. Fluorescence: absorption coefficient ratio - tracing photochemical and microbial degradation processes affecting coloured dissolved organic matter in a coastal system. Mar. Chem. 125, 26-38.

Romera-Castillo, C., Sarmento, H., Álvarez-Salgado, X.A., Gasol, J.M., Marrasé, C., 2011b. Net production/consumption of fluorescent coloured dissolved organic matter by natural bacterial assemblages growing on marine phytoplankton exudates. Appl. Environ. Microbiol. Accepted.

Rosenstock, B., Zwisler, W., Simon, M., 2005. Bacterial Consumption of Humic and Non-Humic Low and High Molecular Weight DOM and the Effect of Solar Irradiation on the Turnover of Labile DOM in the Southern Ocean. Microb. Ecol. 50, 90-101.

Schnitzer, M., 1985. Nature of nitrogen of humic substances from soil. In: Aiken, G.R., Mcknight, D.M., Wershaw, R.L., MacCarthy, P. (Eds.), Humic Substances in Soil, Sediment and Water. John Wiley & Sons, New York, pp. 303– 325.

Schrum, C., Staneva, J., Stanev, E., Özsoy, E., 2001. Air-sea exchange in the Black Sea estimated from atmospheric analysis for the period 1979-1993. J. Mar. Syst. 31, 3-19.

Skoog, A., Wedborg, M. and Fogelqvist, E., 1996. Photobleaching of fluorescence and the organic carbon concentration in a coastal environment. Mar. Chem. 55, 333-345.

Spencer, R.G.M., Stubbins, A., Hernes, P.J., Baker, A., Mopper, K., Aufdenkampe, A.K., Dyda, R.Y., Mwamba, V.L., Mangangu, A.M., Wabakanghanzi, J.N., Six, J., 2009. Photochemical degradation of dissolved organic matter and dissolved lignin phenols from the Congo River. J. Geophys. Res., 114, G03010.

Stedmon, C.A., Markager, S., 2005. Tracing the production and degradation of autochthonous fractions of dissolved organic matter using fluorescence analysis. Limnol. Oceanogr. 50, 1415-1426.

Stedmon, C.A., Bro, R., 2008. Characterizing dissolved organic matter fluorescence with parallel factor analysis: a tutorial. Limnol. Oceanogr.: Methods 6, 572–579.

Steinberg, D.K., Nelson, N.B., Carlson, C.A., Prusak, A.C., 2004. Production of chromophoric dissolved organic matter (CDOM) in the open ocean by zooplankton and the colonial cyanobacterium Trichodesmium spp. Mar. Ecol. Prog. Ser. 267, 45-56.

Sulzberger, B., Durisch-Kaiser, E., 2009. Chemical characterization of dissolved organic matter (DOM): A prerequisite for understanding UV-induced changes of DOM absorption properties and bioavailability. Aquat. Sci. 71, 104-126.

Swan, C.M., Siegel, D.A., Nelson, N.B., Carlson, C.A., Nasir, E., 2009. Biogeochemical and hydrographic controls on chromophoric dissolved organic matter distribution in the Pacific Ocean. Deep Sea Res. I: Oceanographic Research Papers, 56, 2175-2192.

Thurman, E.M., 1985. Organic geochemistry of natural waters. Chapter 10. Aquatic humic substances. Eds. Martinus Nijhoff and Dr W. Junk Publishers.

Turro, N.J., 1991. Modern molecular photochemistry. University Science Books.

Vähätalo, A.V., Salkinoja-Salonen, M., Taalas, P. and Salonen, K., 2000. Spectrum of the quantum yield for photochemical mineralization of dissolved organic carbon in a humic lake. Limnol. Oceanogr. 45, 664-676.

Vodacek, A., Hoge, F.E., Swift, R.N., Yungel, J.K., Peltzer, E.T., Blough, N.V., 1995. The use of in situ and airborne fluorescence measurements to determine UV absorption coefficients and DOC concentrations in surface waters. Limnol. Oceanogr. 40, 411-415.

Vodacek, A., Blough, N.V., 1997. Seasonal variation of CDOM in the Middle Atlantic Bight: Terrestrial inputs and photooxidation. Proceedings of SPIE-The International Society for Optical Engineering, 2963(Ocean Optics XIII), 132-137.

Weishaar, J.L., Aiken, G.R., Bergamaschi, B.A., Fram, M.S., Fujii, R., Mopper, K., 2003. Evaluation of specific ultraviolet absorbance as an indicator of the chemical composition and reactivity of dissolved organic carbon. Environ. Sci. Technol. 37, 4702-4708.

Wheeler, J.R., 1976. Fractionation by molecular weight of organic substances in Georgia coastal water. Limnol. Oceanogr. 21, 846-852.

Yakushev, E.V., Podymov, O., Chasovnikov, V.K., 2005. Seasonal changes in the hydrochemical structure of the black sea redox zone. Oceanography, 18, 48-5.

Yamashita, Y., Tanoue, E., 2008. Production of bio-refractory fluorescent dissolved organic matter in the ocean interior. Nat. Geosci. 1, 579-582.

Zepp, R.G., Sheldon, W.M., Moran, M.A., 2004. Dissolved organic fluorophores in southeastern US coastal waters: correction method for eliminating Rayleigh and Raman scattering peaks in excitation-emission matrices. Mar. Chem. 89, 15-36.

Chapter IV

Fluorescence: absorption coefficient ratio – tracing photochemical and microbial degradation processes affecting coloured dissolved organic matter in a coastal system

Chapter IV

Co-authors:

M. Nieto-Cid, C.G. Castro, C. Marrasé, J. Largier, E.D. Barton and X.A. Álvarez-Salgado.

Abstract

The optical properties of coloured dissolved organic matter (CDOM) —absorption coefficient, induced fluorescence, and fluorescence quantum yield — were determined in the coastal eutrophic system of the Ría de Vigo (NW Spain) under two contrasting situations: a downwelling event in September 2006 and an upwelling event in June 2007. Significantly different optical properties were recorded in the shelf surface (higher absorption coefficient, lower quantum yield) and bottom (lower absorption coefficient, higher quantum yield) waters that entered the embayment during downwelling and upwelling conditions, respectively. Continental waters presented distinctly high CDOM levels. The spatial and temporal variability of the induced fluorescence to absorption coefficient ratio during the mixing of shelf and continental waters was used to quantify the relative importance of photochemical and microbial processes under these contrasting hydrographic conditions. Photochemical processes were dominant during the downwelling episode: 86% of the variability of CDOM can be explained by photochemical degradation. On the contrary, microbial processes prevailed during the upwelling event: 77% of the total variability of CDOM was explained by microbial respiration.

Chapter IV

Introduction

Coloured dissolved organic matter (CDOM) is the main UV-absorbing component in aquatic systems, contributing to prevent DNA damage in aquatic organisms, especially in a global change context of stratospheric ozone reduction (Häder and Sinha, 2005 and references therein). CDOM also absorbs radiation in the visible spectral range interfering with satellite-derived chlorophyll estimates, a fact that has stimulated the study of these materials in coastal and open ocean systems (e.g. Hoge et al., 1993; Vodacek and Blough, 1997; Siegel et al., 2002). A fraction of CDOM can emit the absorbed radiation as fluorescent light (Coble, 1996, 2007). In most estuaries and coastal areas, CDOM constitutes a dominant fraction of the DOM pool and good positive correlations are obtained between the induced fluorescence emission of CDOM, the absorption coefficient at the fluorescence excitation wavelength, and the concentration of dissolved organic carbon, DOC (e.g. Hoge et al., 1993; Vodacek et al., 1995; 1997; Ferrari et al., 1996; Ferrari, 2000; Del Vecchio and Blough, 2004; Del Castillo and Miller, 2008; Kowalczuk et al., 2010). In most of these cases, the more sensitive, simpler and quicker fluorescence spectroscopy measurements have been used to estimate CDOM absorption and DOC concentrations, especially for the calibration of remote sensing colour sensors. The goodness of the linear relationships between induced fluorescence and absorption coefficient, and between absorption coefficient and DOC, depend on the narrow variability of the fluorescence to absorption coefficient ratio, i.e. the fluorescence quantum yield, and the absorption coefficient to DOC ratio, i.e. the carbon specific absorption coefficient (Green and Blough, 1994; Vodacek et al., 1995). In some areas, CDOM absorption coefficient or induced fluorescence measurements can be used together with salinity to solve the mixing of three coastal water masses (e.g. Klinkhammer et al., 2000; Stedmon et al., 2010). The benefit of this approach depends on how conservative the behaviour of the optical properties of CDOM is during water mass mixing.

However, it is well known that DOC and CDOM are produced and consumed by biogeochemical processes during the mixing of water masses of contrasting origins. The most important CDOM sink is photo-degradation mediated by natural UV-light, which break down the coloured molecules into smaller and colourless ones (Chen and Bada, 1992; Moran et al., 2000). On the other hand, the main source of CDOM is aerobic autotrophic and heterotrophic microbial respiration (Yentsch and Reichert, 1961; Kramer and Herndl, 2004; Nieto-Cid et al., 2006; Romera-Castillo et al., 2010, see Chapter I) and, to a lesser extent, abiotic reactions of photo-humification (Kieber et al., 1997). DOC and CDOM absorption and fluorescence have a different response to these processes, thus altering the fluorescence quantum yield and carbon specific absorption coefficient (e.g. De Haan, 1993; Moran et al., 2000; Lønborg et al., 2010).

The in situ production of fluorescent CDOM is 5-fold the terrestrial inputs measured in the ocean interior (Yamashita and Tanoue, 2008). Although in coastal areas more affected by freshwater

discharges terrestrial inputs will gain importance, net fluorescent CDOM production rates in the eutrophic embayment of the Ria de Vigo (NW Spain) still were 3-fold the continental inputs as calculated from Nieto-Cid et al. (2005). This observation, together with the dynamic nature of this coastal inlet intermittently affected by wind-driven upwelling and downwelling events (Doval et al., 1997; Álvarez-Salgado et al., 2001), makes the Ría de Vigo an excellent location to study the spatial and temporal variability of the optical properties of CDOM under contrasting hydrographic conditions and infer the relative importance of photochemical and microbial processes during the mixing of continental and oceanic waters in a coastal upwelling system.

Materials and methods

Survey area

The Ría de Vigo is a large (3.12 km^3) V-shaped coastal embayment in the NW Iberian Peninsula (Fig. 1). The River Oitaben-Verdugo is the main freshwater source, with an average annual flow of 15 m^3 s^{-1} (Gago et al., 2005). It drains into San Simon Bay, a sedimentary basin in the innermost part of the embayment. The mouth of the ría, where it opens to the Atlantic Ocean, is divided by the Cíes Islands into northern (2.5 km wide, 25 m deep) and southern (5 km wide, 60 m deep) entrances. The hydrography of the Ría de Vigo is dictated by coastal wind stress, which is upwelling-favourable from April-May to September-October and downwelling-favourable the rest of the year (Wooster et al. 1976; Torres et al. 2003). The upwelling-favourable season appears as a succession of wind stress/relaxation cycles of period 10-20 days (Álvarez-Salgado et al., 1993), when the cold nutrient-rich and DOC-poor Eastern North Atlantic Central Water (ENACW) enters the ría (Doval et al., 1997; Álvarez-Salgado et al., 2001; Nieto-Cid et al., 2005). The transition from the upwelling- to the downwelling-favourable seasons occurs from mid September to mid October and it is characterised by the entry of warm, nutrient-poor and DOC-rich shelf surface waters into the ría (Doval et al., 1997; Álvarez-Salgado et al., 2001; Nieto-Cid et al., 2005). Whereas during the upwelling-favourable season the microplankton community (> 20 μm) is dominated by diatoms and the net community metabolism is autotrophic, in the transition from the upwelling- to the downwelling-favourable season dinoflagellates prevail and the metabolism is balanced or net heterotrophic (Figueiras and Ríos, 1993; Cermeño et al., 2006; Piedracoba et al., 2008).

Sampling program

Water samples were collected aboard R/V Mytilus during two contrasting periods: from 26 to 30 September 2006, during the transition from the upwelling- to the downwelling-favourable season,
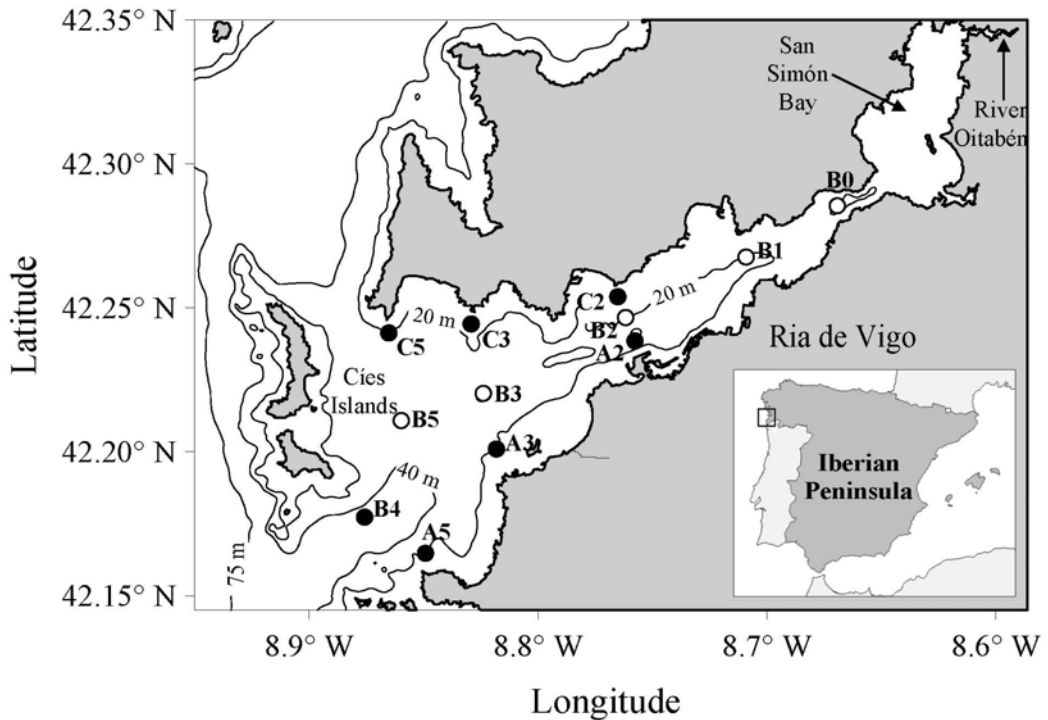
Fig. 1. Map showing the bathymetry and location of sampling stations in the Ría de Vigo (NW Spain).

and from 25 to 28 June 2007, during the upwelling season. On 26 and 30 September 2006 and 25 and 28 June 2007, the twelve stations indicated in Fig. 1 were visited. On 28 September 2006 and 27 June 2007 the sampling concentrated on the middle sector (stns A3, B3 and C3), on 27 September 2006 in the outer sector (stns A5, B5 and C5), and on 29 September 2006 on the inner sector (stns A2, B2 and C2) of the Ría de Vigo. Surface samples were taken from the continuous non-toxic underwater supply at 2 m depth. At stations B0, B1, B2, B3, B4 and B5 full-depth continuous conductivity-temperature-depth (CTD) profiles were recorded with a SBE 9/11 CTD probe incorporated into a rosette sampler equipped with twelve 12-L Niskin bottles. Conductivity measurements were converted into practical salinity scale values with the equation of UNESCO (1985). Water samples from 3 to 5 depths were collected depending on the bathymetry of the stations.

Aliquots for the analysis of dissolved oxygen (O_2), nutrient salts (NH_4^+, NO_2^-, NO_3^-, HPO_4^{2-} and H_4SiO_4), dissolved organic carbon (DOC), absorbance and fluorescence of coloured dissolved organic matter (CDOM) were collected from both the non-toxic underwater pipe and the Niskin bottles.

Coastal wind data over the study periods were obtained from a mooring located about 60 km offshore of Cabo Silleiro (Fig. 1) ran by Spanish Port Authority (Puertos del Estado, http://www.puertos.es). Hourly data were checked for outliers, and any gaps of less than 6 hours were filled by interpolation with a cubic spline before the series was low pass filtered to remove periods less than 40 h and then sub-sampled to produce 6 hourly series.

Temperature observations were available from TidBit thermistor loggers and SeaBird MicroCat SBE37 recorders moored at 42º 12.4'N, 8º 48.6'W in 21 m depth, close to stn A3 on the southern side of the central ría (Fig. 1). The data were compared with CTD profiles made at the site to check that accuracy lay within the quoted manufacturers' specifications. The TidBits have a nominal accuracy of ±0.2ºC and precision of ±0.02ºC, while the MicroCats have quoted values of ±0.002ºC precision and ±0.0001ºC resolution. The temperature series, recorded at 2 minute intervals, were edited for outliers before averaging to 1 hour intervals.

Chemical analysis

Dissolved oxygen was determined by the Winkler method with potentiometric endpoint detection using a Titrino 72' analyser (Metrohm) with an analytical precision of ±0.5 μmol kg^{-1}. Oxygen concentrations were referred to the oxidation state of nitrate (O$_2$cor) by considering that the ammonium and nitrite of the samples were oxidised to nitrate. Since 0.5 mol of oxygen is necessary to oxidise 1 mol of nitrite to nitrate and 2 mol of oxygen is required to oxidise 1 mol of ammonium to nitrate.

$$O_2cor = O_2 - \frac{1}{2} \cdot NO_2^- - 2 \cdot NH_4^+ \tag{1}$$

This correction allows comparison of dissolved oxygen consumption versus nutrient salts and CDOM production independently of the oxidation state of the inorganic nitrogen form involved in the organic matter mineralisation process. The corrected Apparent Oxygen Utilisation (AOU), i.e. the difference between the dissolved oxygen concentration at saturation and the actual corrected oxygen concentration of the sample, was calculated following UNESCO (1986).

Samples for nutrient salts analysis were collected in 50 mL polyethylene bottles and preserved at 4ºC until determination in the base laboratory within 4 h of collection using standard segmented flow analysis (SFA) procedures. The precisions of the methods are ±0.02 μmol kg^{-1} for nitrite, ±0.1 μmol kg^{-1} for nitrate, ±0.05 μmol kg^{-1} for ammonium, ±0.02 μmol kg^{-1} for phosphate and ±0.05 μmol kg^{-1} for silicate.

Samples for DOM analyses were taken in 500 mL acid-washed glass flasks and transported into the base laboratory within 4 hours of collection. Once in the laboratory, aliquots for DOC, and absorbance and fluorescence of CDOM were immediately filtered through precombusted (450ºC, 4 h) Whatman GF/F filters in an acid-cleaned all-glass filtration system, under positive pressure with low N_2 flow.

Approximately 10 mL of the filtrate were collected for DOC determination in precombusted (450ºC, 12 h) glass ampoules. These samples were acidified with H_3PO_4 to pH < 2 and the ampoules were heat-sealed and stored in the dark at 4ºC until analysis. DOC was measured with a Shimadzu TOC-CVS organic carbon analyser. The system was standardised daily with potassium hydrogen phthalate. The concentration of DOC was determined by subtracting the instrument blank area from the average peak area and dividing by the slope of the standard curve. The precision of the equipment was ±0.7 μmol L^{-1}. The accuracy was tested daily with the DOC reference materials provided by Prof. D.A. Hansell (Miami University). We obtained average concentrations of 45.7 ± 1.6 μmol L^{-1} for the deep ocean reference (Sargasso Sea deep water, 2600 m) minus blank reference materials. The nominal DOC value provided by the reference laboratory is 44.0 ± 1.5 μmol L^{-1}.

Optical measurements

Absorbance of CDOM was measured within 4 hours of collection using a Beckman Counter DU 800 spectrophotometer equipped with a 10 cm quartz round cell. Spectral scans were collected in a wavelength range of 250-700 nm at a constant room temperature of 25ºC. Pre-filtered (0.2 μm) Milli-Q water was used as the reference for all samples. Absorption coefficients were calculated using the equation:

$$a_{CDOM}(\lambda) = \frac{2.303}{1} \cdot ABS(\lambda) \qquad (2)$$

where $ABS(\lambda)$ is the absorbance at wavelength λ, and l is the cell length in meters.

Using the Levenberg-Marquardt algorithms implemented in the Stat Soft Inc. STATISTICA software we obtained the coefficients $a_{CDOM}(340)$, S and K that best fit the equation:

$$a_{CDOM}(\lambda) = a_{CDOM}(340) \cdot \exp(-S \cdot (\lambda - 340)) + K \qquad (3)$$

where $a_{CDOM}(340)$ is the absorption coefficient at wavelength 340 nm (in m^{-1}), S is the spectral slope (in nm^{-1}) and K is a background constant caused by residual scattering by fine size particle fractions, micro-

air bubbles or colloidal material present in the sample, refractive index differences between sample and the reference, or attenuation not due to organic matter (in m⁻¹). The estimated detection limit of this spectrophotometer is 0.001 absorbance units or 0.02 m⁻¹. The carbon specific CDOM absorption coefficient at 340 nm, $a^*_{CDOM}(340)$, was calculated dividing $a_{CDOM}(340)$ by the DOC concentration.

Induced fluorescence of CDOM (FDOM) was measured after 4 hours of collection with a Perkin Elmer LS 55 luminescence spectrometer, equipped with a xenon discharge lamp, equivalent to 20 kW for 8 μs duration. The detector was a red-sensitive R928 photomultiplier and a photodiode worked as reference detector. Slit widths were 10.0 nm for the excitation and emission wavelengths. Measurements were performed at a constant room temperature of 25ºC in a 1cm quartz fluorescence cell. MQ water was used as a reference blank for fluorescence analysis. Fluorescence intensity was measured at a fixed excitation/emission wavelength of 340 nm/440 nm, $F(340/440)$, which is characteristic of humic-like substances (Coble, 1996). The spectrofluorometer was calibrated daily with quinine sulphate in 0.1 N sulphuric acid. $F(340/440)$ was expressed in μg L⁻¹ of quinine sulphate, hereafter quinine sulphate units (QSU). The equivalent concentration of each peak was determined by subtracting the MQ blank peak height from the sample average peak height, and dividing by the slope of the standard curve. The precision was ± 0.1 QSU.

The quantum yield of fluorescence at 340nm, $\Phi(340)$, is the portion of the light absorbed at 340 nm, $a_{CDOM}(340)$, that is re-emitted as fluorescent light. $\Phi(340)$, for the samples was determined as in Romera-Castillo et al. (submitted, see Chapter III) using the ratio of the absorption coefficient at 340 nm and the corresponding fluorescence emission between 400 and 600 nm from the quinine sulphate standard in 0.1 N H_2SO_4 using the equation (Green and Blough, 1994):

$$\Phi(340) = \frac{F(400\text{ - }600)}{a_{CDOM}(340)} \cdot \frac{a_{CDOM}(340)_{QS}}{F(400\text{ - }600)_{QS}} \cdot \Phi(340)_{QS} \qquad (4)$$

where $a_{CDOM}(340)$ and $a_{CDOM}(340)_{QS}$ are the absorption coefficients of the sample and the QS standard (in m⁻¹), respectively; $F(400\text{-}600)$ and $F(400\text{-}600)_{QS}$ are the average integrated fluorescence spectra between 400 and 600 nm at a fixed excitation wavelength of 340 nm (in μg QS L⁻¹) of the sample and the QS standard, respectively; and $\Phi(340)_{QS}$ is the dimensionless fluorescence quantum yield of the QS standard, equal to 0.54 according to Melhuish (1961).

Although fluorescence spectra between 400 and 600 nm, $F(400\text{-}600)$, were recorded in 34 out of the 197 samples collected in the Ría de Vigo, the very good linear correlation between $F(340/440)$ and $F(400\text{-}600)$ ($R^2 = 0.87$, n = 34, p < 0.001) reveals that $F(400\text{-}600)$ can be estimated from $F(340/440)$ using the dimensionless conversion factor of 0.62 ± 0.05. Therefore, the ratio $F(400\text{-}600)/a_{CDOM}(340)$ can be obtained from the ratio $F(340/440)/a_{CDOM}(340)$ for all the samples collected in this study, in such a way that eq. (4) can be rewritten as:

$$\Phi(340) = \beta \cdot \Phi(340)_{QS} \cdot \frac{F(340/440)}{a_{CDOM}(340)} = 2.2(\pm0.2) \cdot 10^{-3} \cdot \frac{F(340/440)}{a_{CDOM}(340)} \qquad (5)$$

where $\beta = 4.2(\pm0.3) \, 10^{-3} \, m^{-1} \, QSU^{-1}$ is a constant that accounts for the conversion factor $F(400\text{-}600)/F(340/440)$ and for the $F(400\text{-}600)_{QS}/ \, a_{CDOM}(340)_{QS}$ ratio. The universality of this constant have been demonstrated in Romera-Castillo et al., (submitted, Chapter III).

Results

Hydrography and dynamics of the Ría de Vigo in September 06 and July 07

From 25 to 30 September 2006 coastal winds evolved from northerly to southerly, i.e. from upwelling- to downwelling-favourable (Fig. 2a). Concomitantly, water temperature at stn A3 (Fig. 2b) traced the replacement of water colder than 16.8 ºC (top 25m) on 25 September by warmer shelf surface water >18ºC (top 25 m) on 30 September. The evolution of surface temperature from 25 September (Fig. 3a) to 30 September (Fig. 3b), indicates that the transition from upwelling- to downwelling favourable winds was not a local phenomenon observed only at stn A3. It affected the entire ría from surface to bottom, and from the outer to the inner segment of the embayment. Salinity varied in a very narrow range, from 35.1 in the surface inner ría (Figs. 3c, d) to 35.7 in the bottom outer ría (not shown).

From 25 to 28 June 2007, as a response to the strong northerly winds that were blowing on the shelf (Fig. 2c), the cold (<13ºC) and salty (>35.7) Eastern North Atlantic Central Water (ENACW) entered the ría through the bottom of the southern mouth. Cooling due to upwelling was perceptible when comparing the sea surface temperature distributions of 25 June (Fig. 3e) and 28 June (Fig. 3f). The 14ºC isotherm was at >30 m depth on 25 June, and reached 15 m depth three days later (Figs. 4a, b). Salinity exhibited in this case a wider range of variability, from 31.1 in the surface inner ría (Figs. 3g, h) to 35.9 in the bottom outer ría (not shown). The warmer and fresher waters observed in the inner ría are the result of the mixing of the oceanic ENACW with the continental waters carried by the river Oitabén-Verdugo, which represent >5% in samples of salinity <34.

Nutrient status under contrasting hydrographic conditions

Shelf surface waters that entered the ría during the downwelling event sampled in September 06 were nutrient-poorer than the waters inside the ría (Figs. 5a, b). Phosphate and silicate distributions (not shown) followed a parallel pattern to the total inorganic nitrogen (TIN) distribution, presenting
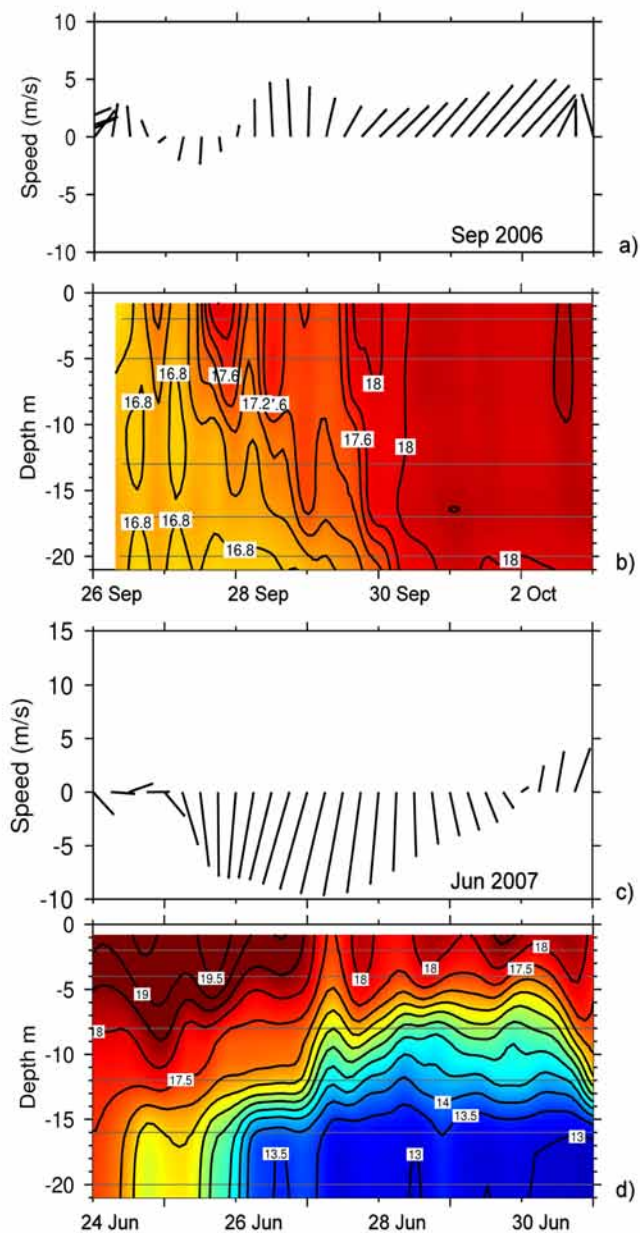
Fig. 2. Coastal winds (a, c) and thermistor records (b, d) at stn A3 during the September 06 and June 07 sampling periods.

significant linear correlations ($R^2 = 0.74$, n = 112, $p < 0.001$ and $R^2 = 0.69$, n = 112, $p < 0.001$) for phosphate and silicate, respectively. The predominant form of inorganic nitrogen was ammonium, which represented $81 \pm 2\%$ of TIN (eq. 1 in Table 1), i.e. pointing to a system dominated by recycled production (Eppley and Peterson, 1979). This contrasts with the negative values of AOU in the nutrient-poor shelf surface waters that entered the ría, lower than those of the water in the inner part of the ría, where positive values of AOU were recorded (Figs. 5c, d). The distribution of DOC (Figs. 5e, f) was more complex: on 25 September, a strong gradient was observed between the DOC-rich (>100 µmol L^{-1}) surface waters coming from the sedimentary basin of San Simon Bay and the DOC-poor (<65 µmol L^{-1}) waters of the bottom outer ría. On 30 September, shelf surface waters, which have an intermediate DOC concentration (about 80 µmol L^{-1}), modified the DOC distribution of the ría.

During the event sampled on June 07, the upwelling of nutrient-rich and dissolved oxygen-poor oceanic ENACW produced a clear impact on the distributions of total inorganic nitrogen (Figs. 4c, d and 6a, b) and AOU (Figs. 4e, f and 6c, d). Nitrate was the predominant inorganic nitrogen form in this case, representing $82 \pm 3\%$ of TIN (eq. 2 in Table 1), which is characteristic of a system dominated by new production (Eppley and Peterson 1979). The DOC distributions of June 07 (Figs. 4g, h and 6e, f) traced the entry of the DOC-poor (< 68 µmol L^{-1}) oceanic ENACW. The signal of the river Oitaben-Verdugo after crossing San Simón bay is also visible in the surface innermost stations, where a DOC value of 112 µmol L^{-1} was recorded.

Optical properties of CDOM under contrasting hydrographic conditions

During the downwelling event sampled in September 06, the DOC-rich waters coming from the sedimentary basin of San Simón bay presented the highest values of $a_{CDOM}(340)$, >0.77 m^{-1} (Figs. 7a, b). Shelf surface waters were characterised by much lower values of $a_{CDOM}(340)$, 0.34 ± 0.02 m^{-1} (average ± SD of the surface sample at stn B5). On the contrary, $\Phi(340)$ were not that different: $0.82 \pm 0.03\%$ for the surface sample of stn B0 and $0.76 \pm 0.02\%$ for the surface sample of stn B5 (Figs. 7c, d). The distribution of $F(340/440)$ (data not shown) was parallel to $a_{CDOM}(340)$: $r^2 = 0.79$, n = 112, $p < 0.001$. The surface distribution of $a_{CDOM}(340)$ on 25 September shows the mixing of the coloured waters from the inner ría with the bleached waters from the adjacent shelf (Figs. 4i & 8a). Five days later, the surface layer of the ría reflected the intrusion of CDOM-poor shelf surface waters into the inner ría (Figs. 4j & 8b). Similar patterns are observed in the distributions of $\Phi(340)$ (Figs. 4k, l & 8c, d).

During the upwelling event sampled on June 07, the oceanic ENACW cooler than 14ºC that occupied the bottom of the ría presented relatively low $a_{CDOM}(340)$ but high $\Phi(340)$ values, 0.23 ± 0.04 m^{-1} and $1.2 \pm 0.3\%$ respectively (Figs. 4i-l), compared with the warmer waters in the ría before the upwelling episode. The influence of the CDOM transported by the river Oitaben-Verdugo through San Simon Bay can also be traced in the low salinity water of the innermost part of the ría, where an
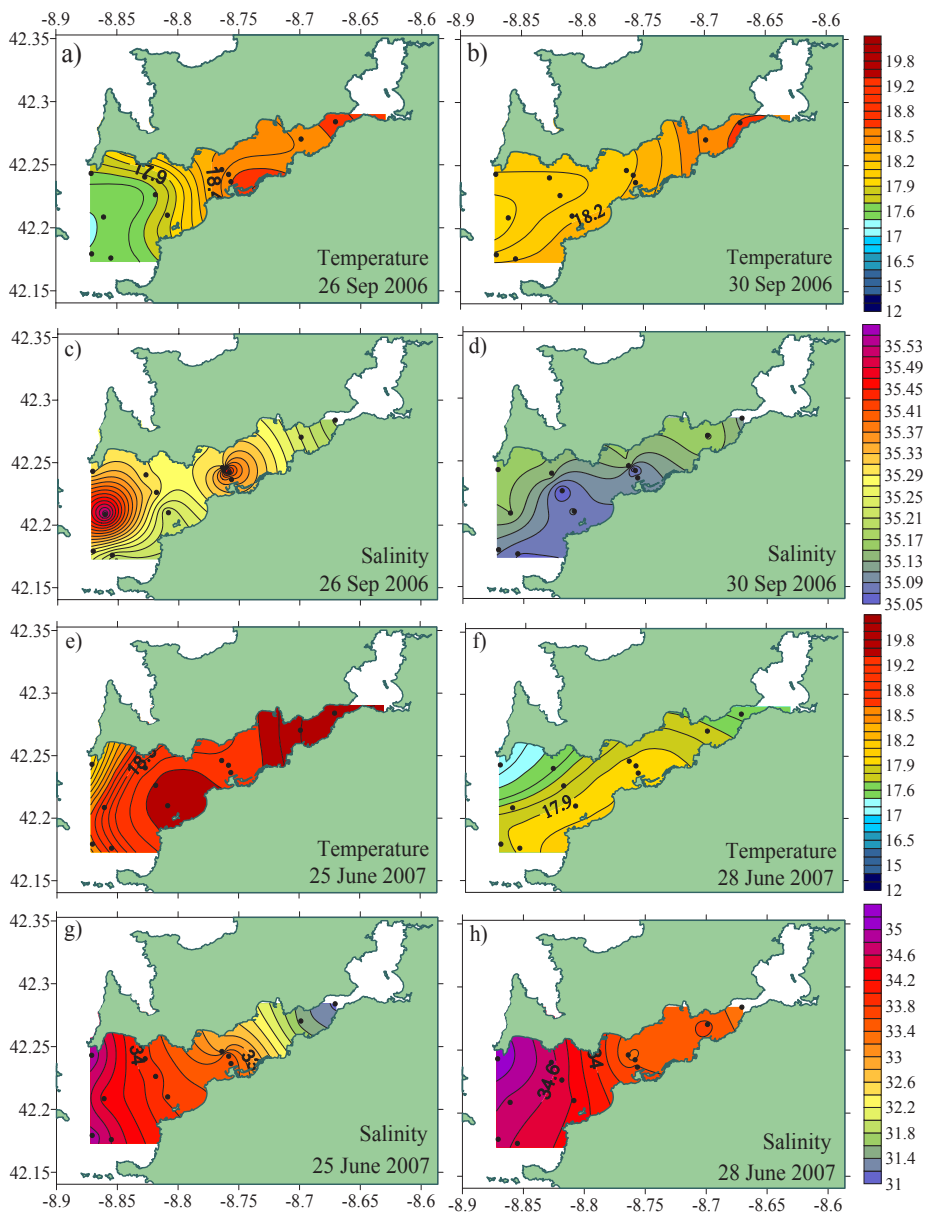
Fig. 3. Sea surface distribution for September 26 and 30 (2006) of temperature (a, b) and salinity (c, d) and sea surface distribution for June 25 and 28 (2007) of temperature (e, f) and salinity (g, h). Temperature in ºC. X-axis is logitude in degrees; Y-axis is latitude in degrees.
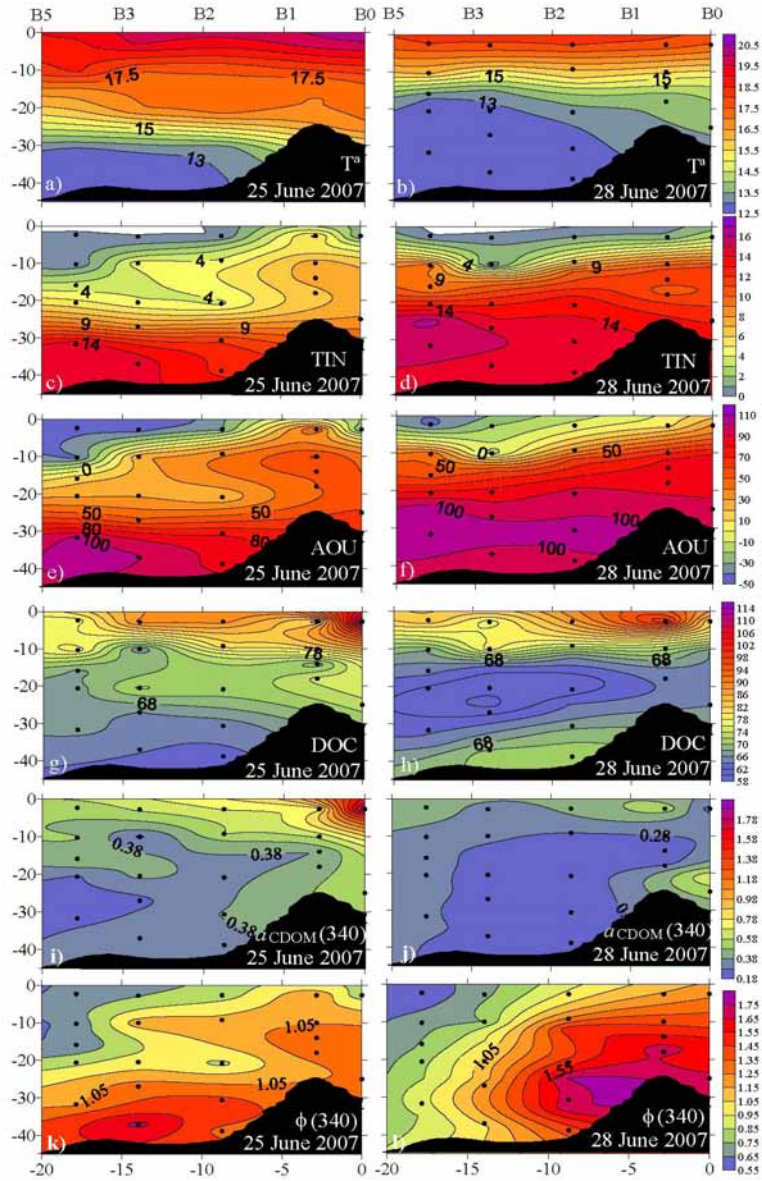
Fig. 4. Vertical distributions for June 25 and 28 (2007) of temperature (a, b) in ºC; total inorganic nitrogen (TIN) (c, d) in $\mu mol \cdot L^{-1}$; apparent oxygen utilization (AOU) (e, f) in $\mu mol \cdot Kg^{-1}$; dissolved organic carbon (DOC) (g, h) in $\mu mol \cdot L^{-1}$; CDOM absorption coefficient at 340nm, $a_{CDOM}(340)$ (i, j), in m^{-1} and CDOM fluorescence quantum yield at 340 nm, $\Phi(340)$ (k, l). X-axis is distance (Km) from station B0; Y-axix is depth (m).

$a_{CDOM}(340)$ value of 1.82 m^{-1} was recorded. The highest values of $\Phi(340)$, 1.6 ± 0.1%, were observed in the inner ría, below 10 m on 28 June. This maximum is coincident with the maxima observed in TIN (Fig. 4d) and AOU (Fig. 4f). In this case, the linear correlation of $F(340/440)$ with $a_{CDOM}(340)$ was lower than in September 06 ($r^2 = 0.60$, n = 80, $p < 0.001$) when the outlying samples B0 (2 m) on 25 June and B3(20 m) on 27 June are excluded from the analysis.

Absorption spectral slopes, S (not shown), were not significantly different during the upwelling and downwelling periods: they ranged between 0.018 nm^{-1} and 0.023 nm^{-1} during the former and between 0.018 nm^{-1} and 0.024 nm^{-1} during the latter period. S varied inversely to $a_{CDOM}(340)$ but the log transformed plot of the two variables (Fig. 9) shows that the slope of the relationship between S and $a_{CDOM}(340)$ (regression model II; Sokal and Rolf, 1995) was significantly higher for the downwelling (-0.26 ± 0.01) than for the upwelling period (-0.16 ± 0.01). For the case of the upwelling period, the two outlying samples (grey dots) were not considered. If they are included in the analysis the determination coefficient of the relationship increases ($r^2 = 0.76$) but the origin intercept and slope of the regression does not change significantly.

Discussion

Optical properties of CDOM in the Ría de Vigo: comparison with other marine systems

The average ± SD values of the absorption coefficient, $a_{CDOM}(340)$, and carbon-specific CDOM absorption coefficient, $a^*_{CDOM}(340)$, at 340 nm in the Ría de Vigo were significantly higher (p < 0.001) during the downwelling (0.43 ± 0.11 m^{-1} and 5.4 ± 1.1 m^2 mol C^{-1}) than during the upwelling event (0.35 ± 0.14 m^{-1} and 4.5 ± 1.3 m^2 mol C^{-1}). On the contrary, $\Phi(340)$ was significantly lower ($p < 0.001$) during the downwelling (0.81 ± 0.11%) than during the upwelling episode (1.03 ± 0.30%, Table 2). Day and Faloona (2009) also found less coloured surface waters in association with intense upwelling episodes in the Northern California coast. The distributions of $a_{CDOM}(\lambda)$ and $a^*_{CDOM}(\lambda)$ in the Ría de Vigo, resulting from the mixing of DOC and CDOM-rich continental waters with DOC and CDOM-poor ocean waters, is characteristic of most coastal systems (e.g. Vodacek and Blough, 1997; Chen et al., 2002; Del Vecchio and Blough, 2004). This mixing pattern results in a decrease of $a_{CDOM}(\lambda)$ with depth. However, in other coastal upwelling regions drier and more irradiated than the NW Iberian Peninsula, $a_{CDOM}(\lambda)$ tends to increase with depth (Coble et al., 1998; Kudela et al., 2006).

The variety of wavelengths used in the literature to determine $a_{CDOM}(\lambda)$ —325, 355, 375 and 443 nm being the most common— makes difficult the direct comparison of this parameter obtained in the Ría de Vigo with other marine systems. In this work, we have used $a_{CDOM}(340)$ to allow the quantitative

estimation of $\Phi(340)$ referred to a quinine sulphate standard of known fluorescence quantum yield. In any case, average ± SD values for the referred wavelengths are reported in Table 2. The significant difference observed in $a_{CDOM}(340)$ between the upwelling and the downwelling episodes sampled in this study (see above) is also observed for the other wavelengths. The average ± SD values of $a_{CDOM}(325)$, $a_{CDOM}(355)$, $a_{CDOM}(375)$ and $a_{CDOM}(443)$ recorded in the Ría de Vigo for both periods —0.54 ± 0.17 m^{-1} , 0.29 ± 0.10 m^{-1}, 0.20 ± 0.07 m^{-1} and 0.051 ± 0.023 m^{-1} (Table 2), respectively— are higher than in continental shelf surface waters but lower than in estuaries and coastal inlets affected by important freshwater inputs (e.g. Vodacek and Blough, 1997; Ferrari, 2000; Babin et al., 2003; Del Vecchio and Blough, 2004; Nelson et al., 2010; Kowalczuk et al., 2010). Our surface values of $a_{CDOM}(\lambda)$ are in the upper end of those reported in other coastal upwelling regions such as Northern California (Day and Faloona, 2009), Mauritania (Bricaud et al., 1981) or Arabia (Coble et al., 1998). They are also significantly higher than in coastal oligothrophic sites such as the Blanes Bay Observatory in the NW Mediterranean, where $a_{CDOM}(325)$ was 0.28 ± 0.09 m^{-1} and $a_{CDOM}(443)$ was 0.016 ± 0.015 m^{-1} (average ± SD) over an annual cycle (Romera-Castillo et al., in prep., see Chapter V) and in oligotrophic open ocean waters (Nelson et al., 2004, 2007, 2010; Swan et al., 2009).

As for the case of $a_{CDOM}(\lambda)$, direct comparison of absolute values of S obtained by different authors is difficult because they have used different fitting procedures across different wavelength ranges and S slightly differs depending on those choices (Ferrari, 2000; Stedmon et al., 2000; Blough and Del Vecchio, 2002). In our case, spectral slopes were determined over the range 250-500 nm, and the observed values, 0.0205 ± 0.0013 nm^{-1} (average ± SD), are close to those reported by Babin et al. (2003), 0.0176 ± 0.0020 nm^{-1} (average ± SD; wavelength range 350-750 nm),who considered a wide variety of coastal and open ocean systems. Our values are also between those reported by Ferrari, (2000) for surface open ocean (0.025 nm^{-1} and more) and coastal waters (0.013-0.018 nm^{-1}) calculated over a wavelength range of 350-480 nm. Bricaud et al., (1981) obtained lower S mean values, 0.0150 ± 0.0023 nm^{-1}, in the Mauritanian upwelling region for a wavelength range of 375-500 nm.

Although absolute values of S are not directly comparable, some common trends can be defined. This is the case of the inverse relationship between S and $a_{CDOM}(\lambda)$ reported in our Fig. 9, which is observed in most coastal and open ocean waters (e.g. Del Castillo and Coble, 2000; Stedmon et al., 2000; Stedmon and Markager, 2001; Nelson et al., 2010). In general, i) CDOM of terrestrial origin is characterised by lower spectral slopes than CDOM of marine origin; ii) microbial degradation processes lowers; and iii) photodegradation rises the spectral slopes (Del Vecchio and Blough, 2004; Nelson et al., 2007, 2010). With these considerations in mind, the remarkably higher slope of the relationship between $a_{CDOM}(340)$ and S for September 06 compared with June 07 suggests a dominance of photodegradation over microbial processes during the downwelling period and the contrary during the upwelling period, especially considering that the effect of continental waters (that would tend to lower the slopes) is larger during the upwelling period.

The concentration of DOC correlated with $a_{CDOM}(340)$ for both periods (eq. 3 and 4, Table 1). Equations 3 and 4 are not significantly different, neither in the y-intercept nor in the slope. Therefore, the relationship between DOC and $a_{CDOM}(340)$ can be presented under an unique regression equation (Eq. 5, Table 1). The y-intercept, $49 \pm 1 \mu mol\ L^{-1}$, represents the colourless DOC. Since the average ± SD concentration of DOC for all the samples taken in the Ría de Vigo in September 2006 and June 2007 is $77 \pm 13\ \mu mol\ L^{-1}$, the coloured DOC would represent $36 \pm 20\%$ of the bulk DOC. This value is within the range of the characteristic values for open ocean, approx. 20%, and coastal areas, up to 70% (e.g. Ferrari,
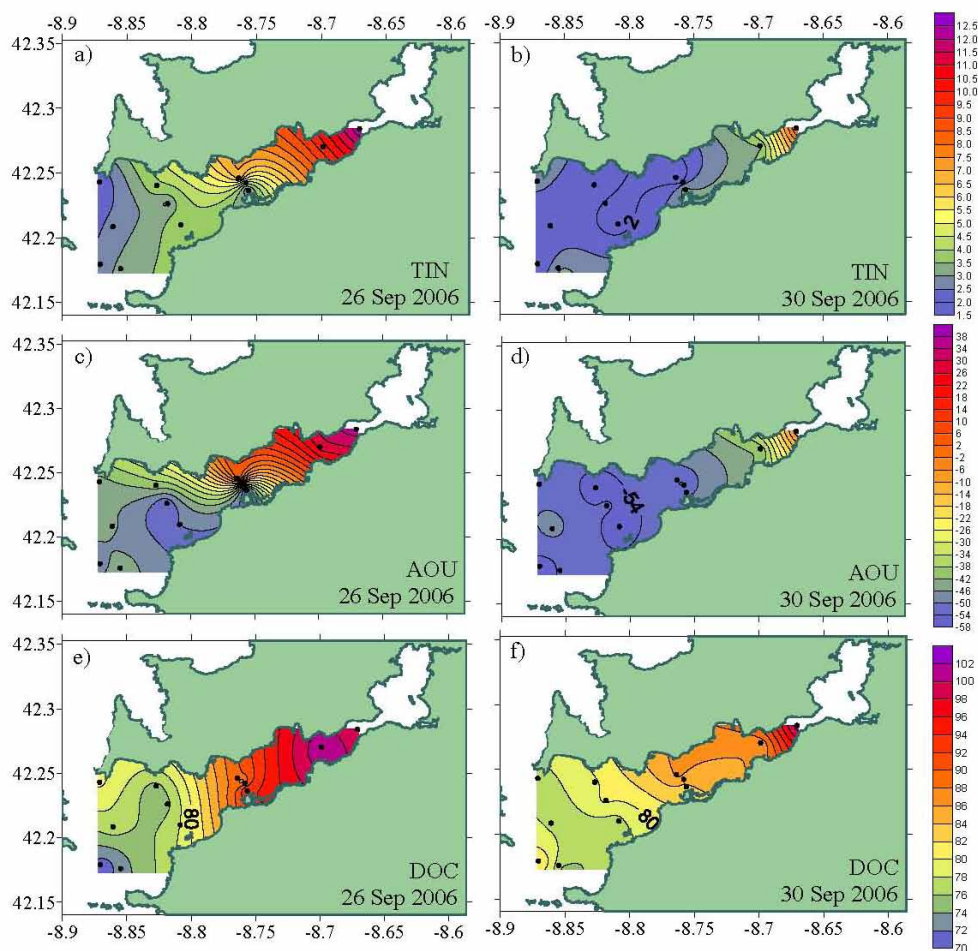

Fig. 5. Sea surface distributions for September 26 and 30 (2006) of total inorganic nitrogen (TIN) (a, b) in $\mu mol \cdot L^{-1}$; apparent oxygen utilization (AOU) (c, d) in $\mu mol \cdot Kg^{-1}$ and dissolved organic carbon (DOC) (e, f) in $\mu mol \cdot L^{-1}$. X-axis is logitude in degrees; Y-axis is latitude in degrees.

1996; Del Vecchio and Blough, 2004; Coble, 2007; Kowalczuk et al., 2010). That appears reasonable because wind-driven upwelling/downwelling systems are coastal areas with enhanced oceanic influence. The inverse of the slope of eq. 5 (Table 1), 14.5 (±0.8) m^2 mol C^{-1}, represents the mean value of the DOC specific absorption coefficient, $a^*_{CDOM}(340)$, for the coloured DOC fraction. Using the factor 0.74 ± 0.02 (to convert $a_{CDOM}(340)$ into $a_{CDOM}(355)$), the mean specific CDOM absorption coefficient of the coloured DOC of Ría de Vigo at 355 nm, $a^*_{CDOM}(355)$, results 20 ± 1 m^2 mol C^{-1}, a relatively high value compared with other coastal areas. $a^*_{CDOM}(355)$ for the coloured DOC in Middle Atlantic Bight
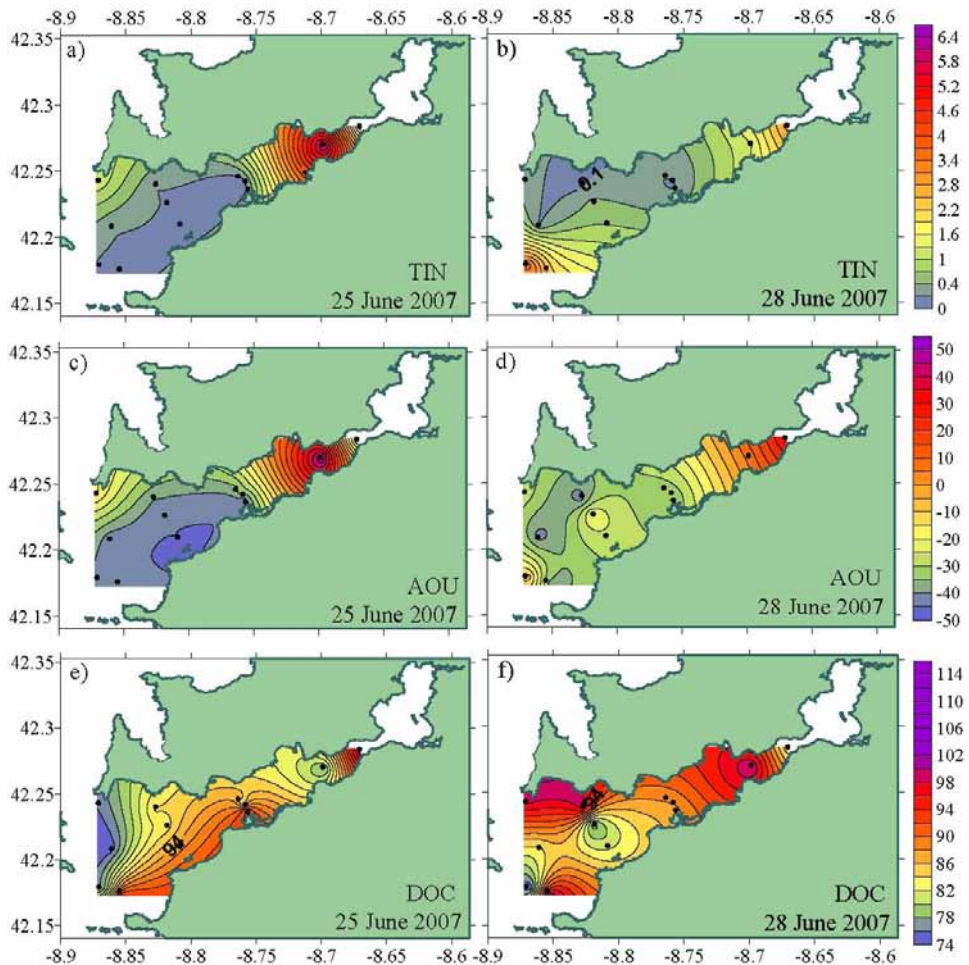

Fig. 6. Sea surface distributions for June 25 and 28 (2007) of total inorganic nitrogen (TIN) in $\mu mol \cdot L^{-1}$ (a, b); apparent oxygen utilization (AOU) (c, d) in $\mu mol \cdot Kg^{-1}$ and of dissolved organic carbon (DOC) (e, f) in $\mu mol \cdot L^{-1}$. X-axis is logitude in degrees; Y-axis is latitude in degrees.

samples with $a_{CDOM}(355) < 1$ m^{-1} (reduced river plume influence) ranged from 8 to 18 m^2 mol C^{-1} (Del Vechhio and Blough, 2004). Regression slopes larger than 20 m^2 mol C^{-1} are obtained only for samples with $a_{CDOM}(355) > 1$ m^{-1} (strong river plume influence). Ferrari et al. (1996) also reported relatively low values of $a^*_{CDOM}(355)$, around 14-15 m^2 mol C^{-1}, in the Southern Baltic Sea, where $a_{CDOM}(355)$ was always above 1 m^{-1}. Lower specific absorption coefficient, 16 m^2 mol C^{-1}, were also obtained by Vodacek and Blough, (1997) in Delaware Bay. In the Gulf of Lions (NW Mediterranean), $a^*_{CDOM}(355)$ ranged from 4 ± 2 m^2 mol C^{-1} in surface marine waters to 23 ± 7 m^2 mol C^{-1} in the river Rhone plume (Ferrari, 2000). On the contrary, a much higher value of $a^*_{CDOM}(355)$, 32 ± 1 m^2 mol C^{-1}, was obtained by Kowalczuk et al., (2010) in the South Atlantic Bight, where $a_{CDOM}(355)$ up to 20 m^{-1} were recorded.

It has been shown in the results section that $F(340/440)$ correlated significantly with $a_{CDOM}(340)$ in the Ría de Vigo during the two study periods. A good linear correlation between the fluorescence emission of CDOM and the absorption coefficient at the fluorescence excitation wavelength has been found in most coastal areas, allowing the estimation of absorption coefficients from fluorescence measurements (e.g. Hoge et al., 1993; Vodacek et al., 1995; 1997; Ferrari et al., 1996; Ferrari, 2000; Del Vecchio and Blough, 2004; Kowalczuk et al., 2010). This is because the variability of $\Phi(\lambda)$ is usually at least one order of magnitude lower than the variability of $a(\lambda)$ (Green and Blough, 1994). Our values of $\Phi(340)$, which range from 0.56% to 1.76%, were close to the 1% reported by other authors for coastal waters (Green and Blough, 1994; Vodacek and Blough, 1997; Ferrari et al., 1996, 2000; Zepp et al., 2004). The coefficients of variation of $a_{CDOM}(340)$ and $\Phi(340)$ were 26% and 14% during the downwelling and 40% and 29% during the upwelling period, respectively. Therefore, although $\Phi(340)$ was less variable than $a_{CDOM}(340)$, the variability was of the same order of magnitude. This is the reason behind the relatively low coefficients of determination found in the Ría de Vigo ($R^2 = 0.79$ for the downwelling and 0.60 for the upwelling period) compared with published values usually higher than 0.90 (Kowalczuk et al., 2010). $\Phi(\lambda)$ is altered by biotic as well as abiotic processes. On the one hand, laboratory experiments on the photobleaching of humic substances show that fluorescence decreases faster than absorption, implying a decrease of $\Phi(\lambda)$ (De Haan, 1993). On the other hand, laboratory experiment on the degradation of natural DOM from the Ría de Vigo showed that fluorescence builds up faster than absorption during the microbial production of CDOM, which implies an increase of $\Phi(\lambda)$ (Lønborg et al., 2010). Consequently, the significantly lower values of $\Phi(340)$ observed during the downwelling than during the upwelling period suggest that photodegradation was more relevant than microbial production under downwelling conditions, when the irradiated shelf surface waters entered the Ría, and the contrary under upwelling conditions, when the aged ENACW upwelled on the shelf and flowed into the ría. This deduction is consistent with the significant difference observed between the regression slopes of the logarithmic plot of $a_{CDOM}(340)$ and S for both periods (see above).

Table 1. Coefficients of selected linear regression equations for the two periods studied in the Ría de Vigo.

Nº	Period	Equation	R^2	n
1	Down	$NH_4^+ = -1.2(\pm 0.1) + 0.81(\pm 0.02)\cdot$ TIN	0.92	109
2	Up	$NO_3^- = -0.8(\pm 0.2) + 0.82(\pm 0.03)\cdot$ TIN	0.94	80
3	Down	DOC $= 50(\pm 2) + 65(\pm 7)\cdot a_{CDOM}(340)$	0.46	106
4	Up	DOC $= 48(\pm 2) + 76(\pm 5)\cdot a_{CDOM}(340)$	0.75	77
5	Down+Up	DOC $= 49(\pm 1) + 69(\pm 4)\cdot a_{CDOM}(340)$	0.63	183
6	Down	$F^*(340/440) = -10(\pm 7) + 0.32(\pm 0.20)\cdot$salinity*	0.03	109
7	Down	$a^*_{CDOM}(340) = 1.7(\pm 1.6) - 0.04(\pm 0.05)\cdot$salinity*	0.01	109
8	Down	AOU $= -2865(\pm 342) + 80 (\pm 10)\cdot$ salinity	0.39	109
9	Up	$F^*(340/440) = 15 (\pm 2) - 0.39(\pm 0.05)\cdot$ salinity	0.43	80
10	Up	$a^*_{CDOM}(340) = 5.0 (\pm 0.3) - 0.13(\pm 0.01)\cdot$ salinity	0.74	80
11	Up	AOU $= -1227 (\pm 153) + 36 (\pm 4)\cdot$ salinity	0.46	80
12	Down+Up	$\Delta F^*(340/440) = 4.8(\pm 0.4)\cdot\Delta a^*_{CDOM}(340)$	0.46	189
13	Down	$\Delta F^*(340/440) = 0.005(\pm 0.001)\cdot\Delta AOU + 2.8(\pm 0.3)\cdot\Delta a^*_{CDOM}(340)$ $\beta_1 = 0.27\pm 0.07$ $\beta_2 = 0.66\pm 0.07$	0.77	109
14	Up	$\Delta F^*(340/440) = 0.008(\pm 0.001)\cdot\Delta AOU + 2.1(\pm 0.4)\cdot\Delta a^*_{CDOM}(340)$ $\beta 1 = 0.66\pm 0.07$ $\beta 2 = 0.36\pm 0.07$	0.63	80

Down: downwelling; Up: upwelling.

For all the equations $p < 0.001$ except for those with * meaning not significant.

Assessment of the influence of water masses mixing, microbial production and photochemical degradation on the distribution of CDOM

Concurrent absorption coefficient, induced fluorescence and DOC measurements in the coastal upwelling system of the Ría de Vigo allowed a study of the relationship among the three variables as well as the fluorescence to absorption coefficient ratios, i.e. the fluorescence quantum yield $\Phi(\lambda)$, and absorption coefficient to DOC ratio, i.e. the C-specific CDOM absorption coefficient $a^*_{CDOM}(\lambda)$.

Since contrasting coastal upwelling and downwelling conditions were sampled, we have been able to characterise the optical properties of the shelf surface waters that enter the rías during downwelling events ($a_{CDOM}(340) = 0.34 \pm 0.02$ m^{-1}, $a^*_{CDOM}(340) = 4.5 \pm 0.5$ m^2 mol C^{-1}, $\Phi(340) = 0.76 \pm 0.02\%$; average $\pm$ SD of surface samples at stn B5 in September 06) and the bottom shelf ENACW that enter the rías during upwelling events ($a_{CDOM}(340) = 0.23 \pm 0.04$ m^{-1}, $a^*_{CDOM}(340) = 3.6 \pm 0.7$ m^2 mol C^{-1}, $\Phi(340) = 1.2 \pm 0.3\%$; average $\pm$ SD of samples colder than 14ºC in June 07). The values of $a_{CDOM}(340)$, $a^*_{CDOM}(340)$, and $\Phi(340)$ of these water types were significantly different (p < 0.001). These two different shelf
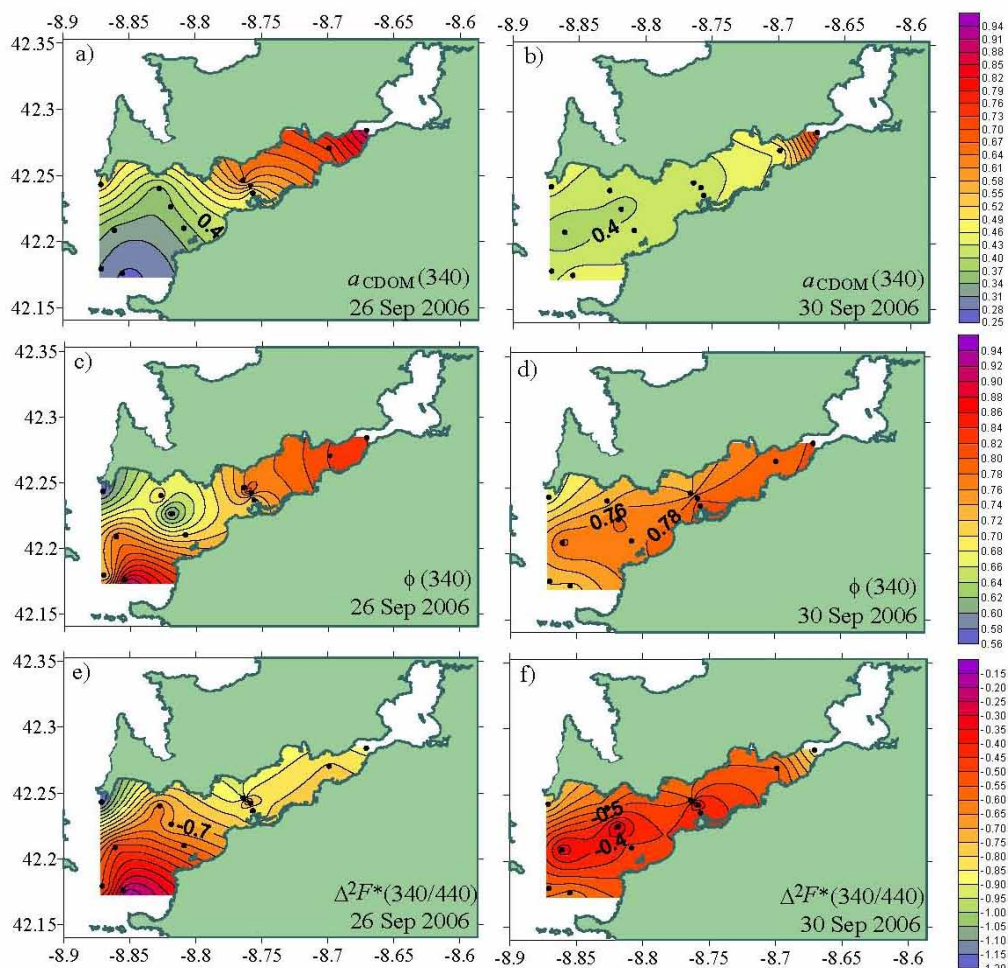

Fig. 7. Sea surface distributions for September 26 and 30 (2006) of CDOM absorption coefficient at 340nm ($a_{CDOM}(340)$) (a, b) in m^{-1}; CDOM fluorescence quantum yield at 340 nm, $\Phi(340)$ (c, d) and $\Delta^2F^*(340/440)$ (e, f). X-axis is logitude in degrees; Y-axis is latitude in degrees.

waters were forced to mix with the significantly more coloured ($a_{CDOM}(340) > 0.7$ m^{-1}, $a^*_{CDOM}(340) > 7.5$ m^2 mol C^{-1}, $\Phi(340) > 0.8\%$) brackish waters, exported from San Simón Bay, by the positive (negative) residual circulation characteristic of upwelling-favourable (downwelling-favourable) conditions.

The distributions of the absorption coefficient and the induced fluorescence of CDOM in any marine ecosystem depend on (1) water masses mixing; and biogeochemical processes of two categories: (2) microbial and (3) photochemical. In the case of the Ría de Vigo, to remove the continental and oceanic waters mixing effects, we considered our system as a two end-member mixing problem (Doval et al.
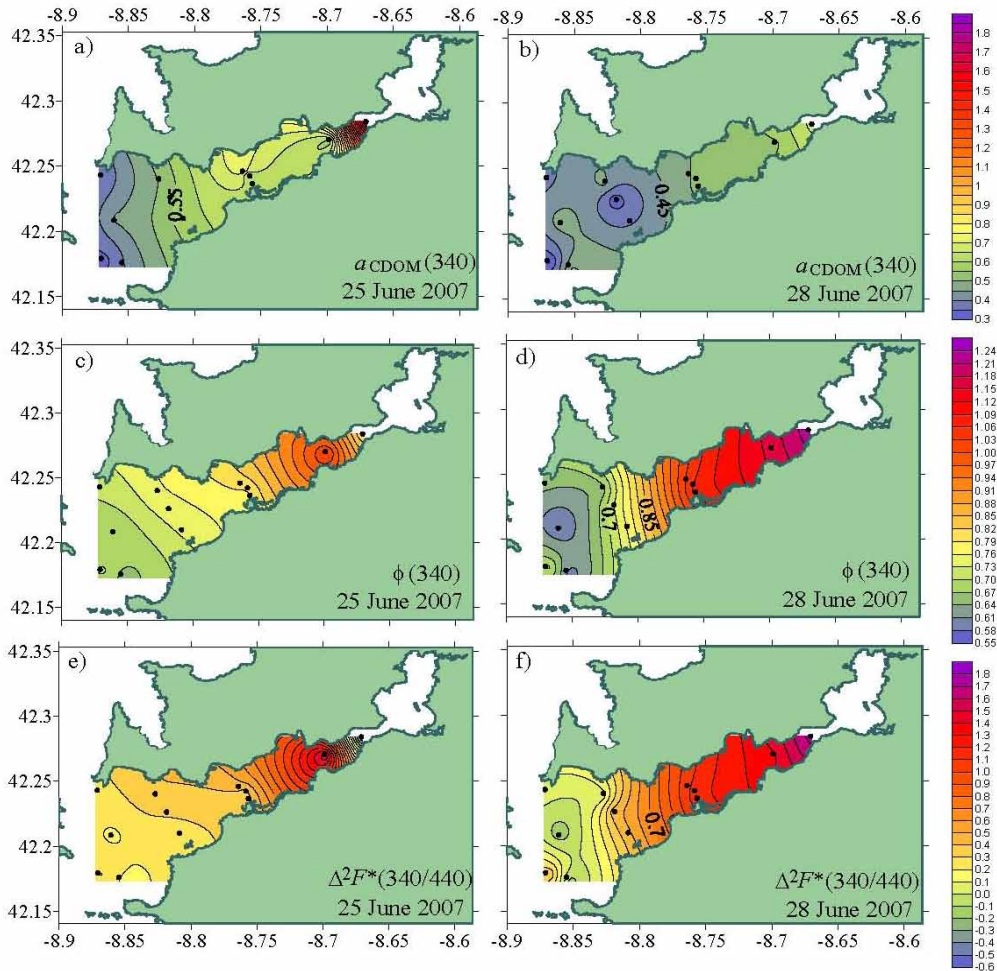

Fig. 8. Sea surface distributions for June 25 and 28 (2007) of CDOM absorption coefficient at 340nm ($a_{CDOM}(340)$) (a, b) in m^{-1}; CDOM fluorescence quantum yield at 340 nm, $\Phi(340)$ (c, d) and $\Delta^2 F^*(340/440)$ (e, f). X-axis is logitude in degrees; Y-axis is latitude in degrees.

1997; Nieto-Cid et al. 2005) that can be solved by considering the residuals of the linear correlations of the absorption coefficient and fluorescence of CDOM with salinity. Given the significant correlation of the optical properties of CDOM with DOC (Eqs. 3-5), absorption coefficient and fluorescence to DOC ratios, $a*_{CDOM}(340)$ and $F*(340/440)$, are used to remove that dependence. During the upwelling event of June 07 the optical properties of DOM were more dependent on water mass mixing than during the downwelling event of September 06, when no significant correlations were found between either $a*_{CDOM}(340)$ or $F*(340/440)$ with salinity (see Eqs 6, 7, 9 and 10 in Table 1). The residuals of the regression of $a*_{CDOM}(340)$ with salinity, $\Delta a*_{CDOM}(340)$, correlated significantly with the residuals of the correlation of $F*(340/440)$ with salinity, $\Delta F*(340/440)$, (see Eq. 12 in Table 1) and the slope of that correlation, 4.8 ± 0.4 m QSU, was not significantly different for both study periods. If this slope of 4.8 ± 0.4 m QSU is multiplied by the conversion factor 2.2 ($\pm$0.2) 10^{-3} m^{-1} QSU^{-1} of eq. 5 produces a value of $1.1 \pm 0.1\%$ that can be considered the average $\Phi(340)$ of the Ría de Vigo, independently of the mixing of water masses and the dominant hydrographic conditions. However, the linear correlation between $\Delta F*(340/440)$ and $\Delta a*_{CDOM}(340)$ explains only 46% of the observed variability ($R^2 = 0.46$ form Eq. 12 in Table 1). Figs. 7e, f and 8e, f show the horizontal distributions of the residuals of the linear regression between $\Delta F*(340/440)$ and $\Delta a*_{CDOM}(340)$, $\Delta^2 F*(340/440)$. The variability of $\Delta^2 F*(340/440)$ is equivalent to the variability of $\Phi(340)$ independent of the mixing of water masses. If the distributions of $\Delta^2 F*(340/440)$ were stochastic it would mean that the values of $\Delta^2 F*(340/440)$ are just a consequence of the errors associated to the collection and determination of $F*(340/440)$ and $a*_{CDOM}(340)$. However, the distributions of $\Delta^2 F*(340/440)$ are systematic: the values are predominantly negative in September 06 (Figs. 7e, f) and predominantly positive in June 07 (Figs. 8e, f). For a given period, they increase down- and shore-wards. A systematic distribution of residuals means that environmental factors, other than the mixing of water masses, are affecting the distributions of $F*(340/440)$ and $a*_{CDOM}(340)$.
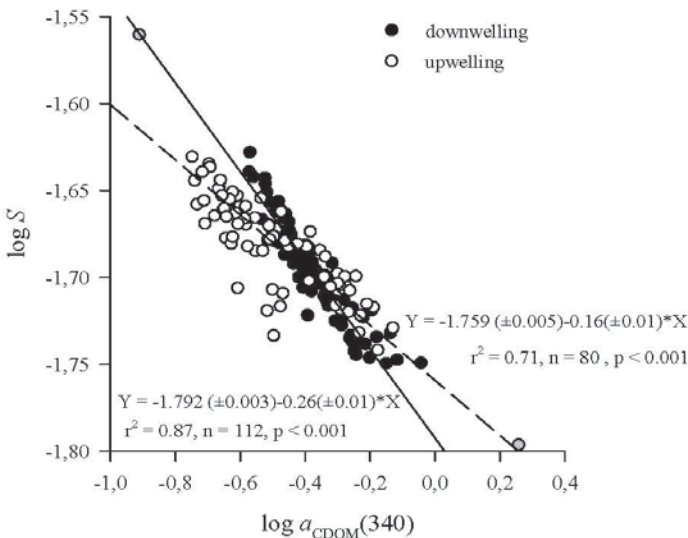

Fig. 9. Logarithmic plot of the spectral slope, S in the range of 250-500nm versus absorption coefficient at 340 nm, $a_{CDOM}(340)$, for the downwelling (black dots) and upwelling period (open dots).

Considering that $\Phi(340)$ decreases during photo-degradation (De Haan, 1993) and increases during microbial degradation processes (Lønborg et al., 2010), and that the variability of $\Delta^2 F^*(340/440)$ is equivalent to the variability of $\Phi(340)$, positive values of $\Delta^2 F^*(340/440)$ indicate a larger relative influence of microbial degradation processes while negative values a larger relative influence of photo degradation processes. Consequently, microbial processes were more relevant in June 07 than in September 06 and within each period, photochemical processes gained importance in the surface layer of the outermost stations.

The relative importance of photochemical and microbial respiration processes on the distributions of $\Delta F^*(340/440)$ and $\Delta a^*_{CDOM}(340)$ can be quantified by means of the parameters of the multiple linear regression of $\Delta F^*(340/440)$ versus ΔAOU and $\Delta a^*_{CDOM}(340)$ for each period (eqs 13 and 14 in Table 1). The AOU reflects the net ecosystem metabolism (NEM; Smith and Hollibaugh, 1997), this is the net production of dissolved oxygen due to primary producers minus the net consumption by the respiration of all the autotrophs and heterotrophs living in the study system. Previous studies in the Ría de Vigo have demonstrated that the oxygen budget of this embayment is controlled by the microbial food web (Cermeño et al., 2006; Piedracoba et al., 2008). In addition, the AOU in the surface mixed layer is affected by the exchange of dissolved oxygen with the atmosphere when moderate to strong winds blow into the ría (Piedracoba et al., 2008). For the particular case of the study period, the average $\pm$ SD local wind speed estimated at 10 m over the sea surface (u_{10}) was 0.79 ± 0.78 m s^{-1} in September 06 and 1.66 ± 0.82 m s^{-1} in June 07. The corresponding piston velocities (k) calculated with the Wanninkhof's (1992) formula, $k = 0.31 \cdot u_{10}^2 \cdot (Sc/589)^{-1/2}$, were 0.04 and 0.20 m d^{-1}, respectively. Sc is the dimensionless Schmidt number. With these values of k, the average AOU of the surface layer (-41 $\pm$ 20 µmol kg^{-1} for September 06 and -25 $\pm$ 25 µmol kg^{-1} for June 07) and considering that the surface layer is 5 m thick, the resulting oxygen fluxes would be as low as 0.36 µmol kg^{-1} d^{-1} in September 06 and 0.97 µmol kg^{-1} d^{-1} in June 07, in both cases from the sea surface to the atmosphere. Given that the flushing time of the surface layer during moderate upwelling and downwelling events in the Ría de Vigo is about 2-3 days (Álvarez-Salgado et al., 2001; Piedracoba et al., 2008), oxygen exchange can be neglected for the purposes of this work. Therefore, AOU is an unequivocal indicator of the aerobic microbial metabolism and ΔAOU are the residuals of the linear regression of AOU with salinity, which is significant during the downwelling event of September 06 and the upwelling event of June 07 (eqs 8 and 11 in Table 1).

When the variables $\Delta F^*(340/440)$, ΔAOU and $\Delta a^*_{CDOM}(340)$ are normalised and the regression slopes are of the same sign, the square of the resulting normalised regression slope (β_1^2) indicates the proportion of the variability of $\Delta F^*(340/440)$ explained by ΔAOU if $\Delta a^*_{CDOM}(340)$ is kept constant. Consistently, β_2^2 indicates the proportion of the variability of $\Delta F^*(340/440)$ explained by $\Delta a^*_{CDOM}(340)$ if ΔAOU is kept constant. Therefore, the ratio $\beta_1^2 /(\beta_1^2 + \beta_2^2)$ indicates the proportion of the biogeochemical ariability of $\Delta F^*(340/440)$ that is due to microbial respiration and

$\beta_2^2 / (\beta_1^2 + \beta_2^2)$ the proportion due to photo degradation. Equations 13 and 14 in Table 1 show the values of β_1 and β_2. For the downwelling period of September 2006, $\beta_1 = 0.27 \pm 0.07$ and $\beta_2 = 0.66 \pm 0.07$. Therefore, the relative contribution of photo- and biodegradation processes would be 86% and 14%, respectively. If the same procedure is followed for the upwelling event of June 07, only 23% of the variability of $\Delta F^*(340/440)$ was due to photochemical process while 77% was due to microbial respiration. Note that $R^2 > \beta_1^2 + \beta_2^2$ in both periods because the two predictor variables, $\Delta a^*_{CDOM}(340)$ and ΔAOU, covaried between themselves. However, using β_1 and β_2 ensures that the dependence of the predictor variables among them is ruled out of the analysis. Therefore, in this section we have been able to quantify the differential impact of microbial and photochemical processes on the optical properties of CDOM under contrasting downwelling and upwelling conditions. These differences had been previously suggested qualitatively by the distributions of $\Phi(340)$ and the regression slopes of the logarithmic plot of $a_{CDOM}(340)$ and S for both periods.

Table 2. Average $\pm$ SD values of the absorption coefficient (m^{-1}) at several wavelengths, the spectral slope over the 250-500 nm wavelength range, and the fluorescent quantum yield at 340 nm for downwelling, upwelling, and both period in the Ría de Vigo. All samples collected in September 06 and June 07 were used to calculate the average $\pm$ SD values for downwelling and upwelling conditions, respectively. The last column of Table 2 was produced with all the samples collected in both periods.

	Downwelling	Upwelling	Downwelling + Upwelling
$a_{CDOM}(325)$	0.57 ± 0.03	0.47 ± 0.19	0.54 ± 0.17
$a_{CDOM}(340)$	0.43 ± 0.11	0.35 ± 0.14	0.40 ± 0.13
$a_{CDOM}(355)$	0.32 ± 0.08	0.26 ± 0.11	0.29 ± 0.10
$a_{CDOM}(375)$	0.21 ± 0.06	0.17 ± 0.08	0.20 ± 0.07
$a_{CDOM}(443)$	0.055 ± 0.02	0.043 ± 0.02	0.051 ± 0.023
S	0.020 ± 0.001	0.02 ± 0.001	0.021 ± 0.001
$\Phi(340)$	$0.81 \pm 0.11\%$	$1.03 \pm 0.30\%$	0.91 ± 0.3

Conclusions

Absorption coefficient and induced fluorescence of CDOM have been recurrently used in the literature to estimate DOC concentrations in coastal systems. The success of the prediction of DOC from $a_{CDOM}(\lambda)$ and/or $F(\lambda)$ depends on a narrow variability of the carbon specific CDOM absorption coefficient, $a^*_{CDOM}(\lambda)$, and the fluorescence quantum yield, $\Phi(\lambda)$. The best estimates have been obtained in coastal areas affected by strong freshwater influences, where the variability of $a^*_{CDOM}(\lambda)$ and $\Phi(\lambda)$ is usually several orders of magnitude lower than $a_{CDOM}(\lambda)$ and $F(\lambda)$. However, our work shows that a detailed study of the limited spatial and temporal variability of $\Phi(\lambda)$ in a particular coastal system can help to elucidate the relative importance of the microbial and photochemical processes that control the changes of the absorption coefficient and induced fluorescence properties produced and consumed in that system. In the case study of the Ría de Vigo, we obtained that 86% of the variability of $\Phi(340)$ during the mixing of shelf surface and continental waters under downwelling conditions was due to the photodegradation of CDOM. On the contrary, during the mixing of bottom shelf and continental waters under upwelling conditions, 77% of the variability of $\Phi(340)$ was due to microbial respiration. Concurrent induced fluorescence and absorption coefficient measurements in other coastal system would allow application of this methodology to infer the biogeochemical processes that control CDOM variability during estuarine mixing.

Acknowledgements

References

Álvarez-Salgado, X.A., Rosón, G. Pérez, F. F., Pazos, Y., 1993. Hydrographic variability off the Rías Baixas (NW Spain) during the upwelling season. J. Geophys. Res. 98**,** 14447–14455.

Álvarez-Salgado, X.A., Gago, J., Miguez, B.M., Perez, F.F., 2001. Net ecosystem production of dissolved organic carbon in a coastal upwelling system: the ria de Vigo, Iberian margin of the North Atlantic. Limnol. Oceanogr. 46, 135-147.

Babin, M., Stramski, D., Ferrari, G.M., Claustre, H., Bricaud, A., Obolensky, G., Hoepffner, N., 2003. Variations in the light absorption coefficients of phytoplankton, nonalgal particles, and dissolved organic matter in coastal waters around Europe. J. Geophys. Res. 108, 3122.

Blough, N.V., Del Vecchio, R. Chromophoric dissolved organic matter (CDOM) in the coastal environment. In: Hansell, D.A. and Carlson, C.A. (Eds), 2002. Biogeochemistry of marine dissolved organic matter. San Diego: Academic Press, p. 509–546.

Bricaud, A., Morel, A., Prieur, L., 1981. Absorption by dissolved organic matter of the sea (yellow substance) in the UV and visible domains. Limnol. Oceanogr. 26, 43-53.

Cermeño, P., Marañón, E., Pérez, V., Serret, P., Fernández, E., Castro, C.G., 2006. Phytoplankton size structure and primary production in a highly dynamic coastal ecosystem (Ría de Vigo, NW-Spain): Seasonal and short-time scale variability. Estuar. Coast. Shelf Sci. 67, 251-266.

Chen, R.F., Bada, J.L., 1992. The fluorescence of dissolved organic matter in seawater. Mar. Chem., 37, 191-221.

Chen, R.F., Zhang, Y., Vlahos, P. and Rudnick, S.M., 2002. The fluorescence of dissolved organic matter in the Mid-Atlantic Bight. Deep Sea Res. II 49, 4439-4459.

Coble, P.G., 1996. Characterization of marine and terrestrial DOM in seawater using excitation-emission matrix spectroscopy. Mar. Chem. 51, 325-346.

Coble, P.G., 2007. Marine Optical Biogeochemistry: The Chemistry of Ocean Color. Chem. Rev. 107: 402-418.

Coble, P.G., Del Castillo, C.E., Avril, B., 1998. Distribution and optical properties of CDOM in the Arabian Sea during the 1995 Southwest Monsoon. Deep-Sea Res. II 45, 2195-2223.

Day, D.A., Faloona, I., 2009. Carbon monoxide and chromophoric dissolved organic matter cycles in the shelf waters of the northern California upwelling system. J. of Geophys. Res. 114, C01006.

De Haan, H., 1993. Solar UV-Light Penetration and photodegradation of humic substances in Peaty Lake water. Limnol. and Oceanogr. 38, 1072-1076.

Del Castillo, C.E., Coble, P.G., 2000. Seasonal variability of the colored dissolved organic matter during the 1994-95 NE and SW Monsoons in the Arabian Sea. Deep Sea Res. II 47, 1563-1579.

Del Castillo, C.E., Miller, R.L., 2008. On the use of ocean color remote sensing to measure the transport of dissolved organic carbon by the Mississippi River Plume. Remote Sensing of Environment 112, 836-844.

Del Vecchio, R., Blough, N.V., 2004. Spatial and seasonal distribution of chromophoric dissolved organic matter and dissolved organic carbon in the Middle Atlantic Bight. Mar. Chem. 89, 169-187.

Doval, M.D., Álvarez-Salgado, X.A., Fiz, F.P.r., 1997. Dissolved organic matter in a temperate embayment affected by coastal upwelling. Mar. Ecol. Prog. Ser. 157, 21-37.

Eppley, R.W., Peterson, B.J. 1979. Particulate organic matter flux and planktonic new production in the deep ocean. Nature 282, 677-680.

Ferrari, G.M., Dowell, M.D., Grossi, S., Targa, C., 1996. Relationship between the optical properties of chromophoric dissolved organic matter and total concentration of dissolved organic carbon in the southern Baltic Sea region. Mar. Chem. 55, 299-316.

Ferrari, G.M., 2000. The relationship between chromophoric dissolved organic matter and dissolved organic carbon in the European Atlantic coastal area and in the West Mediterranean Sea (Gulf of Lions). Mar. Chem. 70, 339-357.

Figueiras, F. G., A. F. Ríos. 1993. Phytoplankton succession, red tides and the hydrographic regime in the Rias Bajas of Galicia. In: Smayda, T. J., Shimizu, Y. (Eds.), Toxic Phytoplankton Blooms in the Sea. Elsevier Science Publishers B.V., pp. 239-244.

Gago, J., Álvarez-Salgado, X.A., Nieto-Cid, M., Brea, S., Piedracoba, S., 2005. Continental inputs of C, N, P and Si species to the Ría de Vigo (NW Spain). Estuar. Coast. Shelf Sci. 65, 74-82.

Green, S.A., Blough, N.V., 1994. Optical absorption and fluorescence properties of chromophoric dissolved organic matter in natural waters. Limnol. Oceanogr. 39, 1903-1916.

Häder, D.-P, Sinha, R.P., 2005. Solar ultraviolet radiation-induced DNA damage in aquatic organisms: Potential environmental impact. Mutation Research 571, 221–233.

Hoge, F.E., Swift, R.N., Yungel, J.K., 1993. Fluorescence of dissolved organic matter: a comparison of North Pacific and North Atlantic Oceans during April 1991. J. Geophys. Res. 98, 22,779-22,787.

Kieber, R.J., Hydro, L.H., Seaton, P.J., 1997. Photooxidation of triglycerides and fatty acids in seawater: implication toward the formation of marine humic substances. Limnol. and Oceanogr. 42, 1454-1462.

Klinkhammer, G.P., McManus, J., Colbert, D., Rudnicki, M.D., 2000. Behavior of terrestrial dissolved organic matter at the continent-ocean boundary from high-resolution distributions. Geochim. Cosmochim. Acta 64, 2765-2774.

Kowalczuk, P., Cooper, W. J., Durako, M. J., Kahn, A. E., Gonsior, M., Young, H., 2010. Characterization of dissolved organic matter fluorescence in the South Atlantic Bight with use of PARAFAC model: Relationships between fluorescence and its components, absorption coefficients and organic carbon concentrations. Mar. Chem. 118, 22-36.

Kramer, G.D., Herndl, G.J., 2004. Photo- and bioreactivity of chromophoric dissolved organic matter produced by marine bacterioplankton. Aquat. Microb. Ecol. 36, 239-246.

Kudela, R.M., Garfield, N., Brulanda, K.W., 2006. Bio-optical signatures and biogeochemistry from intense upwelling and relaxation in coastal California. Deep Sea Res. II 53, 2999–3022.

Lønborg, C., Alvarez-Salgado, X.A., Martinez-Garcia, S., Miller, A.E.J., Teira, E., 2010. Stoichiometry of dissolved organic matter and the kinetics of its microbial degradation in a coastal upwelling system. Aquat. Microb. Ecol. 58, 117-126.

Moran, M.A., Sheldon, W.M., Zepp, R.G., 2000. Carbon loss and optical property changes during long-term photochemical and biological degradation of estuarine dissolved organic matter. Limnol. and Oceanogr. 45, 1254-1264.

Melhuish, W.H., 1961. Quantum efficiencies of fluorescence of organic substances: effect of solvent and concentration of the fluorescent solute. J. Phys. Chem. 65, 229-235.

Nelson, N.B., Craig, A.C., Steinberg, D.K., 2004. Production of chromophoric dissolved organic matter by Sargasso Sea microbes. Mar. Chem. 89, 273– 287.

Nelson, N.B., Siegel, D. A., Carlson, C. A., Swan, C., Smethie, Jr W. M., Khatiwala, S., 2007. Hydrography of chromophoric dissolved organic matter in the North Atlantic. Deep Sea Res. I 54, 710-731.

Nelson, N.B., Siegel, D.A., Carlson, C.A., Swan, C.M., 2010. Tracing global biogeochemical cycles and meridional overturning circulation using chromophoric dissolved organic matter. Geophys. Res. Letters 37, L03610.

Nieto-Cid, M., Álvarez-Salgado, X.A., Gago, J., Pérez, F.F., 2005. DOM fluorescence, a tracer for biogeochemical processes in a coastal upwelling system (NW Iberian Peninsula). Mar. Ecol. Prog. Ser. 297, 33-50.

Nieto-Cid, M., Álvarez-Salgado, X.A., Pérez, F.F., 2006. Microbial and photochemical reactivity of fluorescent dissolved organic matter in a coastal upwelling system. Limnol. and Oceanogr. 51, 1391-1400.

Piedracoba S., Nieto–Cid, M., Teixeira, I.G., Garrido, J.L., Álvarez–Salgado, X.A., Rosón, G.., Castro, C.G., Pérez, F.F., 2008. Physical–biological coupling in the coastal upwelling system of the Ría de Vigo (NW Spain). II: An in vitro approach. Mar. Ecol. Progr. Ser. 353, 41–53.

Romera-Castillo, C., Sarmento, H., Álvarez-Salgado, A.X., Gasol, J.M., Marrasé, C., 2010. Production of chromophoric dissolved organic matter by marine phytoplankton. Limnol. Oceanogr, 55, 446–454.

Romera-Castillo, C., Nieto-Cid, M., Marrasé, C., Repeta, D.J., Álvarez-Salgado, X.A. Optical properties of ultrafiltered dissolved organic matter (UDOM) from contrasting aquatic environments and their alteration by sunlight. Submitted.

Siegel, D.A., Maritorena, S., Nelson, N.B., 2002. Global distribution and dynamics of colored dissolved and detrital organic materials. J. Geophys. Res. 107, 3228.

Smith, S.V., Hollibaugh J.T., 1997. Annual cycle and interannual variability of ecosystem metabolism in a temperate climate embayment. Ecol. Monogr. 67, 509-533.

Stedmon, C.A., Markager, S., Kaas, H., 2000. Optical properties and signatures of chromophoric dissolved organic matter (CDOM) in Danish coastal waters. Estuar. Coast. Shelf Sci. 51, 267-278.

Stedmon, C.A., Markager, S., 2001. The optics of chromophoric dissolved organic matter (CDOM) in the Greenland Sea: an algorithm for differentiation between marine and terrestrially derived organic matter. Limnol. Oceanogr, 46, 2087–2093.

Stedmon, C.A., Osburn, C.L., Kragh, T., 2010. Tracing water mass mixing in the Baltic–North Sea transition zone using the optical properties of coloured dissolved organic matter. Estuar. Coast. Shelf Sci. 87, 156-162.

Swan, C.M., Siegel, D.A., Nelson, N.B., Carlson, C.A., Nasir, E., 2009. Biogeochemical and hydrographic controls on chromophoric dissolved organic matter distribution in the Pacific Ocean. Deep Sea Res. I 56, 2175-2192.

Sokal, F. F., F. J. Rohlf. 1995. Biometry. Freeman.

Torres, R., Barton, E.D., Miller, P., Fanjul, E., 2003. Spatial patterns of wind and sea surface temperature in the Galician upwelling region. J. Geophys. Res. 108, 3130.

Vodacek, A., Hoge, F. E., Swift, R. N., Yungel, J. K., Peltzer, E. T., Blough, N. V., 1995. The use of in situ and airborne fluorescence measurements to determine UV absorption coefficients and DOC concentrations in surface waters. Limnol. and Oceanogr. 40, 411-415.

Vodacek, A., Blough, N.V., 1997. Seasonal variation of CDOM and DOC in the Middle Atlantic Bight: Terrestrial inputs and photooxidation. Limnol. Oceanogr. 42, 674-686.

Wanninkhof, R. 1992. Relationship between wind speed and gas exchange over the ocean. J. Geophys. Res. 97, 7373-7382.

Wooster W.S., Bakun A., McLain D.R., 1976. The seasonal upwelling cycle along the eastern boundary of the North Atlantic. J. Mar. Res. 34, 131–140.

Yamashita, Y., Tanoue, E., 2008. Production of bio-refractory fluorescent dissolved organic matter in the ocean interior. Nature Geosci. 1, 579-582.

Yentsch, C.S., Reichert, C.A., 1961. The interrelationship between water-soluble yellow substances and chloroplastic pigments in marine algae. Bot. Mar. 3, 65-74.

Zepp, R.G., Sheldon, W.M., Moran, M.A., 2004. Dissolved organic fluorophores in southeastern US coastal waters: correction method for eliminating Rayleigh and Raman scattering peaks in excitation-emission matrices. Mar. Chem. 89, 15-36.

Chapter V

Seasonal variability of different dissolved organic matter fractions followed by absorption and fluorescence spectroscopy in an oligotrophic coastal system (Blanes Bay, NW Mediterranean)

Chapter V

Co-authors:

C. Marrasé, X.A. Álvarez-Salgado, J.M. Gasol et al.

Abstract

Harmonic analysis of 2 ½ years of data collected with fortnight to monthly frequency in the oligotrophic Bay of Blanes (NW Mediterranean) revealed that the water column mixing-stratification cycle imposed by natural radiation and wind events dictates the seasonal built up of the bulk and different coloured fractions of dissolved organic matter (DOM). Dissolved organic carbon, DOC, accumulated during the spring and summer reaching the annual maximum by mid September, one month later than water temperature. The seasonal cycle of the fluorescence of aromatic protein-like substances, $F(280/350)$, a labile fraction of DOM, was in phase with DOC, suggesting that malfunctioning of the microbial loop by severe nutrient limitation is the reason behind the late summer accumulation of these materials. The absorptivity of the conjugated carbon double bonds characteristic of refractory DOM, $a^*_{CDOM}(254)$, a tracer of microbial respiration, reached annual maximum values in late April. Conversely, the fluorescence of aromatic humic-like substances absorbing in the UV-A region, $F(340/440)$, presented an annual minimum in early August, because of the prevalence of photo-degradation over microbial production of this fluorophore.

Chapter V

Introduction

Coloured dissolved organic matter (CDOM) includes all dissolved organic compounds that absorb ultraviolet and visible radiation. It is the major factor controlling the attenuation of UV radiation in the ocean (Kirk, 1994), which affect both primary and bacterial production (Herndl et al., 1993; Smith and Cullen, 1995). The absorption properties of CDOM are due to the occurrence of conjugated carbon double bonds; when they form aromatic rings, fluorescence emission of the absorbed light often occurs (Stedmon and Alvarez-Salgado, 2011). CDOM absorption coefficients and spectral slopes have been used as tracers for the chemical structure and origin of DOM in aquatic environments (Dahlén et al., 1996; Nelson et al., 2004; Helms et al., 2008). The C-specific absorption coefficient at 254 nm, $a^*_{CDOM}(254)$, has been found to be a good tracer for the aromaticity of aquatic humic substances (Weishaar et al., 2003) and the ratio of absorption coefficients at 254 and 365 nm, $a_{CDOM}(254/365)$, has been used as an index of the average molecular weight of DOM (Dahlén et al., 1996; Engelhaupt et al., 2003). The fraction of CDOM that emits as fluorescence the absorbed UV radiation is called fluorescent dissolved organic matter (FDOM). The consecution of emission fluorescence spectra collected at different wavelengths of excitation results in excitation emission matrices (EEMs) where different peaks characteristics of humic- and protein-like aromatic compounds can be distinguished (Coble et al., 1996). Named peaks –C, –M and –A are due to humic-like fluorophores while peaks –T and –B are due to protein-like fluorophores. Florescence intensity measurements at these peaks can help to follow the dynamics of different DOM pools that not always have the same sources and sinks. The fluorescence to absorption coefficient ratio at 340 nm, a proxy to the fluorescence quantum yield at 340 nm, works as another aromaticity index (Birks, 1970; Turro, 1991).

The variability of absorption and fluorescence properties of DOM has been found to be a useful tracer of biogeochemical processes in coastal systems (Nieto-Cid et al., 2005; Romera-Castillo et al., 2011a, see Chapter IV). Main biogeochemical processes affecting the optical properties of DOM are 1) photodegradation, which usually provokes a loss of absorption and fluorescence (e.g., Del Castillo et al., 1999; Moran et al., 2000; Nieto-Cid et al., 2006); 2) organic matter biodegradation, usually originating an increase of absorption and fluorescence (Kramer and Herndl, 2004; Lønborg et al., 2010). Therefore, the study of the fluctuations of both variables, as well as the indices obtained from them, allows to identify and somewhat quantify the main processes affecting DOM in the studied system. Seasonal cycles of physical and chemical properties in the marine environment can be directly forced by changes in wind intensity, light incidence and air-temperature. In coastal areas, where flows are confined to small basins or continental shelves, the strength of seasonal cycles is more notable than in the open ocean, where processes as mesoscale turbulence or global thermohaline overturning act attenuating the seasonality (Bringham and Lukas, 1996). However, from a planktonic point of view, seasonality is more accentuated in the open ocean than in coastal areas since the latter are more exposed

to nutrients from land and anthropogenic inputs (Cloern and Jassby, 2008; Romero et al., 2010). Despite that fluorescence and absorbance of DOM are two parameters easily measurable, information about the temporal variability of the CDOM and/or FDOM pools in monitoring time-series is still scarce (Nelson et al., 1998; Para et al., 2010).

The Blanes Bay Microbial Observatory is a reference station in the NW Mediterranean Sea placed 1 Km offshore of the town of Blanes (Fig. 1). Due to the low concentration of nutrients and the production limited by phosphorous most part of the year, it is considered an oligotrophic system (Lucea et al., 2005). Rain and mixing episodes, frequent in autumn and early winter, followed by a prolonged period of high atmospheric pressure and the associated well irradiated and calm waters in late winter is the main seasonal trigger in the NW Mediterranean Sea, setting the development of phytoplankton blooms (Duarte et al., 1999; Guadayol et al., 2009). This station has been well studied for a long period of years (e.g., Margalef, 1945; Gasol et al., 1995; Duarte et al., 1999; Guadayol et al., 2009) with special emphasis in plankton surveys (Alonso-Sáez et al., 2008; Galand et al., 2010). However, there are some gaps in the understanding of the dissolved organic matter dynamics in this system. The aim of this work is to study the seasonal cycles of different sub-fractions of the DOM pool through their optical properties and the physical and biogeochemical processes conditioning their variability.

Material and methods

Survey area and sampling strategy

The Blanes Bay Microbial Observatory in Blanes Bay (NW Mediterranean Sea, 41º 40'N, 2º48'E), is located in the continental side of the shelf/slope front, between the submarine Blanes Canyon placed in the north and the mouth of the La Tordera River in the south (Fig. 1). Maximum bottom depth is between 20 and 24 m.

Seawater samples were taken with fortnightly to monthly frequency from March 2008 to August 2010. They were collected from the surface layer (0.5 m depth), pre-filtered through a 200 µm nylon mesh to remove larger mesozooplankton and transported to the base laboratory (Barcelona) in acid-washed 25 L polycarbonate carboys within 2 hours. In situ water salinity and temperature were measured with a CTD model SD204 de SAIV A/S.
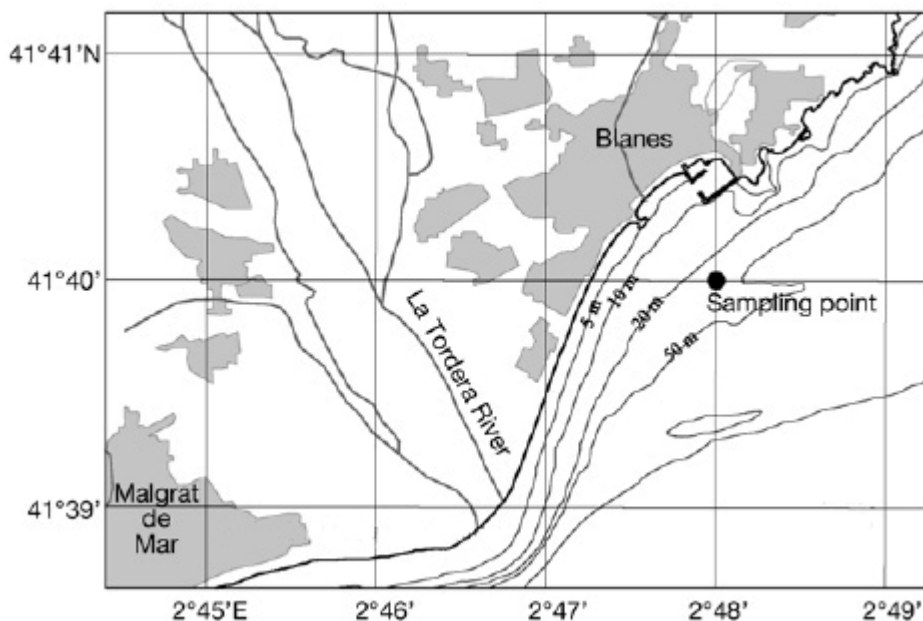
Fig. 1. Sampling station map.

Chemical analysis

For the analysis of the carbon content and the absorption and fluorescence properties of DOM, samples were filtered through Whatman GF/F filters using an acid-cleaned glass filtration system. Approximately 10 mL of water were collected in pre-combusted (450ºC, 12 h) glass ampoules for dissolved organic carbon (DOC) determination. H_3PO_4 was added to acidify the sample to pH < 2 and the ampoules were heat-sealed and stored in the dark at 4ºC until analysis. DOC was measured with a Shimadzu TOC-V organic carbon analyser. The system was standardized daily with potassium hydrogen phthalate. Each ampoule was injected 3–5 times and the average area of the 3 replicates that yielded a standard deviation <1% were chosen to calculate the average DOC concentration of each sample after subtraction of the average area of the freshly-produced UV-irradiated milli-Q water used as a blank. Reference materials provided by Prof. D. Hansell (University of Miami) were analysed to test the performance of the analyser. A concentration of 45.2 ± 0.3 μmol C L^{-1} was obtained for the deep ocean reference (Sargasso Sea deep water, 2600 m) minus blank reference materials. The nominal DOC value provided by the reference laboratory is 45 μmol C L^{-1}.

Samples for CDOM and FDOM determination were measured immediately after filtration, between 2 and 3 h after collection.

CDOM absorption was measured in a Varian Cary spectrophotometer equipped with a 10 cm quartz cell. Spectral scans were collected between 250 and 750 nm at a constant room temperature of 20ºC. Milli-Q water was used as blank. The absorption coefficient at any wavelength, $a_{CDOM}(\lambda)$ (in m^{-1}), was calculated as 2.303·Abs(λ)/l, where Abs(λ) is the absorbance at wavelength λ, and l is the cell length in meters. Using the Levenberg-Marquardt algorithms implemented in the Stat Soft Inc. STATISTICA software, we obtained the coefficients $a_{CDOM}(254)$, S and K that best fit the equation:

$$a_{CDOM}(\lambda) = a_{CDOM}(254) \cdot \exp(-S \cdot (\lambda - 254)) + K \qquad (1)$$

where $a_{CDOM}(254)$ is the absorption coefficient at wavelength 254 nm (in m^{-1}), S is the spectral slope (in nm^{-1}) and K is a background constant caused by residual scattering by fine size particle fractions, micro-air bubbles or colloidal material present in the sample, refractive index differences between sample and the reference, or attenuation not due to organic matter (in m^{-1}). The carbon specific absorption coefficient at 254 nm, $a^*_{CDOM}(254)$ or SUVA$_{254}$ (Weishaar et al., 2003), was calculated dividing $a_{CDOM}(254)$ by the DOC concentration.

CDOM induced fluorescence (FDOM) was determined with a LS 55 Perkin Elmer Luminescence spectrometer, equipped with a xenon discharge lamp, equivalent to 20 kW for 8 μs duration. The instrument has 2 monochromators that ranged between 200 and 800 nm for excitation wavelengths and between 200 and 900 nm for emission wavelengths. The detector was a red-sensitive R928 photomultiplier, and a photodiode worked as reference detector. Slit widths were fixed to 10 nm for the excitation and emission wavelengths and the scan speed was 250 nm min^{-1}. Measurements were performed at a constant room temperature of 20°C in a 1 cm quartz fluorescence cell. Single measurements at specific excitation-emission wavelengths (Ex/Em) were performed. To compare with other works, the wavelengths chosen for the Ex/Em pair measurements were those previously established by Coble (1996): 280 nm/350 nm (peak-T) for protein-like substances; and 320 nm/410 nm (peak-M) and 340 nm/440 nm (peak-C) for humic-like substances absorbing in the UV-C. The fluorescence of UV-radiated Milli-Q at those Ex/Em pairs was subtracted to all samples. Following Coble (1996), fluorescence intensities were expressed in quinine sulphate units (QSU) by calibrating the instrument at Ex/Em: 350 nm/450 nm against a quinine sulphate dihydrate (QS) standard made up in 0.05 mol L^{-1} sulphuric acid. Fluorescence intensities of peak-T, peak-M and peak-C in QSU has been named as $F(280/350)$, $F(320/410)$ and $F(340/400)$, respectively.

Finally, the quantum yield of fluorescence at excitation 340 nm, $\Phi(340)$, was obtained from

the ratio of the fluorescence intensity at peak-C, $F(340/440)$, to the absorption coefficient at 340 nm, $a_{CDOM}(340)$, multiplied by the universal factor of $2.2(\pm 0.1)$ 10^{-3} m^{-1} QSU^{-1} obtained by Romera-Castillo et al. (submitted, 2011a, see Chapter III and IV, respectively):

$$\Phi(340) = 2.2 \cdot 10^{-3} \cdot \frac{F(340/440)}{a_{CDOM}(340)} \qquad (2)$$

Harmonic analysis of the time series

To obtain the annual mean (b1), amplitude (b2) and diphase (b3) parameters defining the seasonal cycle of any variable (Y), a harmonic analysis of the annual component (period, 365 days) of each time series has been performed. Again, using the Levenberg-Marquardt algorithms implemented in the Stat Soft Inc. STATISTICA software, we fitted the data of water temperature, salinity, DOC, $a_{CDOM}(254)$, $a*_{CDOM}(254)$, S, $F(340/440)$, $\Phi(340)$, and $F(280/350)$ to the following trigonometric equation:

$$Y = b1 + b2 \cdot \cos(\frac{2\pi}{365} \cdot t + b3) \qquad (3)$$

where t is the Julian day (ranging from 1 to 365/366). From the diphase parameter, b3, we calculated the Julian day at which each time series achieved the annual maximum value.

Results

Annual cycles of the bulk and coloured fractions of DOM

Sea surface temperature in Blanes Bay followed a well-defined annual cycle (Fig. 2a) that explains 90% of the variability of the time series with an average annual mean of 16.8 ± 0.2 ºC (Table 1). The lowest temperatures, 11.5ºC, occurred by mid February at the time of maximum winter mixing, and the highest, 22.1 ºC, were recorded by mid August (Julian day, 231 ± 3), when summer stratification was highest. Conversely, the annual cycle explained only 24% of the variability of the time series of salinity (Fig. 2b). Salinity was quite stable around the annual average of 37.98 ± 0.04, the amplitude being just 0.18 ± 0.02, except during a few particular dates associated with rainwater episodes.

Table 1. Value ± standard error of the estimation of the parameters of eq. 3 for the time series of the study variables: annual mean (b1), amplitude (b2) and diphase (b3). Coefficients b1 and b2 are expressed in the units of each variable and b3 is expressed in radians. The Julian day when the annual maximum of each variable occurred was calculated from b3. R^2, coefficient of determination of the regression equation; n, number of data of each time series. $p < 0.01$ for all the estimated coefficients.

Variable	Annual mean (b1)	Amplitude (b2)	Diphase (b3)	R^2	n	Time series maximum (Julian day)
Temperature (°C)	16.8 ± 0.2	-5.3 ± 0.3	24.30 ± 0.05	0.90	37	231 ± 3
Salinity	37.98 ± 0.04	0.18 ± 0.06	-18.06 ± 0.32	0.24	37	319 ± 19
DOC (μmol L⁻¹)	81 ± 2	-17 ± 4	5.1 ± 0.1	0.56	32	252 ± 9
$a_{CDOM}(254)$ (m⁻¹)	1.58 ± 0.02	-0.18 ± 0.04	-0.5 ± 0.2	0.53	25	210 ± 10
$a^*_{CDOM}(254)$ (m² mol C⁻¹)	19 ± 1	-3 ± 1	1.18 ± 0.34	0.40	23	114 ± 20
$a_{CDOM}(254/365)$	15.3 ± 0.6	-2.3 ± 0.9	17.7 ± 0.4	0.25	25	248 ± 21
$S(250\text{-}500)$ (nm⁻¹)	0.0257 ± 0.0004	-0.0016 ± 0.0005	-1.1 ± 0.3	0.32	25	248 ± 18
$F(340/440)$ (QSU)	0.50 ± 0.02	0.13 ± 0.03	-0.6 ± 0.2	0.47	35	34 ± 10
$F(280/350)$ (QSU)	1.11 ± 0.05	0.25 ± 0.07	8.1 ± 0.3	0.27	35	260 ± 16
Q.Y. (%)	0.65 ± 0.02	0.16 ± 0.03	-0.3 ± 0.2	0.50	25	17 ± 10

DOC and the optical properties of CDOM also described statistically significant annual cycles. Eq. 3 explained 56% of the variability of DOC. The annual mean concentration of DOC was 81 ± 2 μmol C L^{-1}; it accumulated in the surface layer of Blanes Bay from the annual minimum of 64 μmol C L^{-1} recorded by early March to the annual maximum of 98 μmol C L^{-1} by mid September (Julian day 252 ± 19; Fig. 2c, Table 1), about one month later than the maximum of sea surface temperature. These are the typical annual concentrations but higher values reaching 140 μmol C L^{-1} has been sporadically registered.

Fifty three percent of the variability of the absorption coefficient at 254 nm, $a_{CDOM}(254)$, an indicator of the abundance of conjugated carbon double bounds (Lakowicz et al., 2006), was explained by eq. 3. Although $a_{CDOM}(254)$ also accumulated through the spring and summer, the annual maximum absorption of 1.75 m^{-1} (Fig. 2d) occurred by late July (Julian day, 210 ± 10), i.e. 42 ± 13 days before the annual maximum of DOC (Table 1). The diphase of DOC and $a_{CDOM}(254)$, led to an annual cycle of $a^*_{CDOM}(254)$ that reaches the annual maximum of 22.4 m^2 mol C^{-1} by late April (Julian day, 114 ± 20). $a^*_{CDOM}(254)$ is used as an aromaticity index since Weishaar et al. (2003) found a good correlation between this variable and the percentage of aromaticity determined by ^{13}C–NMR spectroscopy. Other useful indices are the absorption coefficient ratio at 254 nm to 365 nm, $a_{CDOM}(254/365)$, and the absorption spectral slope, S (Fig. 2e), which are inversely correlated with the average molecular weight of DOM (Dahlén et al., 1996; Engelhaupt et al., 2003). In our study, both variables described statistically significant annual cycles that explained 25-32% of the total variability of the time series and were in phase with the annual cycle of DOC (Table 1).

The fluorescence of aromatic humic-like substances absorbing in the UV-A region of the spectrum, $F(340/440)$, followed an annual cycle that explained 47% of the variability of the time series and was out of phase with $a_{CDOM}(254)$ and DOC. $F(340/440)$ evolved from an annual maximum of 0.63 QSU by early February to a minimum of 0.36 QSU by early August (Fig. 2f). The time course of the fluorescence quantum yield at 340 nm, $\Phi(340)$, an spare aromaticity index (Birks, 1970; Turro, 1991), followed also a statistically significant seasonal cycle that explained 50% of its variability and was in phase with $F(340/440)$ (Table 1). Annual average $\Phi(340)$ was $0.65 \pm 0.02\%$, ranging from an annual maximum of 0.81% to a minimum of 0.49%. Conversely, the fluorescence of aromatic protein-like substances (Fig. 2g) described an annual cycle that explained 27% of the variability of the time series and was in phase with DOC, reaching the annual maximum by mid September (Julian day, 260 ± 16; Table 1).

Deseasonalized time series

The studied variables were deseasonalised by subtracting the annual cycles modelled with eq. 3 (dotted lines in Fig. 2) from the original times series (open dots in Fig. 2). The deseasonalised time
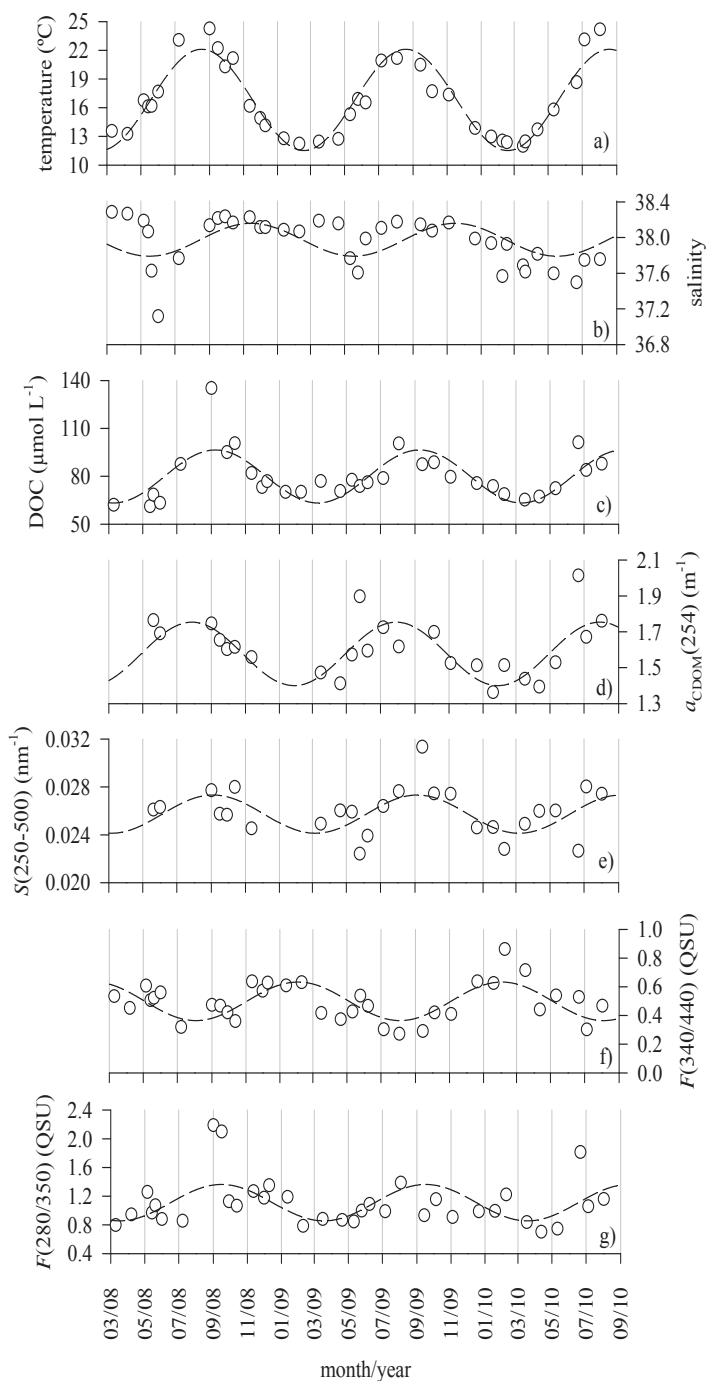
175

Fig. 2. Seasonal distribution of a) temperature (ºC), b) salinity, c) DOC (μmol·L^{-1}), d) $a_{CDOM}(254)$ (m^{-1}), e) Spectral slope at 250-500 range (nm^{-1}), f) peak-C or $F(340/440)$ and g) peak-T or $F(280/350)$. Modelled values (dotted line) and measured values (open dots).

series of the fluorescence of the humic-like peak-C, $\Delta F(340/440)$ (Fig. 3a), was generally opposite to the deseasonalised time series of salinity, ΔSal (Fig. 3b). In fact, a significantly negative linear correlation (R^2 = 0.44, $p < 0.01$) existed between $\Delta F(340/440)$ and ΔSal (Table 2). ΔSal was also negatively correlated with the aromaticity index $\Phi(340)$ ($R^2 = 0.33$, $p < 0.01$). On the other hand, the deseasonalised time series of the protein-like peak-T, $\Delta F(280/350)$ (Fig. 3c), and that of the bulk DOC, ΔDOC (Fig. 3d), followed the same trend; a significantly positive linear correlation ($R^2 = 0.49$, $p < 0.01$) existed between $\Delta F(280/350)$ and ΔDOC (Table 2).

Discussion

The Blanes Bay Microbial Observatory is representative for oligotrophic coastal ecosystems which sporadically receives nutrients and terrestrial carbon inputs during stormy periods (Gudadayol et al., 2009). The annual cycle of sea surface temperature traces the seasonal evolution from winter mixing to summer stratification characteristic of temperate latitudes. Increasing water column stratification throughout the spring and summer prevents the flux of new inorganic nutrients to the surface layer, leading to severe oligotrophic conditions (Sommaruga et al., 2005; Alonso-Sáez et al., 2008). Nutrient concentrations during the summer seasons of the studied years were around 0.03 µmol L^{-1} for phosphate, 0.3 µmol L^{-1} for inorganic nitrogen, and 0.1 µmol L^{-1} for silicate (data not shown). The typical annual range of DOC concentrations recorded during the study period, from 64 µmol L^{-1} in late winter to 98 µmol L^{-1} in late summer, has been previously observed in Blanes Bay (Lucea et al., 2005; Alonso-Sáez et al., 2008) as well as in other temperate marine ecosystems relatively unaffected by terrestrial inputs (Nelson et al., 1998; Álvarez-Salgado et al., 2001). The summer accumulation of DOC of 40 µmol C L^{-1} observed in Blanes is similar to that reported in the temperate stations of Hawaii Ocean Time Series (40 µmol C L^{-1}, http://hahana.soest.hawaii.edu/hot/) but doubles that of Bermuda Atlantic Time Series Study (15 µmol C L^{-1}, Nelson et al., 1998).

The refractory and labile aromatic dissolved materials traced by $a_{CDOM}(254)$ and peak-T, respectively, accumulated also in Blanes Bay during the spring and summer. However, $a_{CDOM}(254)$ reached its annual maximum about 1 ½ months before than peak -T that, in turns, was in phase with DOC. Therefore, the optical properties of CDOM allowed distinguishing the differential accumulation of two DOC pools of contrasting bioavailability. Among the by-products of microbial respiration there are compounds with conjugated carbon double bonds traced by $a_{CDOM}(254)$ since microorganisms produce fluorescent humic-like substances absorbing around Ex 261 nm and emitting around Em 463 nm (Romera-Castillo et al., 2011b, see Chapter II). This fluorescent maximum is within the range established by Coble (1996) for peak-A (Ex/Em 260/400-460). The annual minimum of $a_{CDOM}(254)$ is recorded in winter likely because of mixing with the subsurface waters and/or the deep offshore

waters of Blanes Bay and it accumulates during the spring and summer because of the dominance of net production by microbial respiration over photochemical degradation in the stratified surface layer. In these sense, it is known that higher losses of fluorescence and absorbance occur at the wavelengths of irradiation (Del Vecchio and Blough, 2002) and that few photons of $\lambda < 295$ nm reach the Earth surface. Coherently, the maximum proportion of conjugated carbon double bonds per unit of organic carbon, $a^*_{CDOM}(254)$, occurred in spring, when biological activity is maximum in Blanes Bay (Alonso-Sáez et al., 2008).

The fact that the annual cycle of peak-T is in phase with DOC, suggests that the DOC accumulated in Blanes Bay contains not only the refractory materials traced by $a_{CDOM}(254)$ but also biologically labile materials, including fluorescent free and combined aromatic amino acids. In this sense, it is known that maintenance of the photosynthetic machinery after nutrient exhaustion is accompanied by excretion of DOM and especially carbohydrates (Norman et al., 1995). Apparently, despite the potential lability of the exuded materials, they cannot be processed by heterotrophic bacteria because of nutrient limitation. Therefore, the summer accumulation of DOC in oligotrophic systems is likely due to a malfunctioning of the microbial loop (Thingstad et al., 1997). The accumulation of DOM is a common mechanism that has also been evidenced in this and other oligotrophic aquatic environments (e.g., Sargasso Sea, Thingstad et al., 1997; Siegel et al., 2002) as well as in experimental mesocosms (Norman et al., 1995). The accumulation of protein-like substances in summer was also observed in Florida Bay (Jaffé et al., 2008). Another plausible reason for the protein-like fluorescence maximum recorded in summer could be that photo-degradation of humic substances release amino acids moieties that present higher fluorescence in the free form (Lakowicz, 2006). This has been previously hypothesized in lab experiments with ultrafiltered DOM from the open ocean when the fluorescence of peak-T increased significantly after exposure to sunlight irradiation (Romera-Castillo, et al., submitted, see Chapter III.).

The annual cycle of the coloured and fluorescent refractory humic-like materials that absorbs natural light at wavelengths >300 nm, i.e. in the UV-B and UV-A range of the spectrum, in Blanes Bay, is the result of the prevalence of consumption by photodegradation over production by microbial respiration of these materials (Coble, 2007). This pattern has been previously observed in other marine ecosystems relatively unaffected by continental runoff such as the oligotrophic BATS site (Nelson et al., 1998; 2004) or the eutrophic Iberian coastal upwelling system (Nieto-Cid et al. 2006; Romera-Castillo et al., 2011a, see Chapter IV) and it is the reason behind the relatively low values of the absorption coefficient (Nelson et al., 2010) and the induced fluorescence (Yamashita and Tanoue, 2008) of CDOM in surface ocean waters. Therefore, we hypothesize that the annual maximum accumulation of $a_{CDOM}(340)$ (not shown) and of peak-C, $F(340/440)$, is recorded in winter mainly because of two possible facts: 1) the occurrence of mixing events with the subsurface waters and/or the deep offshore waters of Blanes Bay and 2) the photodegradation during the spring and summer as a consequence of intense photobleaching in the stratified surface layer. Note that this annual pattern is opposite for
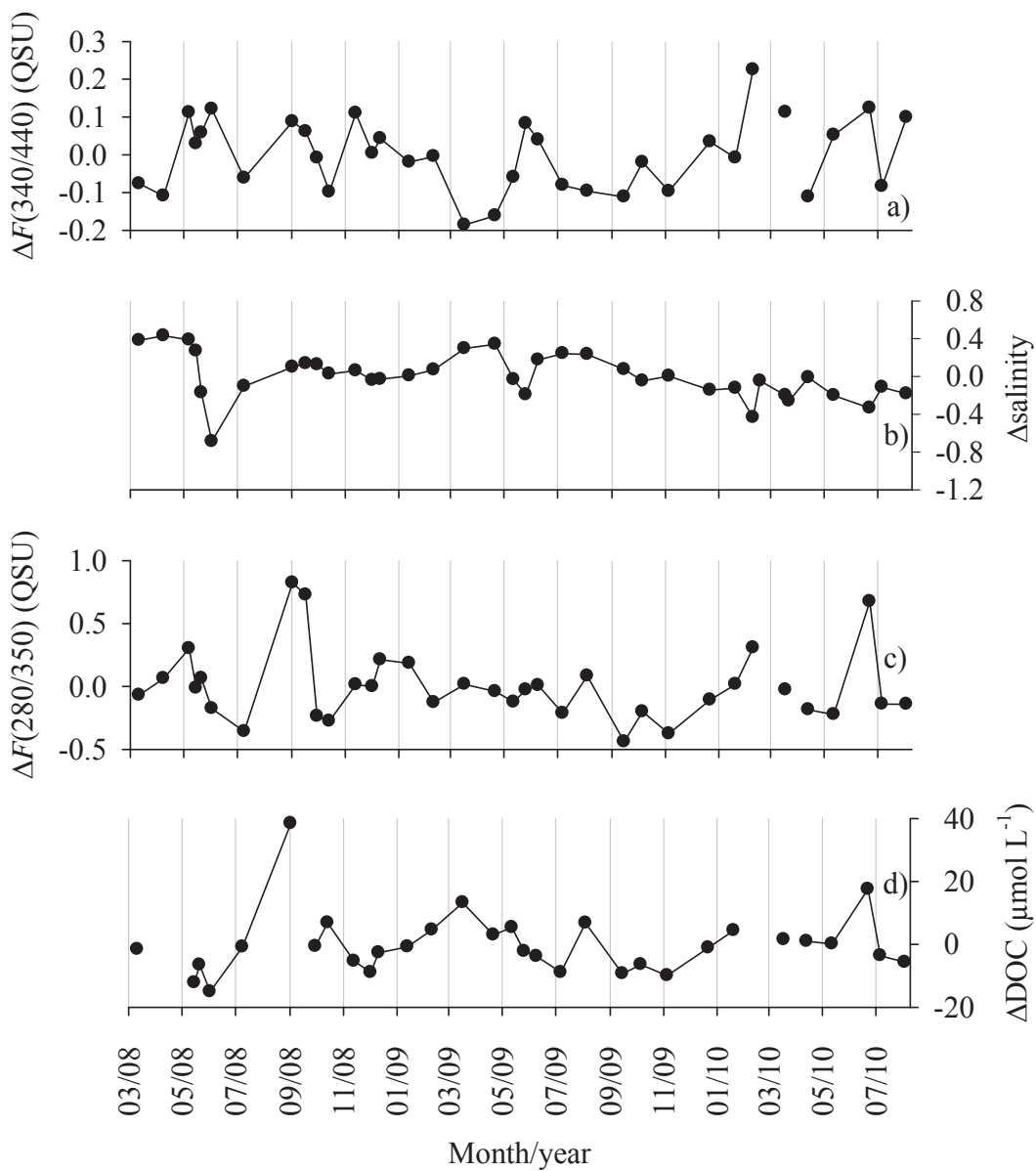
Fig. 3. Seasonal distribution of the deseasonalized time series of a) peak-C or $F(340/440)$, b) salinity, c) peak-T or $F(280/350)$ and d) DOC (μmol L^{-1}).

the refractory coloured materials absorbing at wavelengths <300 nm, represented here by $a_{CDOM}(254)$, which is less affected by photobleaching.

Annual mean $a_{CDOM}(340)$ in Blanes Bay, 0.17 ± 0.01 m^{-1}, does not differ from the average values reported for the NW Mediterranean in the Bay of Marseilles (Ferrari, 2000; Para et al., 2010). These absorption coefficients are higher than those found in oligotrophic open ocean waters (Nelson et al., 2010) but lower than in eutrophic coastal upwelling areas (Coble et al., 1998; Day and Faloona, 2009; Romera-Castillo et al., 2011a, see Chapter IV). In the particular case of the Ría de Vigo (NW Spain), $a_{CDOM}(340)$ ranged from 0.43 ± 0.11 m^{-1} for downwelling to 0.35 ± 0.14 m^{-1} for upwelling conditions (Romera-Castillo et al., 2011a, see Chapter IV). Given that the average DOC concentration in the Ría de Vigo, 78 μmol L^{-1}, and Blanes Bay, 81 μmol L^{-1}, are quite comparable, the carbon specific absorption coefficient at 340 nm was about twice in the eutrophic than in the oligotrophic coastal system.

Photobleaching is the probable reason for the reduction of $F(340/440)$ in Blanes Bay by 42% from the annual maximum in early February to the annual minimum in early August. This proportion is close to that reported in the Middle Atlantic Bight where it was reduced to ~30% (Vodacek and Blough, 1997) and in the eutrophic coastal system of the Ría de Vigo (40-50%, Nieto-Cid et al., 2006).

Photobleaching of humic-like materials produces a dramatic loss of aromaticity and a decrease of the molecular weight of the irradiated materials (Moran and Zepp, 1997; Osburn et al., 2001). Coherently, our annual cycles of the aromaticity indices $a^*_{CDOM}(254)$ and $\Phi(340)$ and the average molecular weight indices $a_{CDOM}(254/365)$ and S values agree with the photodegradation of aromatic and high molecular weigh compounds during the summer to generate colourless more aliphatic and lower molecular weigh products, CO and CO_2 (Moran and Zepp, 1997). Therefore, the fraction of CDOM that reaches maximum concentrations by mid-September seems to be of relatively low average molecular weight and aromaticity. Although labile compounds are formed during photodegradation

Table 2. Coefficients of the linear regression equations between the deseasonalised time series of the fluorescence of peak-C, $F(340/440)$, and peak-T, $F(280/350)$, the absorption coefficient at 254 nm, $a_{CDOM}(254)$, and the fluorescence quantum yield at 340 nm, $\Phi(340)$, with salinity and DOC. R^2, coefficient of determination of the regression equation; p, level of significance; n, number of data of each time series.

Equation	R^2	p	N
$\Delta F(340/440) = -0.27 (\pm 0.05) \cdot \Delta Sal$	0.44	< 0.01	34
$\Delta \Phi(340) = -0.25 (\pm 0.07) \cdot \Delta Sal$	0.33	< 0.01	26
$\Delta F(280/350) = 0.018 (\pm 0.003) \cdot \Delta DOC$	0.49	< 0.01	31

processes (Moran and Zepp, 1997; Obernosterer et al., 1999), the previously referred malfunctioning of the microbial loop leads to the accumulation of these materials in the stratified surface layer.

The annual mean ± amplitude of the absorption spectral slope, 0.0257 ± 0016 nm^{-1}, obtained in Blanes Bay (Table 1) is relatively high when it is compared with the values reported for surface waters of the Gulf of Lions (0.017 ± 0.003 nm^{-1}, Ferrari, 2000) and the Bay of Marseilles (0.019 ± 0.003 nm^{-1}, Para et al., 2010), both in the NW Mediterranean Sea, or for an eutrophic coastal embayment as the Ría de Vigo (0.0205 ± 0.0013 nm^{-1}; Romera Castillo et al., 2011a, see Chapter IV). As in Blanes, absorption spectral slopes in Marseille are relatively lower during winter and higher during summer (Para et al., 2010) as a consequence of the characteristic seasonal increase of photo-degradation at temperate latitudes. Continental CDOM inputs tend to decrease and photodegradation processes tend to rise absorption spectral slopes (Del Vecchio and Blough, 2004; Nelson et al., 2010). Since natural irradiation is not far different between both Mediterranean and Atlantic studied sites, with values around 160 W m^{-2} (Ruiz et al., 2008; www.meteogalicia.es), the reason behind the relatively higher values of S in Blanes Bay is likely because it has less terrestrial influence than the Bay of Marseille, which is close to the major source of freshwater and terrigenous particles of the NW Mediterranean Sea (Rhône River, Pont, 1996), or the Ría de Vigo, which directly receive Oitaben-Verdugo river waters with an average annual flow of 15 m^3 s^{-1} (Nogueira et al., 1997).

The annual mean ± amplitude of the fluorescence quantum yield at 340 nm found in Blanes Bay, $0.65 \pm 0.16\%$, is within the range of values reported for the Gulf of Lions but lower than the average yields recorded in the more eutrophic Rhône river plume (0.96%; Ferrari, 2000) and Ria de Vigo ($0.91 \pm 0.30\%$). Laboratory experiments have shown that photobleaching produces a decrease, and microbial degradation an increase, of the fluorescence quantum yield (De Haan, 1993; Lønborg et al., 2010). Therefore, the distinct values of $\Phi(340)$ found in oligotrophic and eutrophic sites can be explained on basis on a larger influence of microbial degradation in the latter sites. Moreover, in the Rhône River, it could be also due to the higher terrestrial contribution since terrestrial organic matter present a higher degree of aromaticity than marine one (Repeta et al., 2002; Benner, 2003).

The seasonal cycle of the fluorescent humic-like substances is disrupted by the episodic arrival of continental waters to the sampling site, which can be traced by a decrease of salinity (Fig. 2b). Lower salinities are usually accompanied by higher values of $F(340/440)$ (Figs. 3a and b); in fact, a significant negative correlation was observed between the deseasonalised times series of salinity, $F(340/440)$ and $\Phi(340)$ (Table 2). This again is because continental waters are characterised by higher humic-like fluorescence values produced by more aromatic compounds than marine waters (Coble, 1996; Repeta et al., 2002; Benner, 2003). $F(340/440)$ measured at the mouth of River Tordera, placed south of the sampling site, on the 15/05/2008 were as high as 53 QSU while DOC and nutrient values were of 263 µmol L^{-1} C and 90.3 µmol L^{-1} NIT, respectively (unpub. data). Furthermore, continental runoff

also transport new inorganic nutrients to the sampling site that can contribute to enhance microbial activity, which is known to also produce humic-like substances (Nieto-Cid et al., 2006; Shimotori et al., 2009; Lønborg et al., 2010; Romera-Castillo et al., 2010, 2011b, see Chapter I and II, respectively). Coherently, the major sources of the interannual differences in the microplanktonic metabolism are the variability in rainfall and continental runoff (Satta et al., 1996; Guadayol et al., 2009). The fact that the marked salinity decrease observed in June 2008 was not accompanied by a large increase of F(340/440) could be due to photodegradation of continental humic substances during water advection to the sampling site and/or a delay in the stimulation of microbes by nutrients transported by continental waters. In fact, Guadayol et al. (2009) found that the effects of continental runoff in Blanes Bay were visible on the autotrophic activity around 11 days after the river discharge.

For the case of the protein-like compounds, the coupling observed between the annual cycles of F(280/350) and DOC, persists when the deseasonalised time series are compared (Fig. 3; Table 2). The extremely high values of F(280/350) recorded in September 2008 and 2010 (Fig. 3c) were accompanied by high concentrations of DOC too (Fig. 3d). Therefore, as previously observed by Lønborg et al. (2010) in the eutrophic Ría de Vigo, the fluorescence of protein-like substances could be used as a tracer for the evolution of DOC at seasonal and shorter time scales.

Conclusions

Absorption and fluorescence spectroscopy measurements of the coloured fraction of DOM in the Blanes Bay Microbial Observatory have allowed distinguishing between DOM pools of different origin and photo- and bio-availability, which resulted in contrasting seasonal cycles. This work shows that the optical properties of DOM, which are simple, fast and relatively inexpensive to obtain, could be incorporated in time-series monitoring programs as a complement to the usual DOC measurements given that they provide relevant information about the physical and biogeochemical processes controlling the stocks and the reactivity of the DOM pool.

Acknowledgements

References

Alonso-Sáez, L., Vázquez-Domínguez, E., Cardelús, C., Pinhassi, J., Sala, M.M., Lekunberri, I., Balagué, V., Vila-Costa, M., Unrein, F., Massana, R., Simó, R., Gasol, J.M., 2008. Factors controlling the year-round variability in carbon fl ux through bacteria in a coastal marine system. Ecosystems 11, 397-409.

Álvarez-Salgado, X.A., Gago, J., Miguez, B.M. and Perez, F.F., 2001. Net ecosystem production of dissolved organic carbon in a coastal upwelling system: the Ria de Vigo, Iberian margin of the North Atlantic. Limnol. Oceanogr. 46, 135-147.

Benner, R., 2003. Molecular indicators of the bioavailability of dissolved organic matter. In: Findlay, S., Sinsabaugh, R. (Eds.), Aquatic ecosystems: interactivity of dissolved organic matter. Academic Press, New York, p.121-137.

Bingham, F.M., Lukas, R., 1996. Seasonal cycles of temperature, salinity and dissolved oxygen observed in the Hawaii Ocean Time-series. Deep Sea Res. Part II 43, 199-213.

Birks, J.B., 1970. Photophysics of aromatic molecules. Willey-Interscience, London.

Cloern, J.E., Jassby, A.D., 2008. Complex seasonal patterns of primary producers at the land–sea interface. Ecol. Lett. 11, 1294-1303.

Coble, P.G., 1996. Characterization of marine and terrestrial DOM in seawater using excitation-emission matrix spectroscopy. Mar. Chem. 51, 325-346.

Coble, P.G., Del Castillo, C.E., Avril, B., 1998. Distribution and optical properties of CDOM in the Arabian Sea during the 1995 Southwest Monsoon. Deep-Sea Res. II 45, 2195-2223.

Coble, P.G., 2007. Marine optical biogeochemistry: the chemistry of ocean color. Chem. Rev. 107, 402-418.

Dahlén, J., Bertilsson, S., Pettersson, C., 1996. Effects of UV-A irradiation on dissolved organic matter in humic surface waters. Environ. Int. 22, 501-506.

Day, D.A., Faloona, I., 2009. Carbon monoxide and chromophoric dissolved organic matter cycles in the shelf waters of the northern California upwelling system. J. Geophys. Res. 114, C01006.

De Haan, H., 1993. Solar UV-Light Penetration and photodegradation of humic substances in Peaty Lake water. Limnol. Oceanogr. 38, 1072-1076.

Del Castillo, C.E., Coble, P.G., Morell, J.M., López, M.J., Corredor, J.E., 1999. Analysis of the optical properties of the Orinoco River plume by absorption and fluorescence spectroscopy. Mar. Chem. 66, 35-51.

Del Vecchio, R., Blough, N.V., 2002. Photobleaching of chromophoric dissolved organic matter in natural waters: kinetics and modeling. Mar. Chem. 78, 231-253.

Del Vecchio, R., Blough, N.V., 2004. Spatial and seasonal distribution of chromophoric dissolved organic matter and dissolved organic carbon in the Middle Atlantic Bight. Mar. Chem. 89, 169-187.

Duarte, C.M., Agustí, S., Kennedy, H., Vaqué, D.,1999. The Mediterranean climate as a template for Mediterranean marine ecosystems: the example of the Northeast Spanish littoral. Progr. Oceanogr. 44, 245-270.

Engelhaupt, E., Bianchi, T.S., Wetzel, R.G., Tarr, M.A., 2003. Photochemical transformations and bacterial utilization of high-molecular-weight dissolved organic carbon in a southern Louisiana tidal stream (Bayou Trepagnier). Biogeochemistry 62, 39-58.

Ferrari, G.M., 2000. The relationship between chromophoric dissolved organic matter and dissolved organic carbon in the European Atlantic coastal area and in the West Mediterranean Sea (Gulf of Lions). Mar. Chem. 70, 339-357.

Galand, P., Gutiérrez-Provecho, C., Massana, R., Gasol, J.M., Casamayor, E.O., 2010. Inter-annual recurrence of archaeal assemblages in the coastal NW Mediterranean Sea (Blanes Bay Microbial Observatory). Limnol. Oceanogr. 55, 2117-2125.

Gasol, J.M., del Giorgio, P.A., Massana, R., Duarte, C.M., 1995. Active versus inactive bacteria: size-dependence in a coastal marine plankton community. Mar. Ecol. Prog. Ser. 128, 91-97.

Guadayol, Ò., Peters, F., Marrasé, C., Gasol, J.M., Roldán, C., Berdalet, E., Massana, R., Sabata, A., 2009. Episodic meteorological and nutrient-load events as drivers of coastal planktonic ecosystem dynamics: a time-series analysis. Mar. Ecol. Prog. Ser. 381, 139-155.

Helms, J.R., Stubbins, A., Ritchie, J.D., Minor, E.C., Kieber, D.J., Mopper, K., 2008. Absorption spectral slopes and slope ratios as indicators of molecular weight, source, and photobleaching of chromophoric dissolved organic matter. Limnol. Oceanogr. 53, 955-969.

Herndl, G.J., Muller-Niklas, G., Frick, J., 1993. Major role of ultraviolet-B in controlling bacterioplankton growth in the surface layer of the ocean. Nature 361, 717-719.

Jaffé, R., McKnight, D., Maie, N., Cory, R., McDowell, W. H., Campbell, J. L., 2008. Spatial and temporal variations in DOM composition in ecosystems: the importance of long-term monitoring of optical properties. J. Geophys. Res. 113, G04032.

Kirk, J. T. O., 1994. Light and photosynthesis in aquatic ecosystems, 2nd edn., Cambridge University. Press, Cambridge.

Kramer, G.D., Herndl, G.J., 2004. Photo- and bioreactivity of chromophoric dissolved organic matter produced by marine bacterioplankton. Aquat. Microb. Ecol. 36, 239-246.

Lakowic, J.R., 2006. Principles of Fluorescence Spectroscopy. Springer.

Lønborg, C., Álvarez-Salgado, X.A., Davidson, K., Martínez-García, S., Teira, E., 2010. Assessing the microbial bioavailability and degradation rate constants of dissolved organic matter by fluorescence spectroscopy in the coastal upwelling system of the Ría de Vigo. Mar. Chem. 119, 121-129.

Lucea, A., Duarte, C.M., Agustí, S., Kennedy, H., 2005. Nutrient dynamics and ecosystem metabolism in the Bay of Blanes (NW Mediterranean). Biogeochemistry 73, 303-323.

Margalef, R., 1945. Fitoplancton nerítico de la Costa Brava catalana (Sector de Blanes). Publ. Biol. Mediterránea 1, 1-48.

Moran, M.A., Zepp, R.G., 1997. Role of photoreactions in the formation of biologically labile compounds from dissolved organic matter. Limnol. Oceanogr. 42, 1307-1316.

Moran, M.A., Sheldon, W.M., Zepp, R.G., 2000. Carbon loss and optical property changes during long-term photochemical and biological degradation of estuarine dissolved organic matter. Limnol. Oceanogr. 45, 1254-1264.

Nelson, N.B., Siegel, D.A., Michaels, A.F., 1998. Seasonal dynamics of colored dissolved material in the Sargasso Sea. Deep Sea Res. I 45, 931-957.

Nelson, N.B., Craig, A.C., Steinberg, D.K., 2004. Production of chromophoric dissolved organic matter by Sargasso Sea microbes. Mar. Chem. 89, 273– 287.

Nelson, N.B., Siegel, D.A., Carlson, C.A. and Swan, C.M., 2010. Tracing global biogeochemical cycles and meridional overturning circulation using chromophoric dissolved organic matter. Geophys. Res. Lett. 37, L03610.

Nieto-Cid, M., Álvarez-Salgado, X.A., Gago, J., Pérez, F.F., 2005. DOM fluorescence, a tracer for biogeochemical processes in a coastal upwelling system (NW Iberian Peninsula). Mar. Ecol. Prog. Ser. 297, 33-50.

Nieto-Cid, M., Álvarez-Salgado, X.A., Pérez, F.F., 2006. Microbial and photochemical reactivity of fluorescent dissolved organic matter in a coastal upwelling system. Limnol. Oceanogr. 51, 1391-1400.

Nogueira, E., Pérez, F.F., Ríos, A.F., 1997. Seasonal and long - term trends in an estuarine upwelling ecosystem (Ría de Vigo, NW Spain). Estuar. Coastal Shelf Sci. 44, 285-300.

Norman, B., Zweifel, U.L., Hopkinson, C.S., Fry, B., 1995. Production and utilization of dissolved organic carbon during an experimental diatom bloom Limnol. Oceanogr. 40, 898-907.

Obernosterer, I., Reitner, B., Herndl, G.J., 1999. Contrasting effects of solar radiation on dissolved organic matter and its bioavailability to marine bacterioplankton. Limnol. Oceanogr. 44, 1645-1654.

Osburn, C.L., Morris, D.P., Thorn, K.A., Moeller, R.E., 2001. Chemical and optical changes in freshwater dissolved organic matter exposed to solar radiation. Biogeochemistry 54, 251-278.

Para, J., Coble, P.G., Charrière, B., Tedetti, M., Fontana, C., Sempéré, R., 2010. Fluorescence and absorption properties of chromophoric dissolved organic matter (CDOM) in coastal surface waters of the Northwestern Mediterranean Sea (Bay of Marseilles, France). Biogeosci. Discuss. 7, 5675-5718.

Pont, D., 1996. Evaluation of water fluxes and sediment supply. Meddelt, Venezia, October 2–5.

Repeta, D.J., Quan, T.M., Aluwihare, L.I. and Accardi, A., 2002. Chemical characterization of high molecular weight dissolved organic matter in fresh and marine waters. Geochim. Cosmochim. Ac. 66, 955–962.

Romera-Castillo, C., Sarmento, H., Álvarez-Salgado, A.X., Gasol, J.M., Marrasé, C., 2010. Production of chromophoric dissolved organic matter by marine phytoplankton. Limnol. Oceanogr., 55, 446–454.

Romera-Castillo, C., Nieto-Cid, M., Castro, C.G., Marrasé, C., Largier, J., Barton, E.D., Álvarez-Salgado, X.A., 2011a. Fluorescence: absorption coefficient ratio - tracing photochemical and microbial degradation processes affecting coloured dissolved organic matter in a coastal system. Mar. Chem. 125, 26-38.

Romera-Castillo, C., Sarmento, H., Álvarez-Salgado, X.A., Gasol, J.M., Marrasé, C., 2011b. Net production/consumption of fluorescent coloured dissolved organic matter by natural bacterial assemblages growing on marine phytoplankton exudates. Appl. Environ. Microbiol. Accepted.

Romera-Castillo, C., Nieto-Cid, M., Marrasé, C., Repeta, D.J., Álvarez-Salgado, X.A. Optical properties of ultrafiltered dissolved organic matter (UDOM) from contrasting aquatic environments and their alteration by sunlight. Submitted.

Romero, E., Peters, F., Arín, L., Guillén, J., 2010. High degree of variability of coastal plankton dynamics in an urbanized location of the NW Mediterranean. In: Sources of plankton variability in an urbanized coastal ecosystem, PhD thesis.

Ruiz, S., Gomis, D., Sotillo, M.G., Josey, S.A., 2008. Characterization of surface heat fluxes in the Mediterranean Sea from a 44-year high-resolution atmospheric data set. Global Planet Change 63, 258–274.

Satta, M.P., Agustí, S., Mura, M.P., Vaqué, D., Duarte, C.M., 1996. Microplankton respiration and net community metabolism in a bay on the NW Mediterranean coast. Aquat. Microb. Ecol. 10, 165-172.

Shimotori, K., Omori, Y., Hama, T., 2009. Bacterial production of marine humic-like fluorescent dissolved organic matter and its biogeochemical importance. Aquatic Microbial Ecol. 58, 55-66.

Siegel, D.A., Maritorena, S., Nelson, N.B., 2002. Global distribution and dynamics of colored dissolved and detrital organic materials. J. Geophys. Res. 107, C12.

Smith, R. C., Cullen, J. J., 1995. Effect of UV radiation on phytoplankton, Rev. Geophys. 33, 1211-1223.

Sommaruga, R., Hofer, J.S., Alonso-Saez, L., Gasol, J.M., 2005. Differential sunlight sensitivity of picophytoplankton from surface Mediterranean coastal waters. Appl. Environ. Microbiol., 71, 2154-2157.

Stedmon, C.A., Álvarez-Salgado, X.A., 2011. Shedding light on a black box: UV-visible spectroscopic characterization of marine dissolved organic matter. In: Jiao, N., Azam, F., Sanders, S. (Eds.), Microbial carbon pump in the ocean. Science AAA/S. pp. 62-63.

Turro, N.J., 1991. Modern molecular photochemistry. University Science Books.

Thingstad, T.F., Hagström, A., Rassoulzadegan, F., 1997. Accumulation of degradable DOC in surface waters: Is it caused by a malfunctioning microbial loop? Limnol. Oceanogr. 42, 398-404.

Vodacek, A., Blough, N.V., 1997. Seasonal variation of CDOM in the Middle Atlantic Bight: terrestrial inputs and photooxidation. Proceedings of SPIE-The International Society for Optical Engineering, 2963(Ocean Optics XIII), 132-137.

Weishaar, J.L., Aiken, G.R., Bergamaschi, B.A., Fram, M.S., Fujii, R., Mopper, K., 2003. Evaluation of specific ultraviolet absorbance as an indicator of the chemical composition and reactivity of dissolved organic carbon. Environ. Sci. Technol. 37, 4702-4708.

Yamashita, Y., Tanoue, E., 2008. Production of bio-refractory fluorescent dissolved organic matter in the ocean interior. Nat. Geosci. 1, 579-582.

Conclusions

Conclusions

Absorption and fluorescence spectroscopy have been used to characterize the origin of the coloured fraction of DOM (CDOM) in marine ecosystems as well as to identify and quantify the different mechanisms that govern its transformations. The main conclusions from this work are:

1) It has been unequivocally proven, for the first time, that marine phytoplankton produce coloured humic-like substances that emit natural fluorescence at 410 nm when irradiated at 320 nm (peak-M). These compounds are bio-available for marine bacteria, which concurrently produce different humic-like substances that emit natural fluorescence at 440 nm when irradiated at 340 nm (peak-C). These results challenge the traditional view of considering peak-M of marine origin and peak-C of terrestrial origin.

2) When normalised to biomass, the production rate of fluorescent DOM, both protein- and humic-like fluorophores, by marine phytoplankton is one order of magnitude lower than by bacteria. The contrasting production rates together with the bioavailability of the humic-like substances produced by marine phytoplankton are the likely reasons behind the lack of correlation between phytoplankton biomass (chlorophyll) and humic-like substances in most aquatic systems.

3) The optical properties of ultrafiltrated dissolved organic matter (1 KDa cut-off) isolated from contrasting aquatic environments indicate that the average molecular weight and aromaticity of the isolates decreased significantly from riverine to open ocean waters and increased significantly with depth. This pattern can be explained on basis of the contrasting continental or marine influence on the samples and their exposure to sunlight radiation prior to collection. Further exposure of the isolates to sunlight produced a decrease of absorption and fluorescence at wavelengths >300 nm, due to the photobleaching of the humic-like fluorophores. Photobleaching was not significant at < 300 nm because very few photons of those wavelengths reach the Earth surface. Moreover, and increase of absorption and fluorescence at wavelengths < 300 nm in open ocean samples was observed. This increase was likely due to conformational changes in the humic substances containing bound proteins or the cleavage of amino acids or protein moieties bound to humic substances by natural radiation.

4) Microbial production and photodegration of CDOM occurs during mixing of continental and oceanic waters in the coastal eutrophic system of the Ría de Vigo (NW Spain). The spatial and temporal variability of the fluorescence: absorption coefficient ratio reveals that photodegradation is the dominant biogeochemical process influencing CDOM variability during the mixing of shelf surface and continental waters under downwelling conditions. By contrast, microbial production was dominant during the mixing of bottom shelf and continental waters under upwelling conditions.

5) Different CDOM fractions follow well-defined seasonal cycles connected to the water column mixing-stratification sequence imposed by natural radiation in the oligotrophic coastal system of Blanes Bay (NW Mediterranean). Bio-available protein-like substances accumulate during the spring and summer, reaching maximum fluorescence intensities by mid September, probably because of a malfunctioning of the microbial loop by severe nutrient limitation. By contrast, the fluorescence of bio-refractory humic-like substances absorbing in the UV-A region was minimun by early August because of photo-degradation. Finally, the absorptivity at 254 nm, characteristic of the conjugated carbon double bonds of refractory DOM, reached annual maximum values in late April, when they accumulate as a by-product of enhanced microbial respiration during the spring bloom.

Institut
de Ciències
del Mar

CSIC
CONSEJO SUPERIOR DE INVESTIGACIONES CIENTÍFICAS

IIM
Instituto de Investigaciones
Marinas de Vigo